1985 Monitoring Surveys at the Central Long Island Sound Disposal Site:

An Assessment of Impacts from Disposal and Hurricane Gloria

Disposal Area Monitoring System DAMOS

Contribution 57
November 1989

US Army Corps of Engineers
New England Division

1985 MONITORING SURVEYS AT THE CENTRAL LONG ISLAND SOUND DISPOSAL SITE:

AN ASSESSMENT OF IMPACTS FROM DISPOSAL AND HURRICANE GLORIA

CONTRIBUTION #57

November 1989

Report No.
SAIC-87/7516&C57

Submitted to:

Regulatory Branch
New England Division
U.S. Army Corps of Engineers
424 Trapelo Road
Waltham, MA 02254-9149

Submitted by:

J.H.Parker
E.C. Revelas
Science Applications International Corporation
Admiral's Gate
221 Third Street
Newport, RI 02840
(401) 847-4210

US Army Corps
of Engineers
New England Division

TABLE OF CONTENTS

			Page
1.0		INTRODUCTION	1
2.0		METHODS	3
	2.1	Bathymetry and Navigation	3
	2.2	Side Scan Surveys	4
	2.3	REMOTS® Sediment-Profile Photography	4
	2.4	Sediment Sampling and Analysis	5
	2.5	Benthic Community Analysis	5
	2.6	In-situ Observations	5
	2.7	Bottom-Mounted Instrumentation Array (DAISY)	6
3.0		RESULTS	6
	3.1	Bathymetry	6
	3.2	Side Scan Surveys	7
	3.3	REMOTS® Sediment-Profile Survey	8
		3.3.1 Stamford-New Haven North (STNH-N)	8
		3.3.2 Stamford-New Haven South (STNH-S)	11
		3.3.3 Cap Sites One and Two (CS-1 and CS-2)	13
		3.3.4 Mill-Quinnipiac River (MQR)	16
		3.3.5 Norwalk (NOR)	18
		3.3.6 New Haven '74 (NH-74)	19
		3.3.7 New Haven '83 (NH-83)	20
		3.3.8 Southeast CLIS (CLIS-SE)	21
		3.3.9 CLIS Transect	22
	3.4	Sediment Characteristics	22
	3.5	Benthic Community	23
	3.6	In-situ Observations	23
		3.6.1 CS-1	24
		3.6.2 CS-2	24
		3.6.3 STNH-N	24
		3.6.4 STNH-S	25
		3.6.5 Field Verification Program (FVP) Mound	25
	3.7	Bottom-Mounted Instrumentation Array (DAISY)	26
		3.7.1 Water Temperature	26
		3.7.2 Salinity	26
		3.7.3 Current Speed and Direction	27
		3.7.4 Surface Wave Characteristics	27
		3.7.5 Suspended Material Characteristics	28
4.0		DISCUSSION	29
	4.1	August Monitoring Cruise at CLIS	29
	4.2	Effects of Hurricane Gloria at CLIS	32
	4.3	Response of the Sediment-Water Interface at NLON to Hurricane Gloria	34
5.0		SUMMARY AND CONCLUSIONS	37
6.0		REFERENCES	38

LIST OF FIGURES

Figure 1-1	Central Long Island Sound (CLIS) Disposal Area.
Figure 1-2	Hurricane Gloria storm track.
Figure 2-1	Bathymetric survey lanes for Central Long Island Sound (CLIS) Disposal Site and Mounds.
Figure 1-3	Barometric pressure record at Avery Point, Groton, CT. September 24-29, 1985.
Figure 2-2	Location (X) of Instrumentation Array Deployment Site.
Figure 3-1	Contour bathymetric chart of CLIS Disposal Site, August 1985.
Figure 3-2	Contour bathymetric chart at STNH-N, October 1985.
Figure 3-3	Contour bathymetric chart at STNH-S, October 1985.
Figure 3-4	Contour bathymetric chart at MQR, October 1985.
Figure 3-5	Contour bathymetric chart at CS-1, October 1985.
Figure 3-6	Contour bathymetric chart at CS-2,October 1985.
Figure 3-7	Contour bathymetric chart at CLIS-SE with sediment stations, August 1985.
Figure 3-8	Side scan survey results at Cap Sites 1 and 2, August 1985.
Figure 3-9	Side scan survey results at CLIS-SE, August 1985. CLIS-SE survey lanes illustrate area covered by detailed bathymetric survey.
Figure 3-10	Photographs of side scan record at CLIS-SE.
Figure 3-11	A map showing the apparent distribution and thickness of dredged material, averaged by station, at the STNH-N site in August 1985.

LIST OF FIGURES (CONT.)

Figure 3-12 A REMOTS image from station 200E showing a mud/sand/mud stratigraphy apparently representing the original sand cap being mixed and covered with more recently deposited silt-clay sediments. Scale = 1X.

Figure 3-13 A REMOTS image from station 600S showing the appearance of dark reducing sediment near the sediment surface. Scale = 1X.

Figure 3-14 The frequency distributions of boundary roughness, redox potential discontinuity (RPD) depths, and Organism-Sediment Index (OSI) values for August 1985 at STNH-N.

Figure 3-15 The mapped average apparent redox potential discontinuity (RPD) depth values at each station in the August survey at STNH-N.

Figure 3-16 The mapped distribution of successional stages for all replicates in the August survey at STNH-N.

Figure 3-17 The mapped distribution of Organism-Sediment Indices (OSI) for all replicates in the August survey at STNH-N.

Figure 3-18 A post-storm benthic "process" map showing the distribution of erosional and depositional features at STNH-N.

Figure 3-19 A REMOTS image from 200N showing shell lag deposits and an exposed polychaete tube indicative of surface erosion. Scale = 1X.

Figure 3-20 The mapped distribution of post-storm redox potential discontinuity (RPD) depths at STNH-N.

Figure 3-21 The mapped distribution of post-storm infaunal successional stages at STNH-N.

Figure 3-22 The mapped distribution of post-storm Organism-Sediment Indices (OSI) at STNH-N.

Figure 3-23 A map showing the apparent distribution and thickness of dredged material, averaged by station at the STNH-S site in August 1985.

LIST OF FIGURES (CONT.)

Figure 3-24 The frequency distributions of boundary roughness, redox potential discontinuity (RPD) depths, and Organism-Sediment Index (OSI) values for August 1985 at STNH-S.

Figure 3-25 The mapped average apparent redox potential discontinuity (RPD) depth values at each station in the August survey at STNH-S.

Figure 3-26 The mapped distribution of successional stages for all replicates in the August survey at STNH-S.

Figure 3-27 The mapped distribution of Organism- Sediment Indices (OSI) for all replicates in the August survey at STNH-S.

Figure 3-28 A post-storm benthic "process" map showing the distribution of erosional and depositional features at STNH-S.

Figure 3-29 A-B REMOTS images from stations 25W and 25E respectively, showing mud clasts, exposed worm tubes, surface shell lag deposits, and reduced sediment patches near the interface. Scale = 1X.

Figure 3-30 A REMOTS image from station 600E showing a physically disturbed bottom. Scale = 1X.

Figure 3-31 The mapped distribution of post-storm apparent mean redox potential discontinuity (RPD) depths at STNH-S.

Figure 3-32 The mapped distribution of post-storm successional stages at STNH-S.

Figure 3-33 The mapped distribution of post-storm Organism-Sediment Indices (OSI) at STNH-S.

Figure 3-34 A map showing the apparent distribution and thickness of dredged material, averaged by station, at Cap Site 1 in August 1985.

Figure 3-35 A map showing the apparent distribution and thickness of dredged material, averaged by station at Cap Site 2 in August 1985.

Figure 3-36 A-B Two REMOTS images from Cap Site 2 station 200W showing silt-clay layers overlying the original sand cap. Scale = 1X.

LIST OF FIGURES (CONT.)

Figure 3-37 A REMOTS image from Cap Site 2 station CTR showing a fine-sand layer at the surface along with disarticulated bivalve shells. Scale = 1X.

Figure 3-38 A REMOTS image from Cap Site 2 station 600S showing dredged material. Scale = 1X.

Figure 3-39 A-B REMOTS images from Cap Site 1 station 200E (A) and Cap Site 2 station 200W (B) showing reduced sediment patches near the sediment surface. Scale = 1X.

Figure 3-40 The frequency distribution of boundary roughness, redox potential discontinuity (RPD) depths, and Organism-Sediment Index (OSI) values at Cap Site 1 for August 1985.

Figure 3-41 The frequency distributions of boundary roughness, redox potential discontinuity (RPD) depths, and Organism-Sediment Index (OSI) values at Cap Site 2 for August 1985.

Figure 3-42 The mapped mean apparent redox potential discontinuity (RPD) depth values (cm) at each station at Cap Site 1 in the August survey.

Figure 3-43 The mapped mean apparent redox potential discontinuity (RPD) depth values (cm) at each station at Cap Site 2 in the August survey. REMOTS photos were not successfully obtained at station 200NE.

Figure 3-44 The mapped distribution of successional stages for all replicates at Cap Site 1 in the August survey.

Figure 3-45 The mapped distribution of successional stages for all replicates at Cap Site 2 in the August survey. REMOTS photos were not successfully obtained at station 200NE.

Figure 3-46 The mapped distribution of Organism- Sediment Indices (OSI) for all replicates at Cap Site 1 in the August survey.

Figure 3-47 The mapped distribution of Organism- Sediment Indices (OSI) for all replicates at Cap Site 2 in the August survey. REMOTS photos were not successfully obtained at station 200NE.

Figure 3-48 A post-storm benthic "process" map of Cap Site 1 showing the distribution of erosional and depositional features.

Figure 3-49 A REMOTS image from Cap Site 1 station 25S showing shell lag deposits and mud clasts.

Figure 3-50 A REMOTS image from Cap Site 1 station 200E showing fine sand sediments over-lying silt-clay. Scale = 1X.

Figure 3-51 A post-storm benthic "process" map of Cap Site 2 showing the distribution of erosional and depositional features. Scale = 1X.

Figure 3-52 A-B REMOTS images from Cap Site 2 station 200S pre-storm (A) and station 200S post-storm, (B) showing the increase of coarse-grained sediments from August to October. Scale = 1X.

Figure 3-53 The mapped distribution of post-storm average apparent redox potential discontinuity (RPD) depth values at Cap Site 1. A REMOTS photo was not successfully obtained at station 25N.

Figure 3-54 The mapped distribution of post-storm average apparent redox potential discontinuity (RPD) depth values at Cap Site 2.

Figure 3-55 The mapped distribution of post-storm successional stages at Cap Site 1. A REMOTS photo was not successfully obtained at station 25N.

Figure 3-56 The mapped distribution of post-storm successional stages at Cap Site 2.

Figure 3-57 The mapped distribution of post-storm Organism-Sediment Indices (OSI) at Cap Site 1. A REMOTS photo was not successfully obtained at station 25N.

Figure 3-58 The mapped distribution of post-storm Organism-Sediment Indices (OSI) at Cap Site 2.

Figure 3-59 The frequency distribution of boundary roughness, redox potential discontinuity (RPD), and Organism-Sediment Index (OSI) values for the August survey at MQR.

LIST OF FIGURES (CONT.)

Figure 3-60 The mapped distribution of apparent redox potential discontinuity (RPD) depth values at the MQR site in August. REMOTS images were not obtained at stations where no values are indicated.

Figure 3-61 The mapped distribution of successional stages for all replicates at the MQR site in August. REMOTS images were not obtained at stations where no values are indicated.

Figure 3-62 The mapped distribution of Organism-Sediment Indices (OSI) values for all replicates at the MQR site in August. REMOTS images were not obtained at stations where no values are indicated.

Figure 3-63 A post-storm benthic "process" map showing the distribution of erosional and depositional features.

Figure 3-64 A post-storm REMOTS image from station 200N showing a smooth bottom colonized by a Stage I assemblage. Scale = 1X.

Figure 3-65 The mapped distribution of post-storm redox potential discontinuity (RPD) depths (cm) at MQR. A REMOTS photo was not successfully obtained at 1000E.

Figure 3-66 The mapped distribution of post-storm infaunal successional stages at MQR. A REMOTS photo was not successfully obtained at 1000E.

Figure 3-67 The mapped distribution of post-storm Organism-Sediment Indices (OSI) at MQR. A REMOTS photo was not successfully obtained at 1000E.

Figure 3-68 A REMOTS image from August, station 200W, showing reduced sediment patches near the interface.

Figure 3-69 The frequency distribution of boundary roughness,redox potential discontinuity (RPD) depths, and Organism-Sediment Index (OSI) values for August 1985 at Norwalk.

Figure 3-70 The mapped average apparent redox potential discontinuity (RPD) depth values at each station in the August survey at Norwalk.

LIST OF FIGURES (CONT.)

Figure 3-71 The mapped distribution of successional stages for all replicates in the August survey at Norwalk.

Figure 3-72 The mapped distribution of Organism- Sediment Indices (OSI) for all replicates in the August survey at Norwalk.

Figure 3-73 The frequency distribution of boundary roughness, redox potential discontinuity (RPD) depths, and Organism-Sediment Index (OSI) values for August, 1985 at NH-74.

Figure 3-74 The mapped average apparent redox potential discontinuity (RPD) depth values (cm) at each station in the August survey at NH-74.

Figure 3-75 The mapped distribution of successional stages for all replicates in the August survey at NH-74.

Figure 3-76 The mapped distribution of Organism- Sediment Indices (OSI) for all replicates in the August survey at NH-74.

Figure 3-77 The frequency distribution of boundary roughness, redox potential discontinuity (RPD) depths, and Organism-Sediment Index (OSI) values for the August survey at NH-83.

Figure 3-78 The mapped average apparent redox potential discontinuity (RPD) depth values (cm) for all replicates in the August survey at NH-83.

Figure 3-79 The mapped distribution of infaunal successional stages for all replicates in the August survey at NH-83.

Figure 3-80 The mapped distribution of Organism-Sediment Index (OSI) values for all replicates in the August survey at NH-83.

Figure 3-81 The frequency distribution of boundary roughness, redox potential discontinuity (RPD) depths, and Organism-Sediment Index (OSI) values for the August survey at CLIS-SE.

Figure 3-82 The mapped distribution of average apparent redox potential discontinuity (RPD) depth values (cm) for all replicates in the August survey at CLIS-SE.

LIST OF FIGURES (CONT.)

Figure 3-83 The mapped distribution of infaunal successional stages for all replicates in the August survey at CLIS-SE.

Figure 3-84 The mapped distribution of Organism-Sediment Indices (OSI) for all replicates in the August survey at CLIS-SE.

Figure 3-85 A grain-size and benthic "process" map of the post-storm CLIS Transect. Major modal grain-size in phi units are indicated for each station.

Figure 3-86 A-B Two post-storm REMOTS images from stations T-3 and T-6 respectively, showing shell lag deposits and mud clasts indicative of bottom disturbance. Scale = 1X.

Figure 3-87 Near-bottom water temperature, Eastern Long Island Sound, September 1985.

Figure 3-88 Near-bottom salinity, Eastern Long Island Sound, September 1985.

Figure 3-89 Near-bottom current speed, Eastern Long Island Sound, September 1985.

Figure 3-90 Near-bottom current direction, Eastern Long Island Sound, September 1985.

Figure 3-91 Spectral plot of near-bottom pressure at New London Disposal Area, 27 September 1985.

Figure 3-92 Near-bottom suspended material concentrations, Eastern Long Island Sound, September 1985.

Figure 4-1 Observed grain-size (in phi units) along REMOTS transect extending from New Haven Harbor entrance to the CLIS-REFERENCE site.

Figure 5-1 Pre and post-storm REMOTS images from station CTR at the FVP site. In June(left), a high reflectance, sandy surface layer is evident at the interface. After the hurricane (right), this layer is no longer apparent, indicating that approximately 5 cm of material has been removed. Scale = 0.65X.

LIST OF FIGURES (CONT.)

Figure 5-2 Pre and post-storm REMOTS images from station 400S at the FVP site. In June (left), a well-developed Redox Potential Discontinuity layer (high reflectance) is evident. After the hurricane (right), much of this oxygenated material is no longer apparent and an exposed worm tube is evident at the interface, indicating the net loss of surface sediments. Scale = 0.65X.

LIST OF TABLES

Table 2-1	Summary of Diver Survey Operations at the CLIS Site.
Table 3-1	Volume Difference Calculations for CLIS Disposal Sites in August and October 1985.
Table 3-2	Central Long Island Sound Disposal Site Results of Chemical Analysis of Sediment CLIS-SE.
Table 3-3	Benthic Community Analysis at CLIS-SE, August 1985.
Table 3-4	Summary of Megafaunal Species and Relative Abundances Observed During Survey Dives Conducted at the CLIS Site.
Table 3-5	Local Climatological Data - Monthly Summary.
Table 4-1	Comparison Chart of Selected Chemical Concentrations, CLIS-SE with CLIS-REF.
Table 4-2	Summary Statistics for Boundary Roughness Values, Redox Potential Discontinuity Depths, and Organism-Sediment Indices at the CLIS Disposal Sites in August and October 1985.
Table 4-3	Estimates of the Extent of Erosion 25 at the CLIS Disposal Sites Based on the Loss of High-reflectance Surface Sediments (Redox layer).

1.0 INTRODUCTION

The Central Long Island Sound (CLIS) disposal site (Figure 1-1) has been under study by the New England Division (NED) since 1974. Several experiments have been conducted at the CLIS site to assess the impact of dredged material disposal on the surrounding environment and to determine the effectiveness of capping contaminated dredged material.

Monitoring efforts have continued throughout the DAMOS program to document recolonization of the site as well as document changes in the sediment characteristics. The field operations conducted at the Central Long Island Sound disposal site in August, 1985 were designed to accomplish the following objectives:

- assess the impact of previous dredged material disposal operations (with special emphasis on the MQR mound) and
- characterize the southeast quadrant of CLIS, in terms of sediment type and possible presence of dredged material, in order to identify a location for future experiments that will not be influenced by dredged material disposal elsewhere at CLIS.

The tasks required to accomplish these objectives included precision bathymetry, REMOTS® sediment-profiling, side scan sonar, sediment sampling for physical, chemical, and biological analysis, and visual observations.

With the occurrence of Hurricane Gloria in September 1985, additional field studies were performed to address the following objectives:

- verify the containment qualities of the CLIS disposal site after exposure to storm conditions and assess the stability of the disposal mounds. This was accomplished with precision bathymetric surveys and REMOTS® sediment-profiling at STNH-N, STNH-S, CS-1, CS-2, and MQR disposal mounds in October.
- document the physical interaction between the water column and disposed dredged material in Long Island Sound before, during, and after the passage of the storm. This task was accomplished by deploying a bottom-mounted instrument array known as the Disposal Area In-situ System (DAISY) at the New London (NLON) disposal site.

The passage of Hurricane Gloria in September provided a rare opportunity to document any significant storm-associated changes in the characteristics of the disposal mounds at the CLIS site as well as to monitor the response of the sediment-water

interface at the NLON site. To obtain these real-time observations at NLON, the DAISY array was deployed shortly before the forecasted storm arrival and maintained on station for approximately 9 days. Analysis of this data set provided a detailed picture of the effects of storm passage on the sediment transport system in the vicinity of a dredged material disposal site. The relative infrequency of major storms makes this data set unique within the realm of DAMOS observations.

Maximum near-surface current speeds in the vicinity of the NLON disposal site equal approximately 70 cm/sec on the westerly flood and 95 cm/sec on the easterly ebb (NOS, 1985). Freshwater streamflows entering from the Thames River produce some seasonal variations in salinity structure and associated vertical density gradients but generally represent a minor determinant within the local circulation system.

Winds affecting the area display a regular seasonal variability with southwesterlies dominating during the late spring, summer, and early fall and northwesterlies prevailing during the winter. Major storms affecting the area tend to be dominated by winds rich in easterly components. Such events can occur at any time during the year but are most common in the early fall and late winter-early spring.

Hurricane Gloria developed first as a tropical storm in the North Atlantic adjacent to the Cape Verde Islands and then tracked to the northwest towards the continental United States and intensified. As the storm approached the Virgin Islands, it reached hurricane intensity and slowly veered to the north along a crescent-shaped path approximately paralleling the U.S. coastline (Figure 1-2). On its track along the coast, the storm continued to increase in strength with barometric pressures at the center of the storm falling below 919 millibars (27.15 inches). As it approached Cape Hatteras, the storm was reported to have the potential to be the most dangerous storm of the century.

On the morning of 27 September 1985, the storm passed offshore of Norfolk, Virginia and continued along a slightly west of north track towards the south shore of Long Island. Barometric pressures at this point were approximately 984 millibars (29.05 inches) having risen slightly from the minimum. Estimated maximum wind speeds equalled approximately 193 km/h (120 mph). The storm tracked quickly to the north at speeds of 32 to 48 km/h (20 to 30 mph) and passed over Fire Island, 64 km (40 miles) to the east of Manhattan, shortly after noon. After crossing Long Island, the speed of advance increased with the storm moving quickly along a west of north track across Connecticut and into Massachusetts and then New Hampshire where it rapidly dissipated.

Reviews of the available data from the National Weather Service station at Bridgeport and the meteorological station

maintained at the University of Connecticut's Marine Sciences Institute at Avery Point in Groton, Connecticut indicate that the primary effects associated with the passage of Gloria were relatively shortlived and essentially confined to a approximately two hour period between 1300 and 1500 EDST on 27 September 1985. The winds during this period were from the south to southeast with an observed maximum speed at Avery Point of approximately 140 km/h (87 mph). At all local stations, detailed observations during the height of the storm were lost due to widespread power outages. Minimum barometric pressures were just below 982 millibars (29.0 inches, Figure 1-3).

2.0 METHODS

2.1 Bathymetry and Navigation

The precise navigation required for all field operations was provided by the SAIC Integrated Navigation and Data Acquisition System (INDAS). A detailed description of INDAS and its operation can be found in Contribution #60 (SAIC, 1986). Positions were determined to an accuracy of ±3 meters from ranges provided by a Del Norte Trisponder System. Shore stations were established over known benchmarks at Stratford Light and Lighthouse Point Light.

The depth was determined to a resolution of 0.1 feet (3.0 cm) using a Raytheon DE-719 Precision Survey Fathometer with a 208 kHz transducer. The fathometer was calibrated with a bar check at fixed depths below the transducer before the survey began. A Raytheon SSD-100 Digitizer was used to transmit the depth values to the SAIC computer system.

During analysis of the bathymetric data, the raw depth values were standardized to Mean Low Water by adjusting for ship draft and for tidal changes for the duration of the survey. All data points in terms of depth and position were checked for unreasonable values due to any malfunctions with the peripheral instrumentation (navigation or bathymetry) so that the final contour plots did not contain errors.

Precision bathymetric surveys were conducted in August at the ten disposal mounds contained within the CLIS disposal site (Figure 2-1). The surveys were designed to cover the areas of the disposal mounds so that volume changes could be calculated by comparison with future surveys. Surveys at the individual mounds were conducted at a 25 m lane spacing for detecting small changes in depth; in addition, a survey of the entire CLIS site was performed at a 50 m lane spacing. In October, identical surveys were conducted at the STNH-N, STNH-S, MQR, CS-1, CS-2, and FVP mounds so that any changes in depth and volume calculations would indicate whether erosion or deposition had occurred.

2.2 Side Scan Surveys

In August, side scan surveys were conducted in the area of CS-1 and CS-2 to assess the distribution of dredged material deposited during the last year; an additional survey was performed at the southeast quadrant of the CLIS site (CLIS-SE) to determine baseline conditions should locations in this area be used for future dredged material disposal points.

The surveys were conducted using a Klein Side Scan Sonar System along surveys lanes spaced at 100 m intervals to allow complete coverage of the seafloor. A detailed description of the Klein side scan system is presented in DAMOS Contribution #48. (SAIC, 1985).

2.3 REMOTS® Sediment-Profile Photography

REMOTS® images were taken with a Benthos Model 3731 Sediment-Profile Camera (Benthos, Inc. North Falmouth, MA). The REMOTS® camera is designed to obtain in-situ profile images of the top 15-20 cm of sediment. A detailed description of REMOTS® camera operation and image analysis is presented in DAMOS Contribution #60 (SAIC, 1986).

The purpose of the August 1985 REMOTS® surveys of the CLIS disposal mounds was to monitor the potential change in the sedimentary characteristics of the dredged material mounds, to document the process of successional recovery of the disposal mounds, and to monitor changes in the ambient fauna and sediments adjacent to the mounds. To accomplish this, surveys were performed at the STNH-N, STNH-S, CS-1, CS-2, MQR, NOR, NH-74, and NH-83 mounds; prior surveys at these mounds had been carried out in September 1984. In addition, sediment-profile photographs were obtained at the new CLIS-SE location.

Approximately one month after the hurricane, REMOTS® surveys were again performed at the same six CLIS disposal mounds as the precision bathymetry: STNH-N, STNH-S, CS-1, CS-2, MQR, and FVP. In the analysis of these post-storm surveys, special emphasis was placed on the detection of erosional/depositional features. Moreover, the temporal proximity of the pre- and post-storm surveys allowed assessment of the storm's effects on benthic conditions at each mound.

Finally, ten REMOTS® stations extending from the New Haven harbor entrance to the CLIS disposal site were surveyed to evaluate the regional distribution of sediment erosion as a function of depth and distance from shore.

2.4 Sediment Sampling and Analysis

Triplicate sediment samples were collected at three stations, the CLIS-SE area, and at the CLIS Reference station in August using a 0.1 m^2 Smith-McIntyre Grab Sampler. The samples were kept cold and returned to the NED laboratory where they were stored at 4C until analyzed. Parameters measured included grain size, trace metals, and several organic constituents.

Sediment analyses were conducted using methods described by the U.S. Environmental Protection Agency (Plumb, 1981). Mercury analysis was performed using acid digestion and cold vapor atomic absorption spectrophotometry; arsenic analysis was accomplished using acid digestion and gaseous anhydride atomic absorption spectrophotometry. The other trace metals (As, Pb, Zn, Cr, Cu, Cd, and Ni) were analyzed using acid digestion and flame atomic absorption spectrophotometry.

Carbon, hydrogen, and nitrogen analyses were conducted with an autoanalyzer using a combustion technique. Oil and grease measurements were made by extracting the sediment with freon and then analyzing the freon by infrared spectrophotometry. PCBs were extracted with hexane and also analyzed by electron capture gas chromatography.

2.5 Benthic Community Analysis

During the August survey, triplicate sediment samples were collected with a Smith-McIntyre grab sampler (0.1 m^2) at three stations at CLIS-SE and sieved to 0.5mm for analysis of the benthic community and comparison with triplicate samples collected at the CLIS Reference station.

In the laboratory, the samples were soaked in rose bengal stain for 24 hours to provide contrast between animals and detritus. Clean sandy or shelly samples were sorted in glass trays under bright lights and with contrasting backgrounds. If organic detritus was present, it was separated by elutriation and sorted under a dissecting microscope. Animals were identified under a dissecting microscope, counted, and preserved in alcohol. Sieve residue was labeled and archived. Standard reference works and some unpublished studies in preparation for the NOAA series "Marine Flora and Fauna of the Northeastern United States" were used to identify the specimens.

2.6 In-situ Observations

During the August survey, visual observations were performed by a team of diver/scientists from SAIC and the University of Connecticut familiar with the underwater features of the CLIS disposal site, including the resident epifauna, benthic

community, and sediment textural characteristics. Photodocumentation was conducted using 35mm still camera apparatus. A diver-operated epibenthic net was utilized to sample the smaller species in abundance along the photo transects. Table 2-1 presents a summary of the dives conducted at CLIS. The Appendix presents photographs from the diver transects at each mound.

2.7 Bottom-mounted Instrumentation Array (DAISY)

The bottom-mounted instrumentation array deployed at the NLON disposal site was similar in character to those used previously within the DAMOS Program. The array contained a variety of instruments including a two-axis electromagnetic current meter, two optical transmissometers to monitor suspended material concentrations, temperature-conductivity probes, and a tide and wave gage. Logic control and data recording were provided by a digital data logger. All data were recorded on magnetic tape cassettes which later were converted into standard IBM compatible format for analysis.

All array instruments were attached to an aluminum framework configured to sample conditions at points approximately 1 m above the sediment-water interface. With the exception of the wave gage, all primary array components were sampled four times each hour for a period of 3 minutes and 10 seconds. The wave gage was sampled twice each hour over periods of approximately 17 minutes each. This sampling provided 4096 wave measurements and 4 measurements of concurrent tidal amplitude. The wave gage and the primary data logger operated from independent time bases. No attempt was made to provide a common standard.

The bottom-mounted instrumentation array was located along the southern margin of the New London disposal site (Figure 2-2). Pre-deployment bathymetric surveys indicated that the depth contours in the area were relatively smooth and gave little indication of obstructions sufficient to affect the near-bottom flow regime. Water depth at the deployment station was approximately 25 meters. Sediments were predominantly fine-grained sandy silts containing moderate concentrations of organic materials. There was no evidence of recent dredged material disposal at the deployment location.

3.0 RESULTS

3.1 Bathymetry

Results of the analysis of the large bathymetric survey (50 m lane spacing) covering the entire CLIS site (Figure 3-1) indicated the location of the ten disposal mounds. Comparison with the same survey conducted in September 1984 did not reveal any large-scale changes in the bottom topography. The surveys at the

individual disposal mounds (25 m lane spacing) were conducted to detect more detailed changes in bottom topography. The results of the bathymetric surveys conducted in October at STNH-N, STNH-S, MQR, CS-1, and CS-2 (Figures 3-2 to 3-6) were compared with those conducted in August to calculate any changes in the volume of dredged material present (Table 3-1). The volume of dredged material at the Field Verification Program (FVP) disposal mound comparing the August survey with the October survey is also included (results from investigations at the FVP mound are discussed separately in DAMOS Contribution #52). The CS-1 mound was the only one which experienced a detectable loss of material (15,390 m^3 ± 3,660; insignificant given the total area of the survey). Because no significant changes in depth at the individual mounds was evident, only the October contour plots are presented in this report.

The results of the August bathymetric survey at the CLIS-SE location (Figure 3-7) showed a relatively flat bottom topography gently sloping to the south with depths from 20.4 to 21.4 meters.

3.2 Side Scan Surveys

The results of the side scan survey at CS-1 and CS-2 (Figure 3-8) showed areas of high acoustic reflectance indicating the mounds of dredged material as well as some isolated patches in the surrounding area that could have been dredged material. The demarcation line in the figure indicates where natural bottom occurred to the west beyond the boundary of the disposal site; the region of intermediate reflectance in the eastern portion of the survey most likely reflects the general area affected by disposal operations.

The results of the side scan survey conducted at the southeast quadrant of CLIS (Figure 3-9) showed areas of high acoustic reflectance located on the western portion of the survey area representing dredged material disposed at the Stamford-New Haven South (STNH-S) disposal mound. The demarcation line indicates where intermediate reflectance occurred along the western edge of the survey area due to dredged material from previous activity at the SP buoy, NH-74, and STNH-N disposal mounds. The area chosen as CLIS-SE (to the east of the demarcation line) was clear of dredged material and sufficiently far from potential interference from the existing dredged material at STNH-S and FVP to the north. A representative portion of the side scan record from the survey at CLIS-SE (Figure 3-10a) showed the relatively "clean" (i.e., lack of any reflective targets) gently sloping bottom. A section of the side scan record from the western portion of the survey area near STNH-S (Figure 3-10b) illustrates the high reflectivity normally attributed to dredged material; these areas of high reflectance did not occur in the CLIS-SE area.

3.3 REMOTS® Sediment-Profile Survey

Results from 1985 pre and post-Hurricane Gloria surveys at the FVP mound are outlined separately in DAMOS Contribution #52. Results from investigations at the remaining disposal mounds at the CLIS site are discussed individually in the sections which follow.

3.3.1 Stamford-New Haven North (STNH-N)

August Survey

REMOTS® surveys have been carried out at the STNH-N disposal mound in January and August 1983, and again in September 1984. Nine stations located on a cross-shaped grid were occupied in each of those surveys. On 9 August 1985, a survey was carried out on a larger grid consisting of 17 stations (Figure 3-11). Three REMOTS® images were taken at each N, S, E, and W station, while a single image was obtained at each corner station (e.g., 200NW).

Although the STNH-N disposal mound was originally capped with a sand layer, most stations (37 of 43 replicates) now exhibited a grain size major mode of >4 phi (coarse silt to clay-sized particles). All images from stations CTR, 200S, and one image at 200W showed a grain-size major mode of very-fine sand. Two replicates at station 200E revealed a mud/sand/mud stratigraphy (Figure 3-12); this apparently represents the original sand cap being both bioturbated and covered with more recently deposited silt-clay sediments. Coarse sediments and evidence of scour were observed at stations CTR and 200E in the last report. The images from the August 1985 survey did not show evidence of scour. One replicate from station CTR showed the presence of fecal mounds at the surface, suggesting that low kinetic conditions periodically existed at this station.

The mapped distribution of apparent dredged material (Figure 3-11) showed the thickness of apparent dredged material exceeding the penetration depth of the camera prism (20 cm) at several stations. In general, this mound was intensively bioturbated. Biogenic mixing of sediments made it difficult to identify a distinct pre-disposal horizon, because this mixing process had "erased" the pre-disposal stratum.

Patches of highly reduced sediment were evident near the sediment surface at 82% of the STNH-N stations (Figures 3-11 and 3-13). The origin of this material is unknown, but its occurrence suggests redistribution of reduced sediment either laterally through erosion or vertically through bioturbation. Similar reduced sediment patches were evident in varying levels of abundance at all of the CLIS and WLIS disposal mounds surveyed in

August 1985. Moreover, in June 1985, reduced sediments were evident at the interface throughout the FVP mound. This recent, widespread appearance of highly reduced sediments near the sediment-water interface indicated these sediments were potentially being redistributed about the seafloor either by bottom currents (unlikely given past current meter measurements) or other disturbance factors (e.g., trawling, megafaunal bioturbation). The extremely patchy nature of this reduced material, both within an image and between images, suggests a biological cause. It is difficult to envision a physical disturbance mechanism which would produce such a distribution of reduced materials. Conversely, biological activity, such as decapod foraging and burrow excavation, could easily result in the upward movement of isolated clumps of highly reduced subsurface sediments.

The boundary roughness (the vertical range of small-scale topographic relief observed in the REMOTS® images) frequency distribution (Figure 3-14) displayed a modal value of 0.4 cm (reduced from 0.8 cm in August 1983). This is attributed to the progressive "smoothing" of the surface both by currents and biogenic reworking. Similar decreases in small-scale boundary roughness have been noted at other DAMOS sites following disposal operations.

The frequency distribution of apparent Redox Potential Discontinuity (RPD) depths (a measure of the apparent depth of aerobic sediment which is indicative of bioturbation activity, Figure 3-14) indicated the majority of RPD values fell within a range of 2 to 5 cm. In the last REMOTS® survey (September 1984), the distribution exhibited a distinct major mode centered at 4.0 cm. The shallowest RPD depths during this survey were found at station CTR (Figure 3-15). Much of the variation in the RPD values seen in the frequency distribution was the result of within-station variability rather than between-station variability, due to the presence of the near-surface patches of reduced sediment in many images.

The mean RPD depth at STNH-N (3.98) and all the CLIS disposal mounds was deeper than at the CLIS-REF station (2.8 cm). The exact reason for the anomalously thin apparent redox at the CLIS-REF station is unknown. However, in the June 1985 survey of the FVP Mound, the CLIS-REF station showed a distinct successional "retrograde" condition with a progressive loss of Stage III infauna. One possible mechanism for this is the intensive sediment and benthic sampling that has been done at this location by the EPA Narragansett Environmental Research Laboratory since 1982.

Based on the theory that organism-sediment interactions follow a predictable sequence after a major seafloor perturbation, the designation of successional stage from REMOTS® image analysis indicates the functional group of infauna present at any particular

location. A Stage III-I designation indicates the presence of Stage I organisms on Stage III. Stage III seres (Figure 3-16) predominated at this mound (79% of the station replicates). This compared with 65% in September 1984 and 82% in August 1983. This mound has exhibited a relatively high-order successional assemblage since the initiation of the REMOTS® monitoring program in 1983.

The frequency distribution of Organism-Sediment Index (OSI) values (a summary statistic based on the RPD and successional stage, Figure 3-14) showed that most of the figures from August were above +7 with a major mode of +11. The spatial distribution of OSI values at this mound (Figure 3-17) showed relatively high values spread over the entire area surveyed, reflecting the relatively deep RPD values and the abundance of Stage III infauna.

Post Storm Survey

A REMOTS® survey of ten stations (Figure 3-18) at the STNH-N disposal mound was performed on 1 November, approximately one month after Hurricane Gloria. The effects of the hurricane on the STNH-N disposal mound were clearly evident in the REMOTS® images. The "process" map of STNH-N (Figure 3-18) includes any erosional or depositional information obtained from the REMOTS® images. These features include mud clasts, shell lag deposits, exposed worm tubes, and bedforms (Figure 3-19). Erosional features were evident at all stations except for 200W. At stations 200N, 25W, 25E, and 200S, the extent of this erosion was estimated by measuring the distance that large worm tubes extend above the interface. These taxa characteristically build their tubes to the level of the sediment-water interface. The sudden removal of surface sediments resulted in these tubes being exposed above the interface. As a result, a minimum depth of material removed could be estimated. Approximately 0.5 cm of material was scoured from the central portion of the disposal mound (Figure 3-18). It is unknown whether or not this erosion represented a net loss of sediment from this region. Distinct depositional layers were not evident in any post-storm images.

Small-scale topographic relief increased significantly since the August survey (Mann-Whitney U-test, $p = 0.0154$). This increase was due to the presence of bedforms and scour surfaces, results of the disturbance produced by Hurricane Gloria.

The post-storm RPD depths at STNH-N (Figure 3-20) were significantly shallower than those observed in August 1985 (compare with Figure 3-15; Mann-Whitney U-test, $p < 0.001$). This decrease was evidently due to the disturbance and erosion of the surface sediments caused by Hurricane Gloria. The shallowest RPD values were concentrated near the center of the disposal mound. This

suggested the top of this topographic feature was more severely disturbed than the surrounding seafloor.

In August, Stage III infauna were evident throughout the mound (Figure 3-16). Evidence of these high-order successional stages (Figure 3-21) was lacking at several stations (25E, 25W, 25S, 200S, and 600E) in the November survey. These stations were concentrated near the center of the mound and indicated greater physical disturbance in that region. The lack of Stage III infauna at station 600E, however, indicated that the surrounding seafloor was also affected.

The post-storm OSI values (Figure 3-22) were significantly lower than those observed in August (compare with Figure 3-17; Mann-Whitney U-test, $p < 0.001$). The low OSI values reflected both the shallower RPD values and the retrograde successional status. Overall, the STNH-N disposal mound, previously one of the most successfully recolonized CLIS disposal mounds, had been markedly disturbed by Hurricane Gloria.

3.3.2 Stamford-New Haven South (STNH-S)

August

The STNH-S disposal mound was surveyed in January and August 1983 and in September 1984. These three surveys consisted of 11 stations located on a cross-shaped sampling grid. On 13 August 1985, a REMOTS® survey was performed on an expanded sampling grid identical to the grid used at STNH-N (Figure 3-23).

No change in the major modal grain-size was detected in this survey. As documented in earlier surveys, all stations had a major textural mode of >4 phi (silt-clay) with admixtures of very fine sand.

A visible pre-disposal datum allowed the measurement of dredged material thickness at many stations (Figure 3-23). An area to the southeast consisting of five stations (400E, 600E, 200SE, 400S, and 600S) did not show evidence of the deposition of dredged material. These stations showed high-reflective, thoroughly bioturbated bottom sediments. Reduced sediment was found at or near the surface at 47% of the STNH-S stations (Figure 3-23).

The frequency distribution for boundary roughness (Figure 3-24) displayed values which were not significantly different from those found in September 1984.

The major mode of apparent RPD depths (Figure 3-24) in September 1984 was centered at 4.0 cm, while the major mode recorded for this survey was 3.0 cm. The mapped RPD values (Figure

3-25) showed the highest values located to the east of station CTR at stations 200NE, 200E, 400E, and 200SE.

The mapped successional seres (Figure 3-26) indicated the western limb of the cross-shaped grid and stations 200NW, 200S and 200SW apparently lacked well-developed Stage III seres. This also was noted in the September 1984 report. The exact reason for this persistent low successional status is unknown; however, it may be related to the proximity of the New Haven '83 (NH-83) disposal mound.

The major mode of OSI values (Figure 3-24) was at the +7 class interval. In the September 1984 survey, the distribution was bimodal with equal values falling within the +7 modes and the +11 mode. The western side of the grid exhibited relatively low OSI values (Figure 3-27) largely reflecting the low-order successional status of this region.

Post Storm Survey

On 1 November, a post-storm REMOTS® survey was performed at the STNH-S disposal mound. This survey consisted of ten stations in the same configuration used at STNH-N (Figure 3-28).

Evidence of recent sediment disturbance was apparent throughout the survey area (Figure 3-29). Images revealed surface shell lag deposits, mud clasts, exposed worm tubes, and reduced sediment patches near the interface (Figure 3-29). Although the off-mound station, 600E, showed some evidence of disturbance, fewer obvious erosional features were evident (Figure 3-30). Estimates of the amount of surface erosion, based on exposed worm tubes, ranged from 0.30 cm to 0.41 cm. This was comparable to erosion estimates obtained at STNH-N.

Post-storm RPD depths at STNH-S (Figure 3-31) were significantly shallower than August values (Mann-Whitney U-test, $p < 0.001$). As at STNH-N, this decrease in RPD depths was apparently due to the physical disturbance caused by the storm. The central portion of the mound exhibited the most dramatic reductions in RPD depths. At station CTR, the apparent RPD decreased from 3.59 cm to 0.71 cm. The off-mound station, 600E, showed the smallest RPD change. As at STNH-N, this suggested that the ambient seafloor was less severely disturbed than the topographically elevated disposal mound.

Unlike the pattern at STNH-N, there was no marked change in the infaunal successional status of the mound since the August survey (Figure 3-32). At that time, the western side of the mound exhibited low-order successional assemblages relative to the rest of the region; this same pattern continued in November. It is noteworthy that the apparently storm-induced retrograde

successional condition observed at STNH-N was not apparent at STNH-S. This may be an artifact of the relatively small sample sizes of these post-storm mound surveys.

The post-storm Organism-Sediment Index values for STNH-S (Figure 3-33) did not change significantly between August and November (Mann-Whitney U-test, $p = 0.5213$). There was no clear difference in the OSI values from on and off the disposal mound. The distribution of OSI values continued to indicate a patchy and relatively disturbed benthic environment. The lack of significant change due to Hurricane Gloria may be related to the mound's relatively "disturbed" pre-storm condition.

3.3.3 Cap Sites One and Two (CS-1 and CS-2)

August Survey

These two experimental capping locations are located on the western edge of the Central Long Island Sound disposal site. A baseline REMOTS® survey was completed in April 1983. In May 1983, Black Rock harbor sediment was barged to these two locations, and two disposal mounds were produced. CS-1 was capped with silt-clay material, while CS-2 was covered with sand. A post-disposal reconnaissance REMOTS® survey was conducted in June 1983 to map the dispersal of the dredged material and the thickness of capping materials. Subsequent REMOTS® surveys were conducted in August 1983 and September 1984. In August 1985, these mounds were again surveyed (Figures 3-34 and 3-35).

CS-1 stations showed a major textural mode at >4 phi (silt-clay), with a range of >4-3 phi (silt to very fine sand) at all stations; the only exception was station 600N which had a major mode of 4-3 phi (very fine to fine sand). This station was apparently located on the southern flank of the sand cap placed on CS-2 (100S). The sediment grain-size major mode and range for CS-1 stations had not changed since the August 1983 survey.

The sand cap at CS-2 initially consisted predominantly of 4-3 phi material. In the last REMOTS® survey (September, 1984), the sand was still apparent but it appeared to be partially covered with silt-clay (>4 phi). The burial and admixture of the sand with mud was attributed both to bioturbation (bringing underlying Black Rock material upward from below) and to the deposition of fine-grained sediments and detritus from the water column. This survey found that these processes were continuing. A distinct surface sand cap was not apparent at most stations. Many images revealed a major grain-size mode of >4 phi (silt-clay). Two replicates from station 200W showed silt-clay layers 4.5 and 6.5 cm thick overlying the original sand cap (Figure 3-36). This would have represented a net sedimentation rate of 2 to 3 cm/yr (June 1983 to August 1985; a period of 26 months). This high sedimentation rate may have been specific to the western side of

the mound. The August 1983 report described the accumulation of a thin surface mud layer at 5 stations located on the western side of the central mound. This phenomena was interpreted as a potential "lee-side" effect, i.e., a low kinetic area related to the interaction of the flow field with the geometry of the disposal mound. Fine-sand (3-2 phi) was found at the surface of station CTR along with disarticulated bivalve shells (Figure 3-37). This suggested that the apex of the mound was being scoured by bottom currents.

The dredged material evident at CS-2 Station 600S (equivalent to 100N, CS-1; Figures 3-35 and 3-38) represented dredged material disposed between 1984 and 1985 at CS-1. The capped mound locations which exhibited evidence of this recent disposal activity were at the center of CS-1 and stations to the immediate north. Near-surface, reduced sediment patches were encountered at 76% of CS-1 stations (Figure 3-34) and 82% of the CS-2 stations (Figures 3-35 and 3-39). This widespread appearance of previously buried dredged materials near the interface suggested that the mounds had been disturbed. As discussed for the STNH-N mound, this disturbance was probably biogenic. Feeding pockets were evident directly beneath the reduced sediment patches (Figure 3-39).

The modal boundary roughness at CS-1 was 0.4 cm (Figure 3-40), and CS-2 had a major mode shared between two class intervals, 0.4 and 0.8 cm (Figure 3-41). These distributions were unchanged from our September 1984 survey. CS-1 had an RPD depth frequency distribution which was symmetrically distributed about a major mode of 4.0 cm (Figure 3-40). There was no apparent spatial trend in the apparent RPD depths (Figure 3-42). Station 200NE had an anomalously shallow RPD value (1.93 cm) relative to the rest of the mound. The distribution of RPD values at CS-2 had a major mode at 5.0 cm (Figure 3-42). The spatial distribution of apparent RPD depths at CS-2 (Figure 3-43) displayed a pattern similar to CS-1. Pictures were not successfully obtained at station 200NE.

High order successional seres were found distributed over both mounds (Figures 3-44 and 3-45). Stations at CS-1 showed predominantly Stage III-I seres; only three stations had all replicates with Stage I or I-II seres (200N, 400S, and 400W). Similarly, only three stations at CS-2 showed all replicates in a Stage I condition (400W, 400S, and 200E). The abundance of Stage III infauna had increased markedly at both capped mounds since the September 1984 survey.

The Organism-Sediment Index frequency distributions at CS-1 and CS-2 revealed major modes at +7 and +11 respectively (Figures 3-40 and 3-41). CS-2 had 14 station replicates with an index of +11 while CS-1 had only 9. There were no obvious spatial trends in the distribution of OSI values (Figures 3-46 and 3-47).

However, three stations at CS-1 had unusually low (less than +6) values (400W, 200NE, and 600S); station 400S at CS-2 was also anomalously low.

Post Storm Survey

On 28 October, one month after Hurricane Gloria, REMOTS surveys were again performed at CS-1 and CS-2. Ten stations were occupied at each mound (Figure 3-48).

Hurricane-produced erosional features such as mud clasts and surface shell lag layers were evident in a number of stations at CS-1 (Figures 3-48 and 3-49). In addition, several stations (25E, 200E, and 200W) exhibited fine sand sediments (4-3 phi) overlying silt-clay (Figure 3-50). Sand layers had not been observed previously at CS-1; this coarse-grained material may have represented lag deposits produced by bottom scour (compare with Figure 3-39A).

A similar pattern of bottom disturbance was evident at CS-2 (Figure 3-51). Shell lag, mud clasts, and sandy surface layers were evident throughout the mound. At a number of stations (25S, 200S, 200E), the apparent percentage of coarse-grained sediments evident in surface sediments had increased since August (Figure 3-52). As at CS-1, this suggested that fine-grained sediments had been winnowed by bottom currents. Unlike STNH-N and STNH-S, evidence of bottom disturbance at the two capped mounds did not appear concentrated at the center of the disposal mounds.

At CS-1, post-storm boundary roughness values were significantly greater than the August values (Mann-Whitney U-test, $p = 0.007$). Conversely, boundary roughness values at CS-2 had not changed significantly (Mann-Whitney U-test, $p = 0.408$). This discrepancy suggested that the sand cap may have been more effective than the silt cap in stabilizing the bottom.

RPD values decreased significantly since the August survey at both CS-1 and CS-2 mounds (Figures 3-53 and 3-54, Mann-Whitney U-tests; $p = 0.048$ and 0.003 respectively). This decrease apparently reflected the disturbance produced by Hurricane Gloria. In general, RPD depths decreased less at these capped mounds due to the storm than at STNH-N and STNH-S.

Comparison of the distributions of the apparent infaunal successional stages at CS-1 and CS-2 (Figures 3-55 and 3-56) with the August data (Figures 3-44 and 3-45) indicates that CS-2 experienced no obvious change in successional status, while CS-1 showed evidence of retrograde succession. In the post-storm survey, only two stations at CS-1 (CTR and 600W) revealed evidence of Stage III infauna. This apparent difference in the impact of

the hurricane on the successional status of each mound again suggested that the degree of bottom disturbance was related to the different capping materials used. The sand cap appeared to reduce the impacts of the hurricane on the benthic community.

The distribution of Organism-Sediment Index values showed lower OSI values at CS-1 (Figure 3-57) than at CS-2 (Figure 3-58), reflecting the paucity of Stage III infauna at the CS-1 mound. As at STNH-S, the OSI values had not changed significantly at either of the capped mounds since the August survey. Overall, although the bottom was obviously physically disturbed by Hurricane Gloria at CS-1 and CS-2, the infaunal benthic assemblages were apparently not as "stressed" as the assemblages at the STNH-N mound. This difference in the impacts of the storm may reflect a gradient in the storm's physical effects or inherent differences in the affected benthic communities.

3.3.4 Mill-Quinnipiac River (MQR)

August Survey

REMOTS surveys have been performed at this mound in January 1983, August 1983 and September 1984. The present survey was conducted on 15 August 1985, approximately 27 months after the disposal of Black Rock Harbor muds followed by capping with New Haven Harbor muds. Earlier surveys, located on a N-S and E-W sampling cross, showed that recolonization of this mound was delayed relative to the other CLIS mounds. The August 1985 survey consisted of an orthogonal grid with stations falling on the quadrants located between the cross, so that the area affected by disposal could be delineated in more detail.

The major modal sediment grain-size was >4 phi (silt-clay) with mixtures of 4-3 phi (very fine sand). The sediment grain-size major mode had not changed from previous surveys conducted here.

Near-surface patches of reduced sediment were evident at only 9% of the MQR stations. Of the CLIS disposal mounds surveyed in August 1985, this was the only mound which did not exhibit widespread evidence of the redistribution of anoxic sediments to the surface. This was most likely related to the mound's low-order successional status.

The major modal value of boundary roughness was at the 0.4 cm class interval (Figure 3-59). In August 1983, the major mode for boundary roughness was 1.2 cm. The reduction in small-scale roughness was probably related to smoothing of the original disposal mound topography by currents.

The major modal values for RPD depths were shared between the 4 and 5 cm class interval (Figure 3-59). In September 1984, the RPD distribution had a modal value of 3 cm. The mapped RPD values (Figure 3-60) showed relatively deep values at all stations except for 300S/100E and 300S/300E, where the apparent RPD was less than 3 cm deep.

All MQR stations exhibited Stage I seres except for stations 500N/500E and 300S/300E (Figure 3-61). Past experience with the recolonization of other DAMOS mounds has shown that Stage III taxa normally appear on disposed materials within one year, initially on the thin flank deposits. The MQR mound is anomalous in this respect; sediment chemical contaminants are a potential cause for the slow recolonization rate of this mound.

Most of the OSI values fell within the modal value of +7 (Figure 3-59), indicative of relatively deep RPD values and low-order successional infauna. In September 1984, the major mode was shared between the +5 and +6 classes. The mapped OSI values showed a remarkably uniform distribution over the mound, suggesting that small-scale heterogeneity was not present (Figure 3-62). The whole mound appeared to be held in a late Stage I condition.

Post Storm Survey

On 29 October 1985, one month after Hurricane Gloria, the MQR disposal mound was surveyed to assess the impacts of the storm. The post-storm benthic process map of the MQR mound (Figure 3-63) indicated much less evidence of physical disturbance than the images from the other CLIS mounds (including FVP). A typical image from the MQR post-storm survey revealed (Figure 3-64) a smooth bottom colonized by a Stage I assemblage (sedimentary methane is also evident in this image). Methane was observed at two stations, 200N and CTR, indicating high sediment BOD and COD. Methane had not been observed in the August survey.

Boundary roughness values did not change at MQR between August and October, supporting the interpretation that bottom disturbance due to the hurricane was minimal at this mound. The post-storm distribution of RPD depths at MQR (Figure 3-65) indicated that, as observed at the other CLIS disposal mounds, RPD values had decreased at MQR since the August survey (compare with Figure 3-60; Mann-Whitney U-test, $p < 0.001$). There was no obvious spatial pattern in the distribution of RPD values indicating a mound-wide disturbance. The presence of methane suggested that organic loading may have been a contributing stress factor. Despite the lack of direct evidence, hurricane-induced disturbance could not be ruled out completely.

The distribution of infaunal successional stages at the MQR mound (Figure 3-66) showed only two stations with Stage III

seres. The MQR mound remained dominated by low-order successional infauna. As discussed above, this persistent lack of Stage III infauna at MQR is anomalous, and it may be related to high levels of sediment contaminants. The OSI values at MQR in October (Figure 3-67) had decreased significantly since the August survey (Figure 3-63, Mann-Whitney U-test, $p = 0.006$). In August, the mound was dominated by OSI values of +7. The decreased values observed in this survey were entirely due to the decreased RPD depths; the infaunal successional status of the mound had not changed. Overall, of the CLIS disposal mounds surveyed subsequent to Hurricane Gloria, the MQR mound showed the least evidence of physical disturbance.

3.3.5 Norwalk (NOR)

Two previous REMOTS® surveys were conducted at the Norwalk mound in January 1983, and September 1984. The cross-shaped sampling grid consisted of nine stations. In August 1985, the sampling grid was extended in both the N-S and E-W directions to produce an expanded view of the disposal mound.

All stations had a major mode grain-size of >4 phi (silt-clay range) as compared to a major mode of >4-3 phi (silt-clay to very fine sand range) in the September 1984 survey. This increase in the abundance of fine-grained sediments suggests that a net deposition of fine-grained material had occurred since the last survey.

Reduced sediment patches were observed near the interface at 53% of the Norwalk stations (Figure 3-68). This material was evident throughout the mound and most likely the result of large-scale biogenic disturbance.

The frequency distribution of small-scale boundary roughness for the August survey (Figure 3-69) displayed a major mode at the 0.4 cm class interval, compared to 0.8 cm in the September survey. This implies small-scale "smoothing" of the bottom had occurred due to currents, sedimentation, and bioturbation.

The shallowest mean RPD values at Norwalk (Figure 3-70) occurred at stations 200E, 600E, 600S, and 600W. However, in 1984 the major mode for RPD depths was located at the 3 cm class interval. In this survey the major mode for RPD depths was at the 5 cm depth class (Figure 3-69), indicating increased bioturbational activity at this mound.

It is apparent that significant recolonization at CTR as well as most of the stations north of center at Norwalk had occurred since September 1984 (Figure 3-71). In the 1984 survey, one image from station CTR revealed an apparently azoic location

with the remaining two images showing evidence of Stage I assemblages. In this survey, two images from station CTR exhibited Stage III-I assemblages. Stage III assemblages were predominant throughout much of the mound except for the southern transect. The origin of the relatively low-order successional status of the southern region of the mound is unknown, but it may have been related to the proximity of the adjacent NH-83 and MQR disposal mounds.

From the 44 images taken at Norwalk, 37 of them had an Organism-Sediment Index of +7 or higher (Figure 3-69). As seen on the frequency distribution histogram, most of the values fell at the +7 and +11 class intervals. In the September 1984 survey, the lowest OSI values were located in the southern transect limb extending from center to 450S (Figure 3-72). This pattern continued, and it may have been related to the influence of the disposal mounds to the south. However, the general recolonization of this mound had progressed markedly since the 1984 survey.

3.3.6 New Haven '74 (NH-74)

This mound has been studied on an irregular basis since the original 1972 baseline study; the first REMOTS® survey of this mound was performed in September 1984. This mound was originally created by the disposal of New Haven Harbor channel muds which were capped with clean sand. The 1985 survey was conducted on 14 August.

As in September 1984, the major modal grain-size was >4 phi (silt-clay). Images from station 200N revealed a relatively mud-free sand cap. This cap ranged in thickness from approximately 1 to 10 cm as measured from the three station replicates. Station 200W also showed a thin layer, 0 to 1.5 cm thick, of very fine sand (4-3 phi) at the sediment surface. This station also had an anomalously thin RPD and low successional status, possibly indicative of a recent erosional event.

As at the Norwalk mound, 53% of the stations at NH-74 showed patches of reduced sediment at the surface. Again, this was apparently due to large-scale biogenic sediment reworking.

The overall distribution of boundary roughness values remained unchanged over those measured in September 1984. The major modal value fell within the 0.40 cm class (Figure 3-73).

The major modal RPD depth for all the stations sampled was at the 4 cm class interval (Figure 3-73), one size-class interval higher than measured in September 1984. However, an examination of only the nine station locations sampled in 1984 revealed the same major modal value (4 cm) in 1985. Station 200W, sampled in both surveys, experienced a dramatic change in its

apparent RPD depth. In September 1984, this station had a mean apparent RPD depth of 3.2 cm. In this survey, the station had a mean apparent RPD depth of 0.88 cm, most likely the result of very localized erosion (this assumption is supported by the presence of a thin layer of washed sand at the surface). The mapped distribution of the mean apparent RPD depth showed that the deepest RPD values were located in an area extending from 400E southwest toward stations 200S and 200SW (Figure 3-74).

Overall, 50% of the replicate images from the NH-74 mound exhibited evidence of Stage III infauna. In September 1984, the NH-74 mound exhibited a patchily distributed Stage III infauna. Two stations, 200E and 200W, showed a marked decrease in successional status since that survey (Figure 3-75). This may be explained by local erosion at station 200W. The sediment profile images at station 200E have relict feeding structures at depth, indicating that Stage III infauna were present at this station in the past. All three images also showed the presence of reduced mud clasts at or near the sediment-water interface; these also suggest either sediment erosion or possibly megafaunal predator foraging. Either of these forces could be potentially responsible for the apparent loss of Stage III infauna from this station.

The frequency distribution of Organism-Sediment Index values was bimodal with peaks at the +7 and +11 class intervals (Figure 3-73). OSI values at the same two stations (200E and 200W) also had decreased dramatically; station 200W had decreased from +9 to +3, and station 200E had decreased from +11 to +6. As described earlier, the reasons for these decreases were most likely related to local erosion (due to either physical or biological forces). The patchy distribution of OSI values (Figure 3-76) reflected the mosaic of Stage I and Stage III infauna present at this mound. Overall, benthic conditions at the NH-74 mound had not markedly changed since the 1984 survey.

3.3.7 New Haven '83 (NH-83)

Three previous REMOTS® surveys were conducted at this disposal mound: a baseline survey in October 1983 and post-disposal surveys in January 1984 and September 1984. The results of the 14 August 1985 survey were compared to the September 1984 survey (stations 200N and 600E were not occupied in the August 1985 survey).

The major modal grain size was >4 phi (silt-clay range) at all stations with subordinate modes of very fine sand (4-3 phi). The medium sand (2-1 phi) observed at station 400N in previous surveys was no longer evident, probably due to both the deposition of additional fine-grained sediments and the bioturbational mixing of the coarse-grained material.

Reduced sediment patches were evident near the surface at 60% of the NH-83 stations. The widespread appearance of reduced sediment at the surface indicated the localized redistribution of bottom sediments and dredged materials both vertically and horizontally. As discussed in previous sections of this report, vertical redistribution of material was most likely due to the activity of large infaunal deposit-feeders.

The frequency distribution for boundary roughness for the August survey (Figure 3-77) indicated that small-scale topographic relief had not changed significantly since the September 1984 survey. Between September 1984 and August 1985, the mean RPD depth for all stations at NH-83 had decreased approximately 1 cm (3.76 to 2.86 cm). There was no obvious spatial pattern in the distribution of the reduced RPD values (Figure 3-78). This decrease is potentially related to recent biogenic disturbance of the bottom.

As observed in 1984, a patchy spatial distribution of Stage I and Stage III successional seres was evident (Figure 3-79). Stage I successional seres were observed in 54% of the replicates. Overall, Organism-Sediment Indices were lower than in September, 1984 (Figure 3-77), due in large part, to the shallower RPD values. The wide range in the distribution of OSI values (Figure 4-80) reflected the patchy mosaic of benthic conditions at this time on the mound.

3.3.8 Southeast CLIS (CLIS-SE)

In August 1985, a REMOTS survey was conducted in the southeast quadrant of the existing CLIS disposal site; one REMOTS image was taken at each of 36 stations on a 6 x 6 orthogonal grid with stations regularly spaced at 200 meter intervals. The purpose of this survey was to determine if any dredged material was already present in this region and to characterize baseline benthic conditions.

No dredged material was evident in the CLIS-SE region. The major modal grain size was >4 phi (silt-clay range) at all stations, with a boundary roughness major mode (Figure 3-81) in the 0.4 cm class interval. Relatively small, rounded mud clasts were observed in six of the REMOTS images from this area. These clasts may have been the result of epifaunal foraging activity. Reduced patches of sediment were also evident in the same number of images (17%). This was the lowest abundance of this near-surface reduced material of any survey grid, except for MQR. As discussed above, this was apparently related to the low abundance of Stage III infauna (see below). In general, the fine-grained sediments and low boundary roughness values indicate that the CLIS-SE area is a low-kinetic area.

The overall mean RPD for this area was 6.1 cm, with the shallowest mean RPD values found at stations 100N/100W and 500S/100W (Figure 3-82). As expected, RPD values were relatively deep at this undisturbed site.

Twenty-five of thirty-six stations at CLIS-SE exhibited Stage I successional seres (Figure 3-83). The relative paucity of Stage III infauna is not readily explained. It is possible Stage III seres exist, but evidence of feeding voids were missed because of the lack of replicate images taken at each station; another possibility is that this area because of its relatively flat topography experiences frequent disturbance due to trawling activities. In any event, because the area appears to be dominated by Stage I assemblages, recovery of this region to its pre-disposal successional status would be rapid (i.e., less than one month).

Of the 36 images analyzed from CLIS-SE, 24 had OSI values of +7, while 7 had index values of +11 (Figure 3-81). The distribution of OSI values reflected the distribution of infaunal successional stages; in general, the higher OSI values (+11) were found in the northern half of the survey area (Figure 3-84).

3.3.9 CLIS Transect

As part of the post-storm survey, a transect of 10 REMOTS® stations extending from the New Haven Harbor entrance to the CLIS disposal site was occupied. Due to inadequate REMOTS® prism penetration because of shell lag deposits at 3 stations, useful images were obtained at only 7 stations along this transect.

The grain-size and benthic "process" map of this transect (Figure 3-86) indicated, as expected, a shoreward increase in modal grain-size. Evidence of bottom disturbance, i.e., shell lag layers, mud clasts, exposed worm tubes, and disturbed RPD layers, were observed throughout the transect (Figure 3-86). There was no obvious indication that bottom disturbance varied over the depth ranges sampled (6 to 20 meters). Moreover, it was apparent from the results of the post-storm disposal mound surveys that the influence of the storm extended well beyond this transect.

3.4 Sediment Characteristics

The sediment collected at CLIS-SE was described by field personnel as a 2-3 cm oxidized layer covering a soft silty clay with both worm tubes and shell hash present. The physical analysis of all the samples (including the CLIS Reference station) by the NED analytical laboratory characterized the sediment as olive gray organic silty clay with traces of sand and shell fragments. Over 95% of the sediment passed the #200 sieve (silt/clay) and had a specific gravity of 2.67 and a pH of 7.1. The concentrations of metals in the sediment from the CLIS-SE area (Table 3-2) reflected

the natural heterogeneity of the region and compared well with the concentrations found at the Reference station. Concentrations of PCB's and DDT's were below detection limits, as was arsenic.

3.5 Benthic Community

The sediment collected at each station in the CLIS-SE area for benthic community analysis was also visually described as soft silty clay with a 2-3 cm oxidized layer at the surface with worm tubes and some shell hash present. The community sampled in August (Table 3-3) was dominated by deposit feeders including Mediomastus ambiseta, Nephtys incisa, Paraonis gracilis, and oligochaete species. The other numerically dominant species included the bivalves Nucula annulata and Yoldia limatula as well as the nemertine worm, Tubulanus pellucidus. All the samples taken at CLIS-SE had similar total number of species and individuals. The largest difference occurred with the dominant species Nucula. The relatively high densities of Nephtys in the samples were due to the recent settlement of young.

The benthic community at the CLIS Reference station was similar to that at CLIS-SE except for low numbers of the polychaetes Cossura, Mediomastus, Spio, and Tharyx. The higher water content of the sediment at this deeper station may have accounted for this difference in population characteristics.

3.6 In-situ Observations

Present at all mounds visited during the CLIS survey were megafaunal assemblages characteristic of that region of Long Island Sound. All species seemed to exhibit normal foraging and motile behavior. The surface sediments at FVP appeared weathered with a thin layer of coarse sand material overlying loosely cohesive clay-muds.

The faunal component at the FVP mound still appeared to be in a state of recolonization. No major evidence of mature or equilibrium infaunal successional seres (i.e., large surface worm tube features, fecal casts) was observed during survey dives. The distribution of the megafaunal component (crustacea and finfish) was very patchy and possibly reflected predation on newly settled patches of prey (i.e., Mulinia or similar rapid colonizer species).

The Black Rock material at the FVP mound was utilized by motile epibenthos, such as shelter-seeking, burrowing taxa like C. irroratus, and other important prey and juveniles of commercially important species. The sediment at CS-1 was cohesive and stable, except for some evidence of eroding clay clumps. The material at CS-2 remained stable and cohesive. The sand cap at STNH-N appeared intact with homogeneous coverage. The material at STNH-S was compacted with no evidence of any major erosional events.

Surface sediments observed at all mounds were oxidized, i.e., no large patches of anoxic sediments were present at the sediment-water interface. Foraging activities of crustaceans, movements of finfish and normal locomotive behavior of gastropods in the area apparently have contributed to oxygenation of surface sediments.

Table 3-4 summarizes the relative abundances of species identified during the dive transects. More detailed descriptions of each mound follow.

3.6.1 CS-1

The survey dive was conducted in a 25 cm/sec (0.5 knot) current. Horizontal visibility was approximately 1 meter. The nepheloid layer was less than 1 cm. The substratum consisted of fine-grained silt throughout. Large clumps of marsh peat, 0.5 - 0.7m diameter, were present at the pile center. Clumps were fouled with hydroids, indicating they had been submerged and exposed for some time. Megafauna utilized the clumps for shelter. Juvenile cunner, Tautogolabrus adspersus, were observed on the lee side of clumps. A single winter flounder, Psuedopleuronectes americanus, was observed in a crevice, sheltered from the current. Lobsters, Homarus americanus, and spider crabs, Libinia emarginata, were observed in lobster traps on the mound. The sediment surface was heavily tracked by crustaceans and finfish. Mud snails were attracted to crustacean foraging excavations and whelk tracks.

3.6.2 CS-2

The survey dive was conducted in a 13 cm/sec (0.25 knot) current. The substratum consisted of a silt-sand matrix, 3 to 5 cm deep. Shell hash cover was approximately 30%, with some shell material fouled by hydroids. The surface had irregular, small ripples spaced at approximately 2 to 15 cm intervals. The sediment surface was heavily tracked by crustacean and finfish activities. Fecal mounds from infauna were common over the surface. Whelks, hermit crabs, mud snails, sand shrimp, and mysids were the major bioturbators observed.

3.6.3 STNH-N

The survey dive was conducted in a slight 5 cm/sec (0.1 knot) current. Horizontal visibility was 1.5 meters with low near-bottom turbidity. The nepheloid layer was not visibly apparent. The bottom consisted of fine silt (less than 1 cm deep) over coarse sand over compacted clay. Small shell hash patches (less than 1 m diameter; Mulinia and Yoldia valves) covered less than 5% of the surface sediment. Hydroids were occasionally anchored to shell hash material. The topography of the survey area was flat with vertical burrows into the sediment 1 to 10 cm diameter. Crustacean foraging depressions were common, and several 15 cm diameter

conical shaped depressions were observed. The typical megafaunal assemblage was observed at this mound as well.

3.6.4 STNH-S

The survey dive was conducted in a 13 cm/sec (0.25 knot) current. The bottom consisted of fine silt (1 to 2 cm deep) over a cohesive clay base. Small vertical burrows (0.5 cm diameter) were common throughout the area (4-5 per m^2). Occasional 10 to 20 cm diameter burrows which had been dug horizontally into the clay base were observed, and patches of hydroids (1 per 10 $m^{2)}$ were common. Eroded clay clump material was also present. The vertical relief over the survey dive was approximately 2 meters; major bioturbators were mud snails, mysids, and whelks.

3.6.5 Field Verification Program (FVP) Mound

Two survey dives were conducted at the FVP mound (center). Current velocity was approximately 10 cm/sec (0.2 knot). The nepheloid layer in the survey area was less than 0.5 cm with horizontal visibility approximately 1 meter. The bottom sediments consisted of a thin oxidized layer of fine-grained silt over coarse sand, grading into anoxic, loosely cohesive mud below. Shell hash composed less than 1% surface cover.

Predominant bioturbators were Pagurus longicarpus, P. pollicaris, and Cancer irroratus. All were actively foraging in surface sediments, creating sediment clouds which were carried away by the current. More than 150 feeding excavation pits were observed with a maximum density of 3 per m^2. In addition to general foraging activities, Pagurus longicarpus would burrow their shells into the sediment surface and use chelae and mandibles to winnow sediments. Juvenile Cancer irroratus (less than 2.5 cm carapace width) excavated 2-3 cm deep vertical burrows for shelter. All individuals of this size class were in softshell condition, and exuviae were present at the entrance of many of the burrows.

Starfish (Asterias forbesi) and sand shrimp (Crangon septemspinosa) were observed in a foraging association. The shrimp would winnow through sediments disturbed by the tube feet of starfish as it moved over the bottom. The mud snail, Nassarius trivittatus, was attracted to the foraging excavations of crustaceans and the plowed tracks of the whelk, Busycon carica. Individual snails were observed to move directly to the area of foraging activity.

Juvenile finfish were also observed on the mound. Both winter flounder, Psuedopleuronectes americanus, and four-spot flounder, Paralichtys oblongus, assumed normal foraging postures during movements over the bottom.

3.7 Bottom-Mounted Instrumentation Array (DAISY)

3.7.1 Water Temperature

During the day preceding the passage of Hurricane Gloria, near-bottom water temperatures at the deployment point (New London Disposal Site, NLON) ranged from a low of approximately 20.4°C to a maximum of 21.2°C (Figure 3-87). Storm passage at 1445 EDST on 27 September suppressed the temperature range and essentially eliminated any evident tidal signature. The effects of this perturbation persisted for nearly 48 hours. Temperatures during the initial 24 hr period after passage of the storm varied by less than 0.2°C and were weakly correlated with tidal phase. After 1500 EDST on 28 September, the temperature range increased slightly and tidal correlations progressively improved. By 0600 EDST on 29 September, pre-storm conditions were re-established and the decrease in water temperature approximated that observed during the period prior to the storm (Figure 3-87). Over the remainder of the deployment period, water temperatures closely followed tidal phase with average values slowly decreasing in response to the coincident decrease in local air temperature (Table 3-5).

3.7.2 Salinity

Near-bottom salinity displayed a response to the passage of Hurricane Gloria similar to that observed within the water temperature records. Prior to the storm, salinities varied in response to the local tidal phase with values ranging from a low of approximately 30.8 ppt to a high of 31.6 ppt (Figure 3-88). Following storm passage, tidal variability was evidently suppressed for a period of approximately 48 hrs and the average salinity slowly decreased in response to increasing freshwater inputs from the Thames River and adjacent streams. The majority of this increased streamflow was the result of the passage of tropical storm Henry earlier in the week and some the direct effect of Gloria. Within southeastern Connecticut, this latter component was expected to be relatively small due to the virtual absence of significant rainfall during Gloria. Reviews of U.S. Geological Survey streamflow data, however, indicate that, over the period 26-27 September, discharge from the Thames River increased from approximately 570 cfs to nearly 1000 cfs. Discharge continued to progressively increase over the next three days and, by 1 October, peaked at approximately 2000 cfs. Over the next three days, values decreased progressively, falling to approximately 1600 cfs, and then remained essentially constant over the remainder of the deployment period. The long term response of near-bottom salinities to this streamflow cycle was evident in the array observations which showed a progressive decrease in average salinity from 26 September to 1 October and a slight increase thereafter (Figure 3-88).

3.7.3 Current Speed and Direction

The passage of Hurricane Gloria along the adjacent continental shelf and over Long Island Sound significantly perturbed the near-bottom current field in the vicinity of the NLON disposal site. Pre-storm currents displayed a regular tidal variability with peak speeds of approximately 35 cm/sec (Figure 3-89). Associated directions were predominantly northeasterly (030° mag) during the ebb tide and southwesterly (225° mag) on the flood tide (Figure 3-90). As Gloria approached, both current speed and direction began to display irregular behavior. Over 26 September and into the early part of 27 September, current speeds during both the flood and ebb remained similar in peak value while displaying some slight increase in short-term variability. This pattern was disturbed during the early morning hours of 27 September and the flood, which commenced at 0529 EDST in The Race (Figure 2-2), displayed a significantly reduced peak value. The subsequent ebb, commencing at 1119 EDST, spanned the period during which Gloria passed over the Sound and displayed significantly higher peak values than those observed during the immediate pre-storm period. Current directions associated with this interval were also significantly perturbed with both the ebb and flood displaying increased northerly components.

Following storm passage, there was an evident suppression of the tidal stream over the next 12 hr tidal cycle with peak flood velocities reduced by approximately 30% relative to pre-storm levels and a near total arrest of the ebb (approx. 2045 EDST on 27 September to 0530 EDST on 28 September in Figure 3-89). This absence of a significant ebb was also apparent in the direction record, where values dominated by southwest to northwest components prevailed over the period from 1745 EDST on 27 September to 0530 EDST on 28 September. This storm-associated perturbation slowly relaxed over the next tidal cycle. Peak speeds during the flood initiated early on the morning of 28 September (0608 EDST) approached pre-storm levels observed just prior to the transit of Gloria across the Sound. The following ebb, beginning at 1119 EDST (28 September), displayed peak values equal to those observed during Gloria and generally well in excess of those found during the pre-storm period. In contrast to the majority of the tidal cycles, these high current speeds persisted over much of the ebb phase resulting in generally high kinetic energy levels. This event appeared to be primarily associated with the relaxation of the tidal system following departure of Gloria. Subsequent tidal cycles displayed characteristics essentially similar to pre-storm conditions.

3.7.4 Surface Wave Characteristics

The bottom-mounted wave and tide gage indicated that the passage of Hurricane Gloria resulted in the generation of a surface

wave field sufficient to significantly perturb the near-bottom pressure field. A summary of the data provided by the gage is shown in Figure 3-91. These plots show the results of simple spectral analysis of near-bottom pressure. Only the higher frequency components representing perturbations in hydrostatic pressure associated with the wind-driven surface wave field were plotted, with variations associated with the tidal system not represented.

The spectral plots clearly show the effects of Hurricane Gloria on the surface wave-associated pressure field. Beginning at approximately 1215 EDST on 27 September, the amplitude of wave-associated bottom pressures progressively increased to a peak near 1415 EDST, approximately coincident with the observed minimum in barometric pressure (Figure 1-3). As previously noted, winds during this period were primarily from the south to southeast directions providing sufficient fetch to allow generation of significant surface wave energy. After this peak occurred, the amplitude of the surface wave-associated pressure perturbation progressively decreased coincident with decreasing wind speeds and a general shift in direction from the south to the southwest and eventually northwest. These data indicate that significant surface wave generation and associated pressure and velocity perturbations produced by the passage of Hurricane Gloria were essentially confined to the immediate storm period. Beyond this time, the sediment-water interface was effectively isolated from surface wave effects by the overlying water column.

3.7.5 Suspended Material Characteristics

Prior to the passage of Hurricane Gloria, near-bottom suspended material concentrations in the vicinity of the deployment point at NLON displayed an average value of approximately 2 mg/l (Figure 3-92). Previous deployments near this site showed that concentrations vary regularly over each tidal cycle (Bohlen, 1982). This signature, although weak, appeared to be present in the pre-storm record. The onset of Gloria produced a significant perturbation in near-bottom concentrations with peak values increased by more than a factor of eight. This perturbation was relatively short-lived, however, and essentially confined to the immediate storm period. This response and the coincidence with the period of maximum surface wave generation suggests that the increase in near-bottom suspended materials resulted primarily from resuspension of materials from the sediment-water interface under the combined effects of wind wave-induced velocities and the tidal stream. As noted above, both of these factors decreased sharply following storm passage, the waves decaying due to variations in the surface wind field and tidal velocity decreasing due to storm-associated perturbations in the local tidal system. In the absence of these forcing functions, the high settling velocities characterizing the reworked materials residing along the sediment-water interface favored a rapid decay in suspended

material concentrations and a return to pre-storm conditions. The slight increase in post-storm concentrations relative to pre-storm levels indicated in the data plot was the result of instrumentation bias introduced from deposition of some of the resuspended materials on the windows of the optical sensor.

Following the post-storm decay, concentrations remained low for a period of approximately 3 hrs and then began a progressive increase to a maximum approaching 30 mg/l (Figure 3-92). This increase was approximately coincident with the rebound of the tidal velocity system; it appeared to be the result of offshore advection of inshore materials suspended during storm passage but retained within the nearshore shallow water areas due to the absence of significant tidal flows. The timing of the occurrence of peak concentrations and its coincidence with the flood suggests that the source of these advected materials was to the east of the deployment location and adjacent to Fishers Island Sound. Timing also clearly eliminated streamflow-associated suspended loads as a possible source of the materials moving past the array. Sediment loads and discharge levels associated with the streams entering the Sound to the east of the deployment point were simply insufficient to produce significant far-field perturbations within the local suspended material field.

After the rebound in suspended sediment concentrations, associated peak concentrations slowly returned to pre-storm levels. The occasional spikes noted in the record during this period as well as those observed on several occasions during the pre-storm interval were most probably the result of the passage of suspended organic detritus and were not considered to be evidence of significant sediment transport activity. Their occurrence could not be simply correlated with either the tidal current record or concurrent temperature-salinity conditions. During the last half of the record, the progressive removal, by ambient tidal flows, of sediment deposited on the windows of the optical sensor most likely resulted in the slow decline of the average apparent suspended sediment concentration. The observed decay was not considered to be evidence of gradual settling of storm-resuspended materials. All indications are that the settling of these materials occurred in a relatively short period of time essentially confined to the immediate post-storm period.

4.0 DISCUSSION

4.1 August Monitoring Cruise at CLIS

The bathymetric surveys conducted at CLIS during August 1985 did not reveal any significant changes (>20 cm) in the topography of the disposal mounds there. The amount of dredged material disposed since the 1984 survey was insufficient to

decrease the depths at the disposal location within the detection limits of the acoustic fathometer system (~10-15 cm).

No significant trends could be found in the sediment chemistry data beyond the sampling and analytical variability. The CLIS-SE results were compared to averages and ranges of selected chemical concentrations for the CLIS reference station (CLIS-REF) over a five year period to see if CLIS-SE chemical concentrations represented values for natural bottom. The CLIS-SE data are within the ranges for CLIS-REF except for oil and grease (Table 4-1). The August 1985 oil and grease results (x = 540 ppm) for CLIS-REF were also higher than normal. If dredged material was present, metal concentrations would be expected to be higher as well. No sediment samples collected during the October field operations were analyzed.

The results of the benthic community analysis of the samples collected at the stations in the CLIS-SE area were generally very similar to one another as well as to CLIS-REF. Some differences did exist in the abundances of some polychaetes (low numbers of Cossura, Mediomastus, Spio, and Tharyx at CLIS-REF) but this was likely due to the higher water content sediment at CLIS-REF. At CLIS-SE, the occurrence of the bivalves Mulinia lateralis and Macoma tenta and the polychaete Mediomastus ambiseta was well below the maximum levels that can be expected here, while Nephtys, Nucula, and Yoldia were more abundant and occupied a deeper, more physically stable habitat. The transition from the former group to the latter might be interpreted as a response to a change in habitat quality or disturbance level. Recent studies at the FVP site by EPA/COE, however, suggest that this transition may be an irregular cycle in relative abundance of these two groups and not related to habitat changes.

Analysis of REMOTS® images taken during the August survey detected a range of benthic conditions from undisturbed to a "stressed" condition. As in the 1984 survey, the STNH-N mound exhibited high OSI values in August 1985, reflecting successful recolonization by Stage III infauna. Also, patches of reduced sediment, the apparent result of large-scale biological sediment reworking, were evident in 82% of the STNH-N images. The STNH-S images showed evidence of "stress" relative to its condition in 1984. RPD depths and OSI values had decreased. The western portion of the STNH-S mound continued to lack high-order successional infauna. Near-surface, reduced sediment patches were evident in 47% of the images.

Images collected at CS-1 and CS-2 exhibited relatively undisturbed benthic environments consisting largely of Stage III infauna and well-developed RPD's. Evidence of new dredged material was observed at approximately 100m north of CS-1. Biogenic

near-surface, reduced sediment patches were evident in 76% of the CS-1 images and 82% of the CS-2 images.

Compared to the 1984 survey, the Norwalk mound showed evidence of continued recovery in 1985. Boundary roughness values were lower, indicating "smoothing" due to currents and bioturbation. Both RPD depths and the abundance of Stage III seres had increased throughout the mound, except for the southern transect. The low-order successional status of this southern region may be related to its proximity to adjacent disposal mounds.

The NH-74 mound did not change markedly between 1984 and 1985. The mound remains a patchy mosaic of Stage I and Stage III seres. Some stations showed obvious retrograde conditions which appear to be due to local erosion, while 53% show biogenic patches of reduced sediment near the interface. Similar to NH-74, the NH-83 mound exhibited a mosaic of Stage I and Stage III infaunal assemblages. Since 1984, RPD values have gotten shallower at this mound.

As in 1984, the MQR mound in August 1985 appeared held in a late Stage I condition. The abnormally slow recolonization rate of this mound coupled with the continued presence of highly-reduced, low-reflectance sediment immediately below the apparent RPD boundary (typical of either freshly deposited dredged material or anoxic sediment with high organic content) indicates a potential for high sediment contaminant levels which could have been responsible for precluding Stage III recolonization. Near-surface patches of reduced sediment, widespread at other CLIS mounds, were evident in only 9% of the MQR images; this was not surprising, given the lack of head-down deposit feeding infauna present in the area. The large-scale (>10 cm) vertical redistribution of sediments at the other mounds was likely due to large, mobile predatory taxa, e.g., decapods or stomatopods, which were excavating burrows or preying on deep-dwelling Stage III infauna. In the absence of these infauna, this large-scale biogenic reworking activity would not take place.

This megafaunal foraging activity apparently overturns patches of relatively deep sediment layers (i.e., greater than 10 cm). On disposal mounds, such burrowing activities may result in the reintroduction of highly reduced (and potentially contaminated) sediments to the sediment-water interface. This reintroduction may also lead to a retrograde succession of the infaunal community. This sequence of events appears to have occurred at the FVP site in June 1985. Until that time, the FVP site had exhibited progressively deepening RPD depths and increasing abundances of Stage III infauna. In June 1985, this pattern was reversed, and patches of reduced sediment were evident near the interface throughout the site. This retrograde condition may represent a new phase in the recolonization of a disposal mound. The pattern of events at the MQR site suggests that, in the absence of

recolonization by Stage III infauna, large-scale megafaunal bottom disturbance does not occur. The presence of Stage III infauna, due to their cryptic habit will lead directly to deeper foraging activities by the larger, predatory epifauna. Alternatively, the inherent qualities of the MQR site, which has apparently prevented (or delayed) recolonization by Stage III infauna, may also be influencing these large mobile taxa.

As indicated in the June FVP survey, the integrity of CLIS-REF as a reference station location appears to be in question, possibly due to the intensive sampling program carried out there since 1982 or other disturbance factors (e.g., regional hypoxia, intense trawling activity). The low RPD depths (Table 4-2) tend to support this conclusion; the loss over time of Stage III infauna are also consistent with a progressive rebound of the apparent RPD at this location. Because the undisturbed integrity of the CLIS-REF station can no longer be assumed coupled with the inherent shortcomings of having only one reference location for a monitoring program (Hurlbert, 1984), new and multiple reference stations have been established for future monitoring at the CLIS site.

A new location (CLIS-SE) for future disposal operations was studied in the southeast quadrant of CLIS. The sediments and benthic infaunal community at CLIS-SE were representative of typical conditions for that region of Long Island Sound (Sanders, 1956; McCall, 1977), and no dredged material was detected with bathymetry, REMOTS® or sidescan surveys. The CLIS-SE location is a low-kinetic region characterized by relatively deep RPD levels, relatively high-reflectance sediment below the RPD boundary, but primarily Stage I assemblages throughout the area surveyed (69% of the images). Only 17% of the images revealed reduced sediment patches near the interface. Recovery of this location to its pre-disposal successional status should be rapid (i.e., less than one month). Influence from disposal mounds to the west (STNH-S, NH-74) and the north (FVP) should be negligible given the low current regime at the CLIS site.

4.2 Effects of Hurricane Gloria at CLIS

Hurricane Gloria passed through the area on 27 September with wind speeds reaching 160 km/h (100 mph). This high energy event created the potential for erosion and redistribution of material at the disposal mounds. Analysis of precision bathymetric surveys conducted in August (pre-storm) and October (post-storm) 1985 did not detect widespread loss of material from the six disposal mounds surveyed (STNH-N, STNH-S, FVP, CS-1, CS-2, MQR). Volume calculations (Table 3-1) revealed that only CS-1 experienced a detectable loss of material. This could have been due to the recent disposal operations occurring there; it is quite probable that the newly disposed material had insufficient time to consolidate completely. The resultant irregular small-scale

topography therefore would have been more susceptible to the hurricane-induced erosional forces. CS-1 was also capped with silt and, therefore, may have experienced increased resuspension and redistribution of material. A loss of 15,390 (±3660) m^3 of material (Table 3-1) evenly distributed over the 800 × 800 meter survey area would result in a change in depth of approximately 2.4 (±0.6) cm.

One month after the storm, evidence of surface sediment disturbance, e.g., mud clasts and shell lag, was present at both the CS-1 and CS-2 mounds. This disturbance was seen over most of the mound surface. RPD depths decreased significantly at both mounds. Boundary roughness and the percentage of Stage I seres increased at CS-1, but not at CS-2; this suggests that the sand cap was more effective than the silt cap in minimizing the impacts of the storm. As mentioned above, volume calculations from bathymetry surveys at CS-1 indicated that a decrease in volume of material occurred. Estimates of the loss of material by comparing RPD depths revealed that approximately 1.04 cm of high-reflective sediment was lost (Table 4-3) with a range of loss of material of 0.2 to 2.2 cm. Other factors influencing the change in thickness of the dredged material layer include consolidation, or compaction. A more extensive sampling grid would have been required to better resolve estimates of erosion from REMOTS® photos compared to bathymetry when dealing in the range of only a few centimeters of material loss over the entire mound.

Unlike the CS-1 and CS-2 mounds, the STNH-N mound showed extensive evidence of disturbance concentrated near the center of the mound. Mud clasts, shell lag, and exposed worm tubes (indicating approximately 0.5 cm of erosion) were apparent in most replicates. Between August and October, boundary roughness values increased, RPD depths decreased, and the mean OSI value dropped nearly 3 units (8.9 to 6.0). The STNH-N disposal mound, previously one of the most successfully recolonized CLIS mound, was significantly disturbed by the storm. Similar conditions were seen at the STNH-S mound, also concentrated at the mound's center. Unlike STNH-N, however, only RPD depths were significantly affected by the storm. The lack of change in successional stages and OSI values was likely due to the mound's "disturbed" pre-storm condition.

The MQR mound exhibited minimal evidence of bottom disturbance due to the storm. Post-storm RPD depths were decreased, and methane was observed in some images; however, most of the images revealed a smooth bottom colonized by a Stage I assemblage. The lack of physical disturbance was very likely due to the binding and sediment-stabilizing properties associated with Stage I communities (Rhoads and Boyer, 1982). The bioturbational activities of the Stage III assemblages, evident in varying

abundances prior to the storm at the other CLIS mounds, tend to reduce sediment shear strength and critical erosion velocities.

The apparent lack of severe bottom disturbance at MQR suggests that the erosional influence of the storm was potentially a function of the infaunal successional stage. Because all the disposal mounds within the CLIS site are located in similar water depths, depth does not appear to be a factor in the pattern of disturbance. Throughout its post-disposal history, MQR has been dominated by Stage I assemblages, displaying an abberantly slow recolonization rate. It has been suggested, based on this observation, that high chemical contaminant levels in the sediment may have been responsible for precluding the recolonization of the site by higher-order successional infauna. Stage I communities are characterized by near-surface, tube-dwelling taxa which bind and stabilize the surface and do not bioturbate sediments deeply. Conversely, Stage III forms rework sediments extensively, resulting in unconsolidated, low shear strength surface sediment layers. Sediments at the MQR site were most likely resistant to erosional forces due to the absence of Stage III infauna. Moreover, the sites which exhibited well-developed Stage III communities in August, such as STNH-N, showed evidence of extensive surface sediment disturbance.

The results of the onshore-offshore REMOTS® and sediment core transect indicate that bottom disturbance was widespread shoreward of the CLIS site (Figure 4-1). Areas shoreward of the 15 m isobath appear to have experienced extensive sediment resuspension. Shell lag deposits and rippled sand layers overlying silt-clay sediments were evident throughout the region. Conversely, the deepest station (CLIS-REF), located in 25 m of water showed little evidence of bottom disturbance. This station was apparently located below the hurricane wave base.

4.3 Response of the Sediment-Water Interface at NLON to Hurricane Gloria

The results of previous studies outlining the effects of storms on the sediment transport system within Long Island Sound include the work of Bokuniewicz and Gordon (1980), studies by McCall (1978), Aller and Cochran (1976), Morton and Miller (1980), and Bohlen (1982), and summaries of the in-progress FVP work. These investigations have shown that the sediment-water interface in the Sound is relatively stable and, for the most part, in equilibrium with the prevailing tidal stream. Disequilibrium can be introduced by disposal-related variations in water depth or a storm-induced increase in boundary shear stress associated with the surface wave field. These studies suggest that the latter effects should be most pronounced inshore of the 25 m isobath. The magnitude of wave-related effects would vary primarily in response to wind direction, with speed and duration representing secondary

contributing factors. Due to the orientation and configuration of Long Island Sound, maximum effects would occur during storm events with winds dominated by easterly or westerly components.

The observed response of the sediment-water interface to energies associated with the passage of Hurricane Gloria supported the findings from the bathymetry and REMOTS® surveys at the CLIS site as well as the earlier findings that the hurricane effects at water depths greater than 25 m were negligible. It also provided additional data to support the hypothesis that, within the eastern Sound, a near-equilibrium prevails between the transport competence of the ambient tidal stream and the erodibility of the surface of the sediment column. Although some amount of alternate resuspension and deposition occurs during each half tidal cycle, major sediment displacements sufficient to measurably disturb the sediment-water interface require a significant supplement to the energies associated with ambient tidal flows. Such energies could be supplied by perturbations sufficient to alter the local tidal regime and/or to generate significant surface waves. The passage of Hurricane Gloria resulted in both effects. However, the short-lived nature of this storm resulted in a temporal separation between these two effects such that a significant disturbance was not produced at the sediment-water interface.

The observed variations in the near-bottom water temperature pattern appear to be primarily the result of a perturbation in the local tidal regime produced by storm passage rather than simple storm-associated mixing of the water column. Average air temperature on 27 September, the day of storm passage, was essentially similar to that observed on the days both before and after the storm (Table 3-5). If mixing were dominant, then the spatial scale of the storm should have resulted in a near homogeneity in water temperatures throughout the Sound and over much of the adjacent continental shelf. Under such conditions, the range of water temperatures observed following storm passage should have been suppressed relative to those existing before the storm. As noted above, water temperature patterns after 0600 EDST on 29 September were essentially similar to those observed prior to the storm. Thus, despite the obvious presence of an extremely energetic wind field and associated surface waves, the temperature perturbations appeared to be primarily associated with the storm-induced variations in the tidal system or storm surge rather than simple response to increased vertical mixing of the water column.

As in the case of the water temperature field, the variations in near-bottom salinity associated with the passage of Hurricane Gloria also appeared to be primarily the result of storm-related perturbations in the tidal field rather than simple mixing of the vertical water column. Beyond 29 September, the variations in salinity appeared similar in magnitude to those observed during

the pre-storm period; the longer term, lower frequency trends were simply related to varying streamflow inputs. Such data provided little indication of any tendency for the storm to produce large spatial scale homogeneity.

The effects of storm-associated surface wave generation were essentially confined to the period of storm passage (≈12 hours) by the geomorphology of Long Island Sound. The long, narrow configuration and the east-west orientation of this basin limit significant wave generation to a relatively well-defined range of wind conditions. These conditions were satisfied during the initial stages of Gloria when south to southeasterly winds prevailed. For the eastern Sound, these wind directions result in relatively large overwater distances, or fetch, favoring maximum wave generation. As the storm proceeded to the north, however, fetch progressively decreased with the wind shift to the southwest. As a result, kinetic energy levels associated with the surface wave field also decreased, reducing the transport competence of the local velocity field. In the absence of these supplemental energies, materials suspended during storm passage settled rapidly, and ambient suspended material concentrations quickly returned to pre-storm levels.

The response of the suspended material field to the storm-associated perturbations of the local tidal system appeared to consist of two primary elements. First the surge-associated retardation of the tidal stream affected both current speed and direction, modifying the interaction between these flows and those induced by the local surface wave field. The net result of this modification was reflected in the well-defined, discrete character of the storm-associated peak in near-bottom suspended material concentrations. This rapid increase in concentration was clearly representative of a system in which transport energies were confined to the storm period and were abruptly terminated following storm passage. Such a response appeared consistent with both the surface wave and current speed data. The virtual absence of factors other than wave-current interactions sufficient to contribute to the storm perturbation makes this a particularly valuable set of data for any efforts to analytically model sediment resuspension in the Sound.

In addition to modifying wave-current interactions, storm-associated perturbations in the local tidal system also altered the tidal height and phase relations. These perturbations were most likely responsible for the secondary peak in near-bottom suspended material concentrations which was observed approximately 12 hours after the direct storm peak. As noted, this secondary peak appeared to be the result of offshore advection of materials suspended during the storm within the inshore areas. The fact that this secondary spike was essentially coincident with the increase in velocity levels and displays maximum suspended sediment concentrations that were independent of peak current speeds tends

to support this supposition. However, these materials could also represent sediment normally in suspension that was deposited during the period of unusually low tidal currents following passage of the storm. Recalling the near-equilibrium hypothesis discussed above, these materials should be particularly susceptible to resuspension following restoration of "normal" tidal current levels. Although additional work is required to resolve the particular cause of this secondary peak, one fact is certain. Its presence was real and not simply associated with direct storm-induced resuspension.

5.0 SUMMARY AND CONCLUSIONS

In the Central Long Island Sound disposal site, the results of the post-storm REMOTS® survey indicate that hurricane-induced redistribution of the top few centimeters of surface sediments was widespread. Evidence of disturbance of the sediment-water interface, such as mud clasts, shell lag deposits, exposed worm tubes and truncated RPD layers was apparent in many of the REMOTS® images (Figures 5-1 and 5-2). However, it must be emphasized that this sediment redistribution was limited in extent to a rather small interval at the sediment-water interface (Table 4-3). The evidence of bottom disturbance generally was limited spatially to the central portions of the disposal mounds. Volume calculations revealed that only one mound (CS-1) experienced a loss of material detectable through precision bathymetry (Table 3-1). This disposal mound was the most recently used CLIS disposal point. The post-storm CLIS transect, extending from the New Haven harbor entrance to the CLIS disposal area, revealed extensive spatial evidence of bottom disturbance in water depths shallower than the CLIS site. There was no indication of any storm-induced disturbance at depths greater than 21 meters.

It is interesting to compare the effects of Hurricane Gloria to an earlier storm which occurred during the DAMOS program, Hurricane David. These two storms displayed significantly different characteristics, with David passing inshore favoring the generation of westerly winds and Gloria crossing the Sound from offshore resulting in southerly winds. In addition, Gloria was generally a more energetic storm. Despite these differences, however, both systems had some effect on the Central Long Island Sound disposal site. Effects from both storms appear to have been confined primarily to the shallower depths (i.e., the apex) of the respective sediment mounds. Although a simple explanation for the cause of these effects is complicated by the differences in sediment type and the dredged material residence time in-place when the two different storms occurred, the resulting response appears to have been largely the result of variations in the magnitude of the sediment boundary shear stress. The important finding from this recent study is that while Hurricane Gloria created perturbations to the normal tidal regime that were short-lived, it did not produce conditions that would cause major movement of

sediment and compromise the containment character of the CLIS site.

It would be difficult to accurately predict a priori the effect of the passage of a major storm (like Gloria or David) on the sediment-water interface. The stage of the tide and the direction of the wave regime will have a profound effect on the amount of shear stress encountered at the bottom. Sites that are fetch-limited in the direction of the storm-generated waves will not experience the full potential of a major storm for resuspension and transport of the bottom sediment. The stage of the tide will control the magnitude of near-bottom current velocities and, again, affect the resuspension and transport of sediment. The depth, sediment type, and benthic faunal assemblage would further complicate any attempts to estimate the overall effect of a major storm on a particular disposal site. Newly disposed dredged material, which has had little time to undergo consolidation and smoothing, will also experience greater resuspension than material deposited at an earlier time; conversely, areas of the seafloor with dense, sediment-binding tubicolous assemblages will be more resistant to erosional processes.

Overall, the disposal mounds at CLIS did experience local redistribution of the top few centimeters of bottom sediment but not to an extent that jeopardized the integrity of the containment characteristics of the disposal site. The effects of low frequency and short duration of major storms like Gloria did not violate the underlying management assumptions that the Long Island Sound disposal sites are containment areas and that the sediment caps on disposal mounds have remained physically intact.

6.0 REFERENCES

Bohlen, W. F. 1979. Long Island Sound and Block Island Sound Tidal Current Charts. US Dept. of Commerce. National Oceanic and Atmospheric Administration. National Ocean Survey. Rockville, MD. 36pps.

Bohlen, W. F. 1982. In-situ monitoring of sediment resuspension in the vicinity of active dredge spoil disposal sites. Proc. of Oceans '82 MTS/IEEE Conference, Washington, DC. pp. 1028-1033

Bokuniewicz, H. J. and R. B. Gordon. 1980. Storm and tidal energy in Long Island Sound. In: Advances in Geophysics, Vol. 22 (B. Saltzman ed). pp. 41-67.

Hurlbert, S. H. 1984. Pseudoreplication and the design of ecological field experiments. Ecological Monographs 54: 187 - 211.

McCall, P. L. 1977. Community paterns and adaptive strategies of the infaunal benthos of Long Island Sound. J. Mar. Res. 35: 221-266.

McCall, P. L. 1978. Spatial and Temporal Distributions of Long Island Sound Infauna: The role of bottom disturbance in a Near-shore Marine Habitat. In: Estuarine Interactions (M. Wiley ed). Academic Press, NY. pp. 191-219.

Morton, R. W. and M. C. Miller. 1980. Stamford-New Haven disposal operation. Monitoring Survey Report #7. Prepared by Science Applications Inc., Newport, RI for New England Division, US Army Corps of Engineers, Waltham, MA. 23pps.

NOS. 1985. Tidal Current Tables. Atlantic Coast of North America. U.S. Department of Commerce. National Oceanic and Atmospheric Administration. National Ocean Service.

Plumb, R. H. 1981. Procedures for handling and chemical analysis of sediment and water samples. Technical Report EPA/CE-81-1.

Rhoads, D. C. and L. F. Boyer. 1982. The effects of marine benthos on physical properties of sediments. In: Animal-Sediment Relations (P.L. McCall & M.J.S. Tevesz, eds.). Plenum Press, New York. pp. 3-52.

SAIC. 1985. Standard operating procedure manual for DAMOS monitoring activities. DAMOS Contribution #48. SAIC Report # SAIC-85/7516&C48.

SAIC. 1986. Seasonal monitoring cruise at the New London Disposal Site, July 1986. DAMOS Contribution #60. SAIC Report # SAIC-86/7540&C60.

Sanders, H. L. 1956. Oceanography of Long Island Sound, 1952-1954. X. The biology of marine bottom communities. Bull. Bing. Oceanogr. Coll. 15: 345-414.

Table 2-1

Summary of Diver Survey Operations at the CLIS Site

DATE	SITE	DIVERS	METERS	START TRANSECT	FINISH TRANSECT
08/13/85	STNH-N	Auster	20.73	26544.2	26544.5
		Paquette		44000.5	44000.2
08/13/85	STNH-S	Shepard	22.86	26541.9	26541.7
		Moreland		43994.2	43993.7
08/13/85	CS-1	Auster	18.90	26555.8	26555.4
		Paquette		44001.4	44001.2
08/13/85	CS-2	Shepard	18.60	26556.7	N/A
		Moreland		44004.5	
08/14/85	FVP	Auster	21.65	26534.9	26535.3
		Shepard		43999.6	43999.7
08/14/85	FVP	Auster	19.51	26535.2	26534.6
		Moreland		43999.7	43999.3

N/A indicates that the final position of the transect was not recorded correctly.

Table 3-1

Volume Difference Calculations
for CLIS Disposal Sites
in August and October 1985

Site	Volume Change*(m^3)	95% Confidence Limits (lower)	(upper)
STNH-N	+3,870	-1,180	+9,620
STNH-S	-3,520	-10,700	+3,660
MQR	-3,930	-11,900	+4,050
CS-1	-15,390	-22,570	-8,210
CS-2	+5,240	-1,940	+12,420
FVP	+50	-4,410	+4,520

*Positive(+) values indicate addition of material in October. Negative(-) values indicate loss of material in October.

Table 3-2

Central Long Island Sound Disposal Site
Results of Chemical Analysis (ppm) of Sediment
CLIS-SE

	Hg	Pb	Zn	Fe	Cd	Cr	Cu	Ni	C:N	O&G
300N/100W										
-1	0.13	40	148	27,600	BDL*	60	72	35	10.1	513
-2	0.09	36	134	25,400	2.0	51	63	37	9.6	611
-3	0.12	40	140	27,300	0.4	52	68	34	9.4	776
Center										
-1	0.10	64	152	26,300	1.6	64	88	37	12.2	807
-2	0.15	64	143	26,300	2.9	53	68	36	9.0	1880
-3	0.17	73	146	29,400	2.3	53	61	37	11.6	454
100S/300W										
-1	0.09	48	132	27,600	2.8	48	56	34	9.6	755
-2	0.12	50	130	25,300	2.9	50	54	34	9.4	494
-3	0.07	60	147	26,600	2.4	56	76	34	9.4	443
Reference										
-1	0.81	43	130	26,100	0.8	47	51	35	9.2	502
-2	0.05	47	118	24,900	1.2	43	51	32	9.9	503
-3	0.02	44	123	25,300	0.8	58	48	27	9.0	616

*BDL = Below Detection Limit

TABLE 3-3.
Benthic Community Analysis At CLIS-SE, August 1985
(0.1 m² grabs sieved to 0.5 mm)

	CENTER			100S-300W			300N-100W			REF		
	1	2	3	1	2	3	1	2	3	1	2	3
CNIDARIA												
Ceriantheopis americanus	7	6	2	2	1	2	6	6	5	6	8	5
Edwardsia elegans	1	.	.	1	1	2	5	8	.	3	2	1
PLATYHELMINTHES												
Platyhelminthes sp.	.	.	.	.	.	.	.	2	.	1	.	.
RHYNCHOECOELA												
Cerebratulus lacteus	.	.	.	.	.	.	.	.	1	.	.	.
Tubulanus pellucidus	46	37	43	29	43	40	52	46	44	25	31	33
MOLLUSCA												
GASTROPODA												
Acteocina canaliculata	.	.	1	2	.	1	8	8	18	12	6	12
Cingula aculeus	1	.	.	.	.	4	.	.	.	.	.	1
Hydrobia sp.	3	1	1	.	.	7	.	2	3	.	.	4
Lunatia heros	.	.	.	.	.	1	.	1	12	.	.	1
Mitrella lunata	.	.	.	.	.	.	.	1	.	.	.	.
Nassarius trivitatus	4	6	.	3	2	3	1	3	.		1	.
Odostomia A	.	6	2	.	.	5	.	2	1	.	1	2
Turbonilla interrupta	4	19	2	1	.	10	.	3	.	3	5	7
BIVALVIA												
Lyonsia hyalina	.	.	.	.	.	.	.	.	.	.	1	1
Macoma tenta	5	2	.	1	.	.	.	1	4	.	.	.
Mulinia lateralis	.	1	1	7	.	.	3	.	5	.	.	.
Nucula annulata	592	526	797	383	665	1083	767	707	903	1162	882	973
Pandora gouldiana	.	2	.	.	5	1	1	.	.	.	.	.
Periploma papyratium	.	2	.	.	.	.	.	.	1	.	.	1
Yoldia limatula	17	16	19	18	24	18	49	12	56	55	33	29
CRUSTACEA												
Ampelisca abdita	1	1	3	.	1	.	1	4	11	.	16	.
Cancer irroratus	.	.	.	.	.	2	.	.	.	.	2	.
Corophium insidiosum	.	.	.	1	.	.	.	.	.	.	.	.
Crangon septemspinosa	.	.	.	1	.	.	.	.	.	.	1	1
Hutchinsoniella macracantha	2	.	1	1	3	1	8	4	7	8	7	.
Microdeutopus anomalus	.	.	.	.	.	.	.	1	.	.	.	.
Parametopella cypris	.	.	.	.	.	.	.	1	.	.	.	.

TABLE 3-3. Continued.

	CENTER			100S-300W			300N-100W			REF		
	1	2	3	1	2	3	1	2	3	1	2	3
POLYCHAETA												
Asychis elongata	.	.	2	1	.	.	4	.	.	.	.	.
Clymenella spp.	1	1	.	3	4	1	5	4	4	2	2	.
Cossura longocirrata	22	199	377	78	35	125	126	84	58	5	5	53
Glycera americana	.	.	.	.	.	.	.	.	.	1	.	1
Mediomastus ambiseta	101	187	262	106	47	184	189	135	119	46	31	69
Melinna cristata	6	6	17	13	6	8	7	7	13	2	5	
Nephtys incisa	90	104	110	70	86	111	146	91	144	86	112	97
Ninoe nigripes	.	.	.	.	.	.	.	.	.	1	1	.
Owenia fusiformis	3	3	.	.	4	1	5	7	.	.	.	.
Paranaitis speciosa	.	.	.	.	.	.	.	1	.	.	.	.
Paraonis gracilis	22	45	34	19	22	18	54	37	52	39	35	23
Pherusa affinis	4	.	.	.	.	6	2	4	5	.	3	.
Polydora ligni	.	.	.	.	.	.	.	2	.	.	.	.
Prionospio malmgreni	.	.	1	3	2	3	.	3	.	.	.	1
Sigambra tentaculata	19	13	16	2	15	13	19	58	14	7	11	16
Spiochaetopterous oculatus	.	1	.	.	.	.	.	1	.	.	.	2
Spio filicornis	8	10	9	3	6	18	22	14	21	6	5	4
Syllis sp.	.	.	.	.	.	2	.	.	.	.	.	.
Tharyx sp.	5	5	15	6	2	8	16	15	7	2	.	3
OLIGOCHAETA												
Oligochaeta spp.	148	233	304	46	53	42	177	122	44	177	93	101
PHORONIDA												
Phoronis muelleri	1	1	.	.	1	.	2	1	4	1	.	.
HEMICHORDATA												
Saccoglossus kowalevskii	1	.	.	1	.	2	3	1	1	.	.	.
Species/sample	26	27	22	27	23	30	28	37	27	23	26	26
Species/station		35			37			43			36	
Individuals/sample	1114	1434	2019	802	1029	1596	1683	1400	1557	1654	1304	1453
Individuals/station		4567			3427			4679			4411	

Table 3-4

Summary of Megafaunal Species and Relative Abundances* Observed During Survey Dives Conducted at the CLIS Site

	STNH-N	STNH-S	CS-1	CS-2	FVP
Cnidaria					
Cerianthiopsis americanus		1			
Gastropoda					
Nassarius trivittatus	>100	>200	>100	>300	>400
Busycon carica	3	20		6	19
Decapoda					
Mysidacea	3-5/.25m^2	2-5/.25m^2	2-5/.25m^2	2-5/.25m^2	
Crangon septemspinosa					15
Libinia emarginata			4		
Cancer irroratus					>85
Pagurus longicarpus	>50		15		>200
Pagurus pollicarus					15
Homarus americanus			2		1
Ovalipes occelatus					15
Echinodermata					
Asterias forbesi	7				20
Pisces					
Paralichtys oblongus					4
Psuedopleuronectes americanus			1	2	2
Tautogolabrus adspersus			5		
Scophthalmus aquosus				1	

*Number of individuals seen by divers while documenting physical and biological characteristics.

Table 3-5

OCT 1985
BRIDGEPORT, CONNECTICUT
NAT'L WEA SER OFC
SIKORSKY MEM. AP. BRIDGEPORT

ISSN 0198-1153

LOCAL CLIMATOLOGICAL DATA

Monthly Summary

SIKORSKY MEMORIAL AIRPORT

LATITUDE 41°10 LONGITUDE 73°08 ELEVATION (GROUND) 7 FEET TIME ZONE EASTERN 94702

OCT 1985
BRIDGEPORT, CONNECTICUT

DATE	TEMPERATURE °F MAXIMUM	MINIMUM	AVERAGE	DEPARTURE FROM NORMAL	AVERAGE DEW POINT	DEGREE DAYS BASE 65°F HEATING (SEASON BEGINS WITH JULY)	COOLING (SEASON BEGINS WITH JAN)	WEATHER TYPES 1 FOG 2 HEAVY FOG 3 THUNDERSTORM 4 ICE PELLETS 5 HAIL 6 GLAZE 7 DUSTSTORM 8 SMOKE, HAZE 9 BLOWING SNOW	SNOW ICE PELLETS OR ICE ON GROUND AT 0700 INCHES	PRECIPITATION WATER EQUIVALENT (INCHES)	SNOW, ICE PELLETS (INCHES)	AVERAGE STATION PRESSURE IN INCHES ELEV. 17 FEET ABOVE M.S.L.	WIND (M.P.H.) RESULTANT DIR.	RESULTANT SPEED	AVERAGE SPEED	FASTEST MILE SPEED	FASTEST MILE DIRECTION	SUNSHINE MINUTES	PERCENT OF TOTAL POSSIBLE	SKY COVER (TENTHS) SUNRISE TO SUNSET	MIDNIGHT TO MIDNIGHT	DATE
1	2	3	4	5	6	7A	7B	8	9	10	11	12	13	14	15	16	17	18	19	20	21	22
01	77	54	66	5		0	1	1 8	0	0.00	0.0					16	20			3		01
02	72	58	65	4		0	0	1 8	0	0.04	0.0					16	34			9		02
03	59	53	56	-4		9	0	1	0	0.44	0.0					17	03			10		03
04	59	54	57	-3		8	0	1 8	0	T	0.0					15	05			10		04
05	70	55	63	3		2	0	23	0	0.58	0.0					21	24			10		05
06	64	49	57	-2		8	0		0	0.00	0.0					18	27			2		06
07	65	43	54	-5		11	0		0	0.00	0.0					17	23			2		07
08	68	44	56	-3		9	0		0	0.00	0.0					16	16			2		08
09	71	57	64	6		1	0		0	0.00	0.0					21	24			7		09
10	77*	60	69*	11		0	4	1 8	0	0.00	0.0					23	26			10		10
11	62	48	55	-3		10	0		0	0.00	0.0					24	35			0		11
12	58	40	49	-8		16	0		0	0.00	0.0					18	02			3		12
13	64	53	59	2		6	0	1 8	0	0.15	0.0					16	24			10		13
14	66	52	59	2		6	0	1 8	0	0.00	0.0					10	18			10		14
15	72	63	68	12		0	3	2 8	0	0.06	0.0					15	22			9		15
16	71	46	59	3		6	0		0	0.00	0.0					23	22			4		16
17	59	40	50	-6		15	0		0	0.00	0.0					14	24			1		17
18	65	42	54	-1		11	0	8	0	0.00	0.0					21	22			7		18
19	69	59	64	9		1	0	1 8	0	T	0.0					25	24			10		19
20	61	48	55	0		10	0		0	0.00	0.0					18	02			10		20
21	59	41	50	-4		15	0		0	0.00	0.0					14	10			4		21
22	59	39	49	-5		16	0		0	0.00	0.0					13	06			1		22
23	63	40	52	-2		13	0		0	0.00	0.0					14	07			0		23
24	69	45	57	4		8	0	1	0	0.20	0.0					17	06			9		24
25	69	52	61	8		4	0	1	0	0.01	0.0					22	28			2		25
26	65	41	53	0		12	0		0	0.00	0.0					17	28			0		26
27	68	45	57	5		8	0		0	0.00	0.0					26	25			8		27
28	59	42	51	-1		14	0		0	0.00	0.0					25	33			0		28
29	53	34	44	-8		21	0		0	0.00	0.0					21	36			3		29
30	52	33*	43*	-8		22	0		0	0.00	0.0					12	01			10		30
31	55	43	49	-2		16	0		0	0.00	0.0					23	07			8		31
SUM	SUM					TOTAL	TOTAL			TOTAL	TOTAL	FOR THE MONTH:						TOTAL	%	SUM	SUM	
2000	1473					278	8			1.48	0.0					26	25		FOR MONTH	174		
AVG.	AVG.	AVG.	DEP.	AVG.		DEP.	DEP.	NUMBER OF DAYS		DEP.						DATE: 27		POSSIBLE		AVG.	AVG.	
64.5	47.5	56.0	0.0			-7	2	PRECIPITATION		-1.85										5.6		

NUMBER OF DAYS				SEASON TO DATE		SNOW, ICE PELLETS		GREATEST IN 24 HOURS AND DATES			GREATEST DEPTH ON GROUND OF SNOW, ICE PELLETS OR ICE AND DATE
MAXIMUM TEMP.		MINIMUM TEMP.		TOTAL	TOTAL	> 1.0 INCH	0				
≥ 90°	≤ 32°	≤ 32°	≤ 0°	334	738	THUNDERSTORMS	1	PRECIPITATION	SNOW, ICE PELLETS		
0	0	0	0	DEP.	DEP.	HEAVY FOG	2	0.58	05	0.0	0
				0	-8	CLEAR 13	PARTLY CLOUDY 4		CLOUDY 14		

* EXTREME FOR THE MONTH - LAST OCCURRENCE IF MORE THAN ONE.
T TRACE AMOUNT.
+ ALSO ON EARLIER DATE(S).
HEAVY FOG: VISIBILITY 1/4 MILE OR LESS.
BLANK ENTRIES DENOTE MISSING OR UNREPORTED DATA.
LESS THAN 24-HOUR WEATHER WATCH FOR DATA IN COLUMN 8.

DATA IN COLS 6 AND 12-15 ARE BASED ON 21 OR MORE OBSERVATIONS AT HOURLY INTERVALS. RESULTANT WIND IS THE VECTOR SUM OF WIND SPEEDS AND DIRECTIONS DIVIDED BY THE NUMBER OF OBSERVATIONS. ONE OF THREE WIND SPEEDS IS GIVEN UNDER FASTEST MILE: FASTEST MILE - HIGHEST RECORDED SPEED FOR WHICH A MILE OF WIND PASSES STATION (DIRECTION IN COMPASS POINTS). FASTEST OBSERVED ONE MINUTE WIND - HIGHEST ONE MINUTE SPEED (DIRECTION IN TENS OF DEGREES). PEAK GUST - HIGHEST INSTANTANEOUS WIND SPEED (A / APPEARS IN THE DIRECTION COLUMN). ERRORS WILL BE CORRECTED AND NOTED IN SUBSEQUENT PUBLICATIONS.

I CERTIFY THAT THIS IS AN OFFICIAL PUBLICATION OF THE NATIONAL OCEANIC AND ATMOSPHERIC ADMINISTRATION, AND IS COMPILED FROM RECORDS ON FILE AT THE NATIONAL CLIMATIC DATA CENTER, ASHEVILLE, NORTH CAROLINA, 28801

Kenneth D Hadeen
DIRECTOR
NATIONAL CLIMATIC DATA CENTER

noaa NATIONAL OCEANIC AND ATMOSPHERIC ADMINISTRATION — NATIONAL ENVIRONMENTAL SATELLITE, DATA AND INFORMATION SERVICE — NATIONAL CLIMATIC DATA CENTER ASHEVILLE NORTH CAROLINA

Table 4-1
Comparison Chart of Selected Chemical Concentrations
CLIS - SE With CLIS-REF

Substance, ppm	Average CLIS-SE(n=9)	CLIS-SE Range	Average CLIS-REF 1980-1985	Range CLIS-REF 1980-1985
oil & grease, ppm	747	443-1880	204*	91-616*
zinc, ppm	141	130-152	182	108-323
lead, ppm	53	36-73	48	<22-69
chromium, ppm	54	48-64	73	43-121
copper, ppm	67	54-88	57	45-93

*Since 1982

Table 4-2

Summary statistics for boundary roughness values, RPD depths, and Organsim-Sediment Indices at the CLIS disposal sites in August and October, 1985. October values which are significantly different from August values are indicated by an * (Mann Whitney U-test, $p < .05$).

Boundary Roughness

SITE	AUGUST		OCTOBER		
	N	MEAN	N	MEAN	
STNH-N	43	.71	12	1.06	*
STNH-S	43	.66	12	.55	
CS-1	41	.81	11	1.74	*
CS-2	43	.88	12	.88	
MQR	32	.59	10	.71	
NORWALK	44	.72			
NH-74	43	.81			
NH-83	35	.67			
SE-CLIS	36	.53			
ClIS-REF	20	.76			

RPD depth

SITE	AUGUST		OCTOBER		
	N	MEAN	N	MEAN	
STNH-N	42	3.97	12	1.97	*
STNH-S	43	4.08	12	2.07	*
CS-1	41	4.02	11	2.97	*
CS-2	43	3.98	12	2.56	*
MQR	32	4.58	10	2.58	*
NORWALK	44	4.39			
NH-74	42	3.83			
NH-83	35	2.86			
SE-CLIS	36	6.09			
CLIS-REF	20	2.81			

Organism-Sediment Index

SITE	AUGUST		OCTOBER		
	N	MEAN	N	MEAN	
STNH-N	40	8.92	12	6.00	*
STNH-S	43	6.14	12	5.75	
CS-1	41	7.80	11	6.45	
CS-2	42	8.35	12	8.00	
MQR	32	7.00	10	5.10	*
NORWALK	44	8.09			
NH-74	42	7.97			
NH-83	35	6.34			
SE-CLIS	34	8.02			
CLIS-REF	20	7.30			

Table 4-3 Estimates of the extent of erosion at the CLIS disposal sites based on the loss of high-reflectance surface sediments (Redox layer).

	Mean depth (cm) of apparent Redox boundary			
SITE	JUNE	AUGUST	OCTOBER	Change in depth (cm)
FVP	2.65		2.21	0.4
STNH-N		3.97	1.97	2.0
STNH-S		4.08	2.07	2.0
CS-1		4.02	2.97	1.0
CS-2		3.98	2.56	1.4
MQR		4.58	2.58	2.0

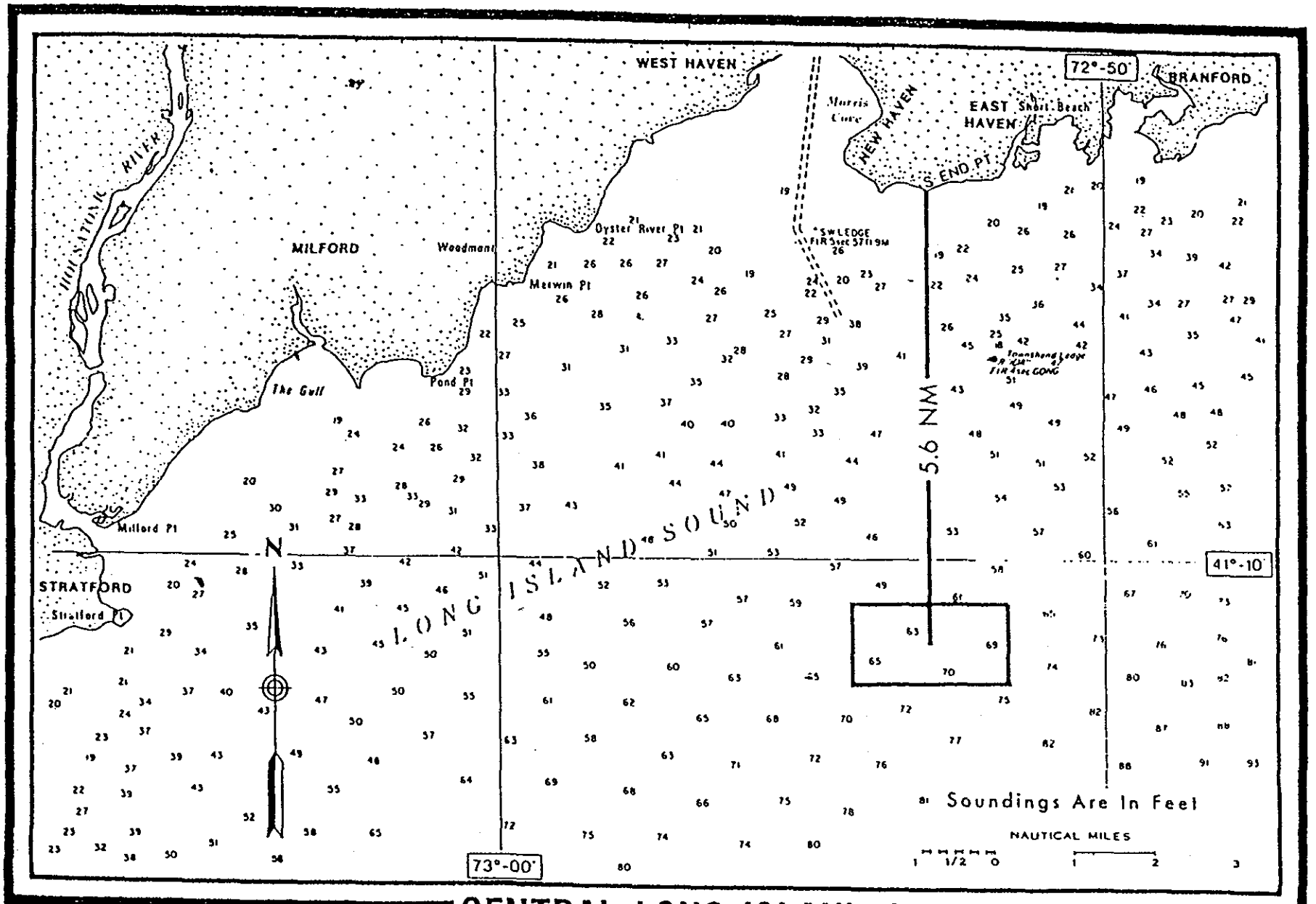

Figure 1-1 Central Long Island Sound (CLIS) Disposal Area.

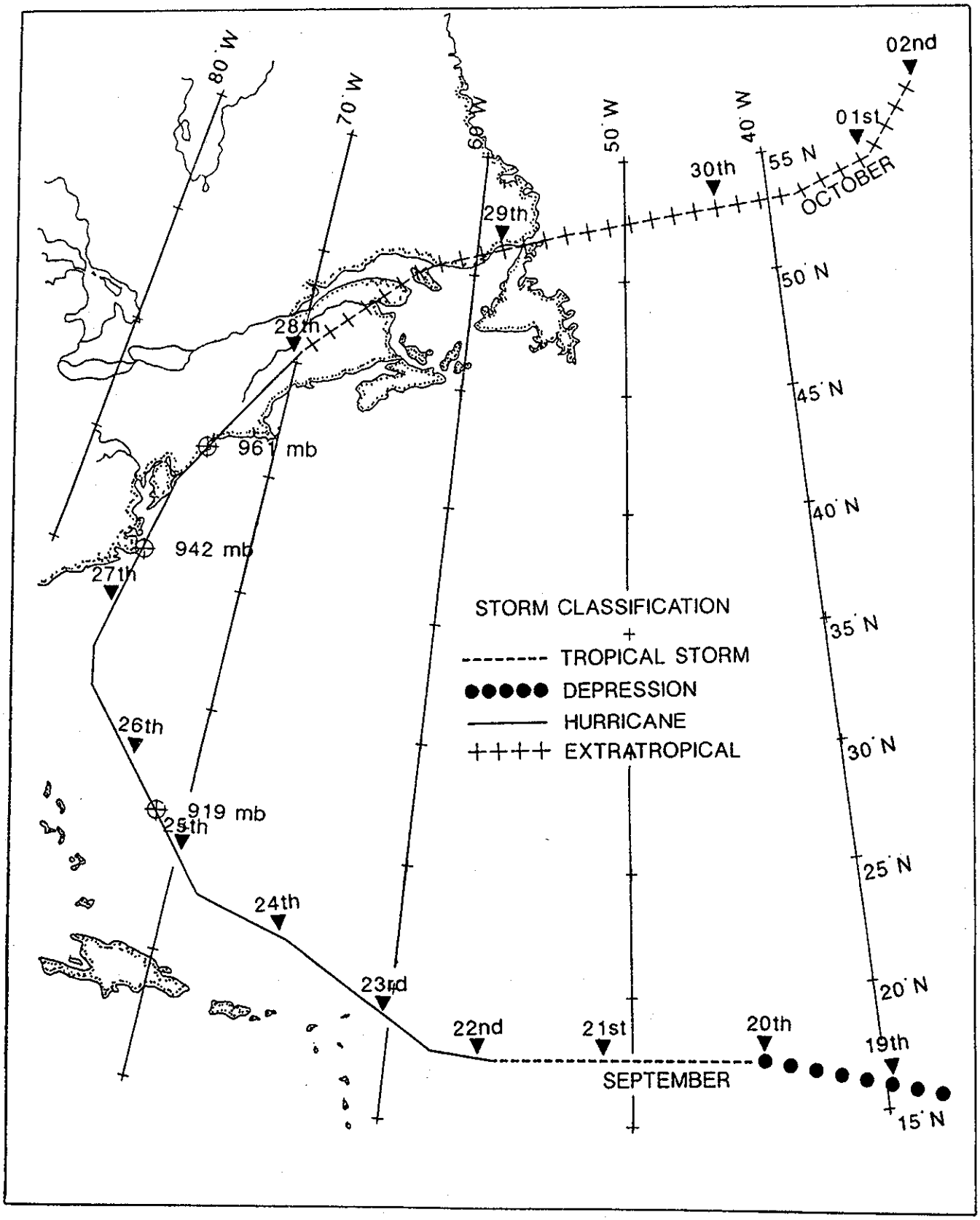

Figure 1-2 Hurricane Gloria storm track.

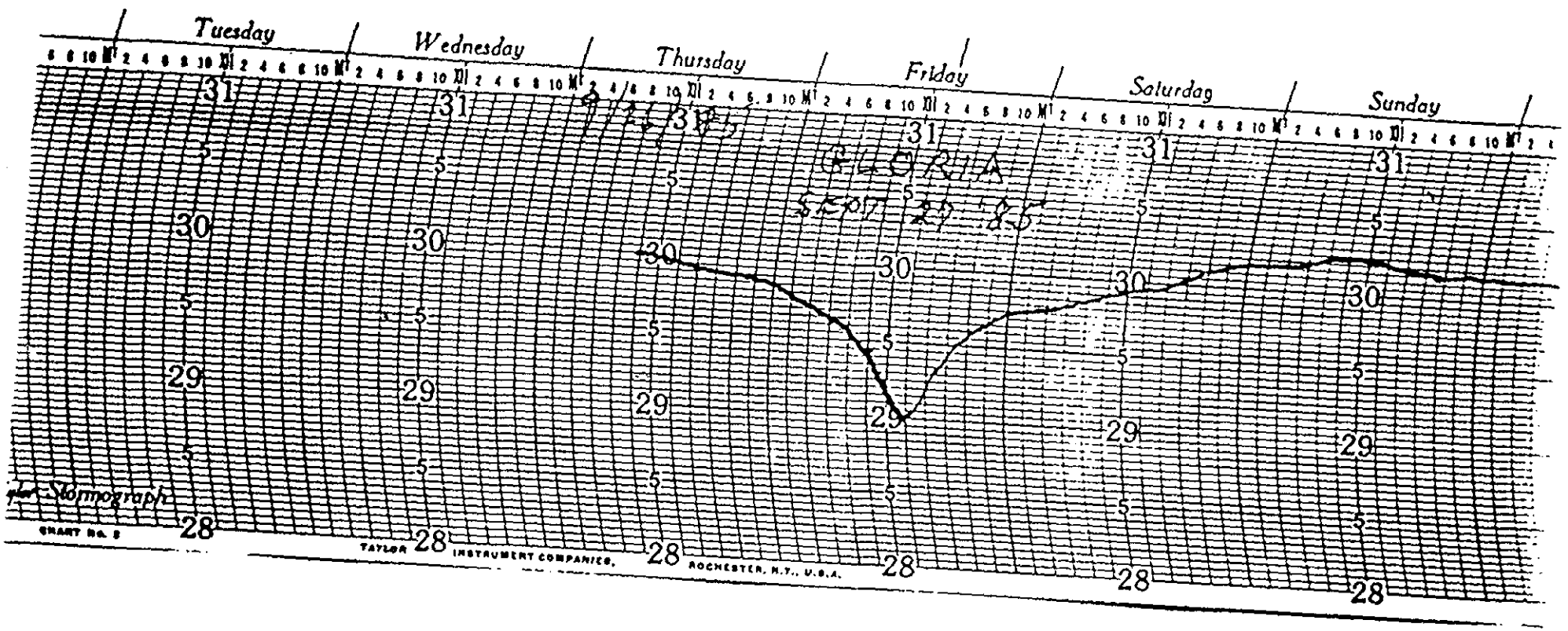

Figure 1-3 Barometric pressure record at Avery Point, Groton, CT. September 24-29, 1985.

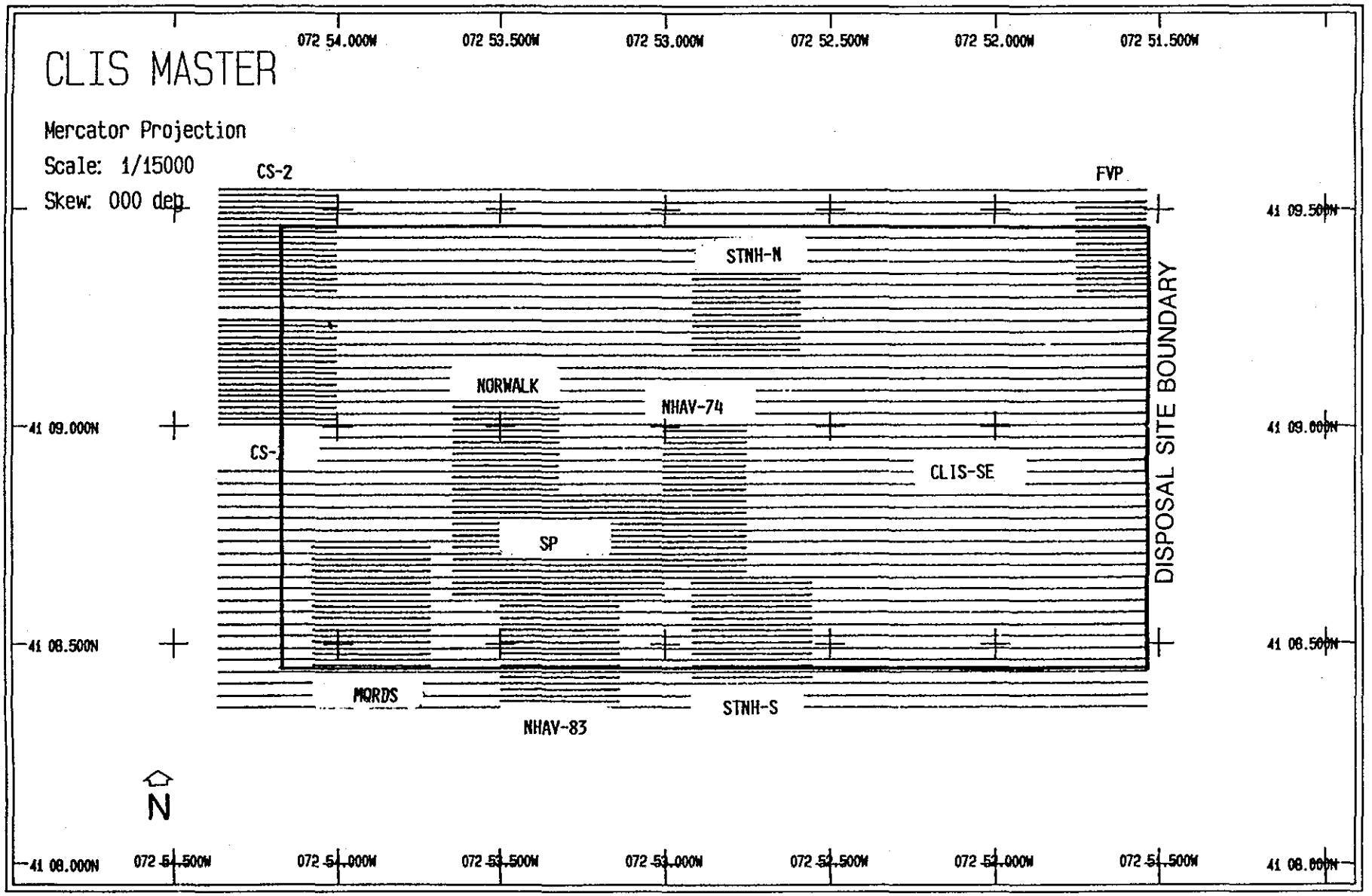

Figure 2-1 Bathymetric survey lanes for Central Long Island Sound (CLIS) Disposal Site and Mounds.

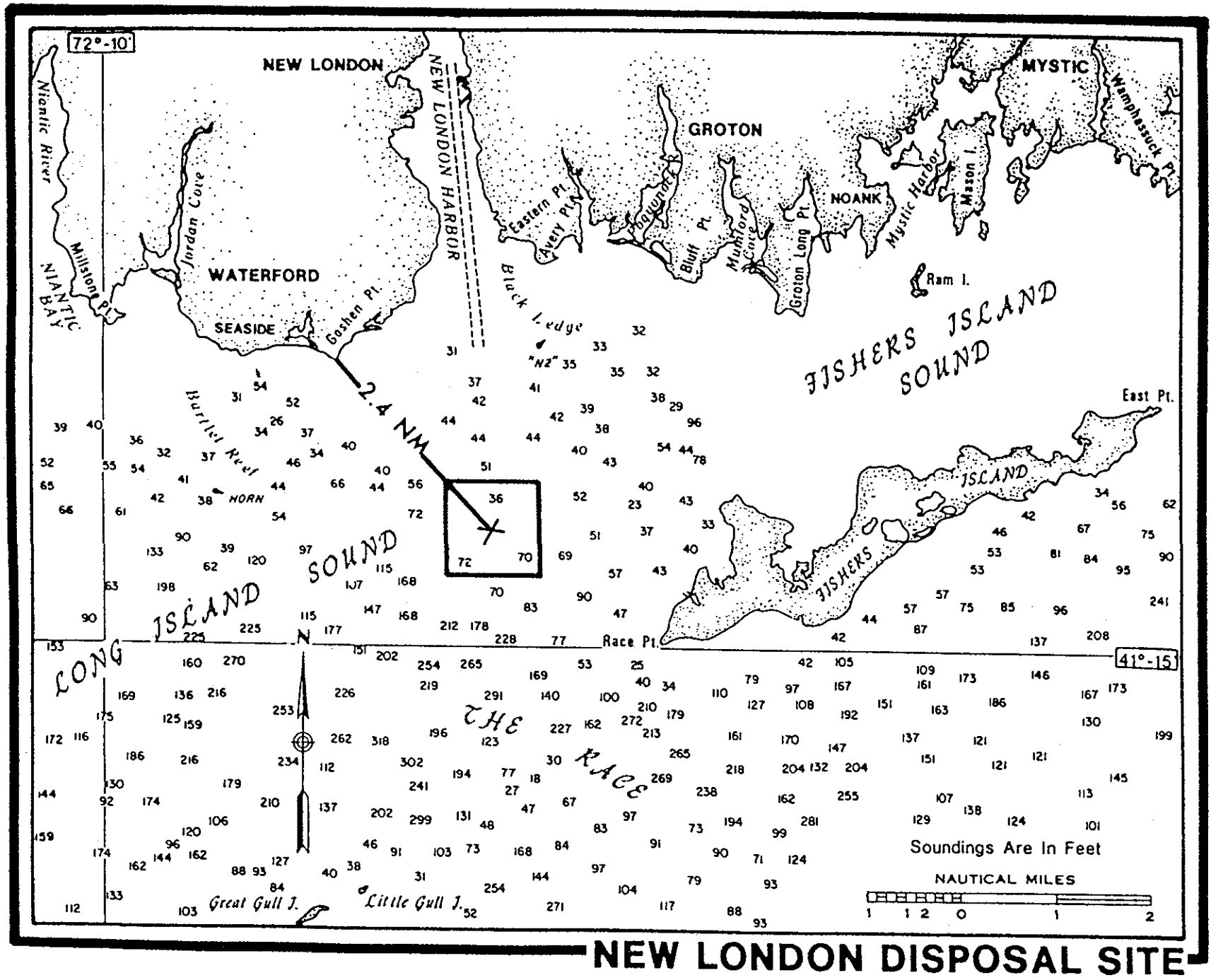

Figure 2-2 Location (X) of Instrumentation Array Deployment Site.

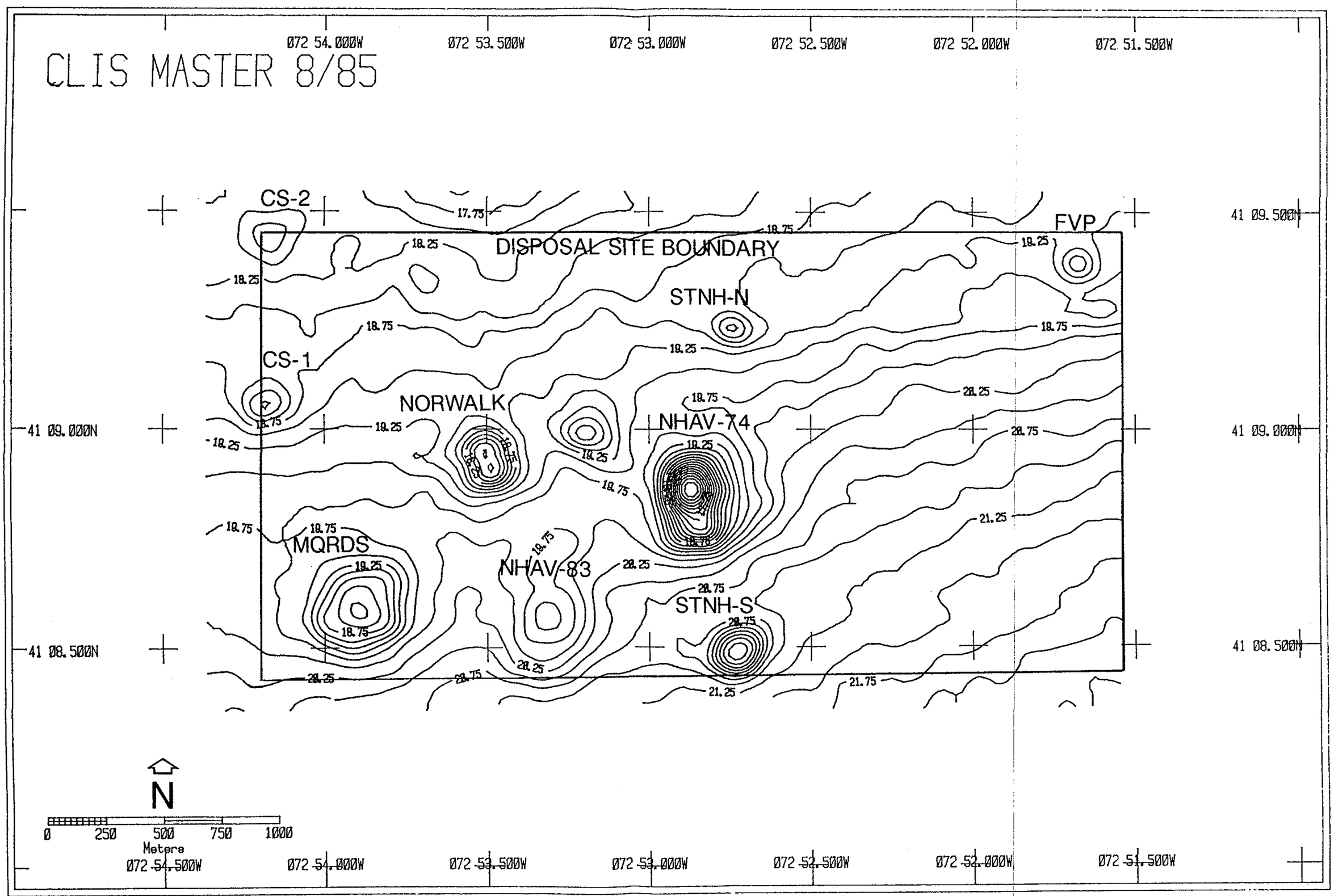

Figure 3-1 Contour bathymetric chart of CLIS Disposal Site, August 1985.

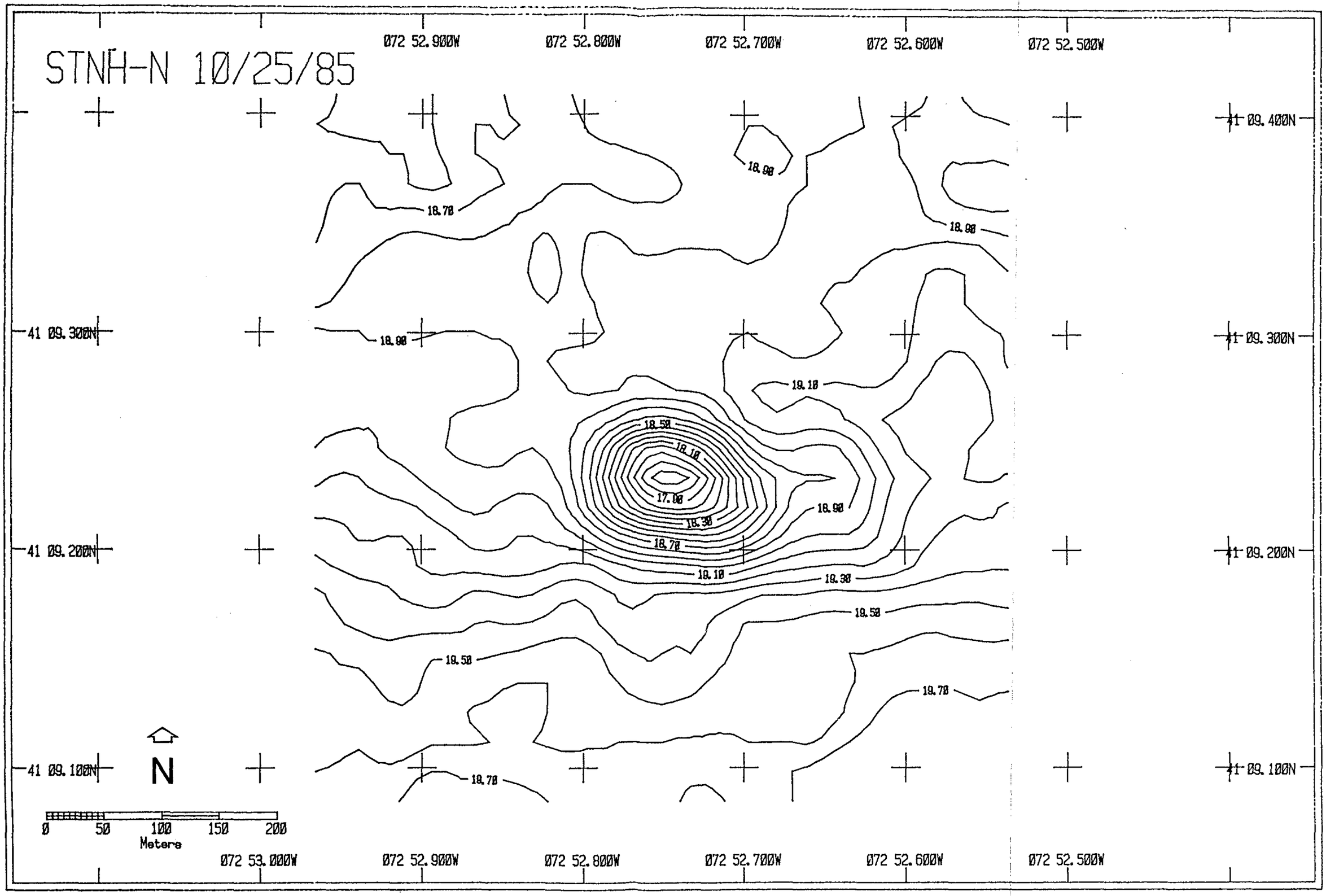

Figure 3-2 Contour bathymetric chart at STNH-N, October 1985.

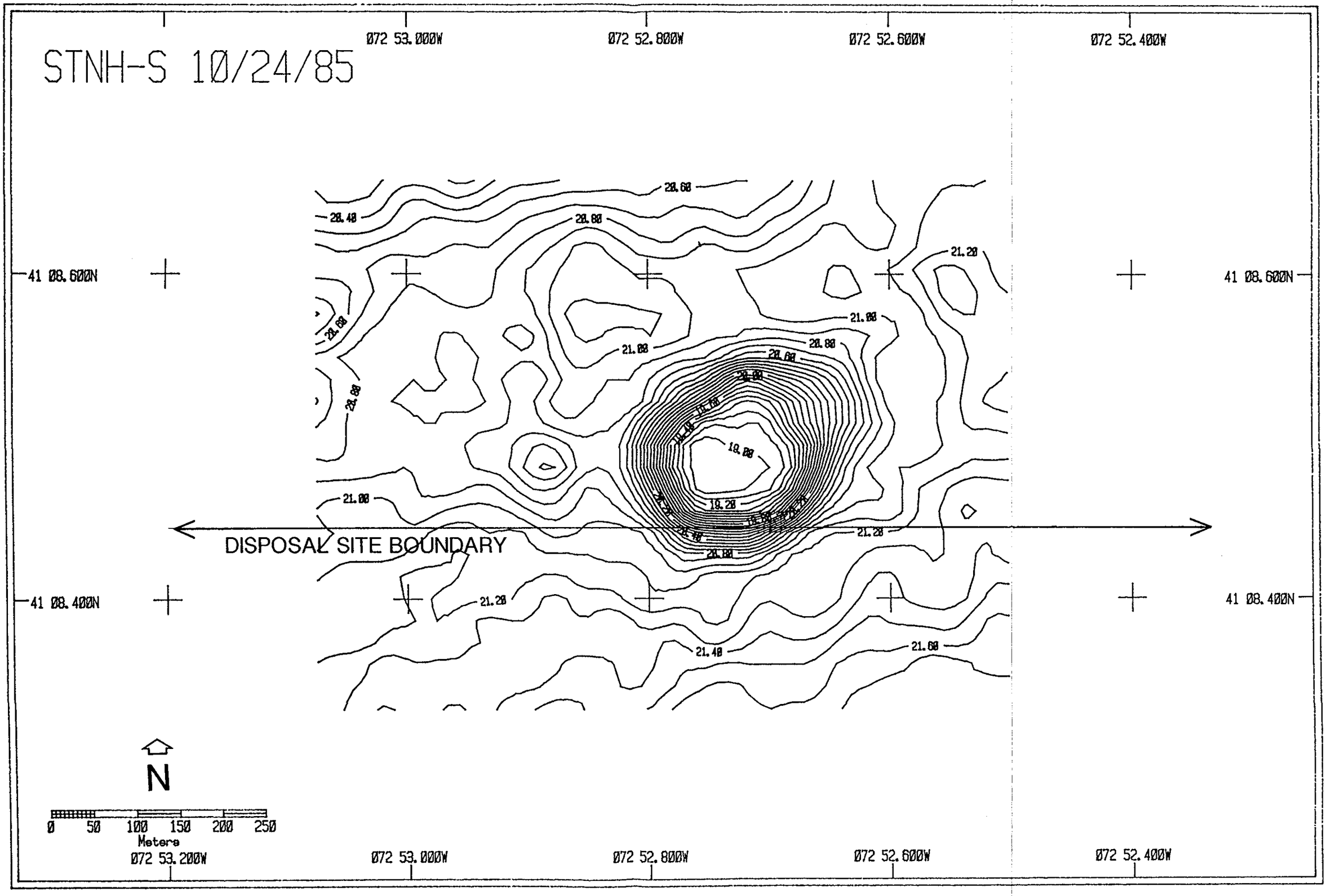

Figure 3-3 Contour bathymetric chart at STNH-S, October 1985.

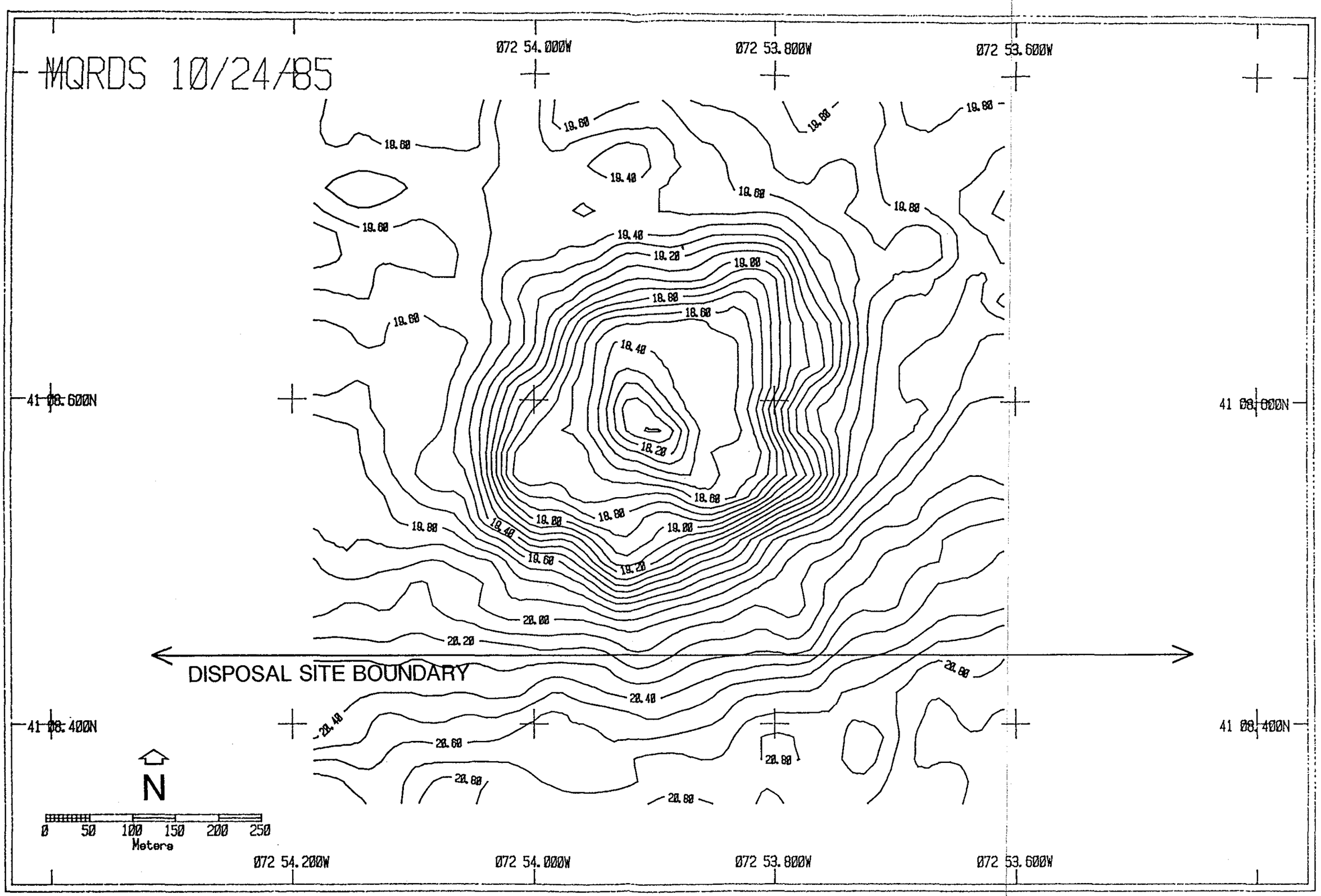

Figure 3-4 Contour bathymetric chart at MQR, October 1985.

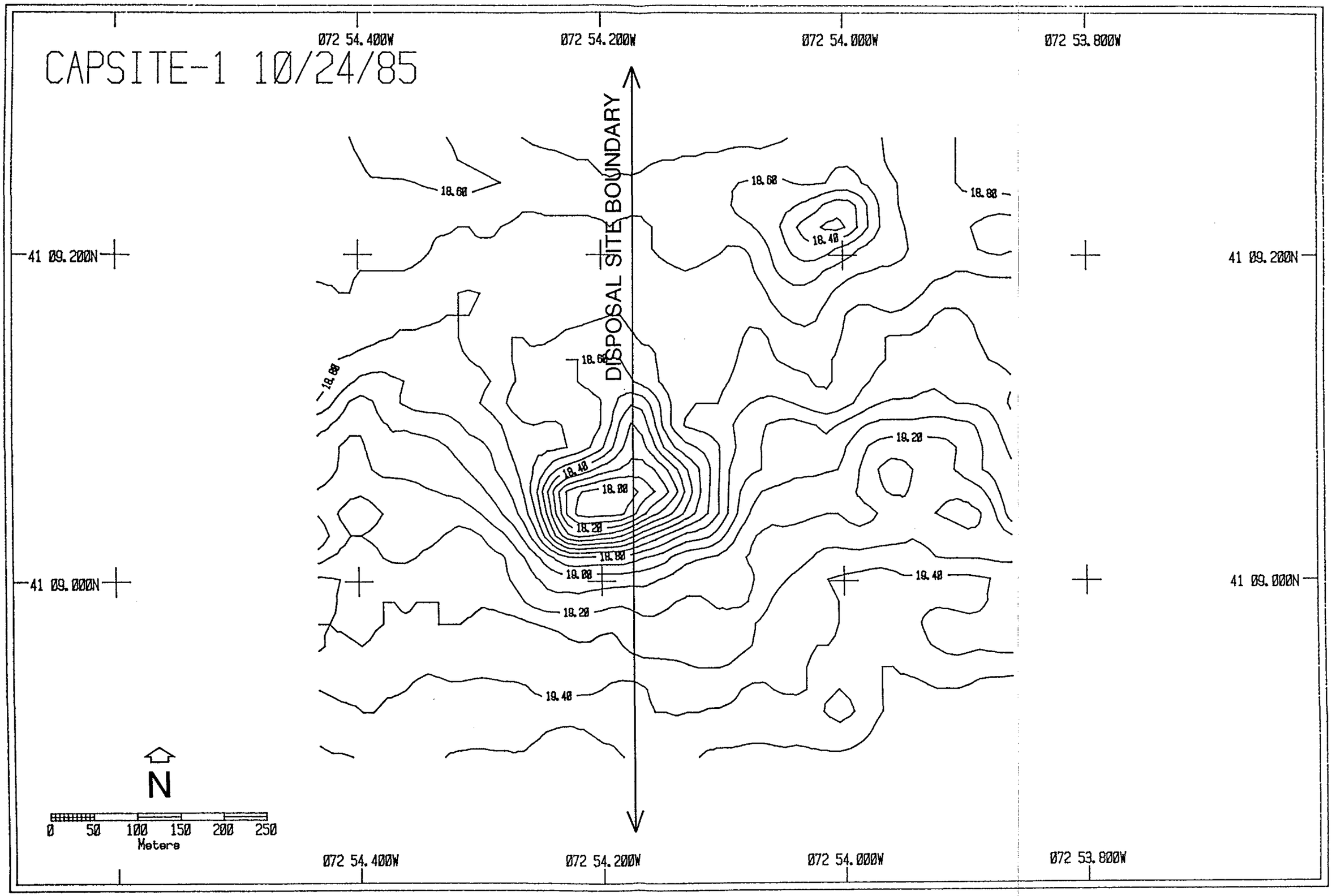

Figure 3-5 Contour bathymetric chart at CS-1, October 1985.

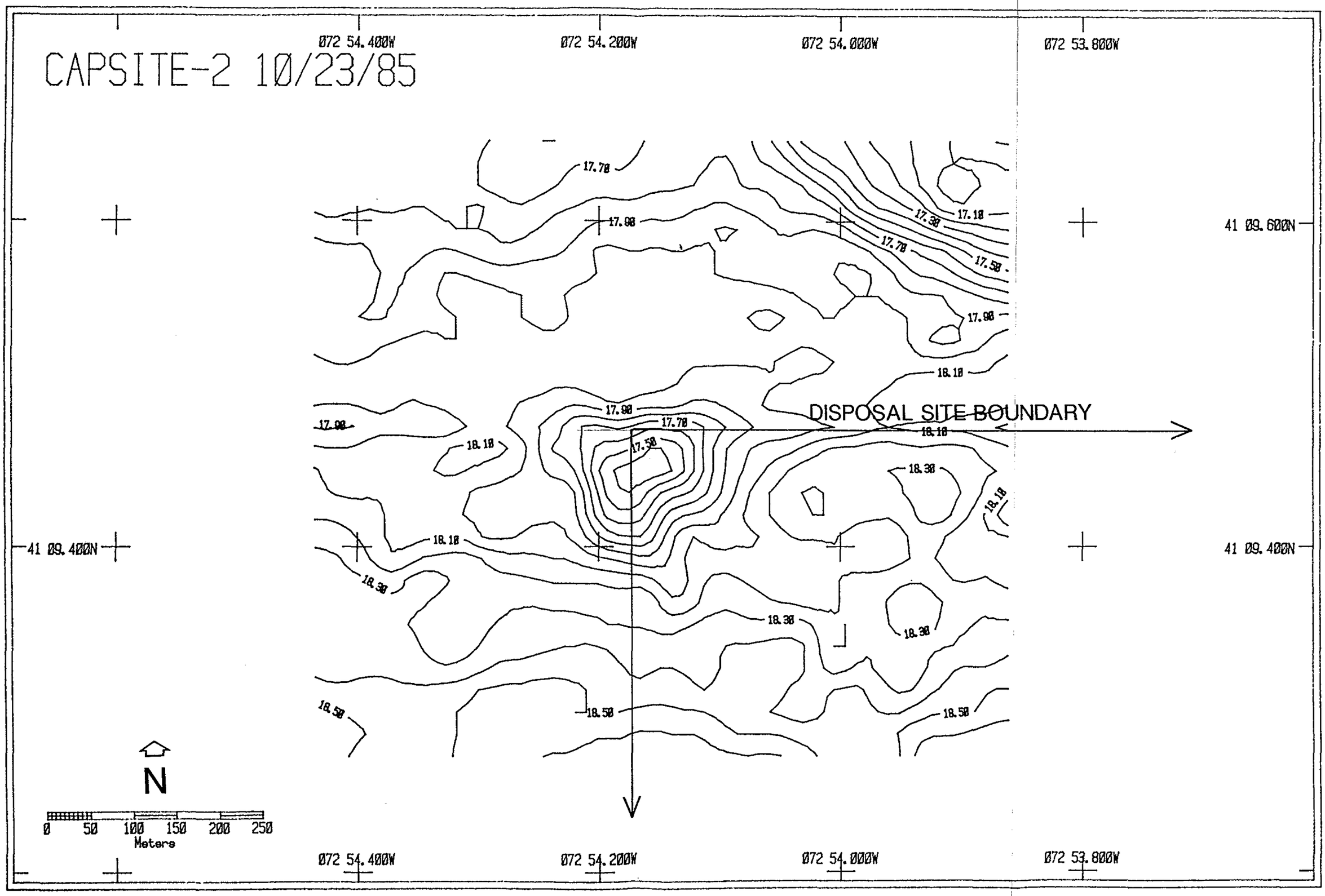

Figure 3-6 Contour bathymetric chart at CS-2,October 1985.

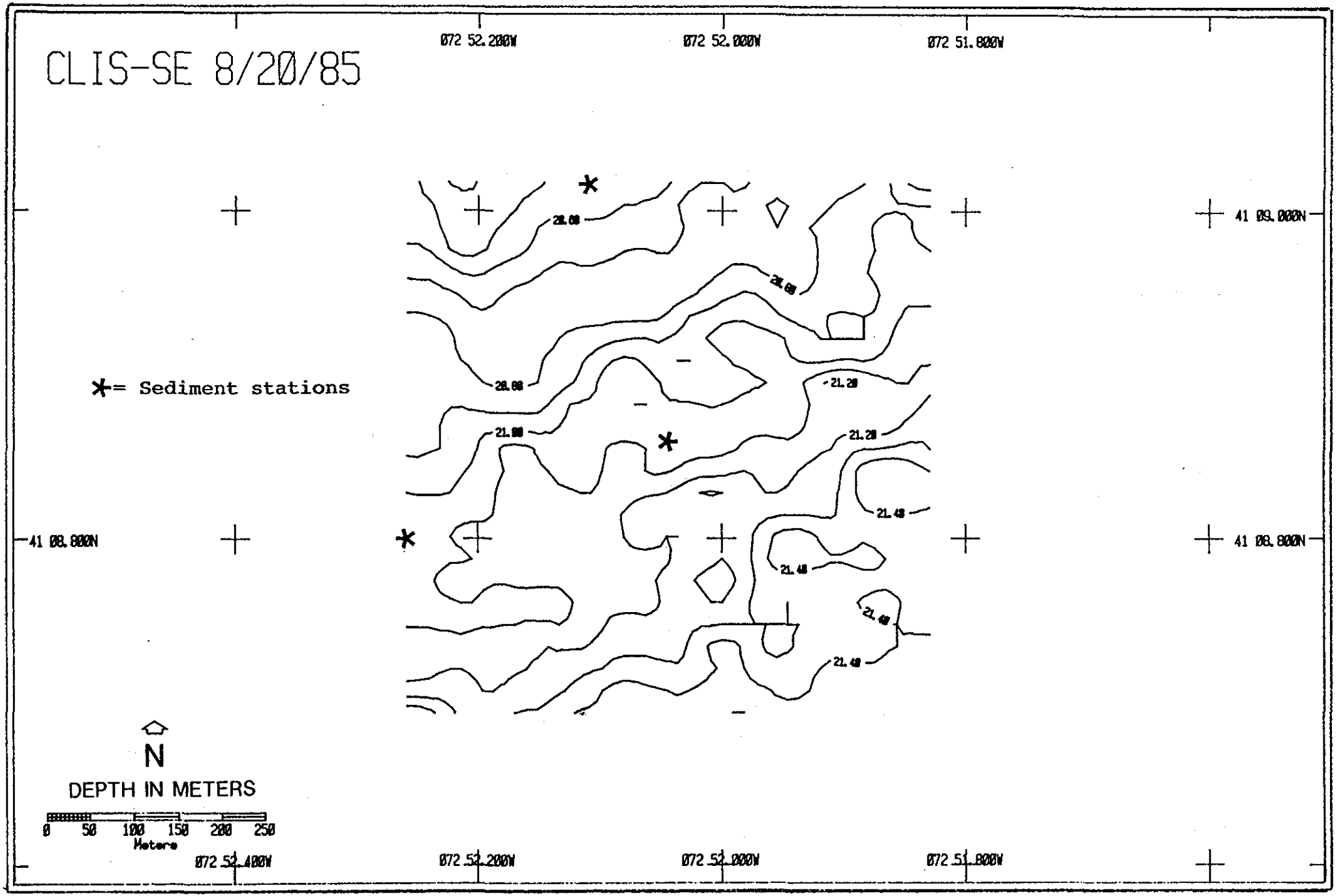

Figure 3-7 Contour bathymetric chart at CLIS-SE with sediment stations, August 1985.

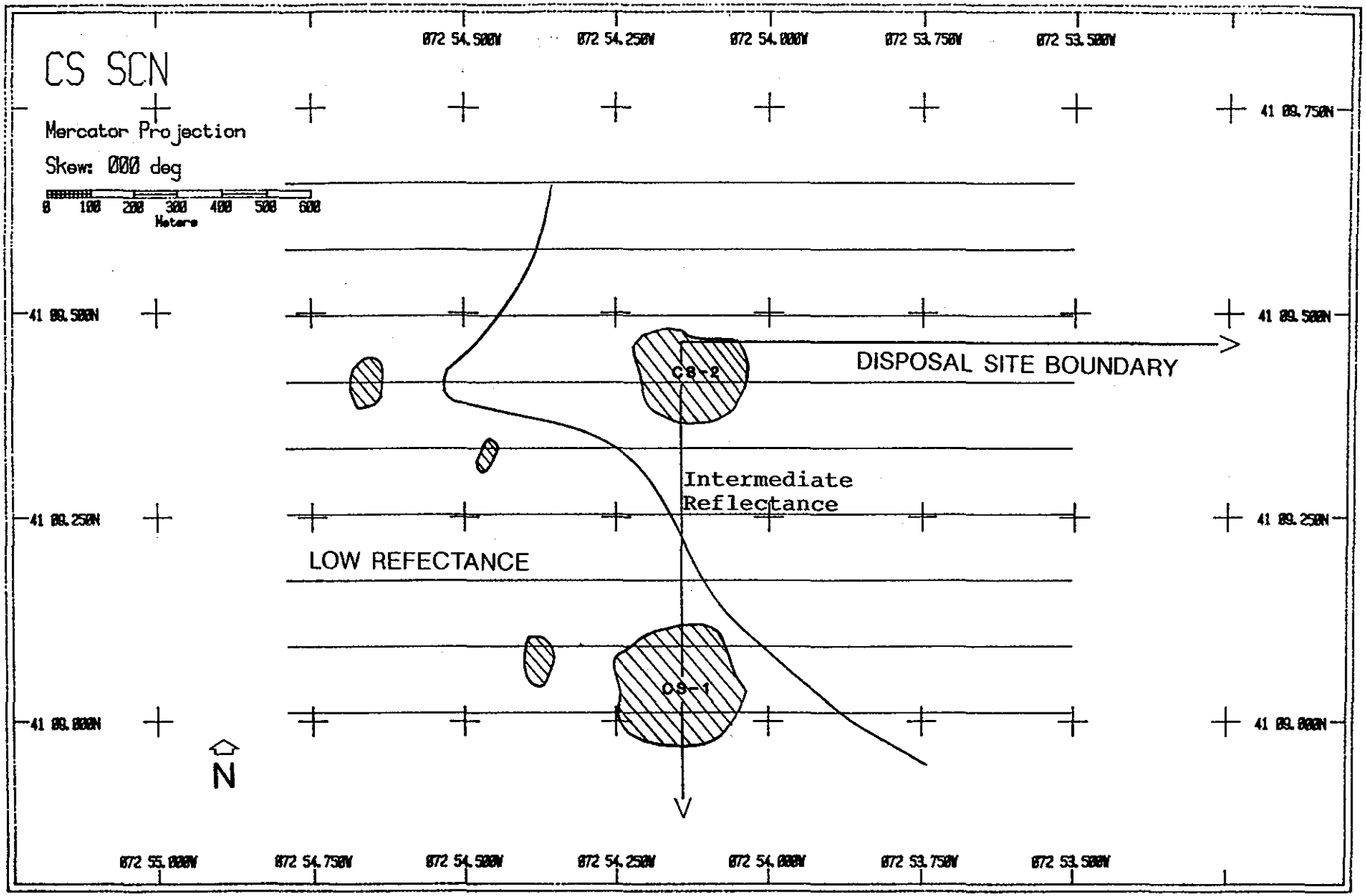

Figure 3-8 Side scan survey results at Cap Sites 1 and 2, August 1985. ▨ indicates heavy reflectance; the solid line marks the boundary of intermediate reflectance.

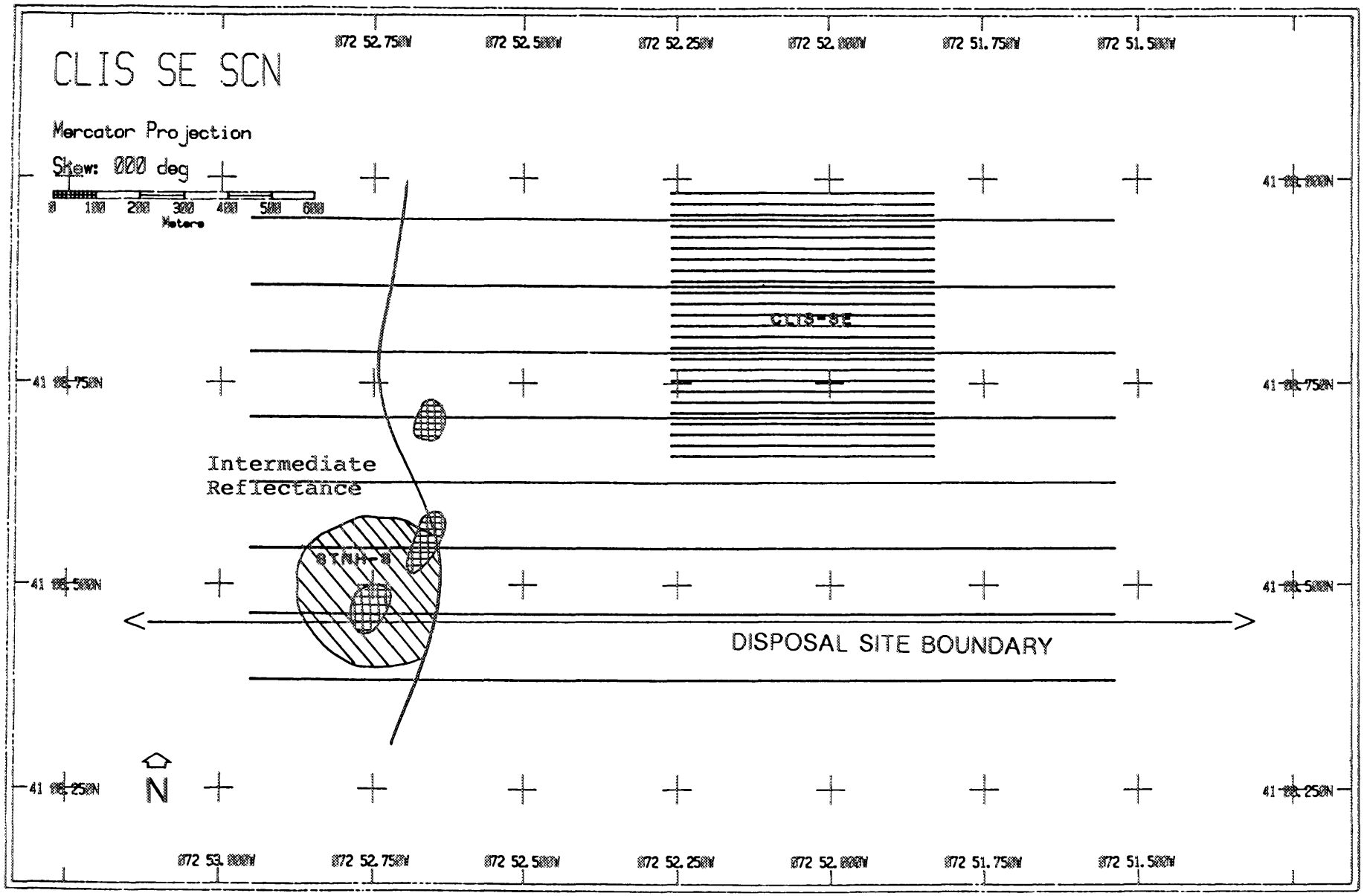

Figure 3-9. Side scan survey results at CLIS-SE, August 1985.

indicates heavy reflectance; indicates distinct areas of very heavy reflectance; the solid line marks the boundary of intermediate reflectance. CLIS-SE survey lanes illustrate area covered by detailed bathymetric survey.

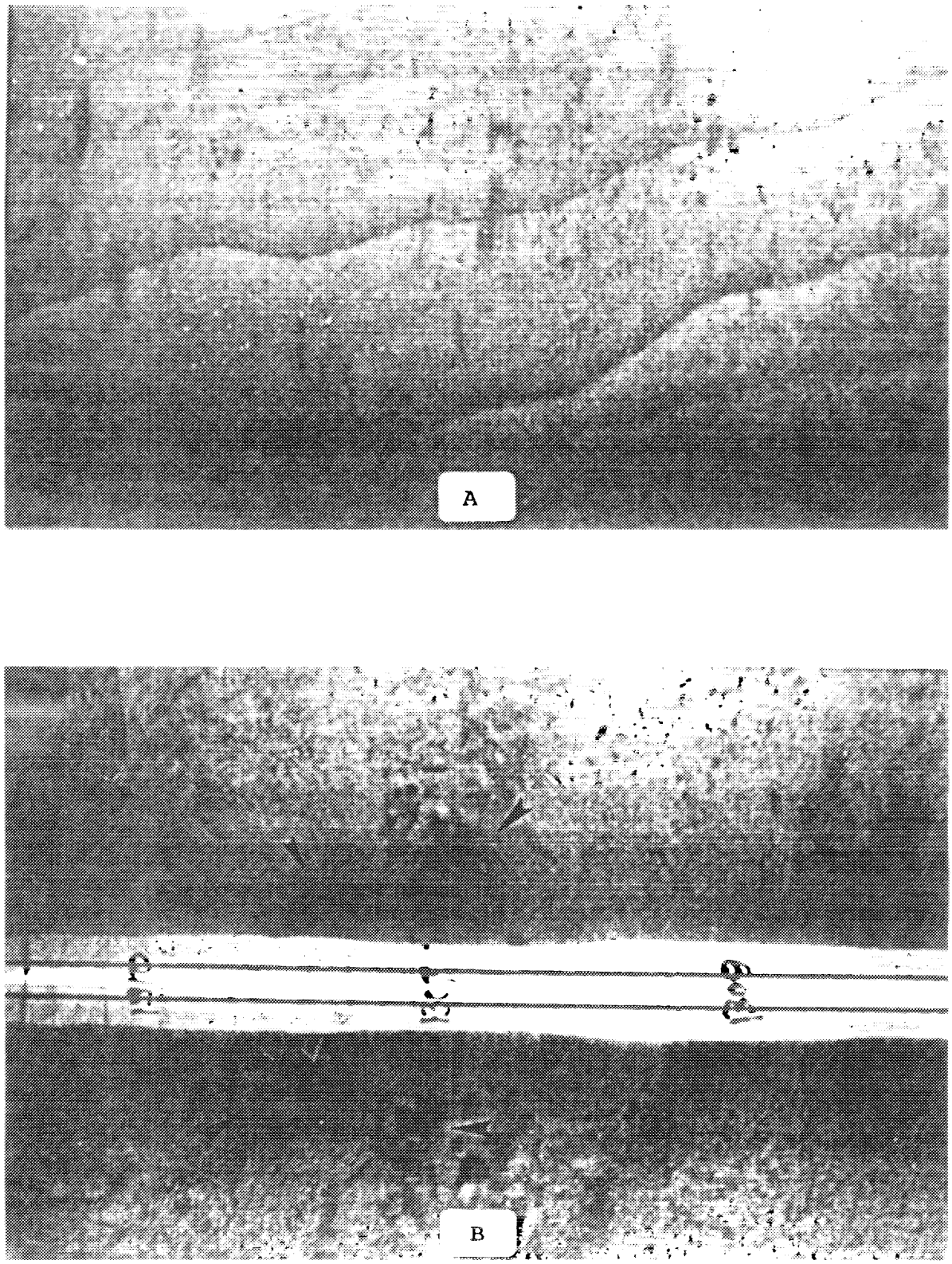

Figure 3-10 Photographs of side scan record at CLIS-SE.

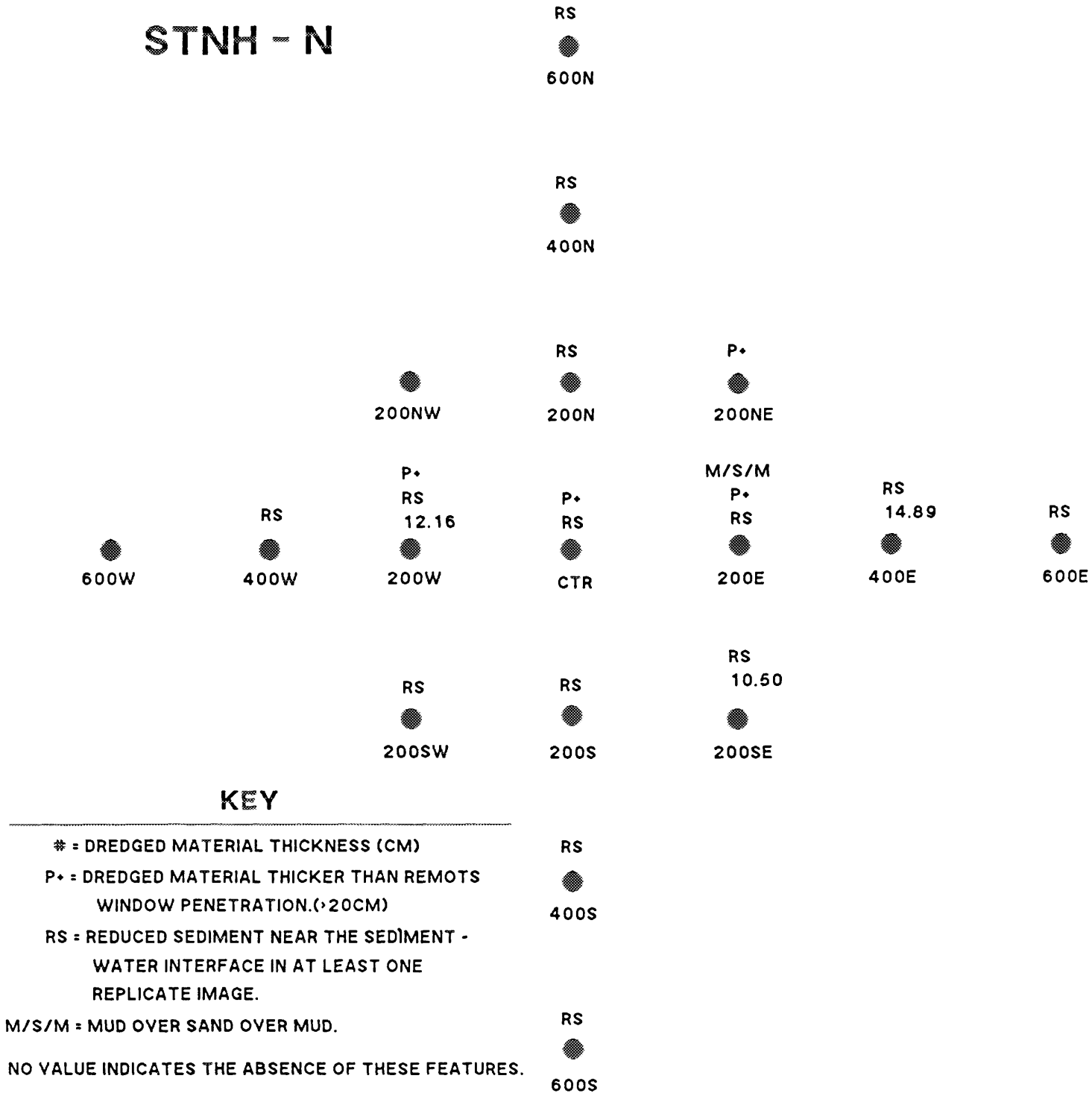

Figure 3-11 A map showing the apparent distribution and thickness of dredged material, averaged by station, at the STNH-N site in August 1985.

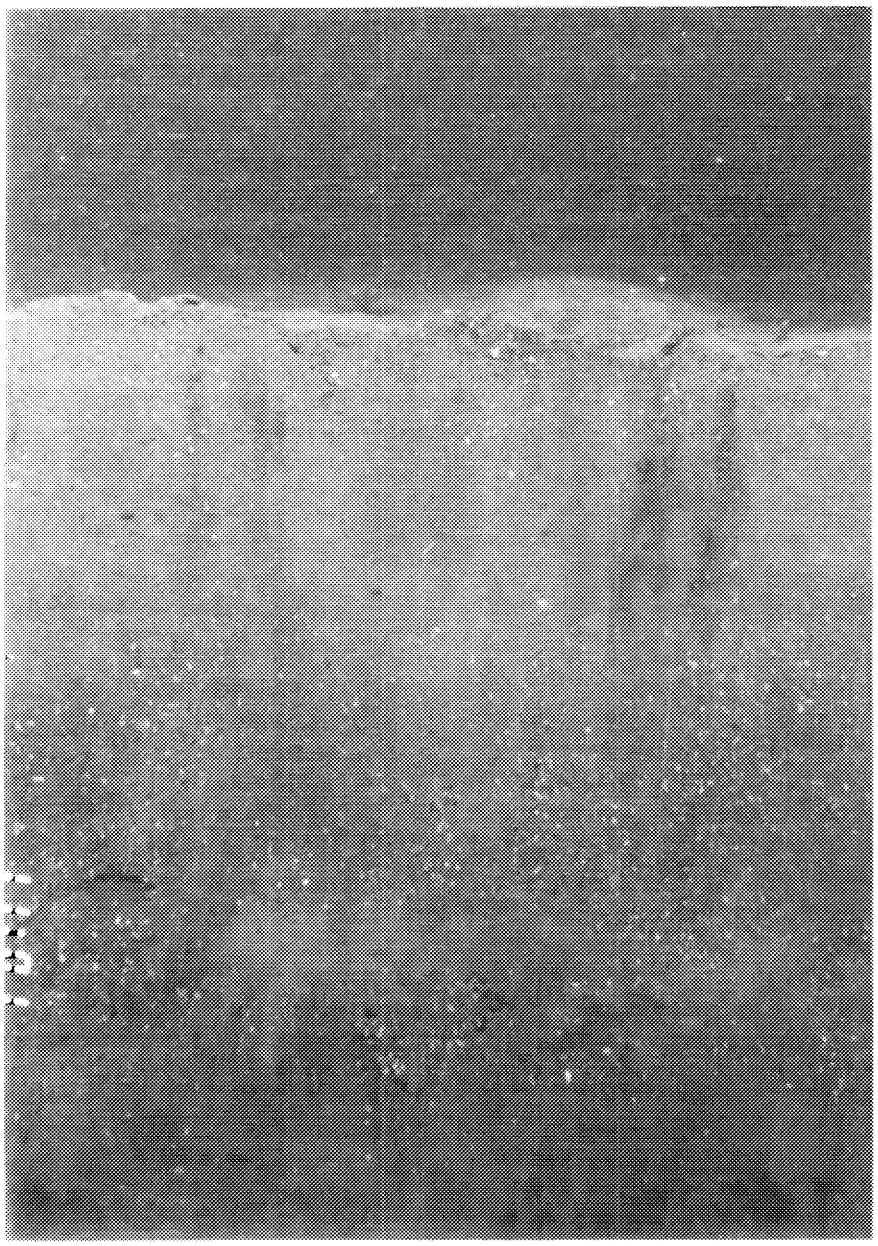

Figure 3-12 A REMOTS® image from station 200E showing a mud/sand/mud stratigraphy apparently representing the original sand cap being mixed and covered with more recently deposited silt-clay sediments. Scale = 1X.

Figure 3-13 A REMOTS® image from station 600S showing the appearance of dark reducing sediment near the sediment surface. Scale = 1X.

STNH-N

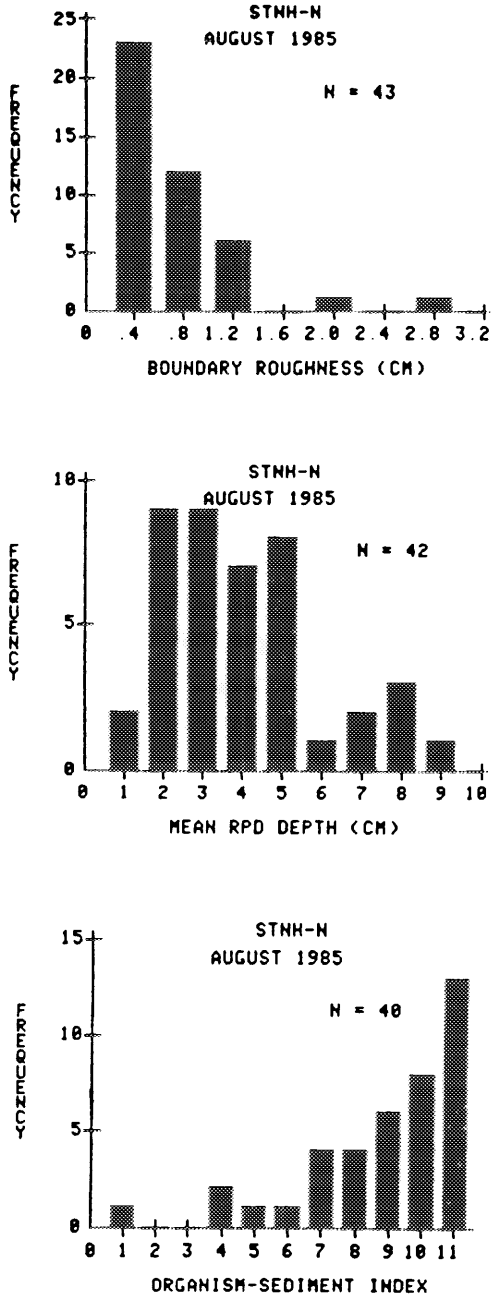

Figure 3-14 The frequency distributions of boundary roughness, redox potential discontinuity (RPD) depths, and Organism-Sediment Index (OSI) values for August 1985 at STNH-N.

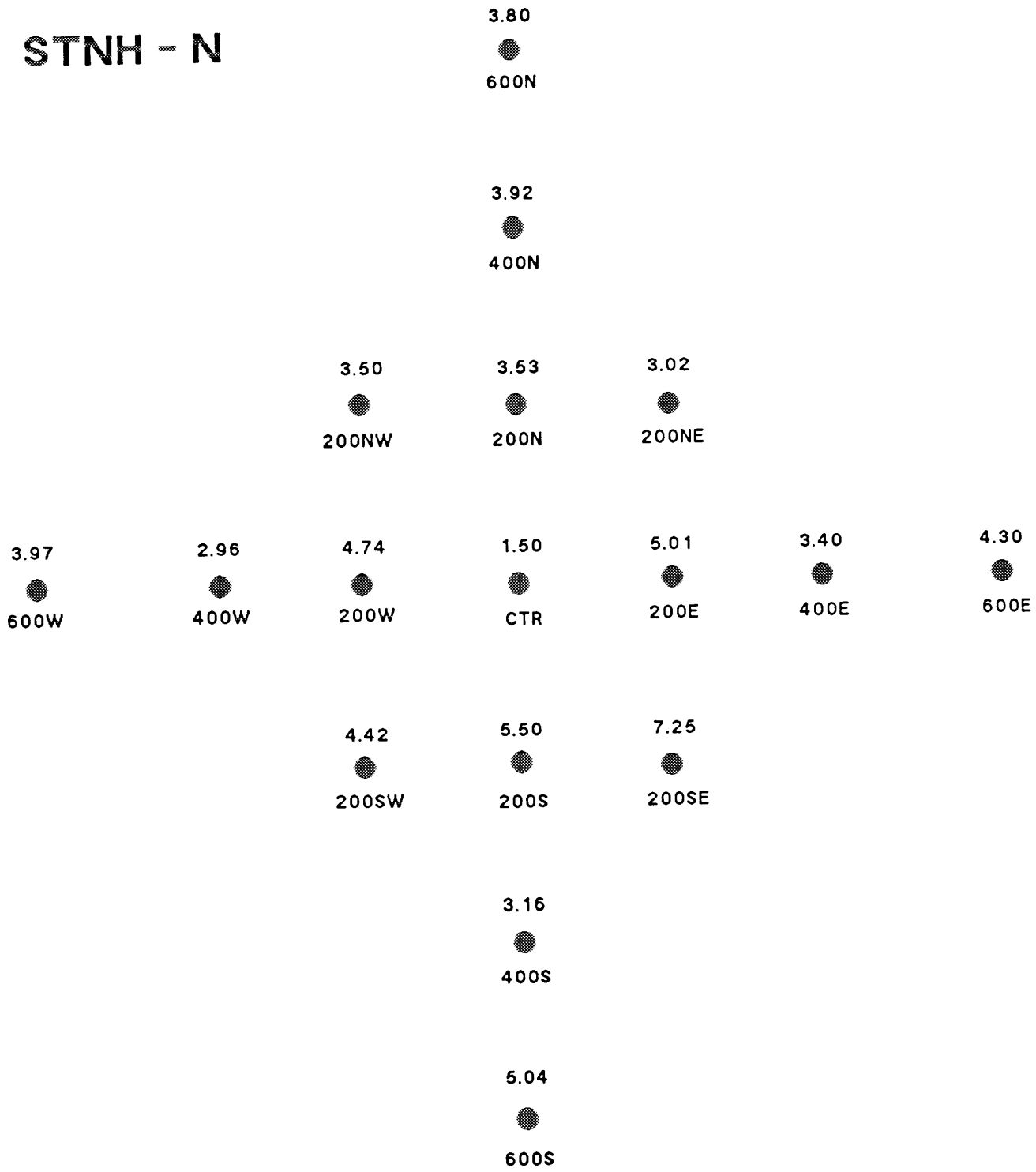

Figure 3-15 The mapped average apparent redox potential discontinuity (RPD) depth values at each station in the August survey at STNH-N.

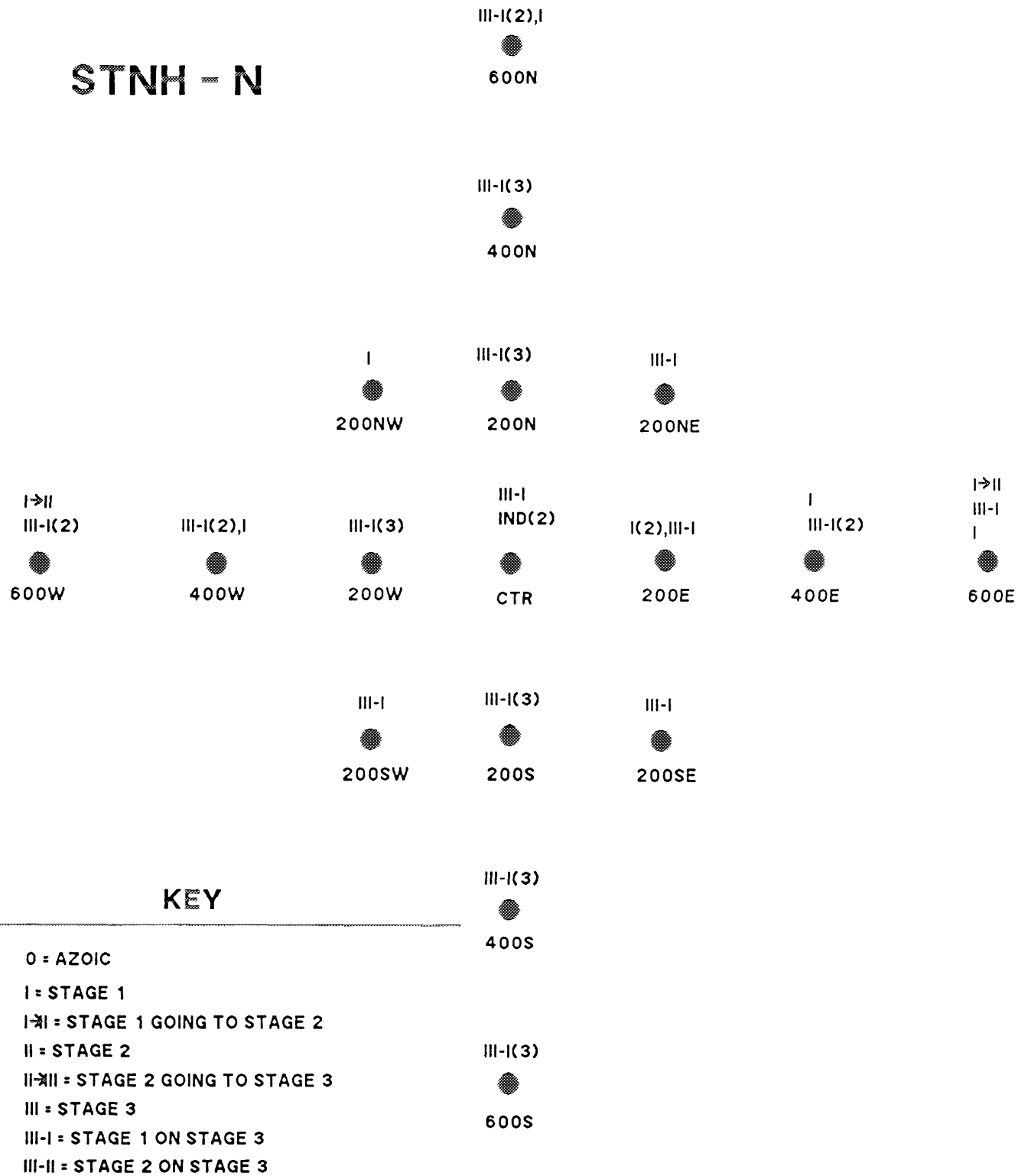

Figure 3-16 The mapped distribution of successional stages for all replicates in the August survey at STNH-N.

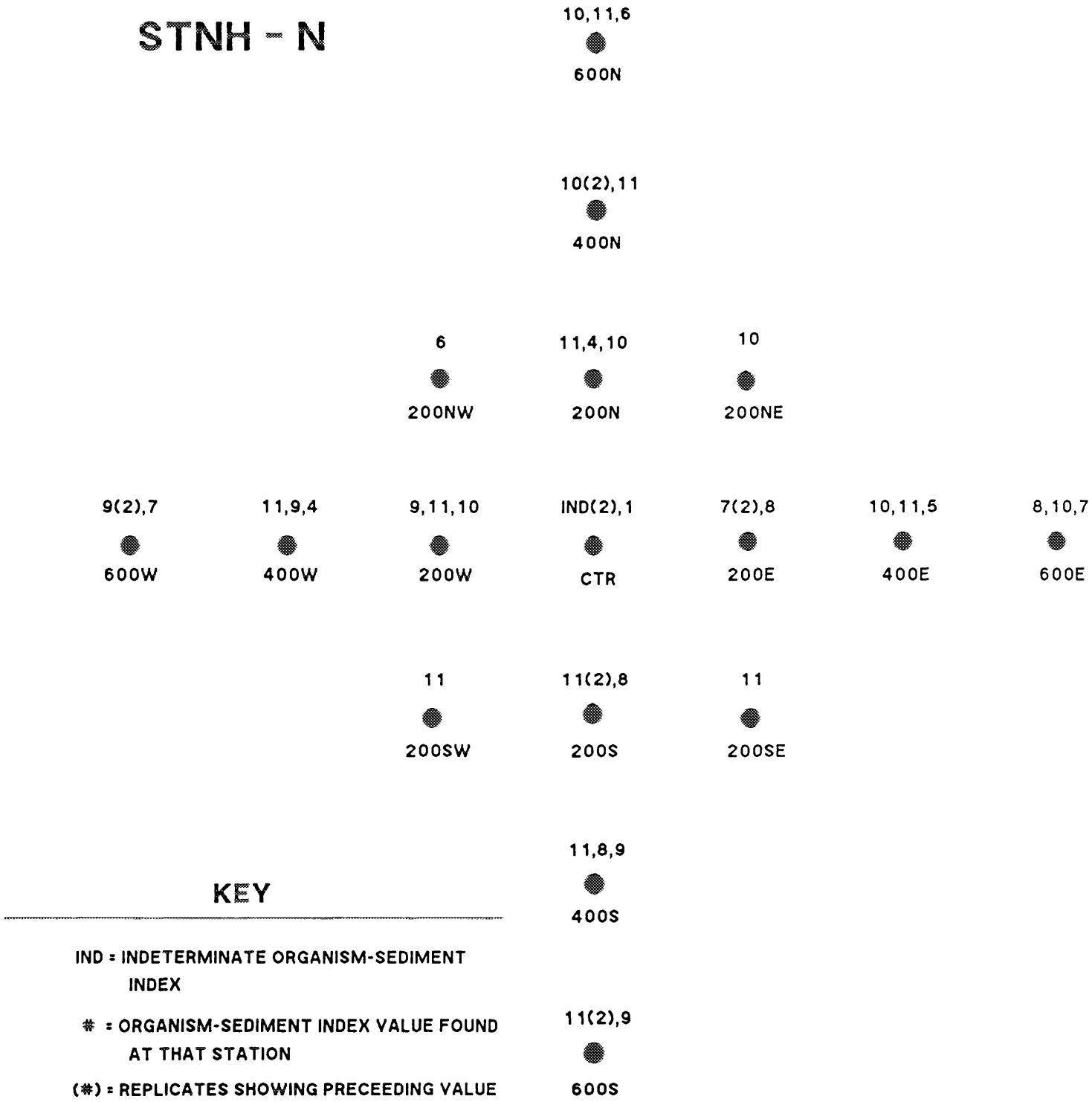

Figure 3-17 The mapped distribution of Organism-Sediment Indices (OSI) for all replicates in the August survey at STNH-N.

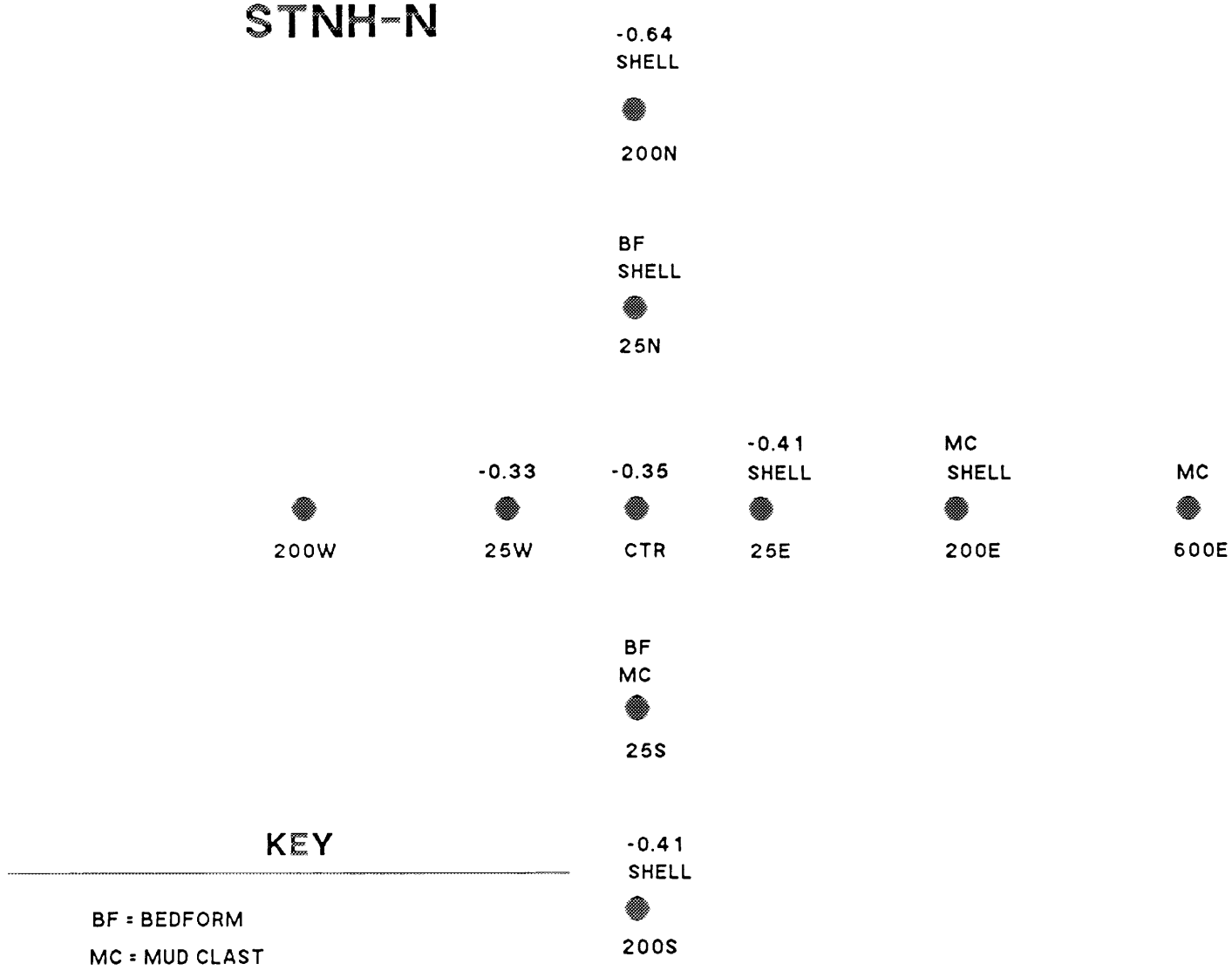

Figure 3-18 A post-storm benthic "process" map showing the distribution of erosional and depositional features at STNH-N.

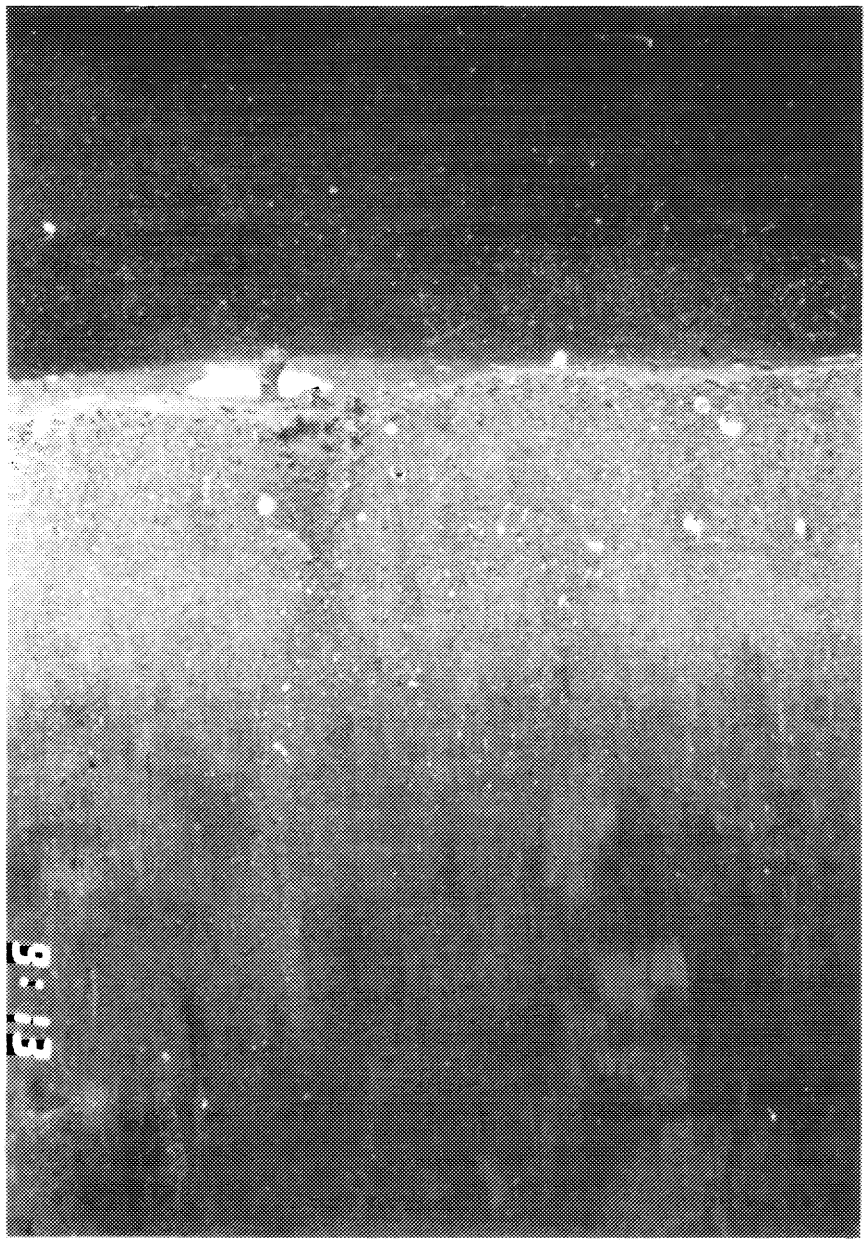

Figure 3-19 A REMOTS® image from 200N showing shell lag deposits and an exposed polychaete tube indicative of surface erosion. Scale = 1X.

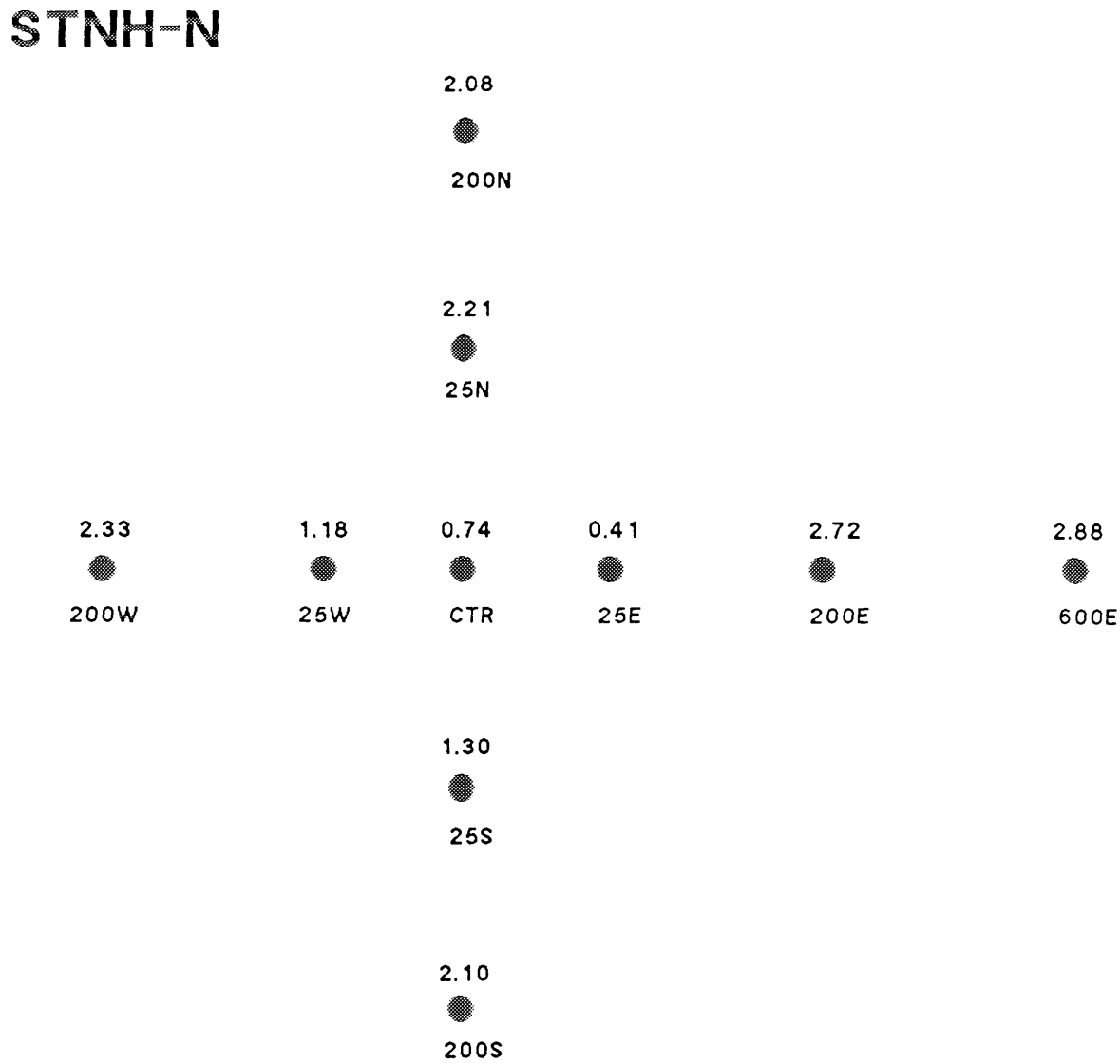

Figure 3-20 The mapped distribution of post-storm redox potential discontinuity (RPD) depths at STNH-N.

STNH-N

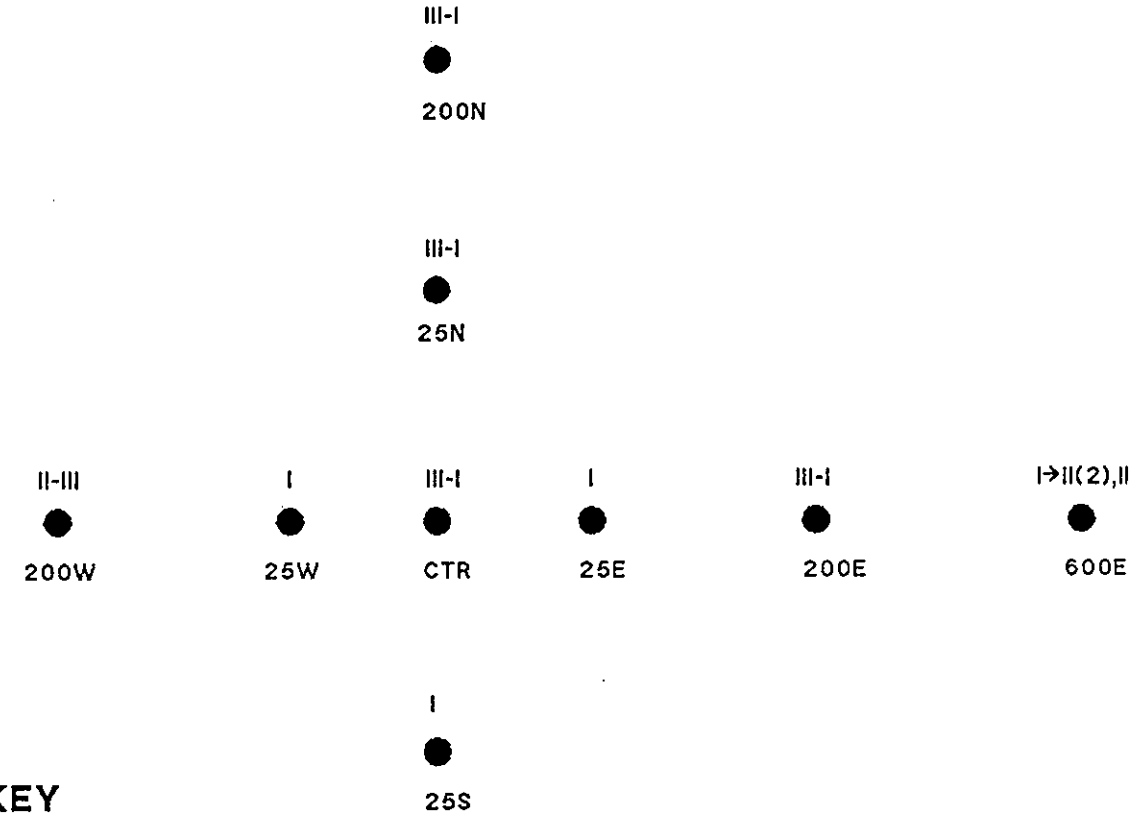

KEY

0 = AZOIC
I = STAGE 1
I→II = STAGE 1 GOING TO STAGE 2
II = STAGE 2
II→III = STAGE 2 GOING TO STAGE 3
III = STAGE 3
III-I = STAGE 1 ON STAGE 3
III-II = STAGE 2 ON STAGE 3

Figure 3-21 The mapped distribution of post-storm infaunal successional stages at STNH-N.

STNH-N

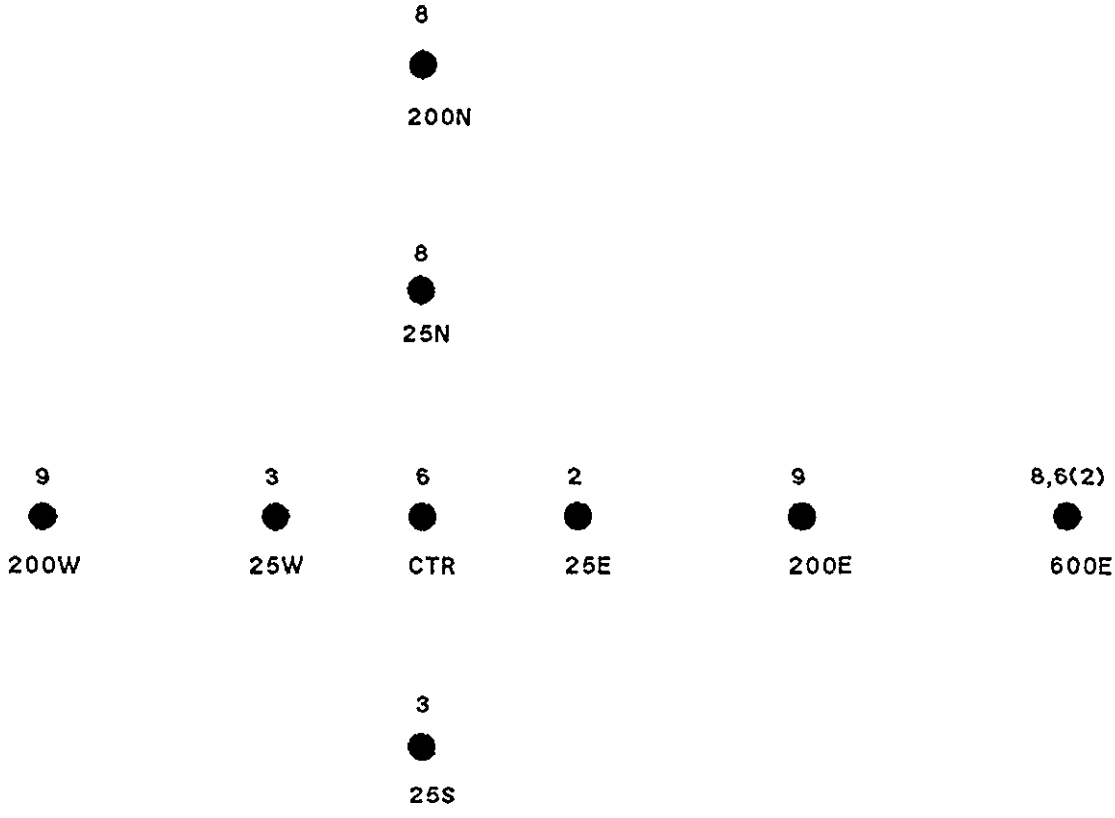

KEY

= ORGANISM-SEDIMENT INDEX VALUE FOUND AT THAT STATION

(#) = REPLICATES SHOWING PRECEEDING VALUE

Figure 3-22 The mapped distribution of post-storm Organism-Sediment Indices (OSI) at STNH-N.

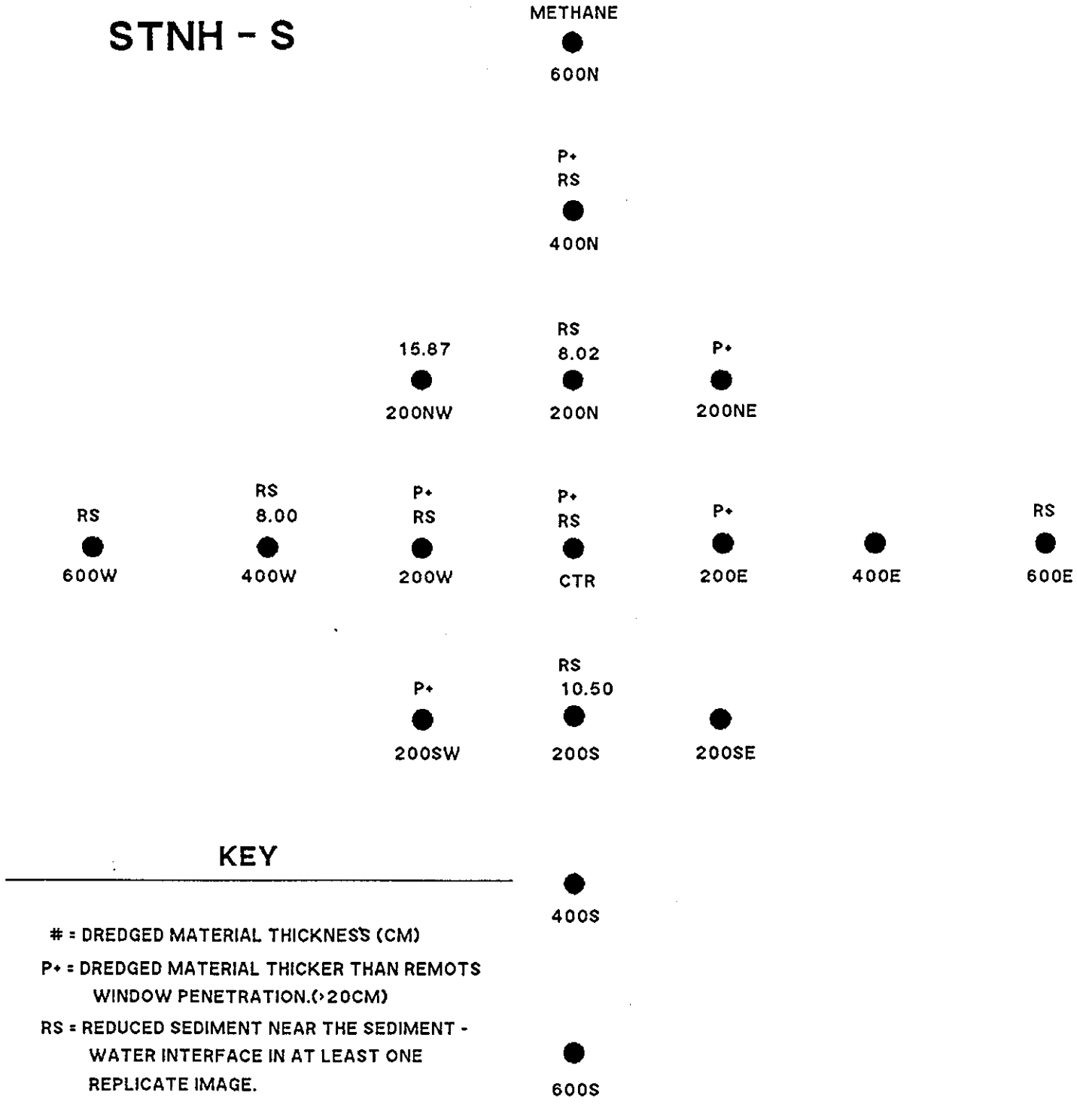

Figure 3-23 A map showing the apparent distribution and thickness of dredged material, averaged by station at the STNH-S site in August 1985.

STNH-S

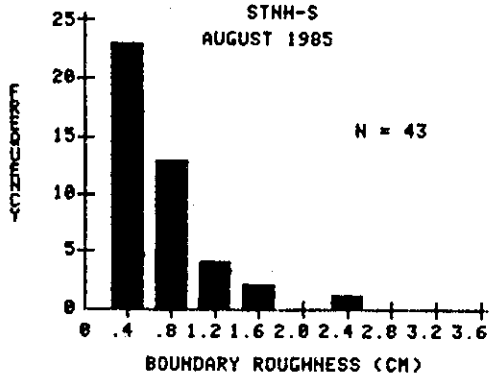

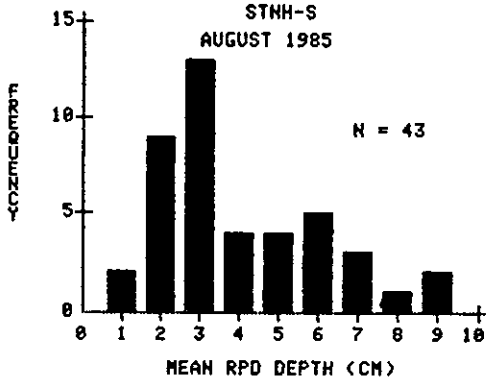

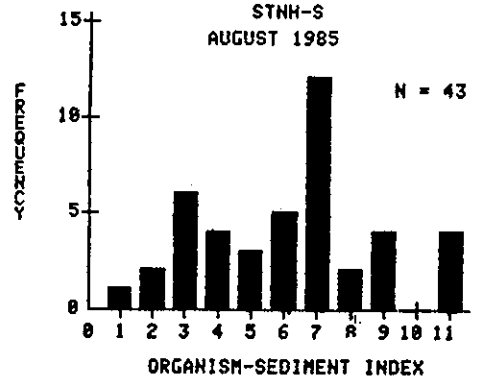

Figure 3-24 The frequency distributions of boundary roughness, redox potential discontinuity (RPD) depths, and Organism-Sediment Index (OSI) values for August 1985 at STNH-S.

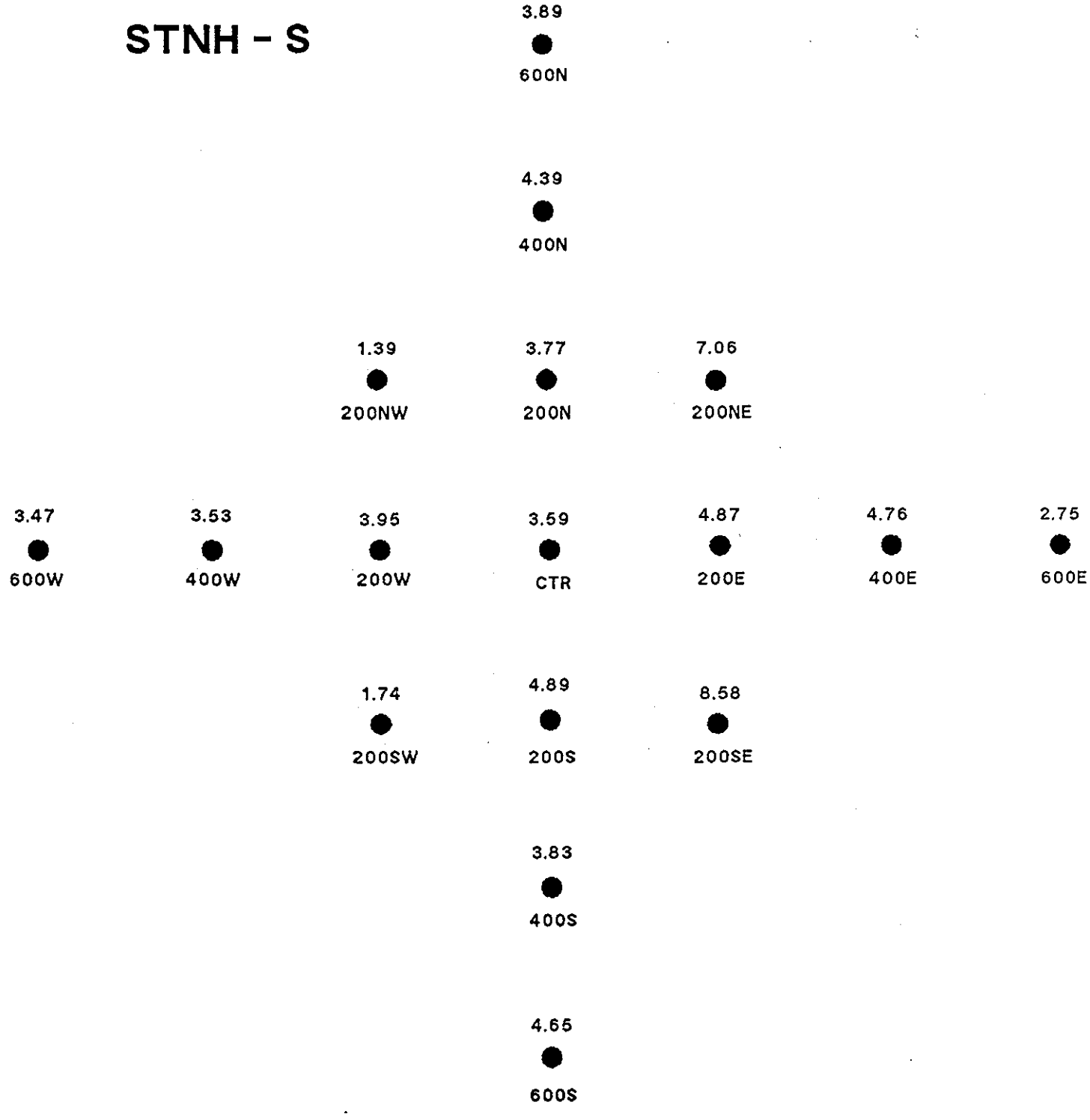

Figure 3-25 The mapped average apparent redox potential discontinuity (RPD) depth values at each station in the August survey at STNH-S.

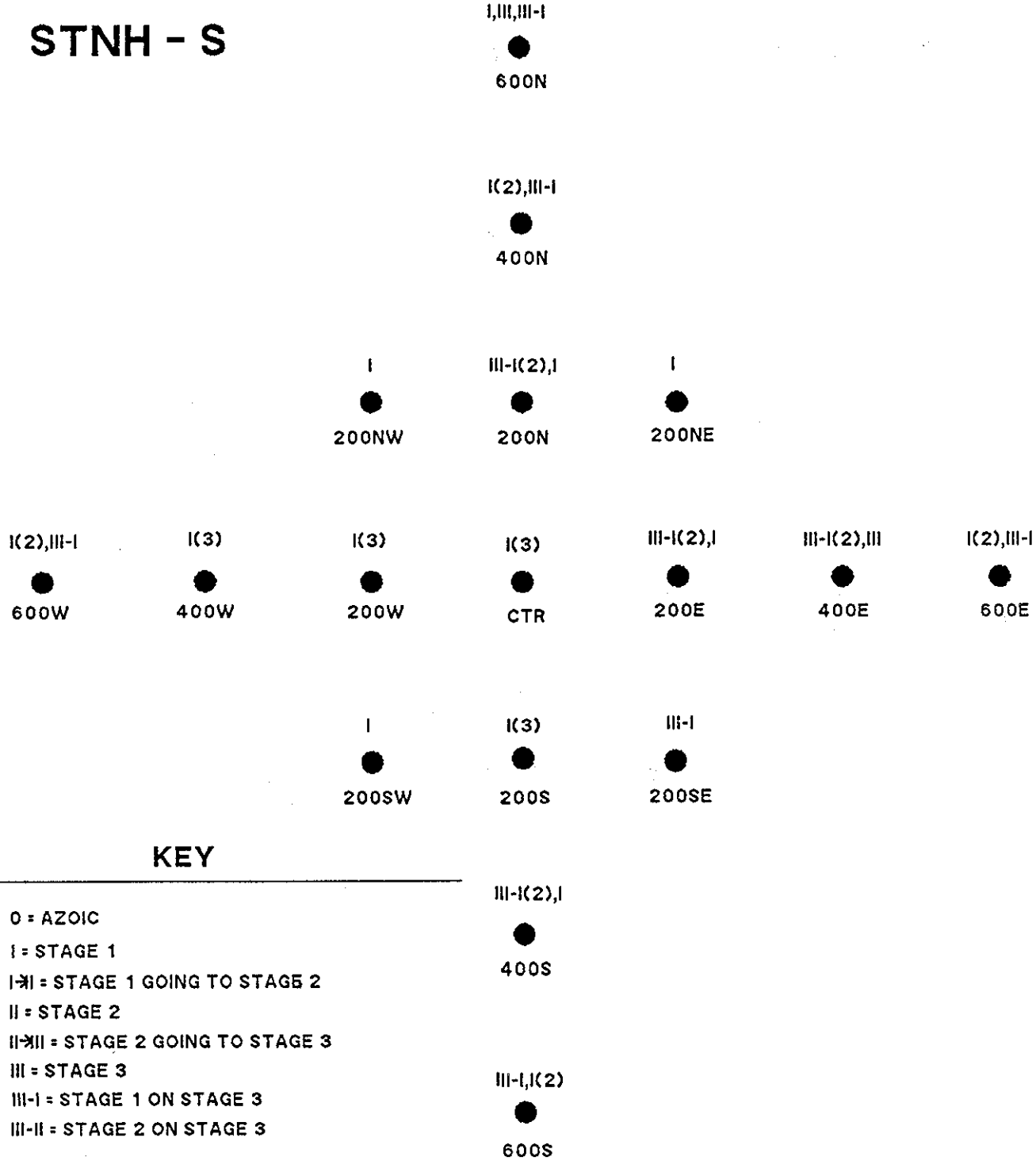

Figure 3-26 The mapped distribution of successional stages for all replicates in the August survey at STNH-S.

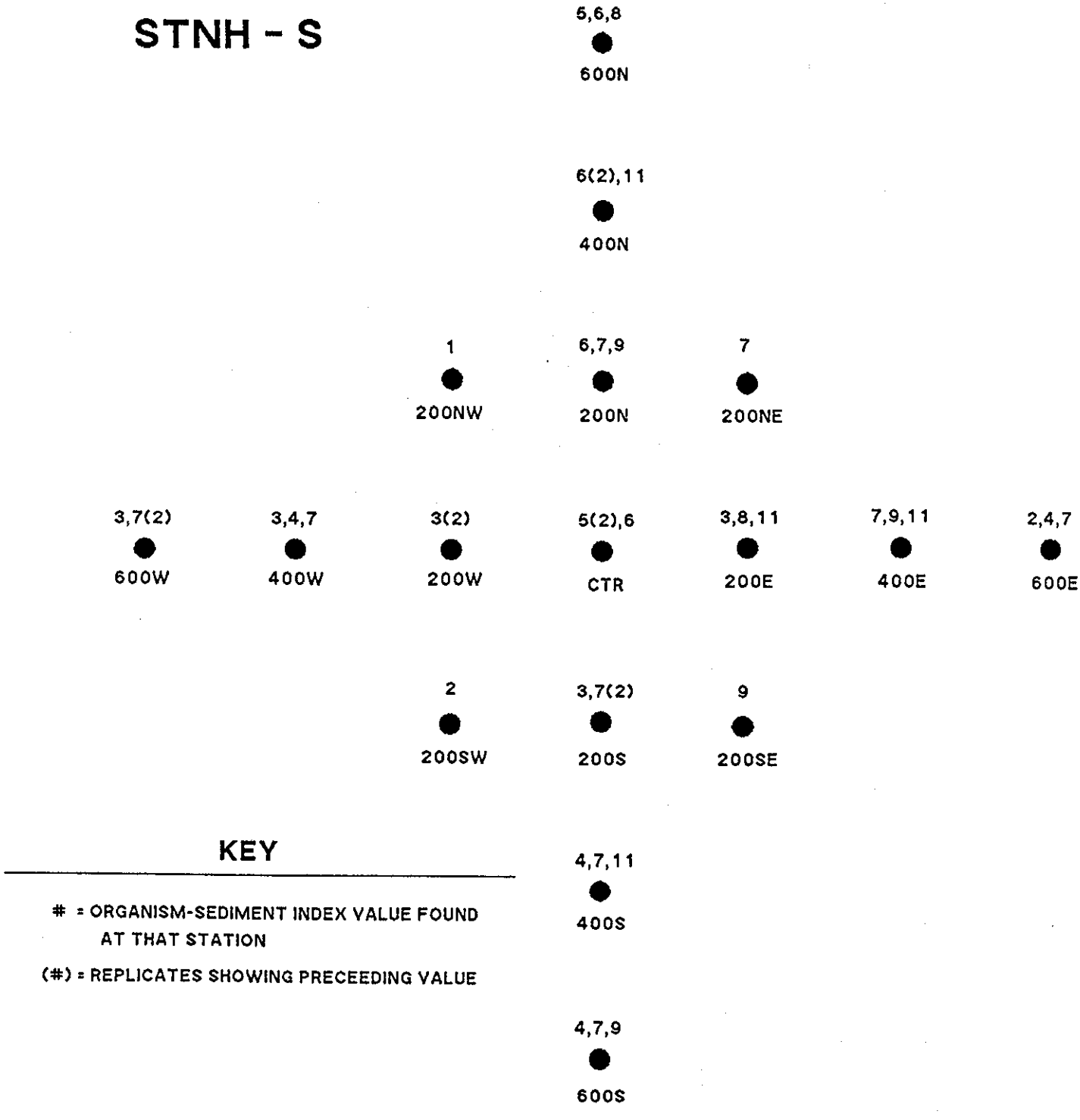

Figure 3-27 The mapped distribution of Organism- Sediment Indices (OSI) for all replicates in the August survey at STNH-S.

STNH-S

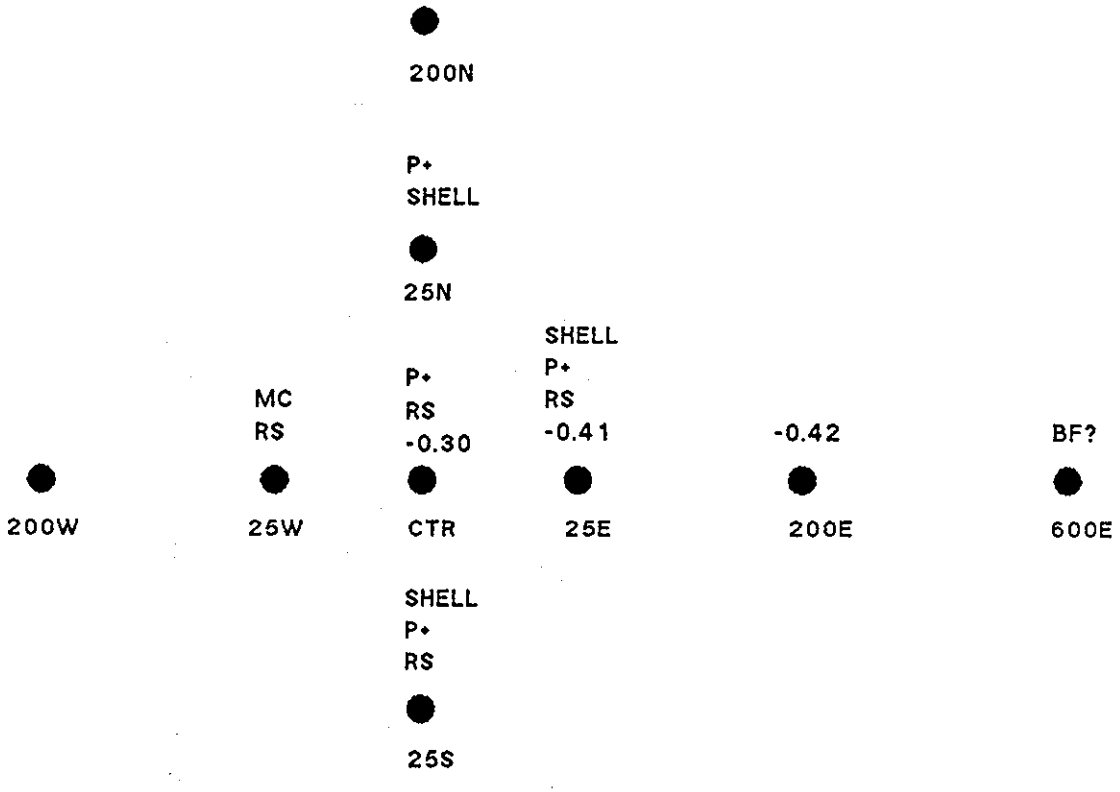

KEY

P+ = DREDGED MATERIAL THICKER THAN REMOTS WINDOW PENETRATION (>20CM)

BF = BEDFORM

MC = MUD CLAST

SHELL = SHELL LAG DEPOSITS

-# = ESTIMATE OF EROSION BASED ON EXPOSED WORM TUBES (CM)

RS = REDUCED SEDIMENT NEAR THE SEDIMENT - WATER INTERFACE IN AT LEAST ONE REPLICATE IMAGE

NO VALUE INDICATES THE ABSENCE OF THESE FEATURES.

Figure 3-28 A post-storm benthic "process" map showing the distribution of erosional and depositional features at STNH-S.

Figure 3-29 A-B REMOTS® images from stations 25W and 25E respectively, showing mud clasts, exposed worm tubes, surface shell lag deposits, and reduced sediment patches near the interface. Scale = 1X.

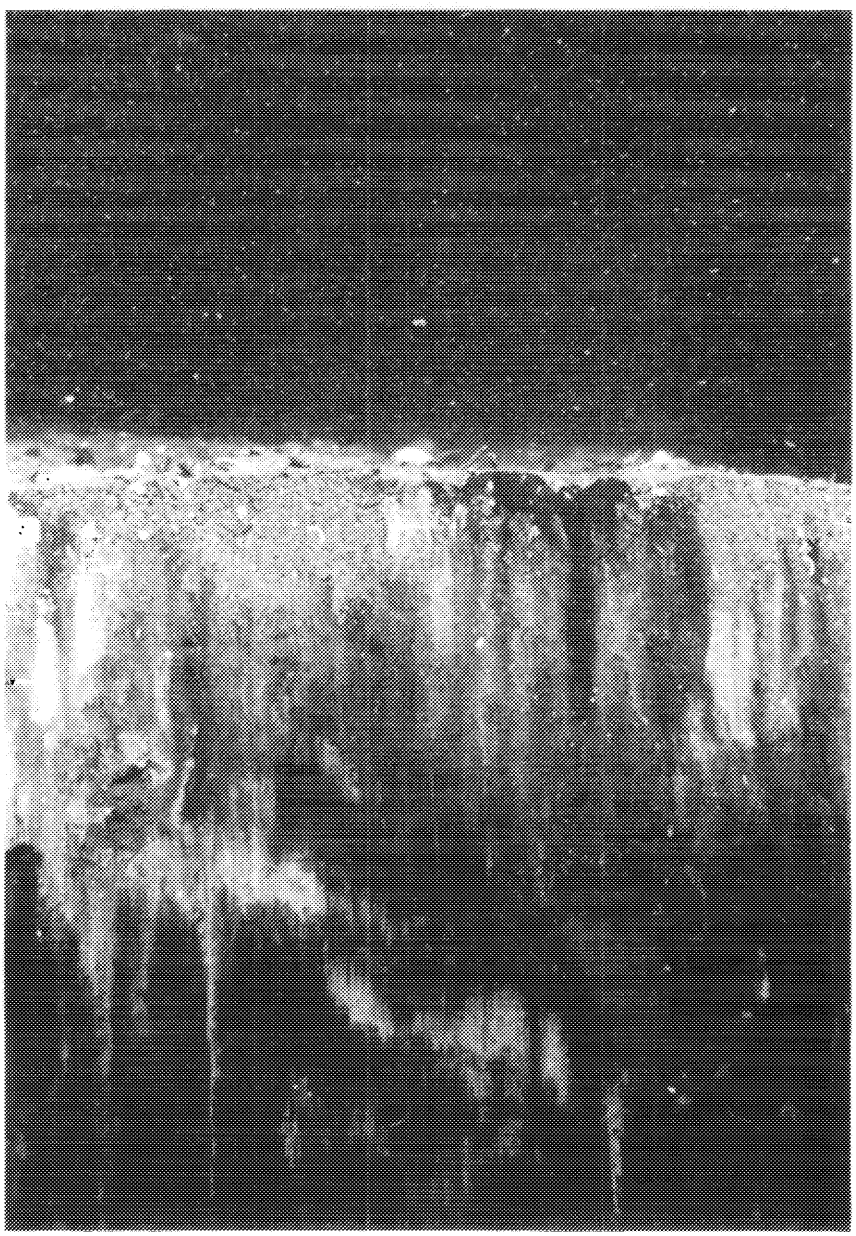

Figure 3-29B Scale = 1X.

Figure 3-30 A REMOTS® image from station 600E showing a physically disturbed bottom. Scale = 1X.

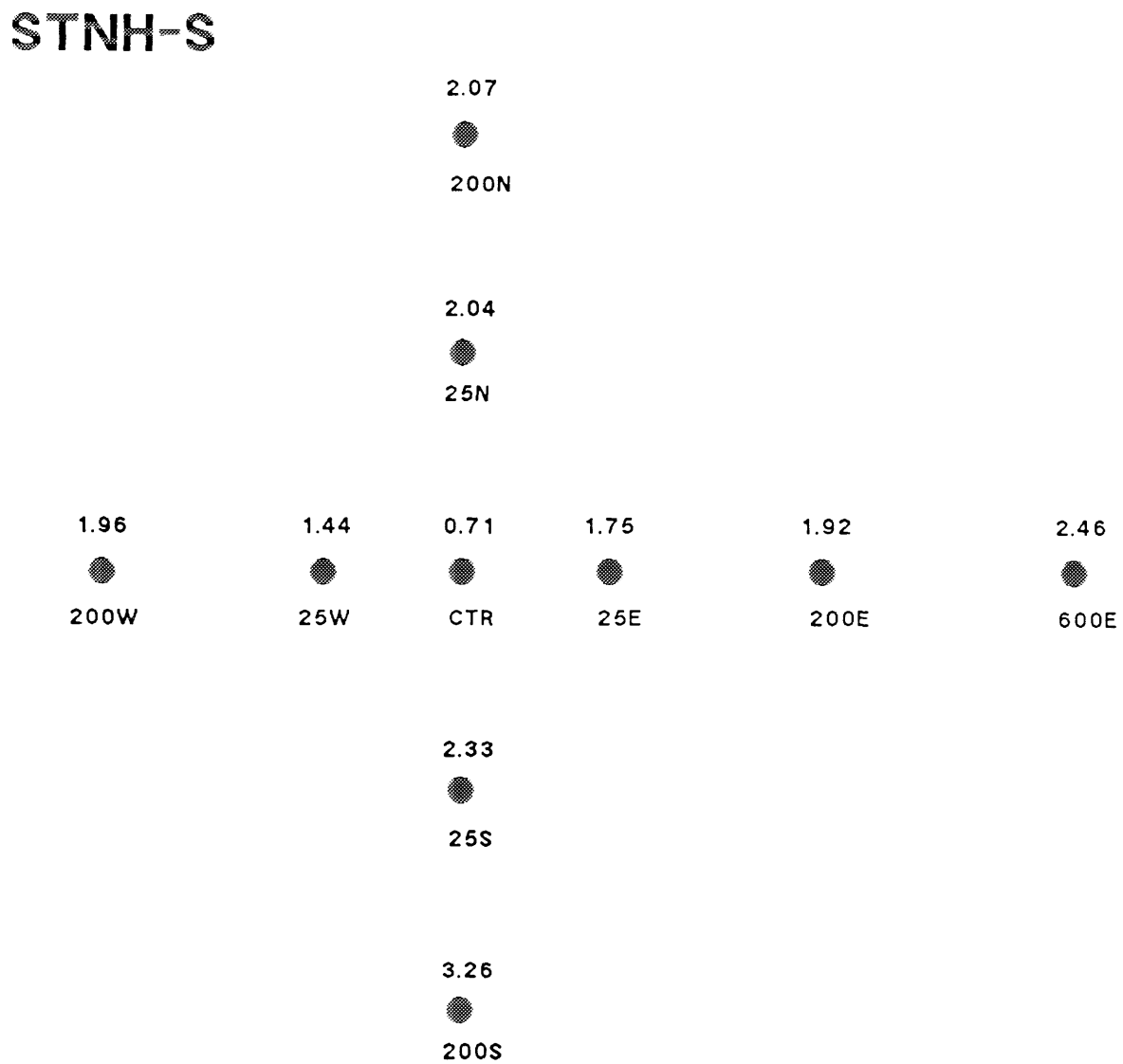

Figure 3-31 The mapped distribution of post-storm apparent mean redox potential discontinuity (RPD) depths at STNH-S.

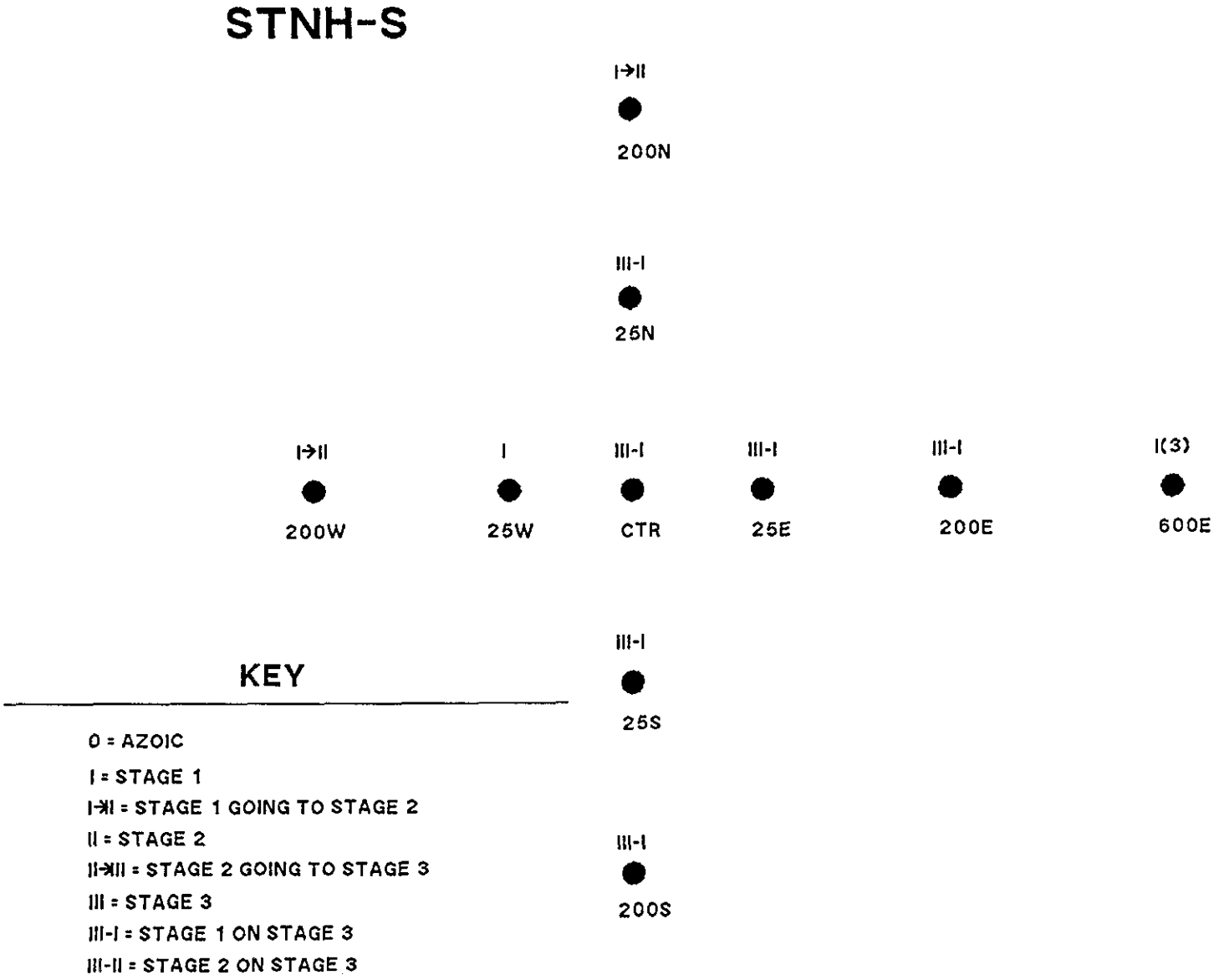

Figure 3-32 The mapped distribution of post-storm successional stages at STNH-S.

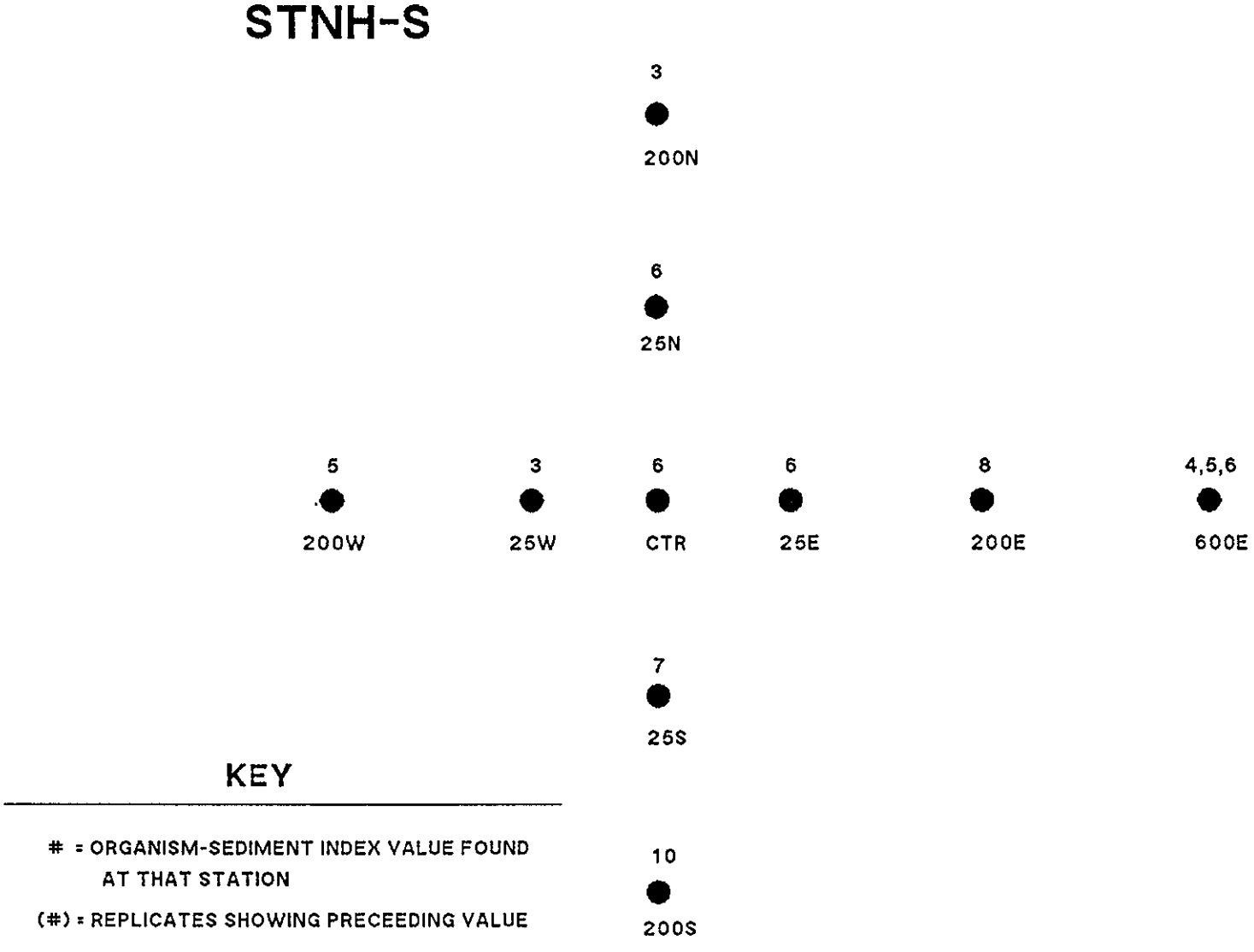

Figure 3-33 The mapped distribution of post-storm Organism-Sediment Indices (OSI) at STNH-S.

CAPSITE - 1

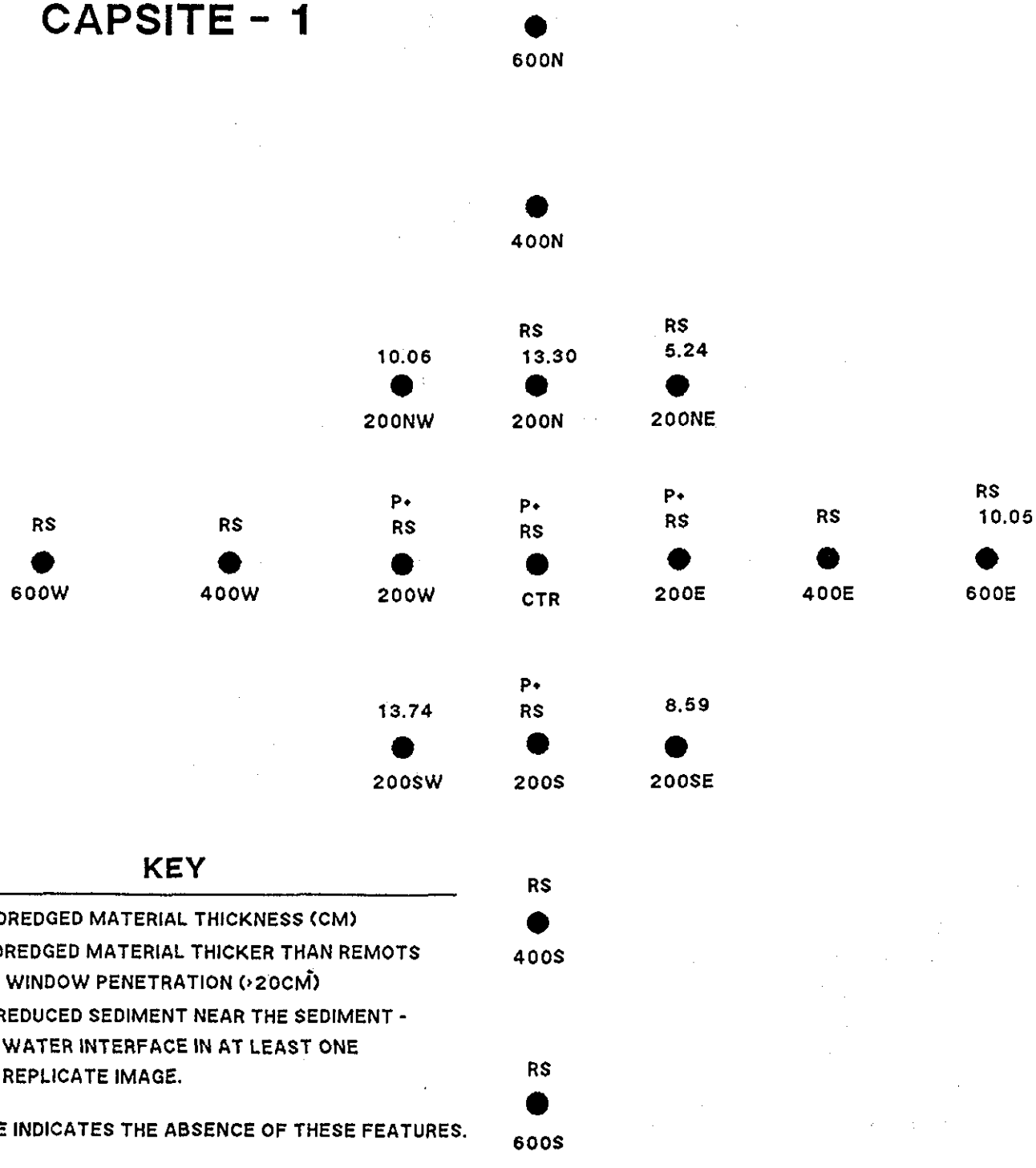

KEY

= DREDGED MATERIAL THICKNESS (CM)

P+ = DREDGED MATERIAL THICKER THAN REMOTS WINDOW PENETRATION (>20CM)

RS = REDUCED SEDIMENT NEAR THE SEDIMENT - WATER INTERFACE IN AT LEAST ONE REPLICATE IMAGE.

NO VALUE INDICATES THE ABSENCE OF THESE FEATURES.

Figure 3-34 A map showing the apparent distribution and thickness of dredged material, averaged by station, at Cap Site 1 in August 1985.

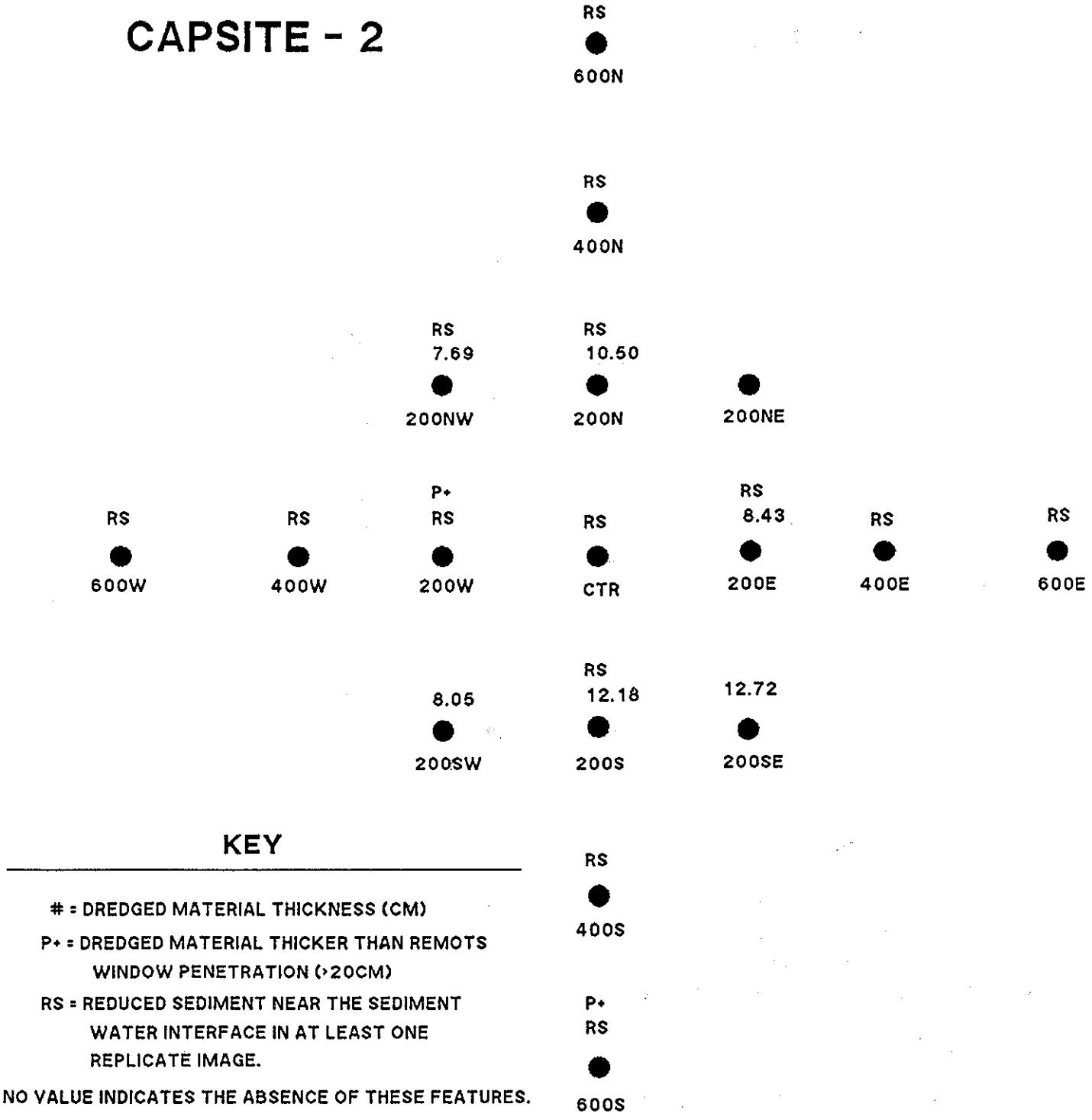

Figure 3-35 A map showing the apparent distribution and thickness of dredged material, averaged by station at Cap Site 2 in August 1985.

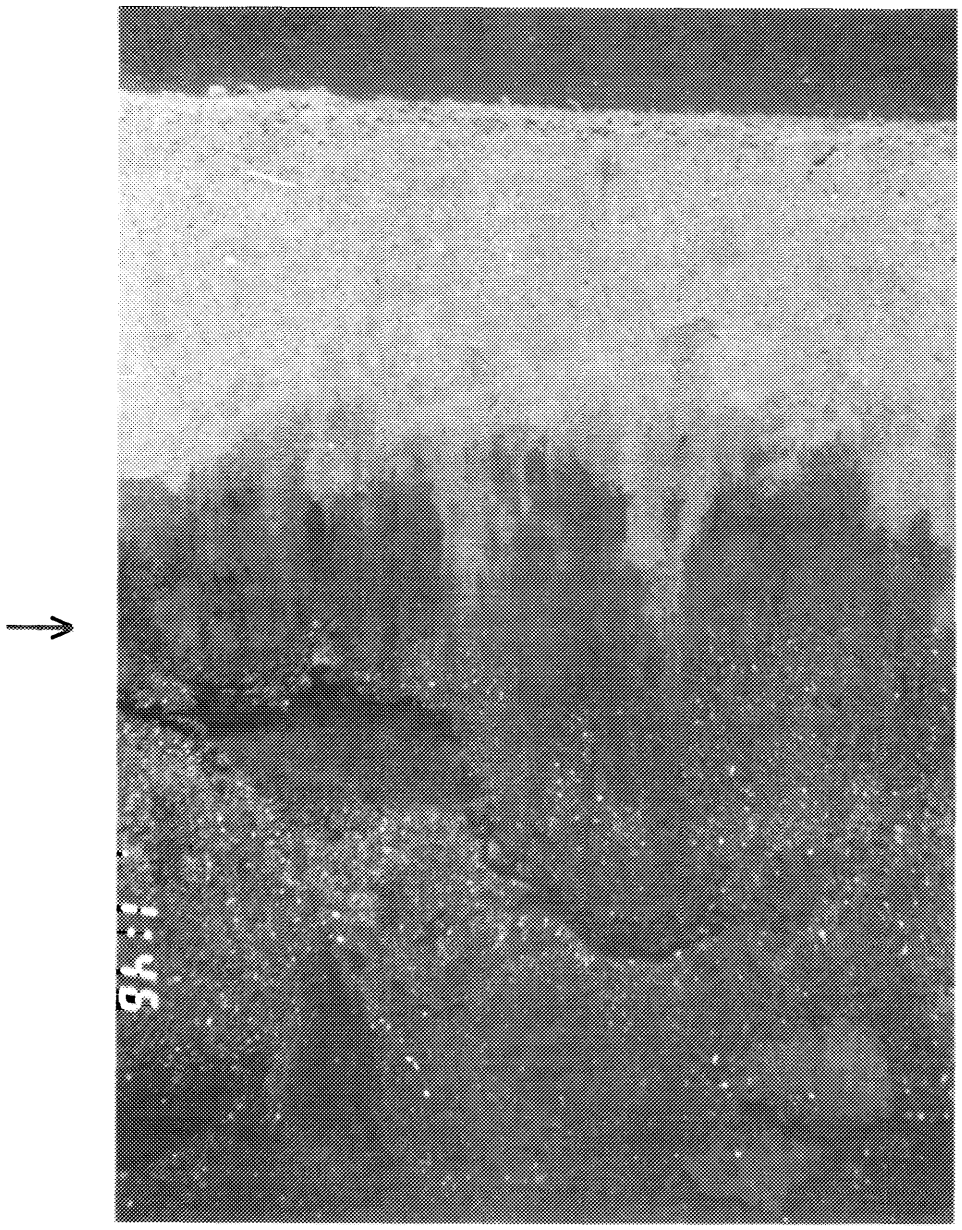

Figure 3-36A-B. Two REMOTS® images from Cap Site 2 station 200W showing a silt-clay layer overlying the original sand cap. The point of contact between the two layers is indicated by the arrow.

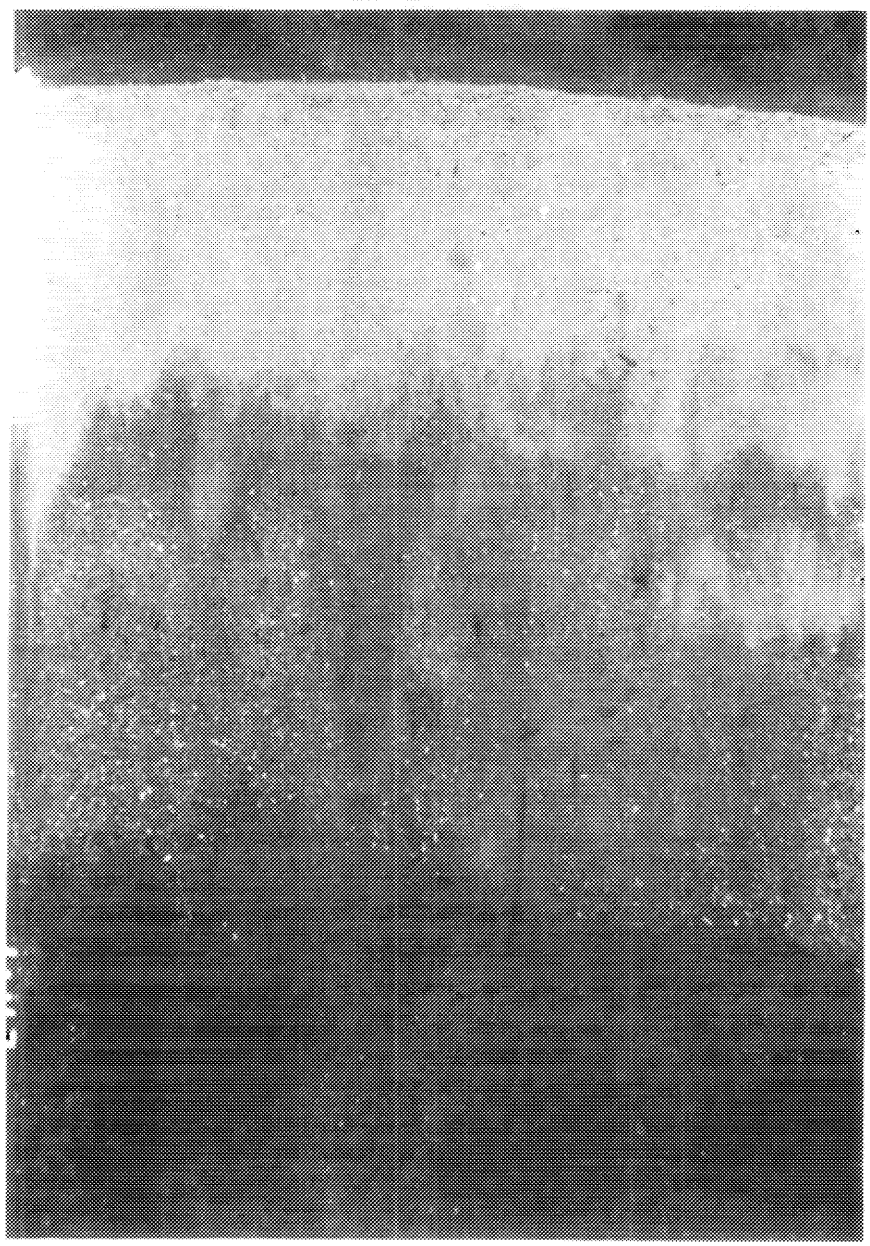

Figure 3-36B Scale = 1X.

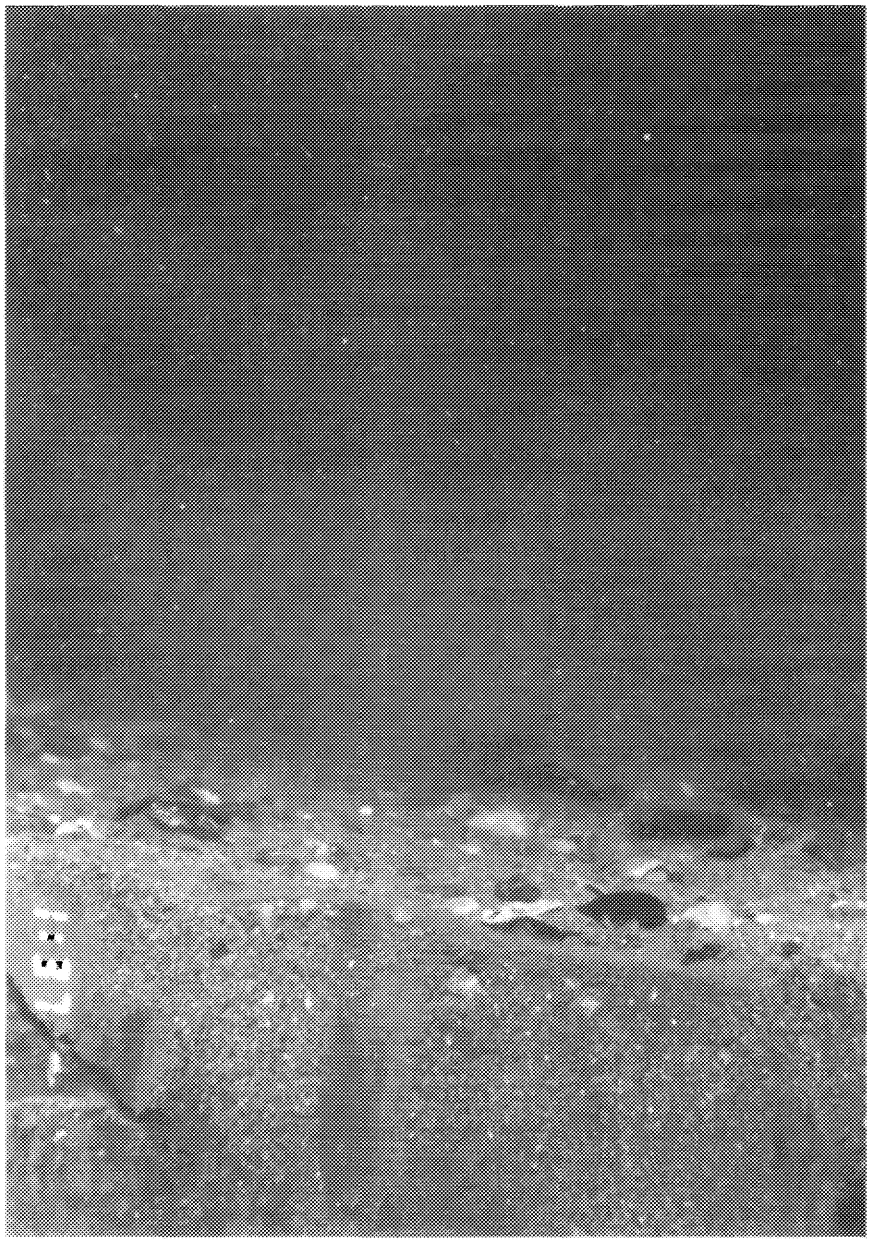

Figure 3-37 A REMOTS® image from Cap Site 2 station CTR showing a fine-sand layer at the surface along with disarticulated bivalve shells. Scale = 1X.

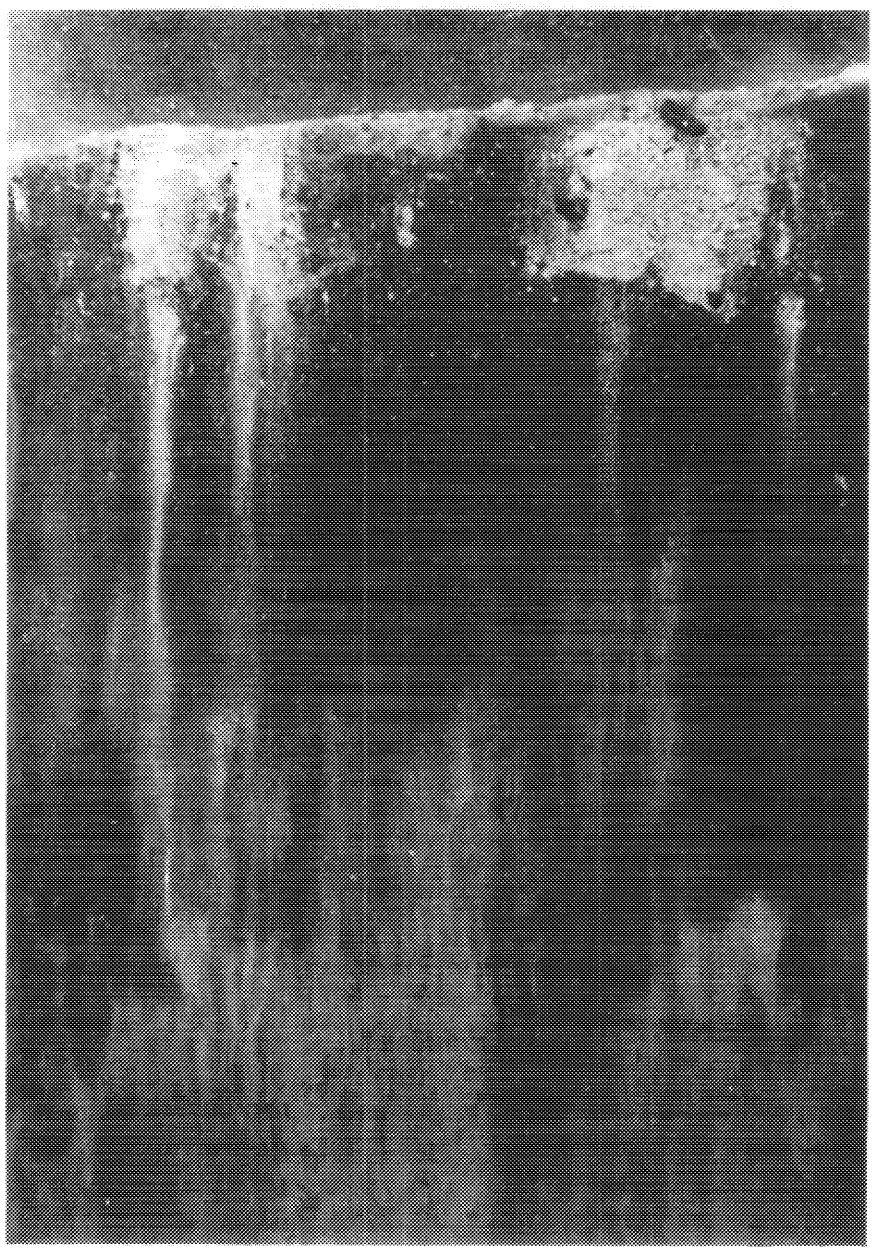

Figure 3-38 A REMOTS® image from Cap Site 2 station 600S showing dredged material. Scale = 1X.

Figure 3-39 A-B REMOTS® images from Cap Site 1 station 200E (A) and Cap Site 2 station 200W (B) showing reduced sediment patches near the sediment surface. Scale = 1X.

Figure 3-39B Scale = 1X.

CAP SITE 1

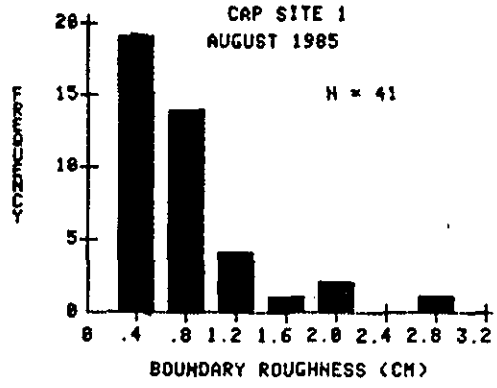

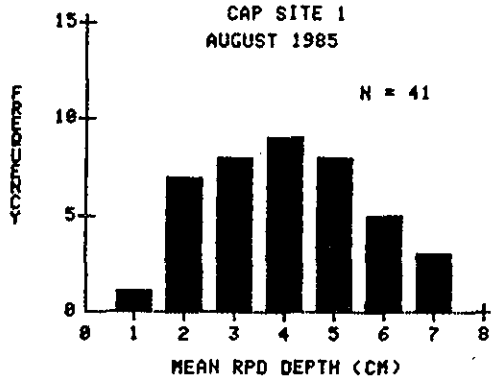

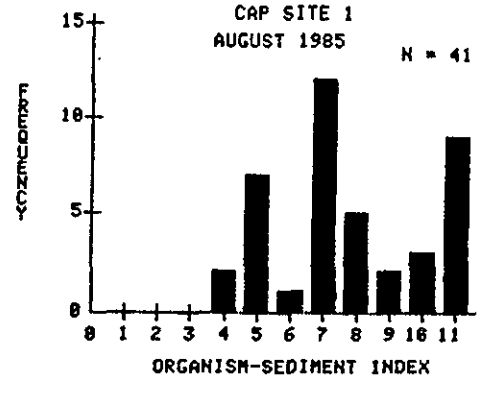

Figure 3-40 The frequency distribution of boundary roughness, redox potential discontinuity (RPD) depths, and Organism-Sediment Index (OSI) values at Cap Site 1 for August 1985.

CAP SITE 2

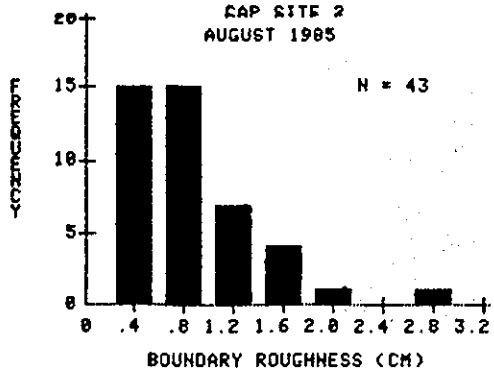

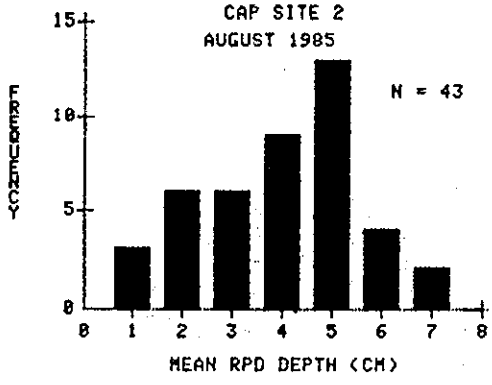

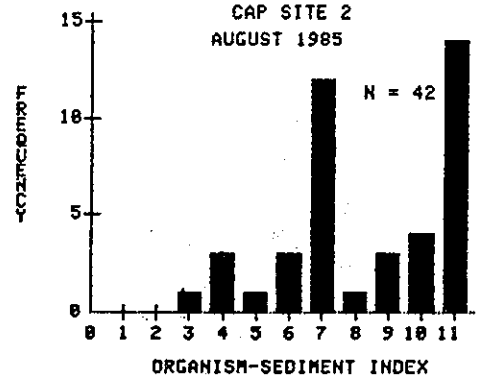

Figure 3-41 The frequency distributions of boundary roughness, redox potential discontinuity (RPD) depths, and Organism-Sediment Index (OSI) values at Cap Site 2 for August 1985.

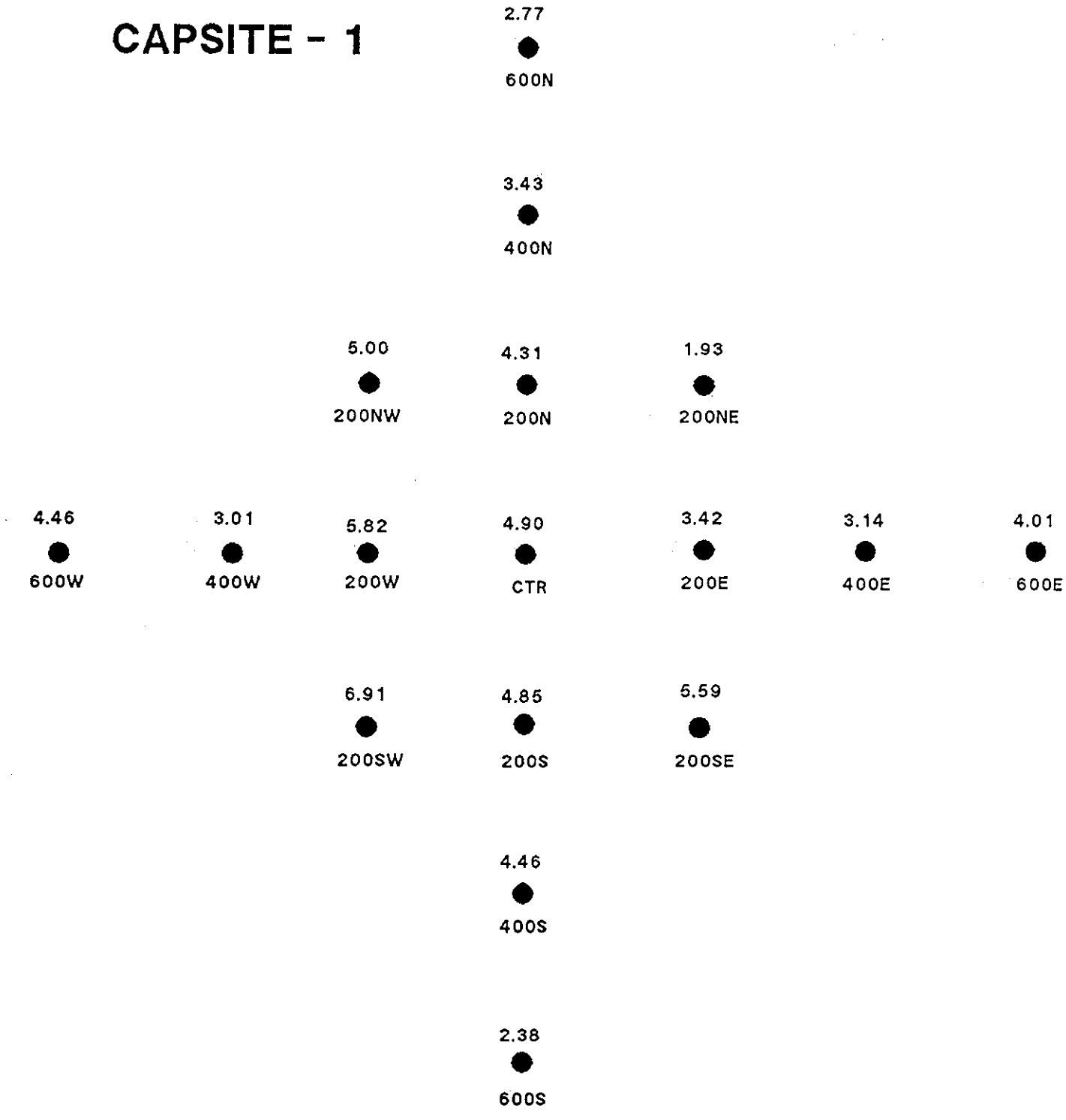

Figure 3-42 The mapped mean apparent redox potential discontinuity (RPD) depth values (cm) at each station at Cap Site 1 in the August survey.

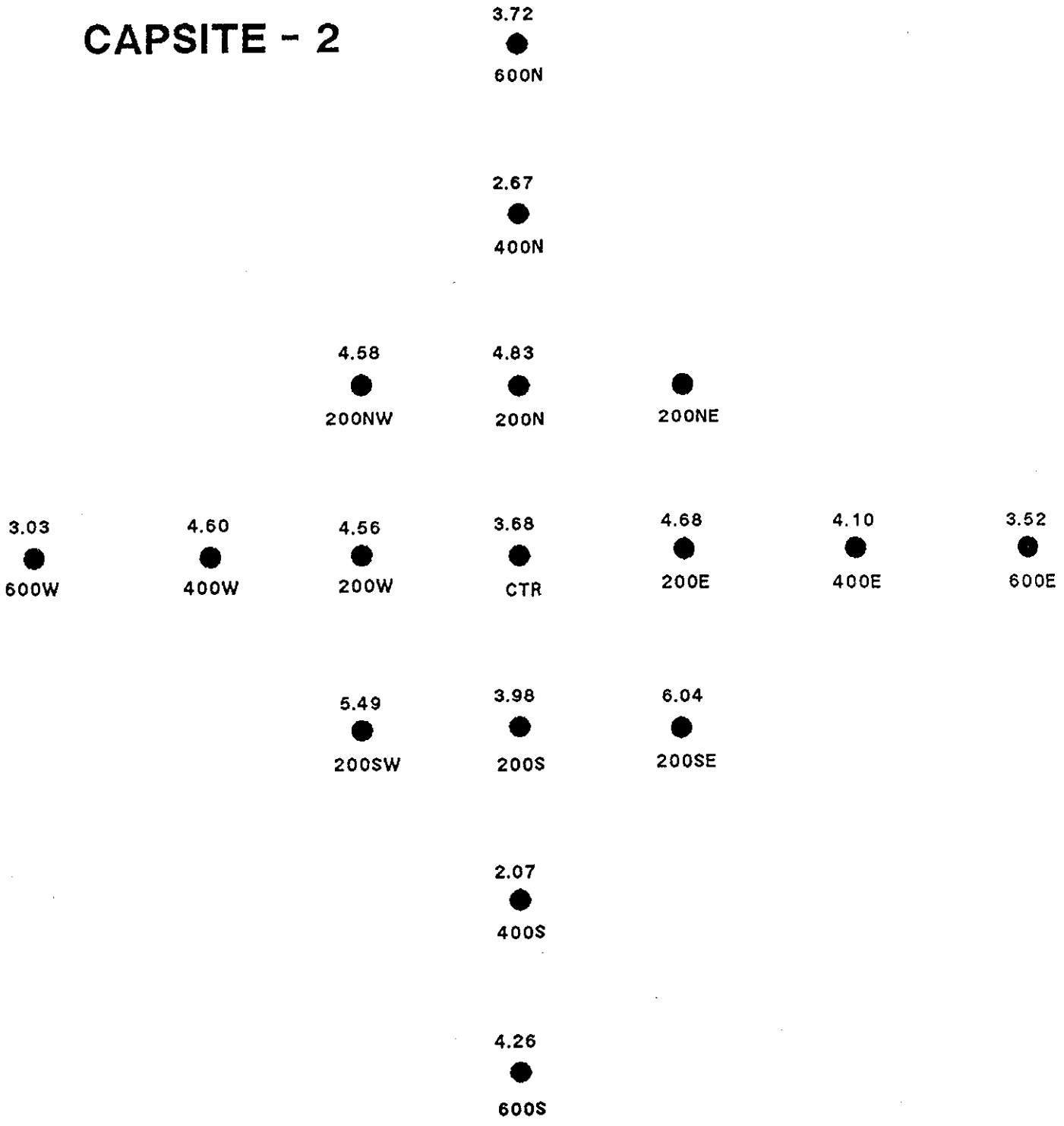

Figure 3-43 The mapped mean apparent redox potential discontinuity (RPD) depth values (cm) at each station at Cap Site 2 in the August survey. REMOTS® photos were not successfully obtained at station 200NE.

CAPSITE - 1

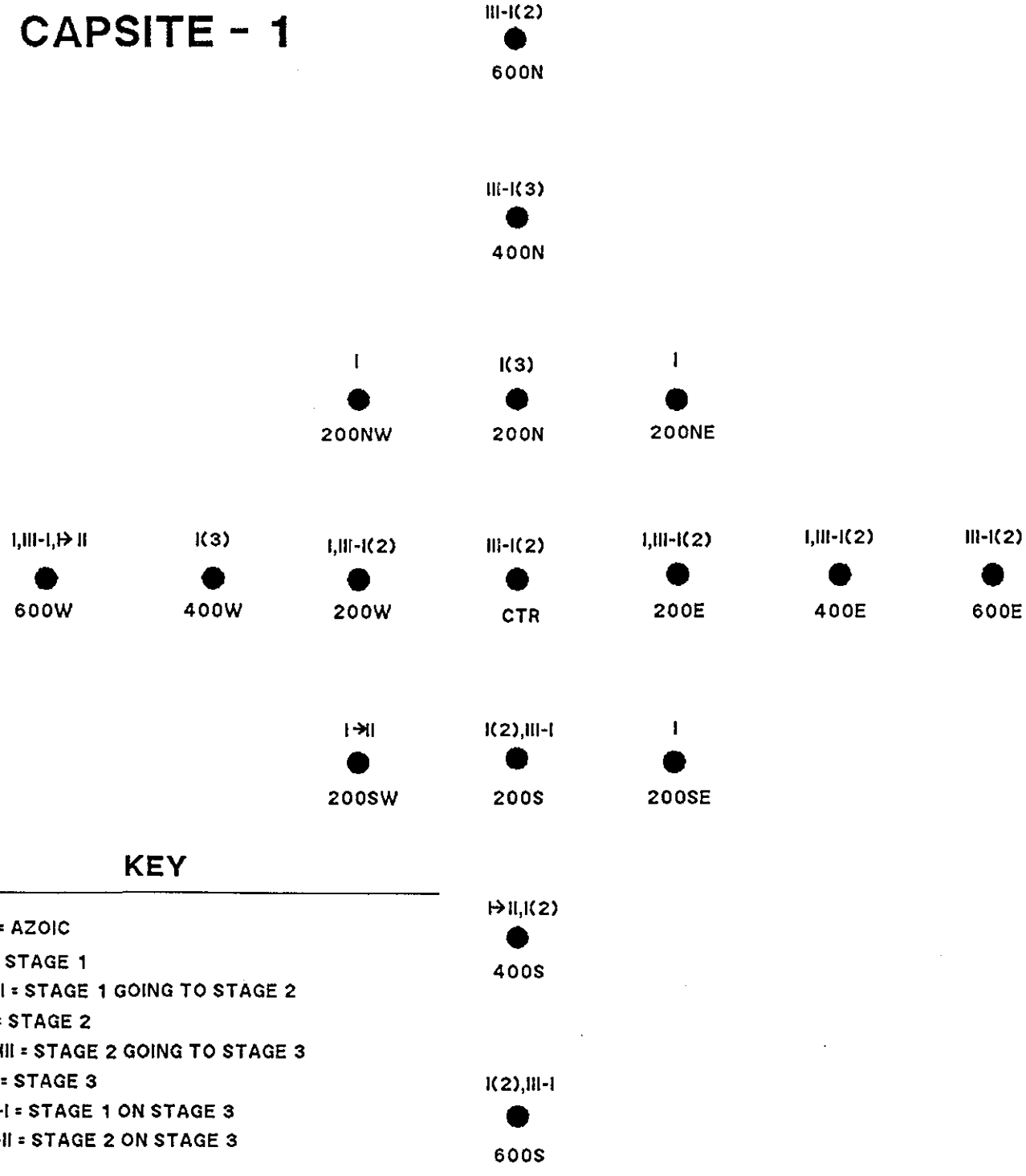

KEY

0 = AZOIC
I = STAGE 1
I→II = STAGE 1 GOING TO STAGE 2
II = STAGE 2
II→III = STAGE 2 GOING TO STAGE 3
III = STAGE 3
III-I = STAGE 1 ON STAGE 3
III-II = STAGE 2 ON STAGE 3

Figure 3-44 The mapped distribution of successional stages for all replicates at Cap Site 1 in the August survey.

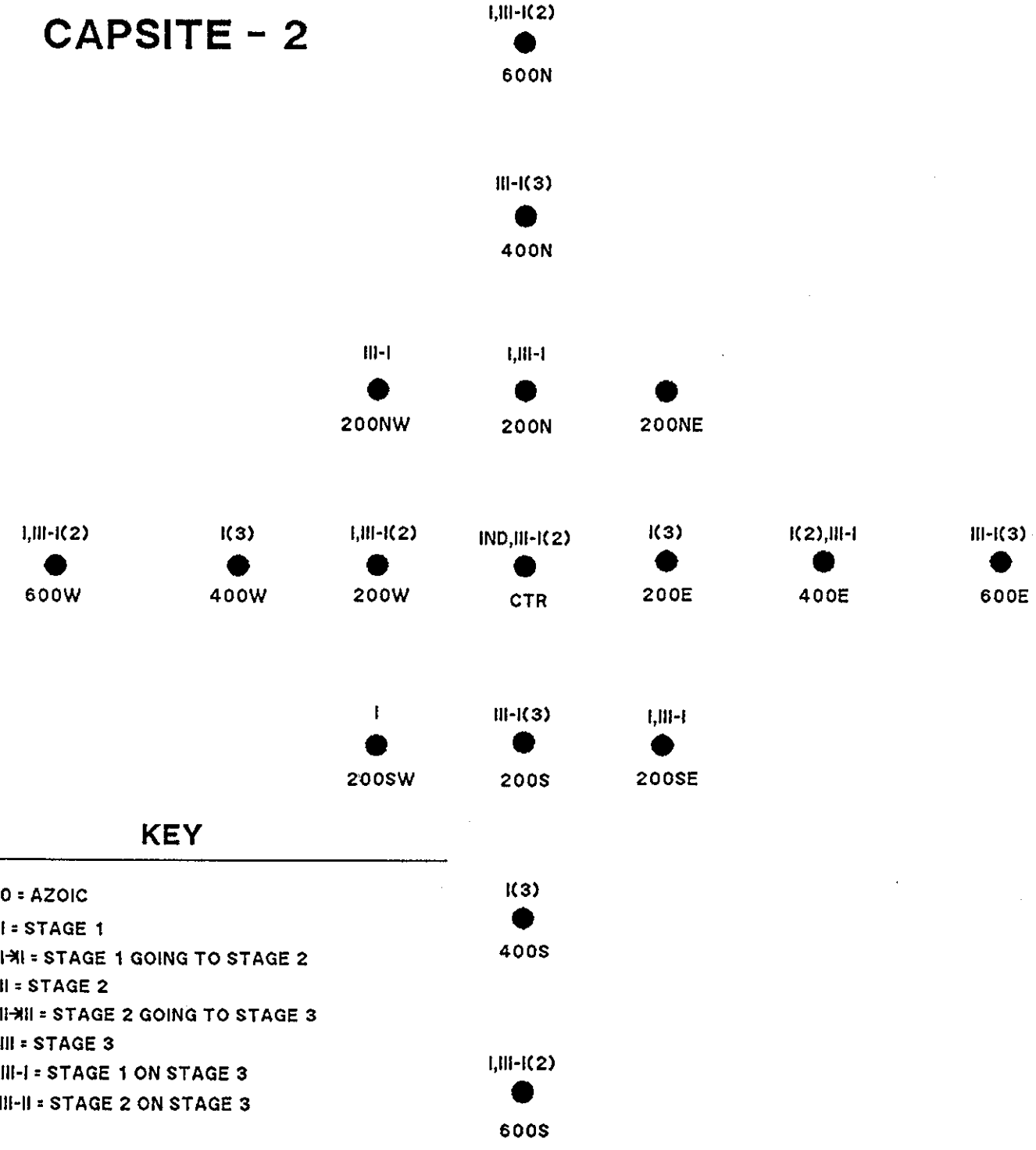

Figure 3-45 The mapped distribution of successional stages for all replicates at Cap Site 2 in the August survey. REMOTS® photos were not successfully obtained at station 200NE.

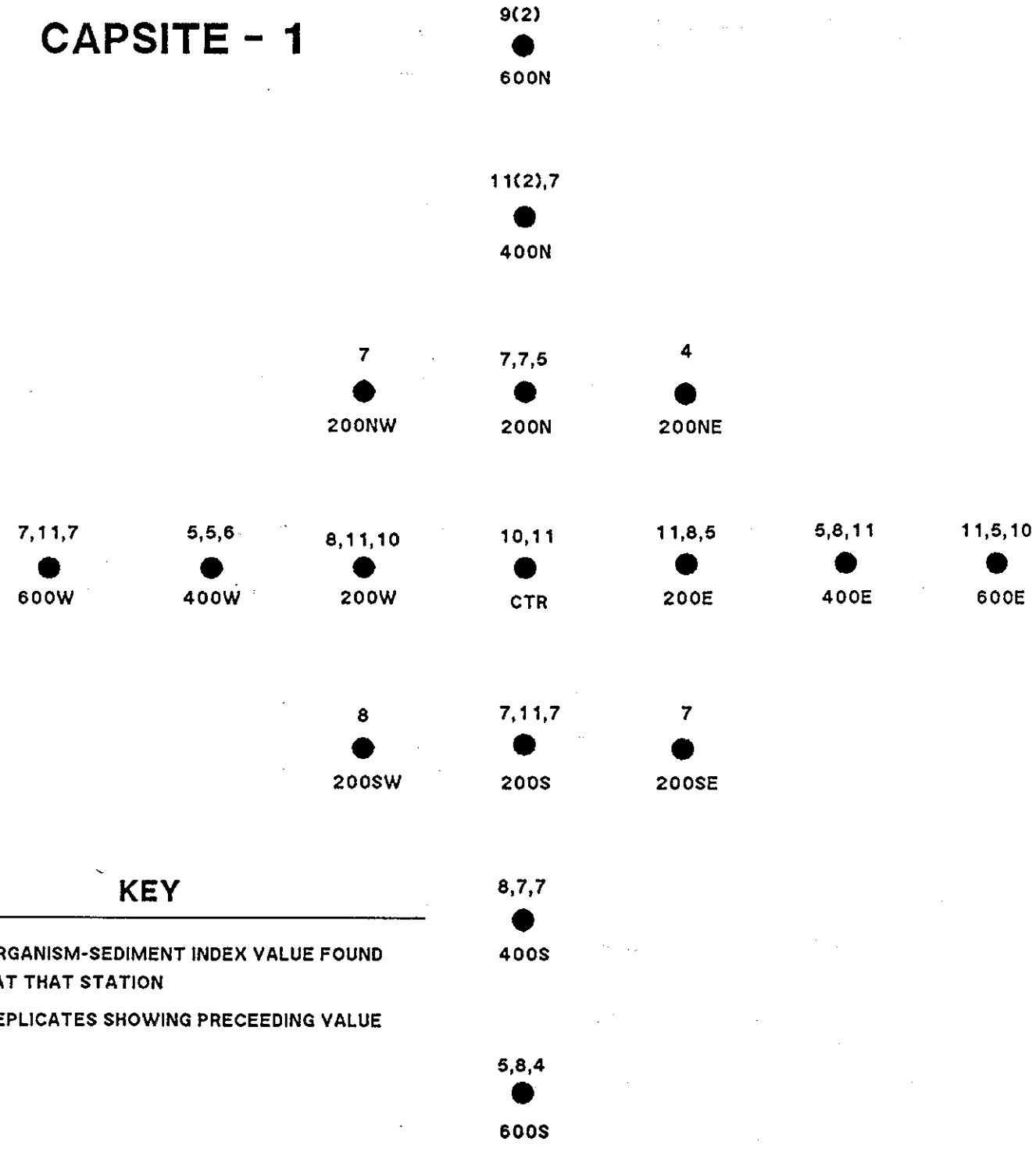

Figure 3-46 The mapped distribution of Organism- Sediment Indices (OSI) for all replicates at Cap Site 1 in the August survey.

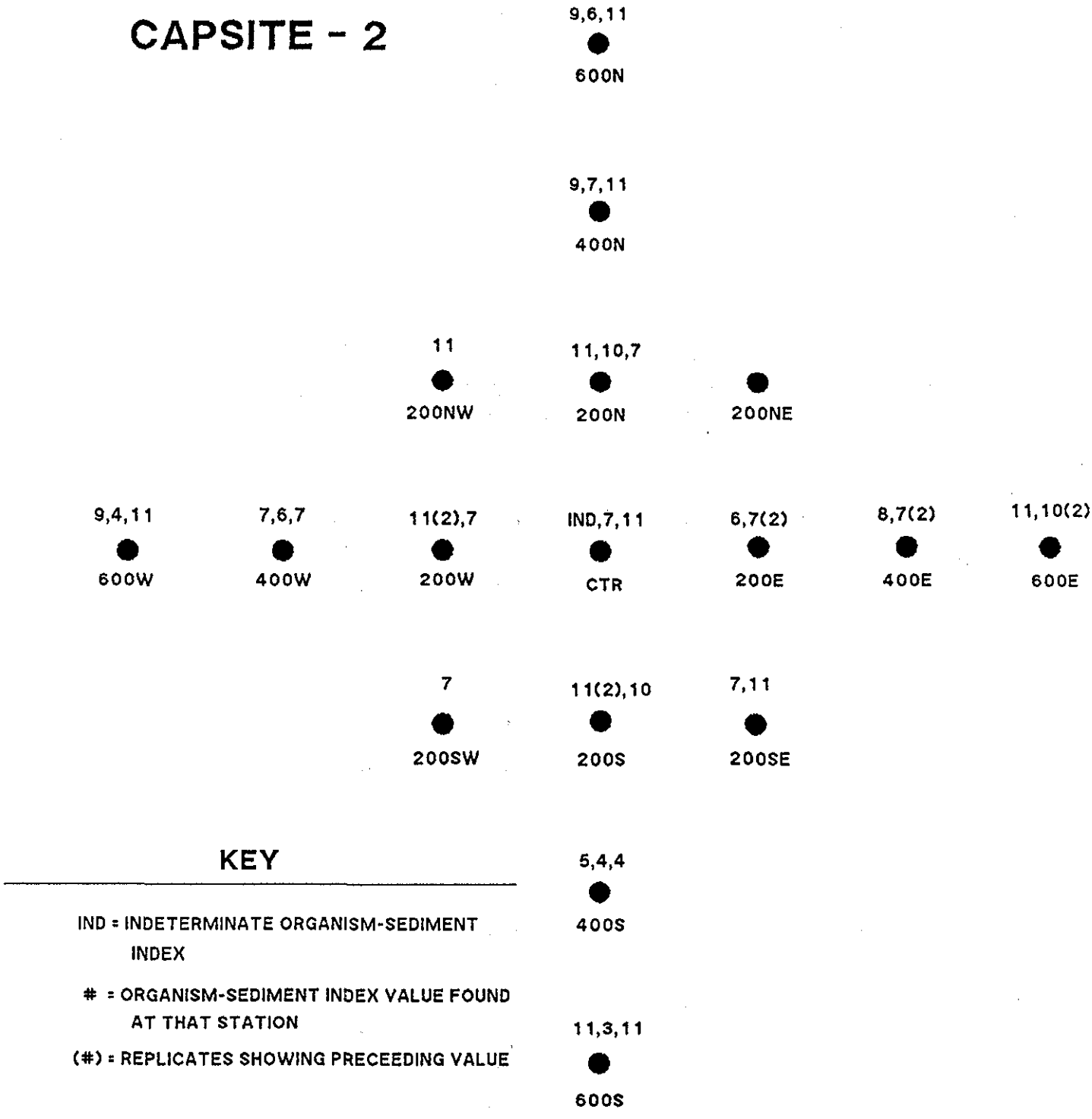

Figure 3-47 The mapped distribution of Organism- Sediment Indices (OSI) for all replicates at Cap Site 2 in the August survey. REMOTS® photos were not successfully obtained at station 200NE.

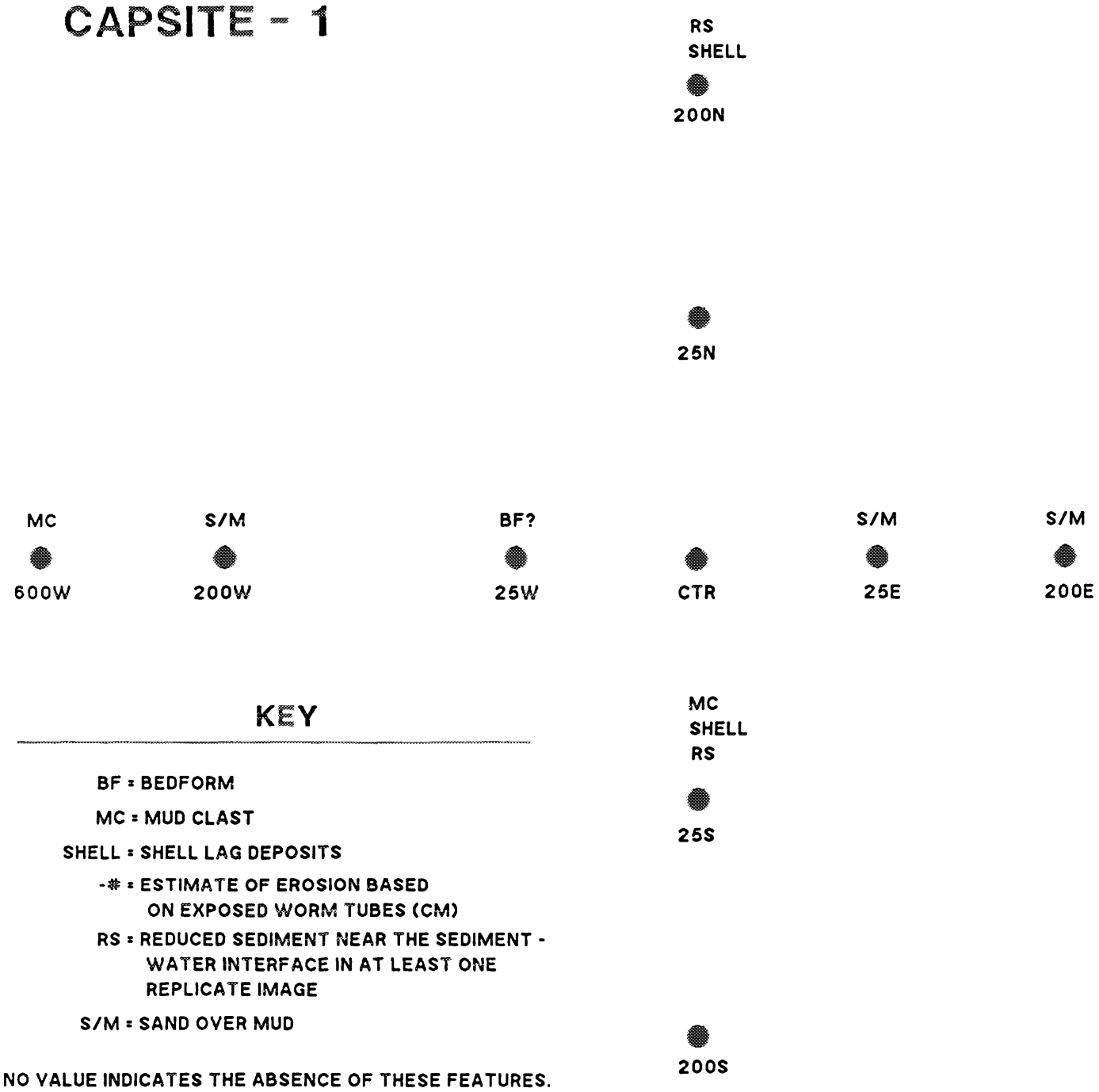

Figure 3-48 A post-storm benthic "process" map of Cap Site 1 showing the distribution of erosional and depositional features.

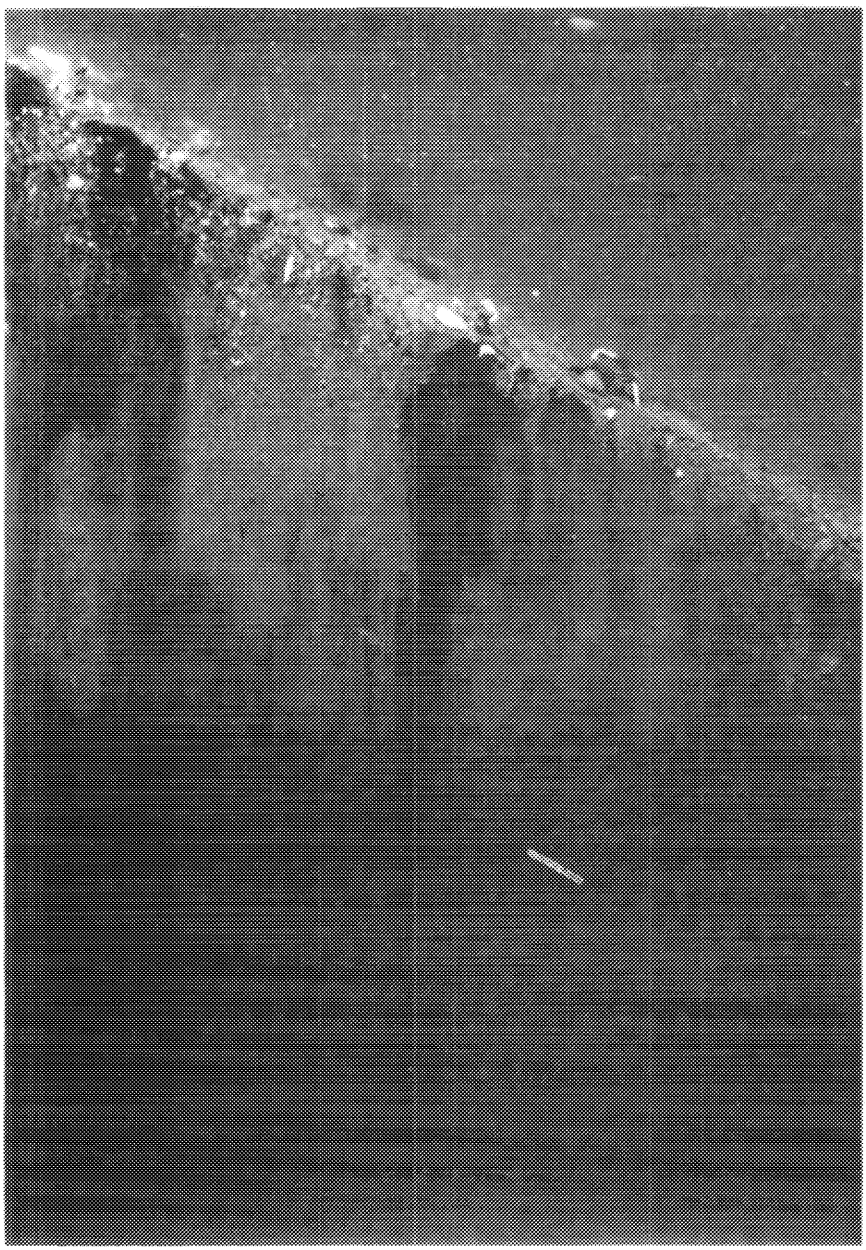

Figure 3-49 A REMOTS® image from Cap Site 1 station 25S showing shell lag deposits and mud clasts.

Figure 3-50 A REMOTS® image from Cap Site 1 station 200E showing fine sand sediments over-lying silt-clay. Scale = 1X.

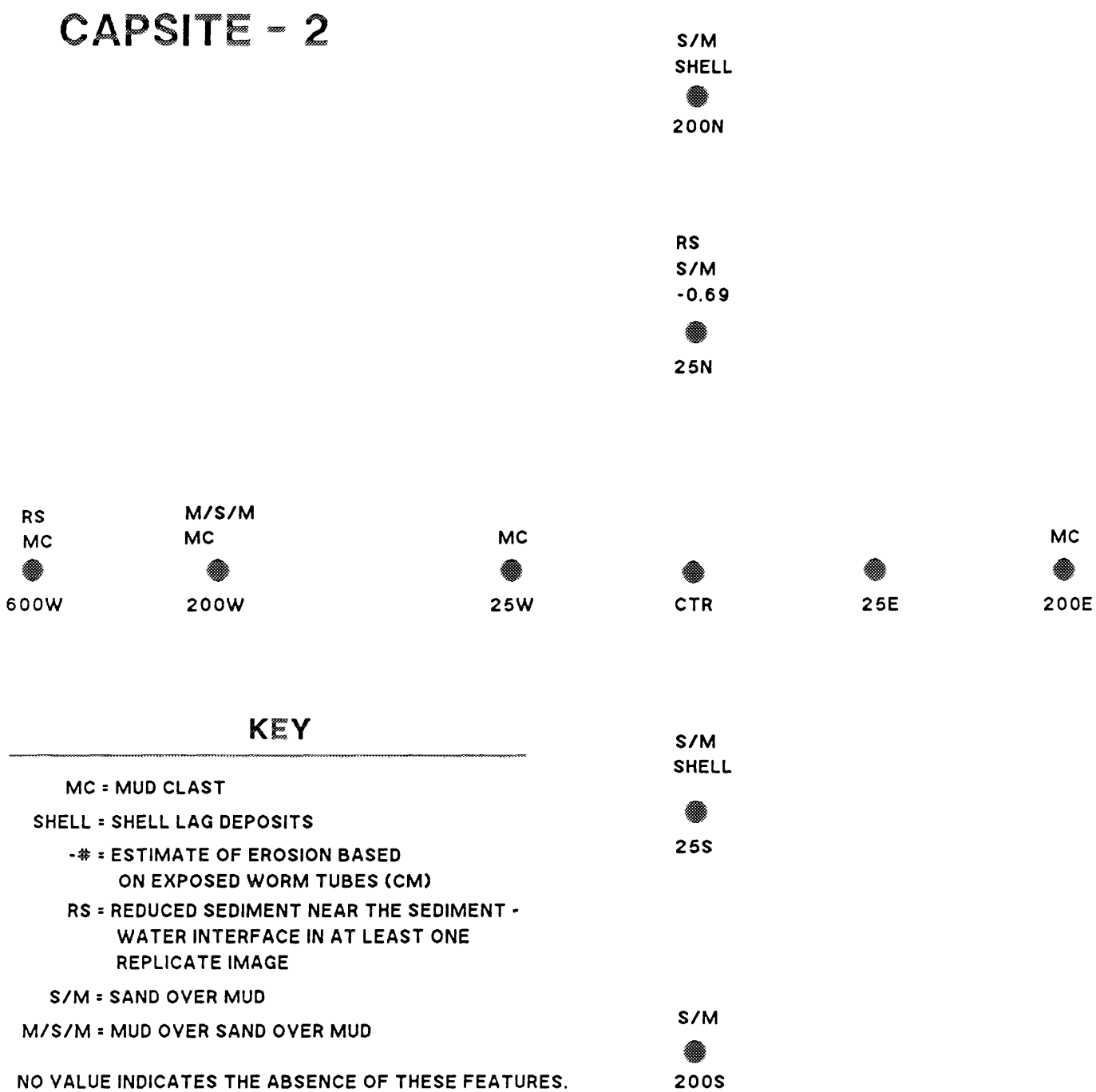

Figure 3-51 A post-storm benthic "process" map of Cap Site 2 showing the distribution of erosional and depositional features.

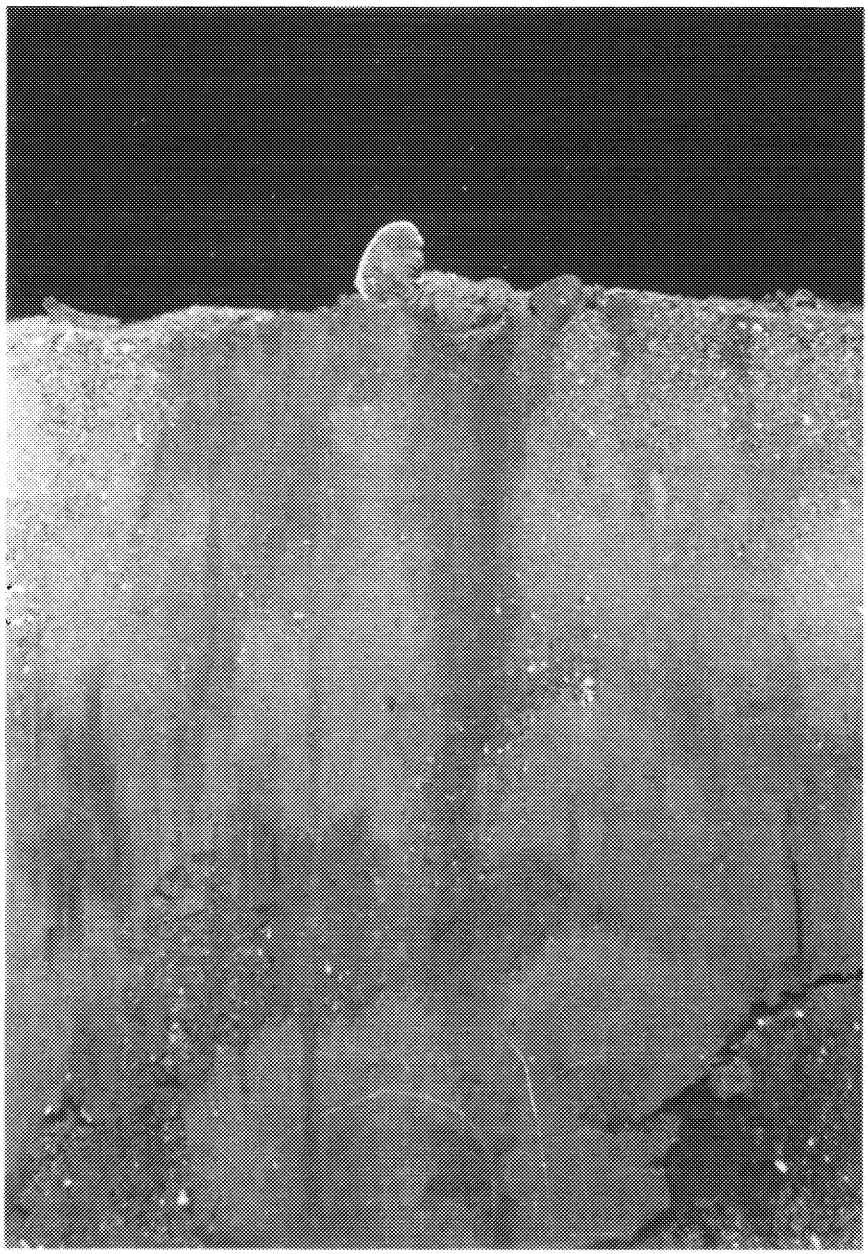

Figure 3-52 A-B REMOTS® images from Cap Site 2 station 200S pre-storm (A) and station 200S post-storm, (B) showing the increase of coarse-grained sediments from August to October. Scale = 1X.

Figure 3-52B scale = 1X.

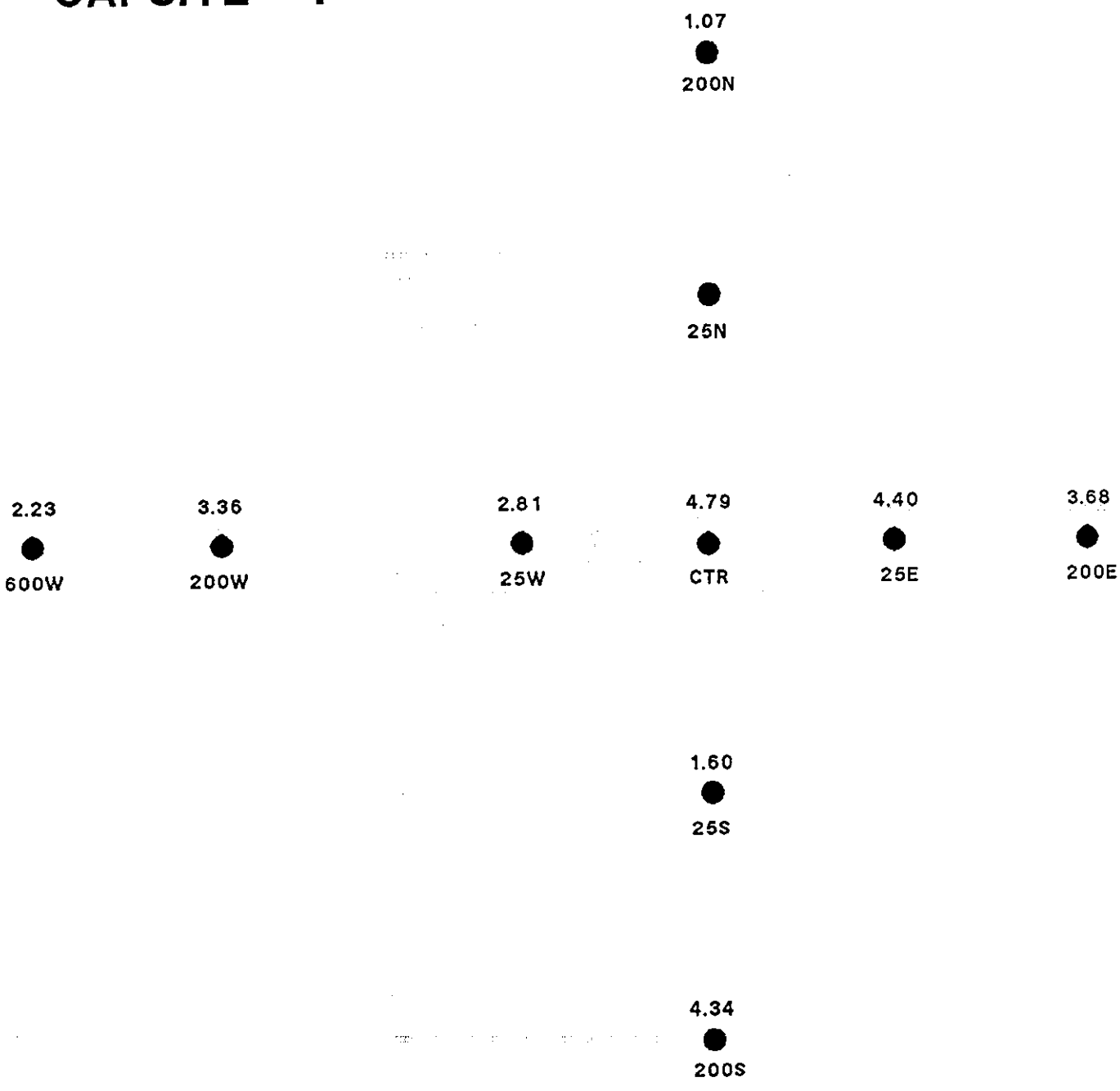

Figure 3-53 The mapped distribution of post-storm average apparent redox potential discontinuity (RPD) depth values at Cap Site 1. A REMOTS® photo was not successfully obtained at station 25N.

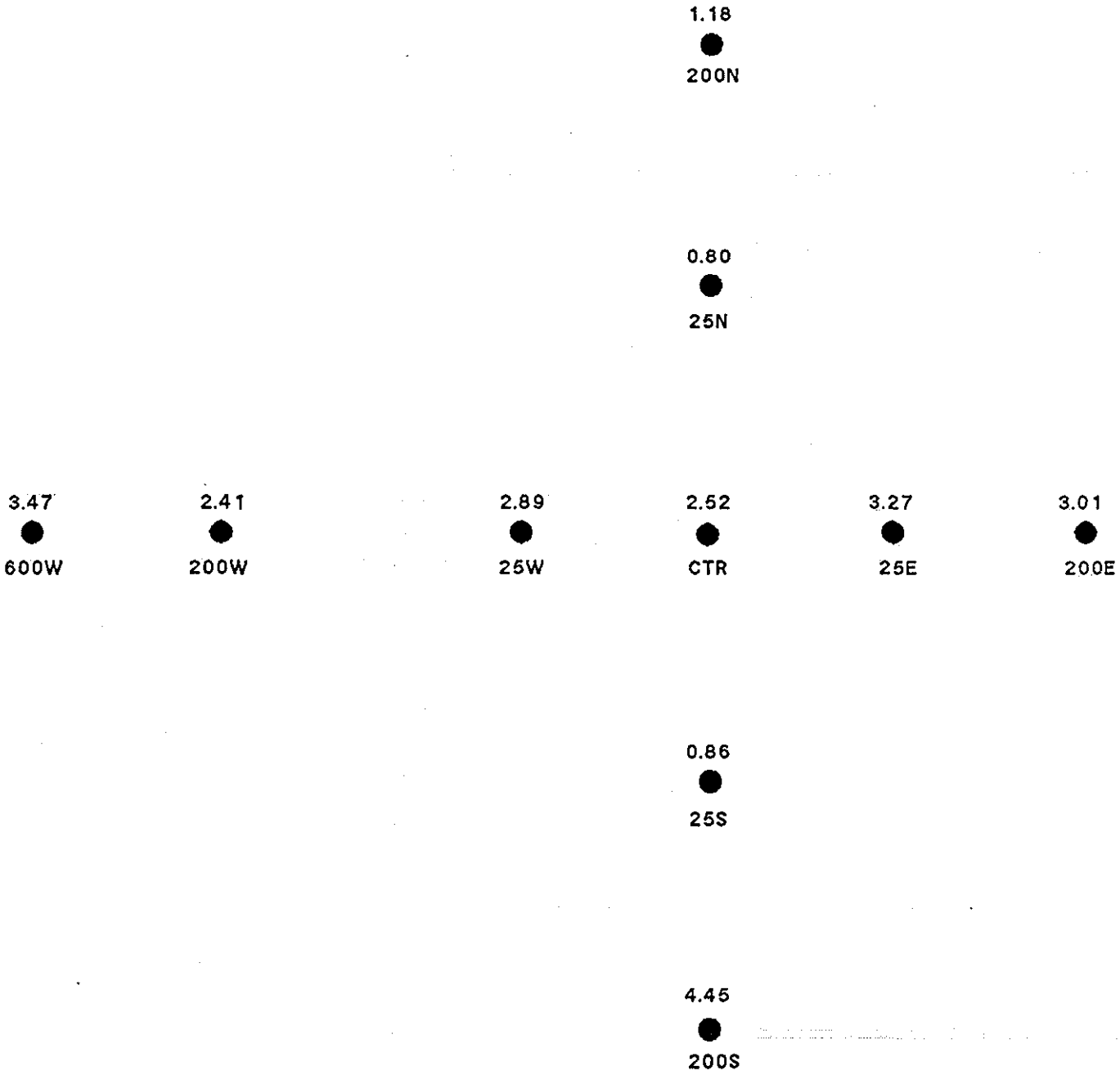

Figure 3-54 The mapped distribution of post-storm average apparent redox potential discontinuity (RPD) depth values at Cap Site 2.

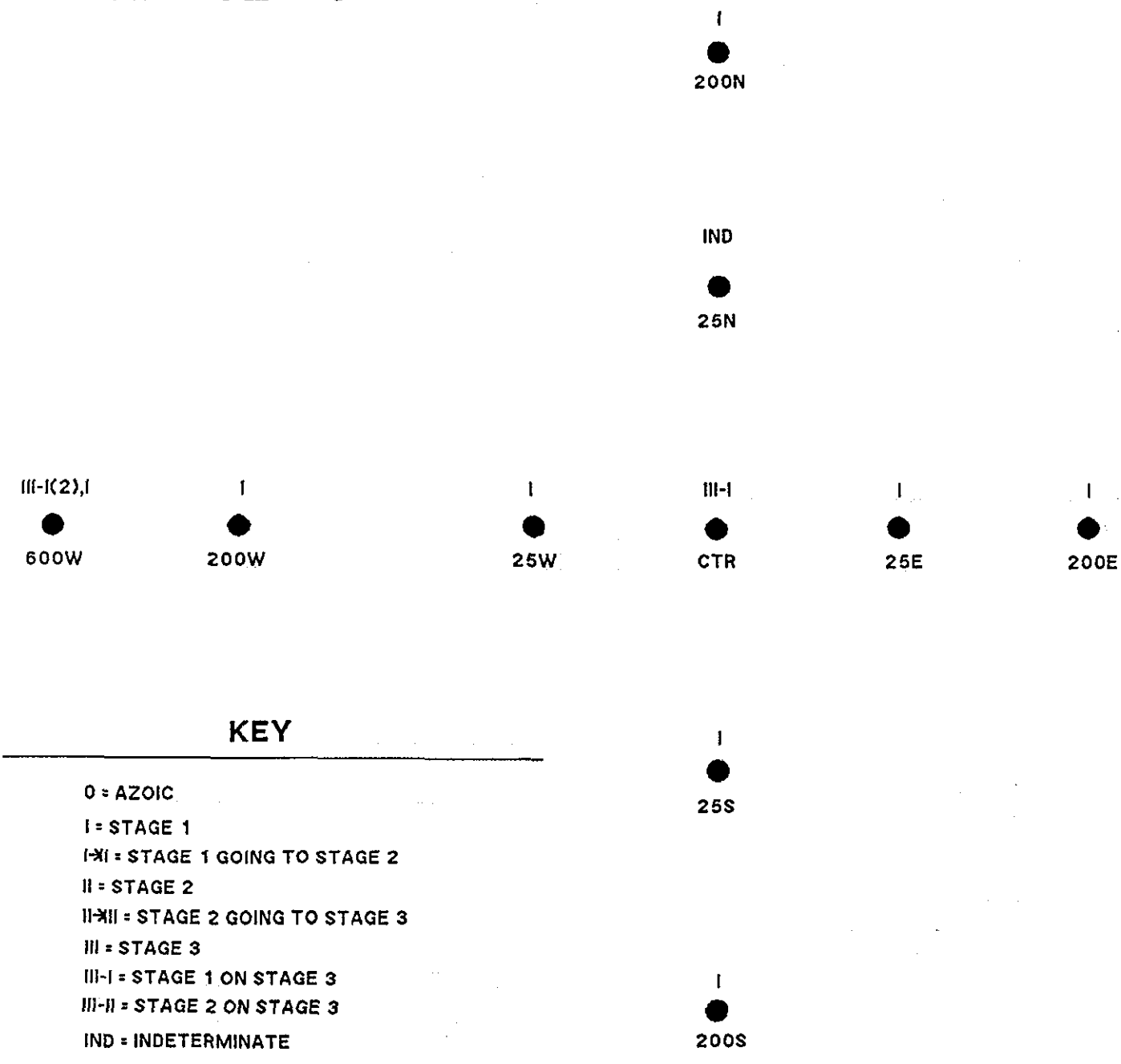

Figure 3-55 The mapped distribution of post-storm successional stages at Cap Site 1. A REMOTS® photo was not successfully obtained at station 25N.

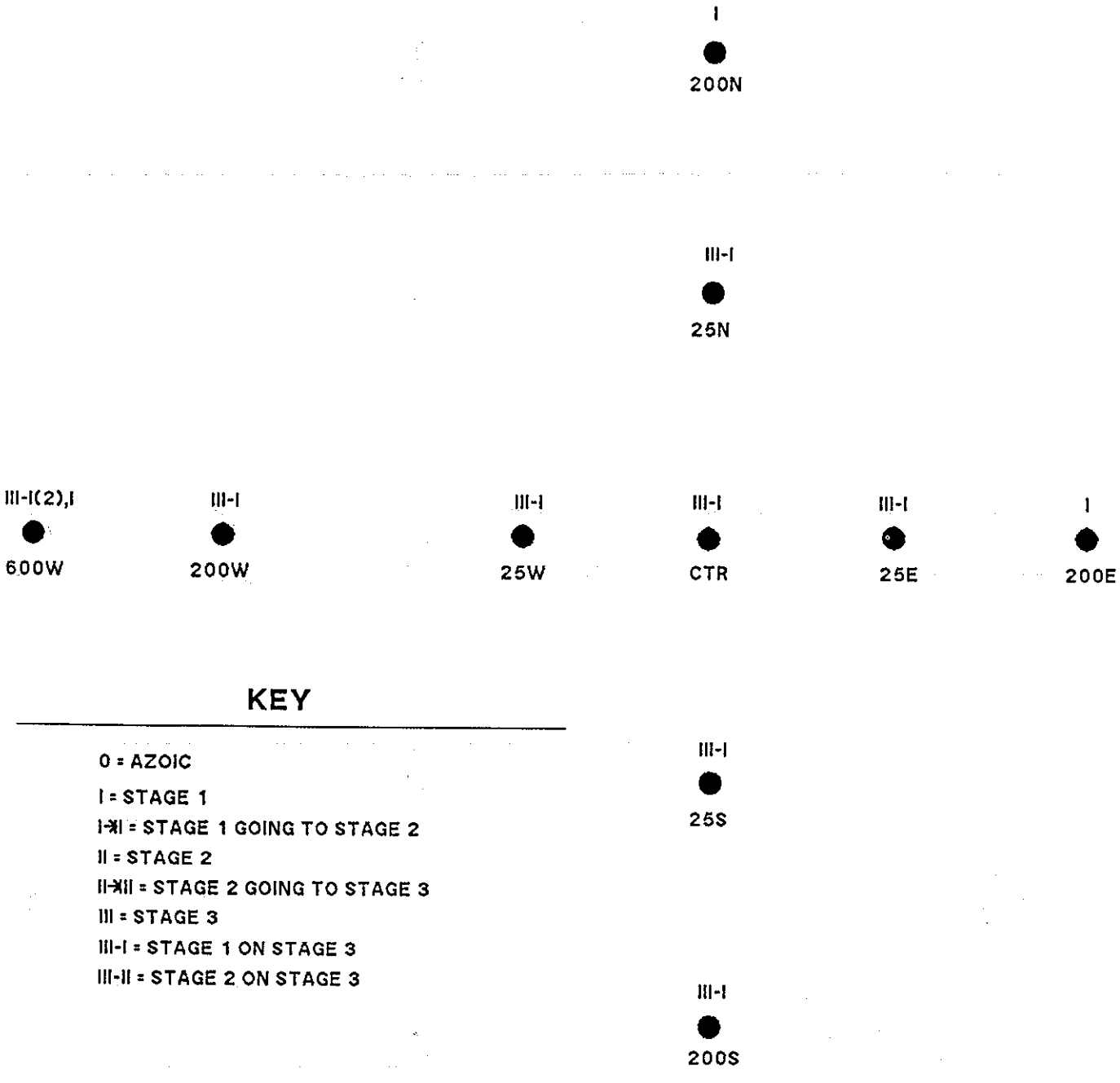

Figure 3-56 The mapped distribution of post-storm successional stages at Cap Site 2.

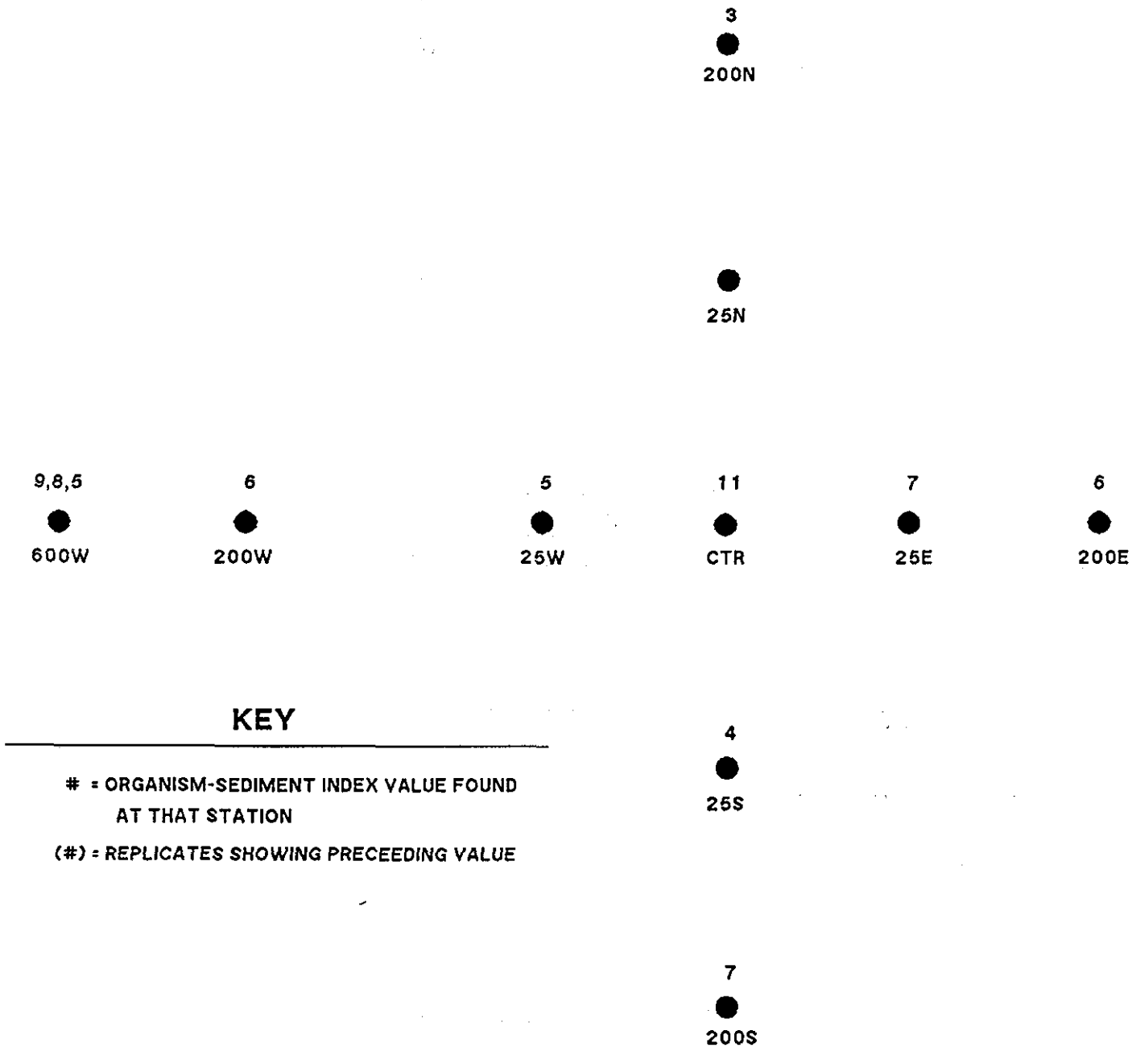

Figure 3-57 The mapped distribution of post-storm Organism-Sediment Indices (OSI) at Cap Site 1.

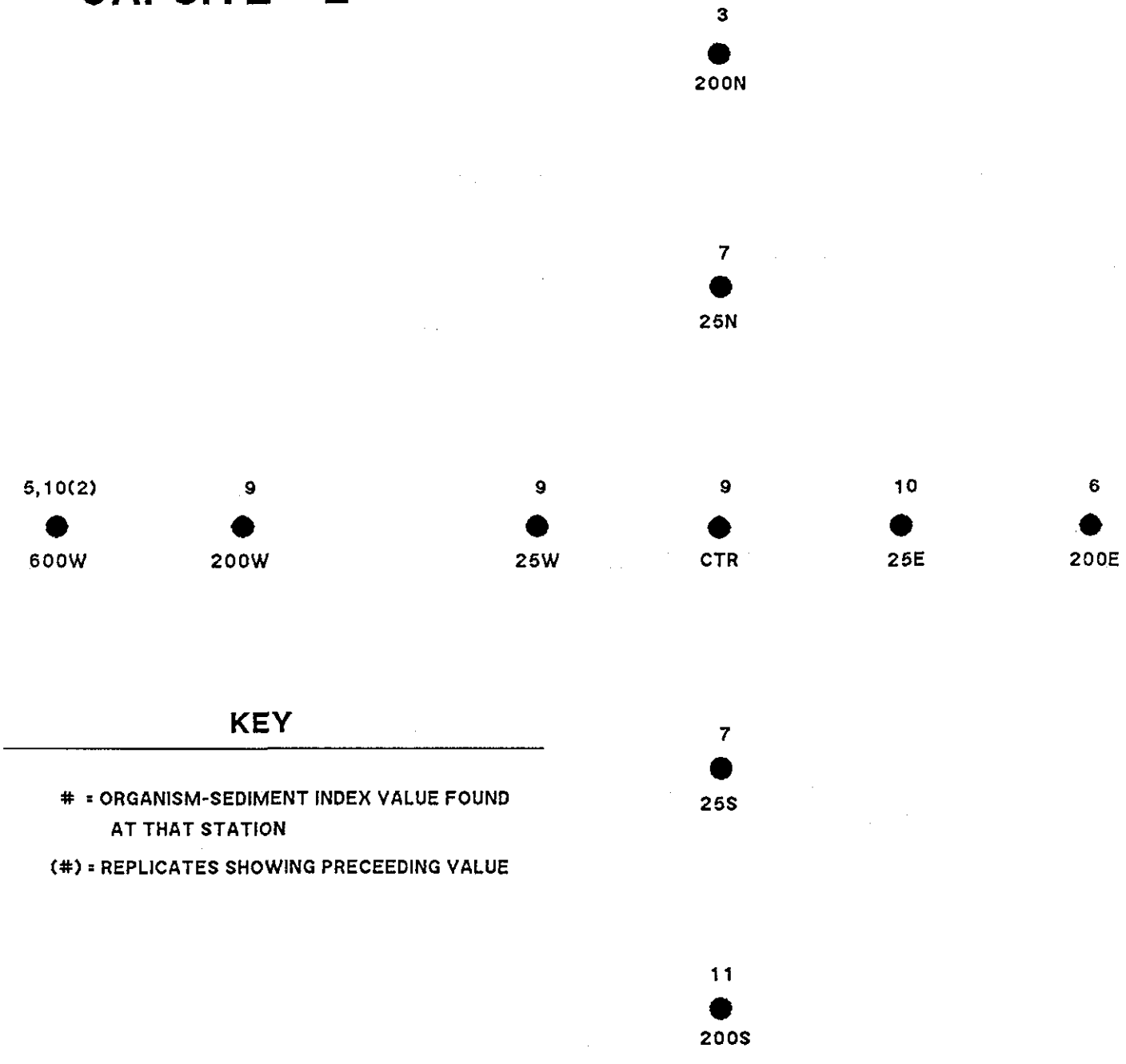

Figure 3-58 The mapped distribution of post-storm Organism-Sediment Indices (OSI) at Cap Site 2.

MQR

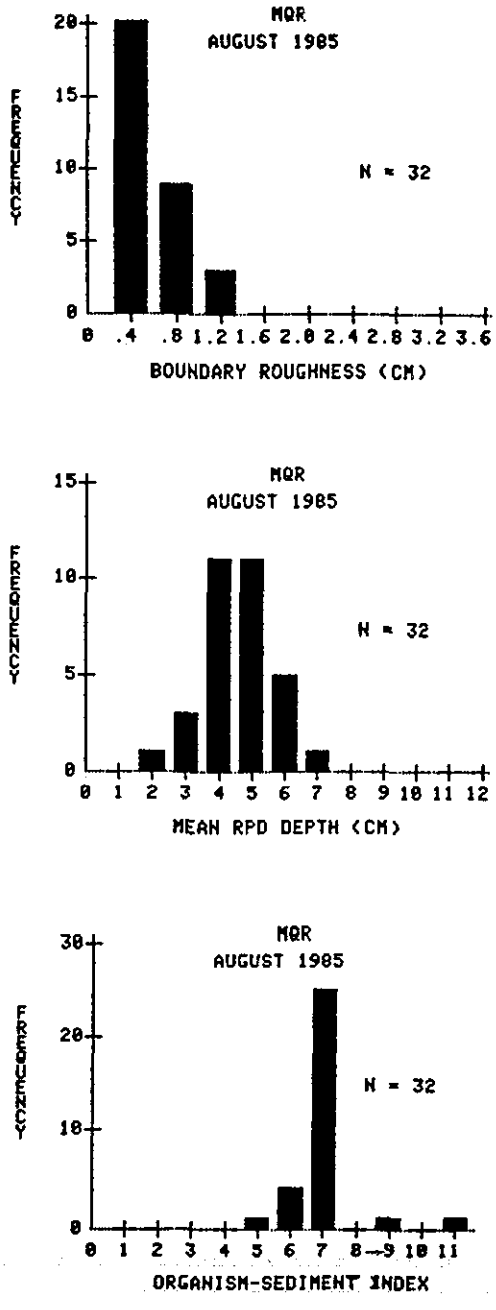

Figure 3-59 The frequency distribution of boundary roughness, redox potential discontinuity (RPD), and Organism-Sediment Index (OSI) values for the August survey at MQR.

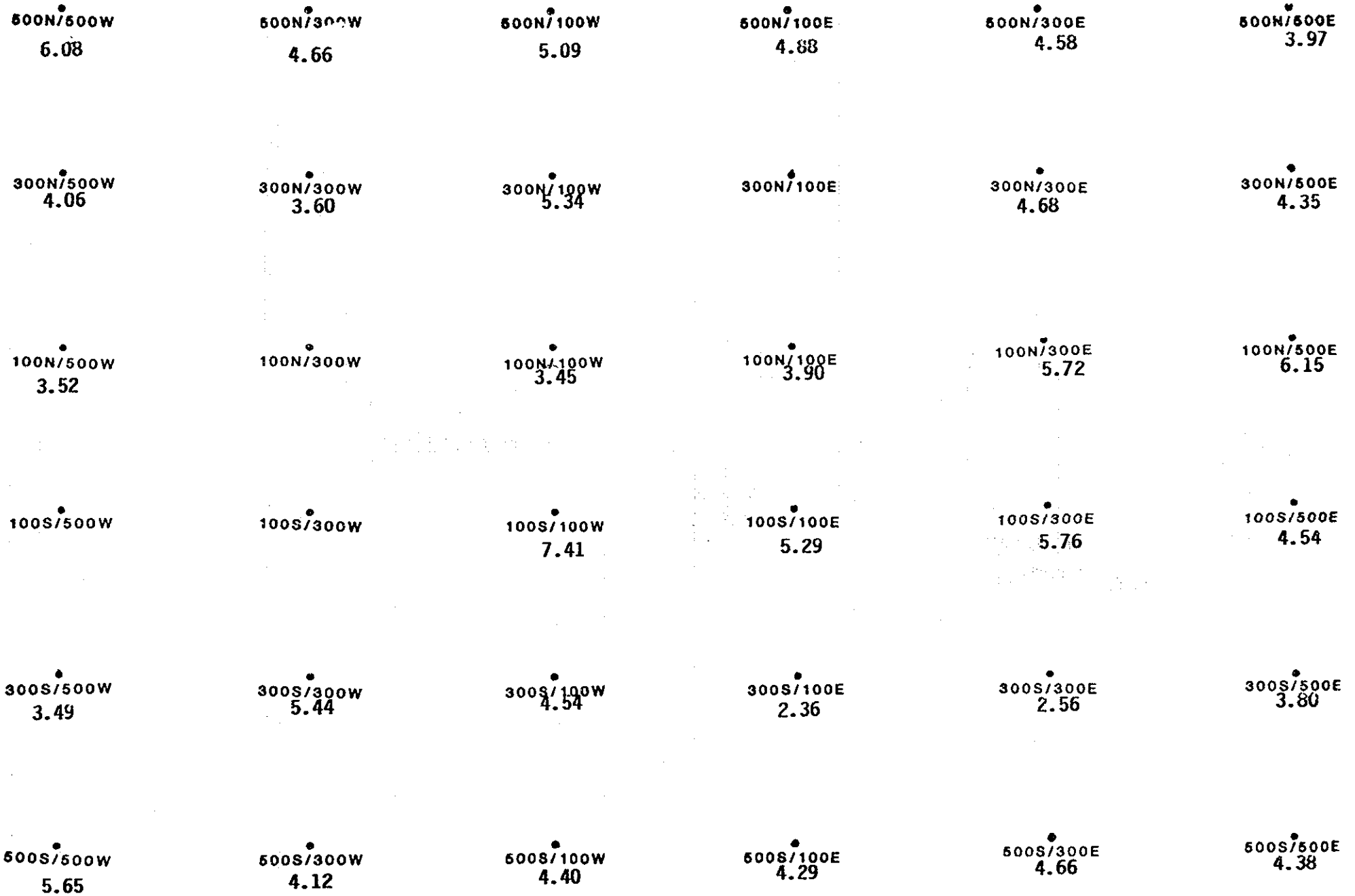

Figure 3-60 The mapped distribution of apparent redox potential discontinuity (RPD) depth values at the MQR site in August. REMOTS® images were not obtained at stations where no values are indicated.

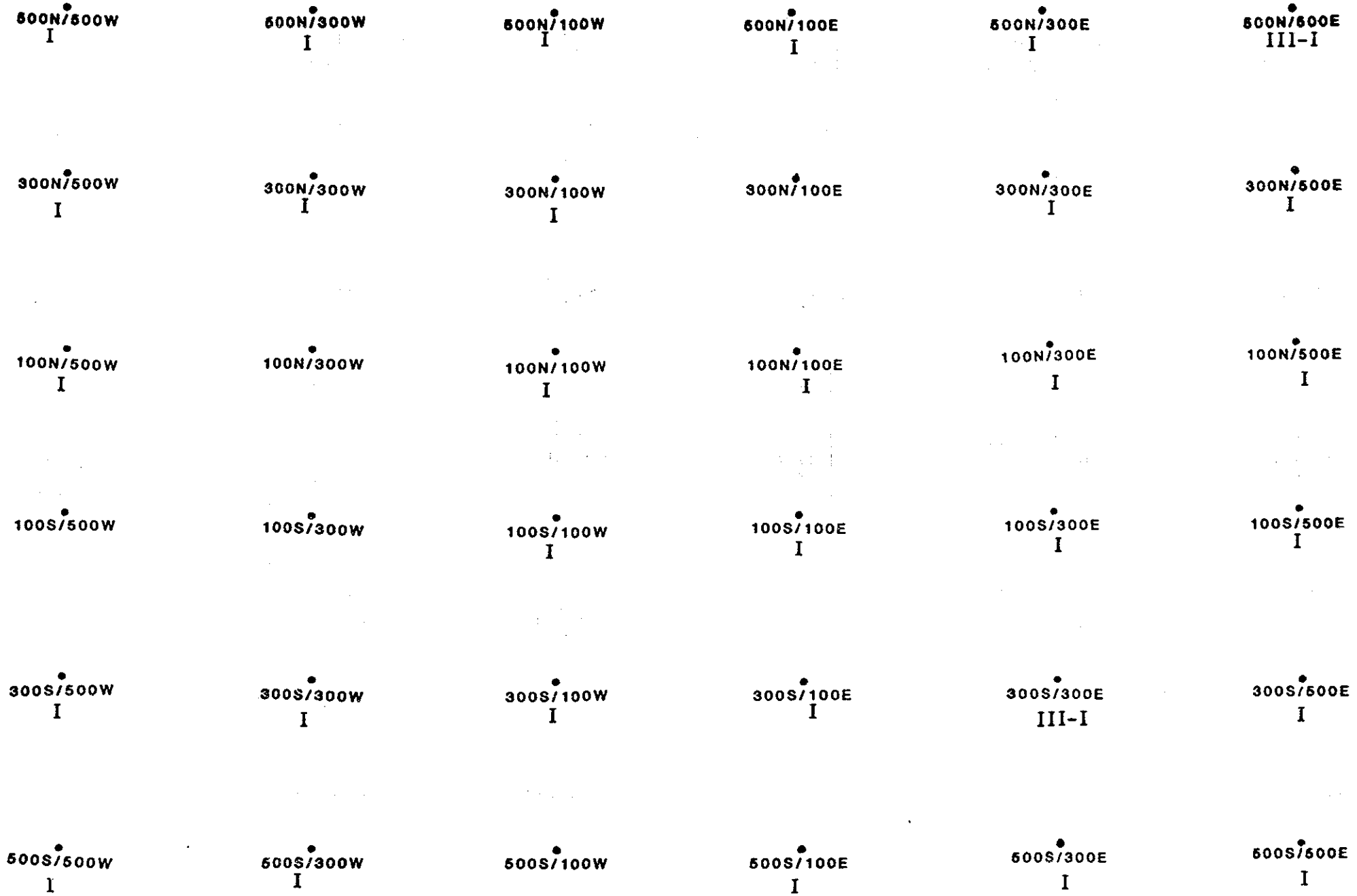

Figure 3-61 The mapped distribution of successional stages for all replicates at the MQR site in August. REMOTS® images were not obtained at stations where no values are indicated.

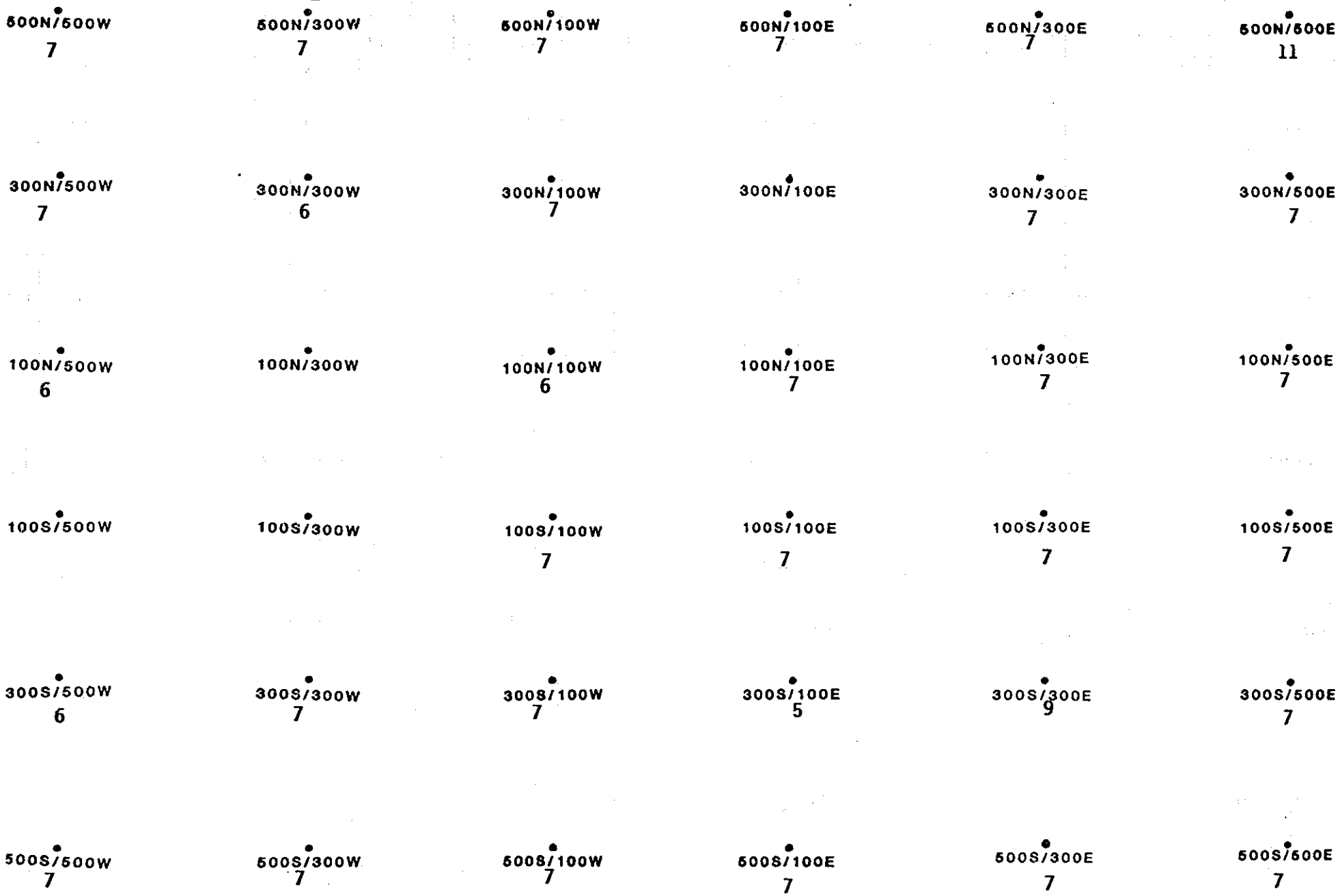

Figure 3-62 The mapped distribution of Organism-Sediment Indices (OSI) values for all replicates at the MQR site in August. REMOTS® images were not obtained at stations where no values are indicated.

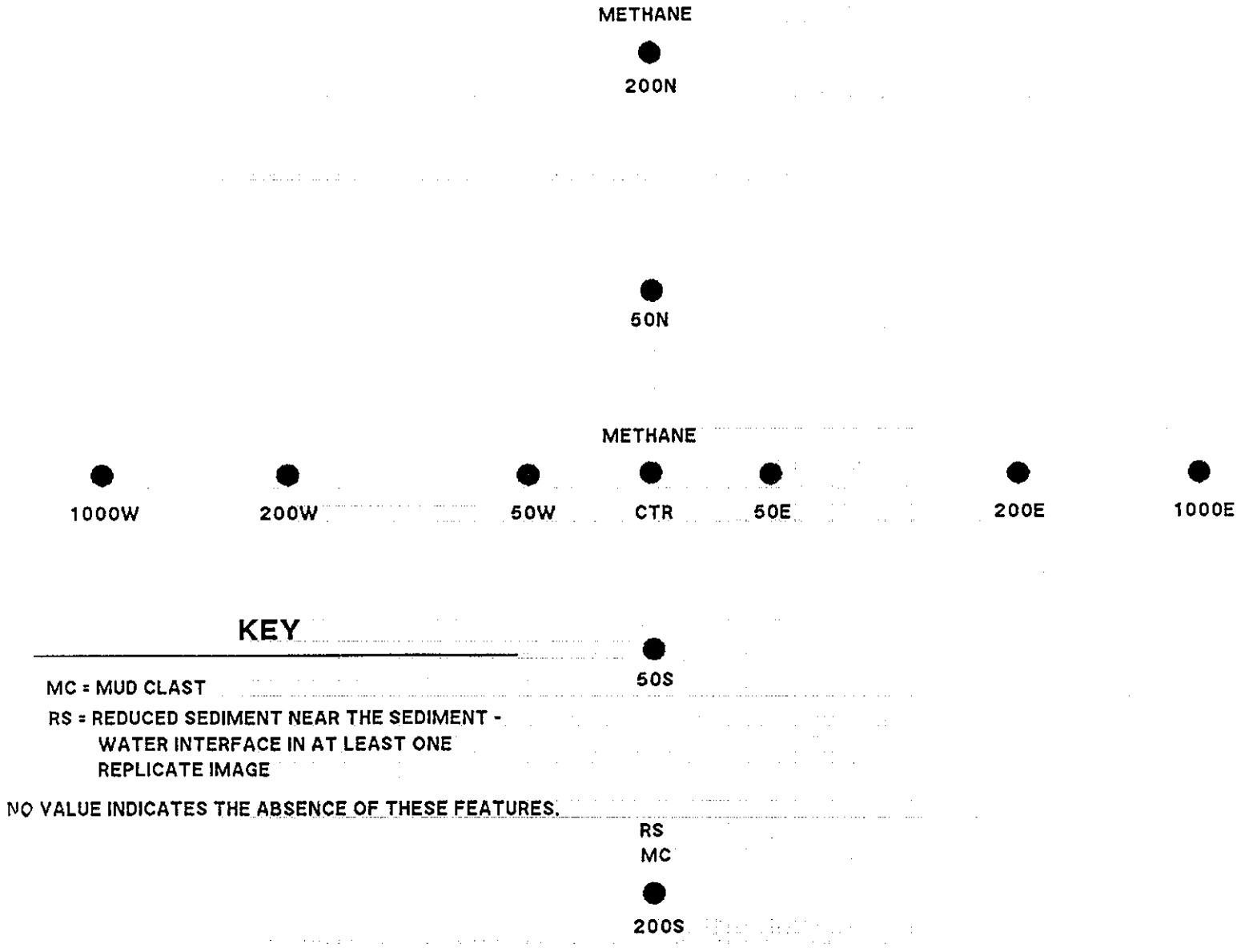

Figure 3-63 A post-storm benthic "process" map showing the distribution of erosional and depositional features.

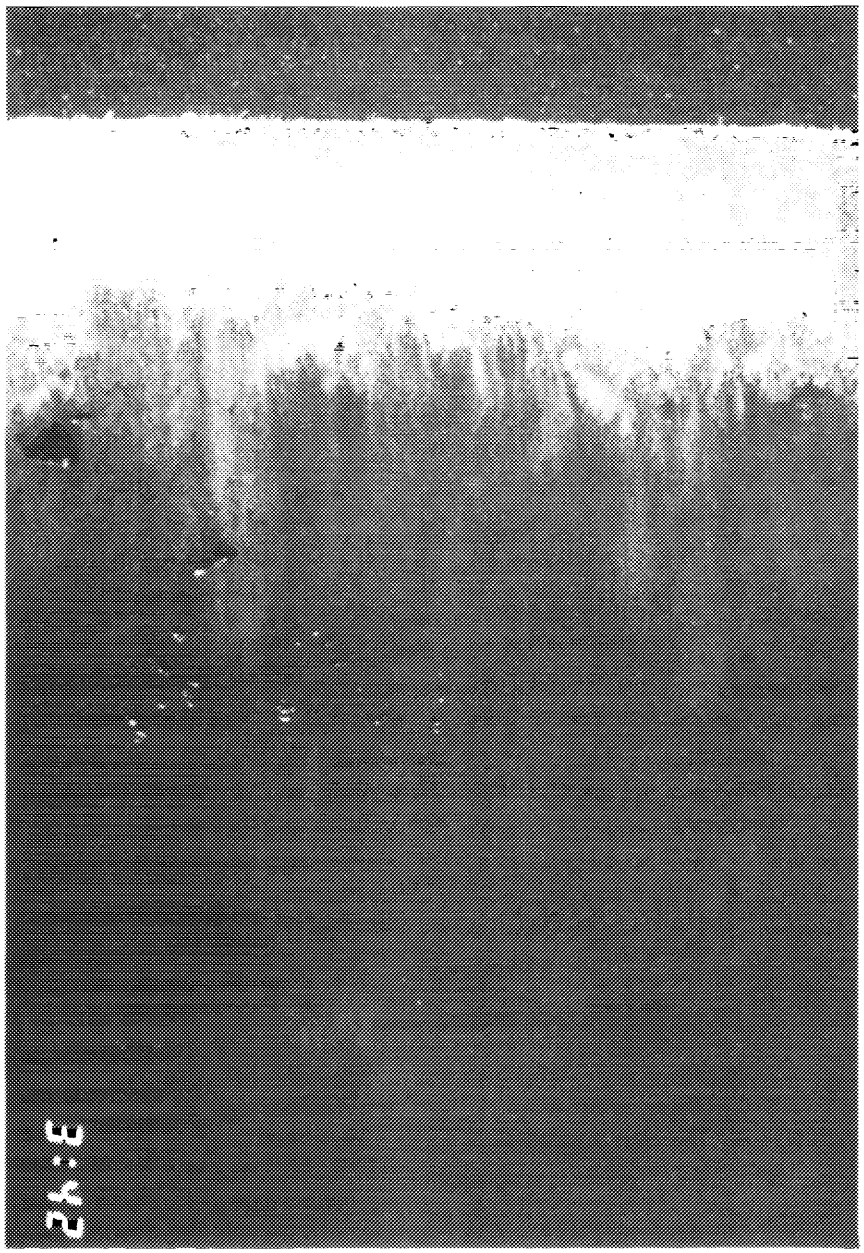

Figure 3-64 A post-storm REMOTS® image from station 200N showing a smooth bottom colonized by a Stage I assemblage. Scale = 1X.

MQR

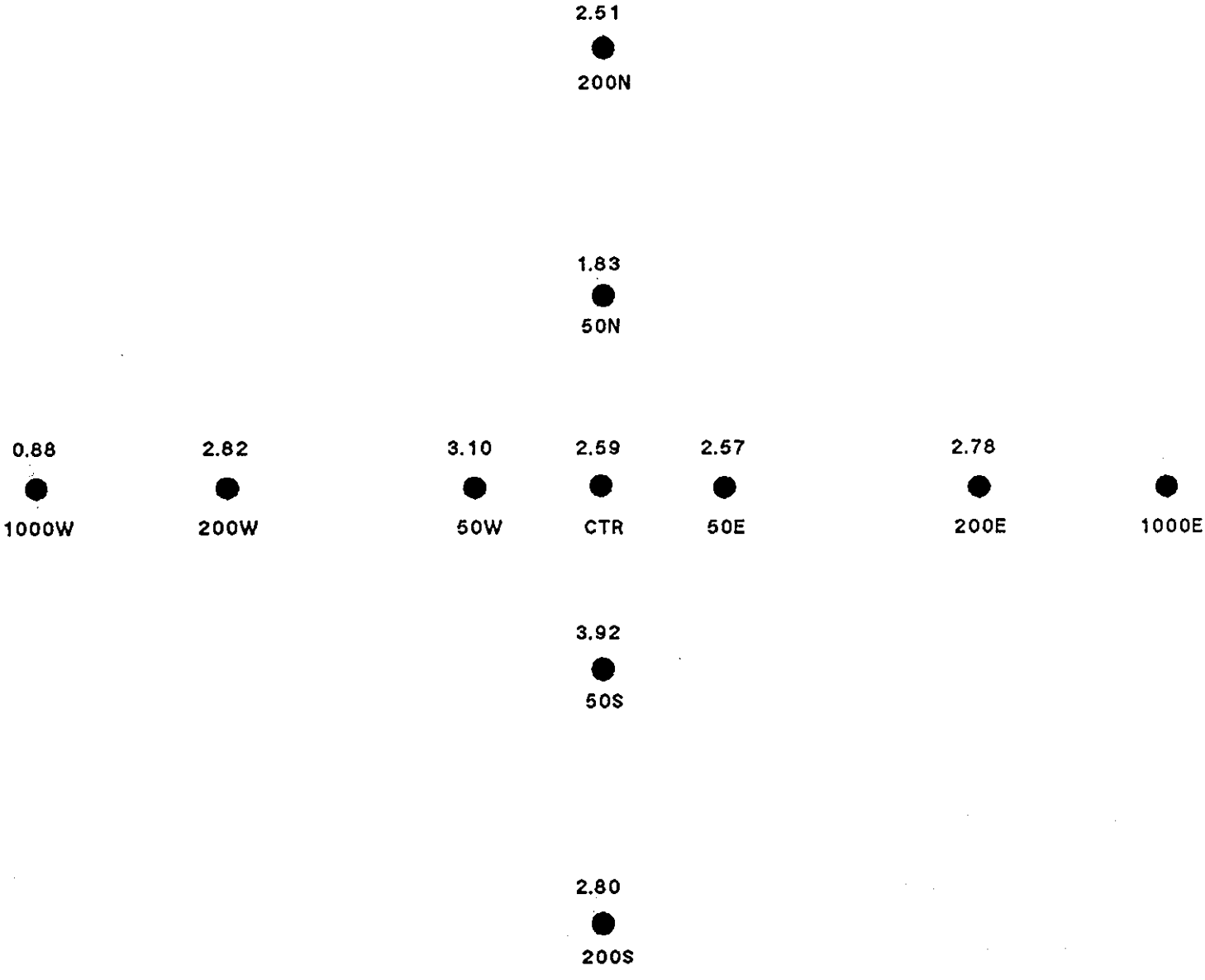

Figure 3-65 The mapped distribution of post-storm redox potential discontinuity (RPD) depths (cm) at MQR. A REMOTS® photo was not successfully obtained at 1000E.

MQR

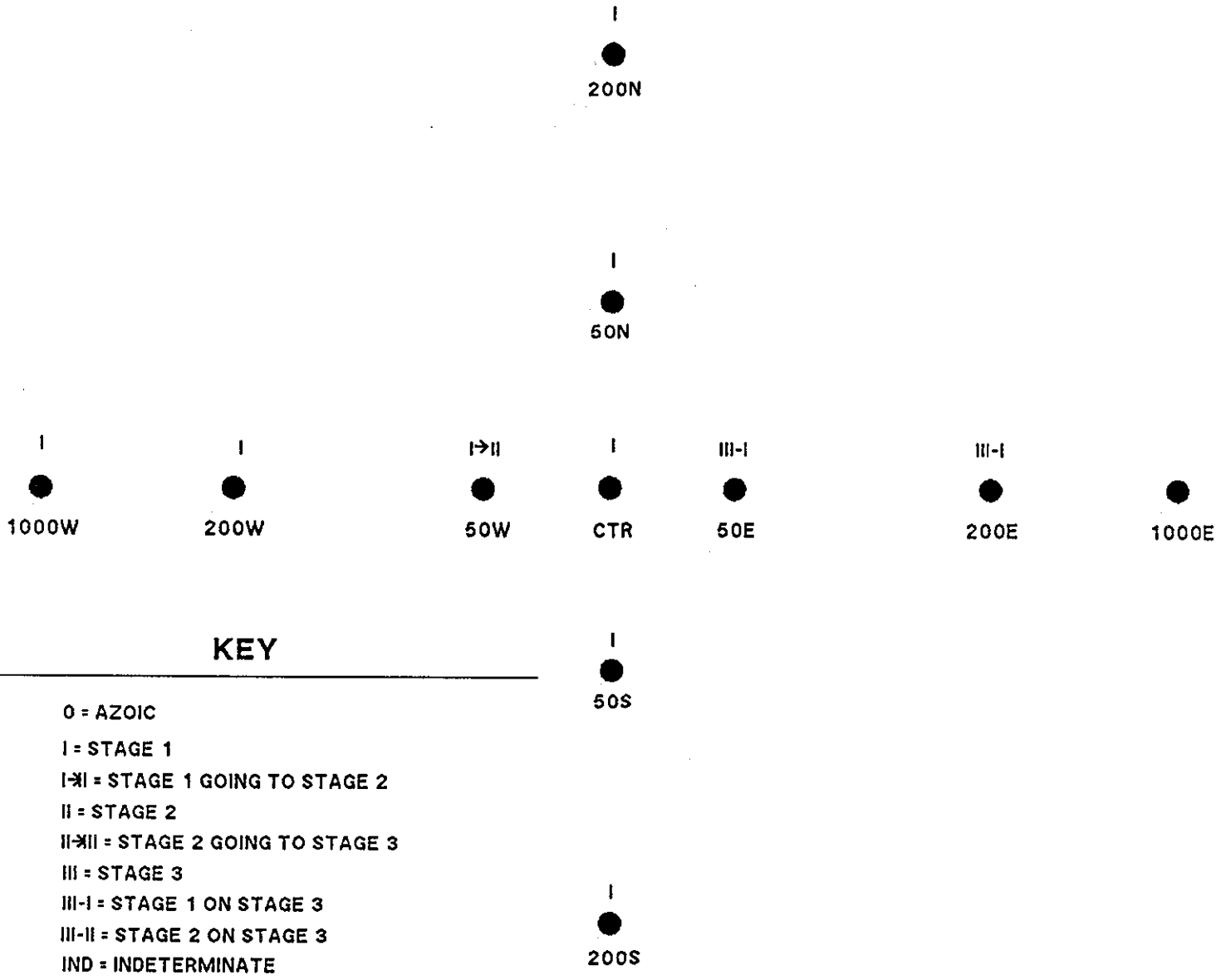

KEY

0 = AZOIC
I = STAGE 1
I→II = STAGE 1 GOING TO STAGE 2
II = STAGE 2
II→III = STAGE 2 GOING TO STAGE 3
III = STAGE 3
III-I = STAGE 1 ON STAGE 3
III-II = STAGE 2 ON STAGE 3
IND = INDETERMINATE

Figure 3-66 The mapped distribution of post-storm infaunal successional stages at MQR. A REMOTS® photo was not successfully obtained at 1000E.

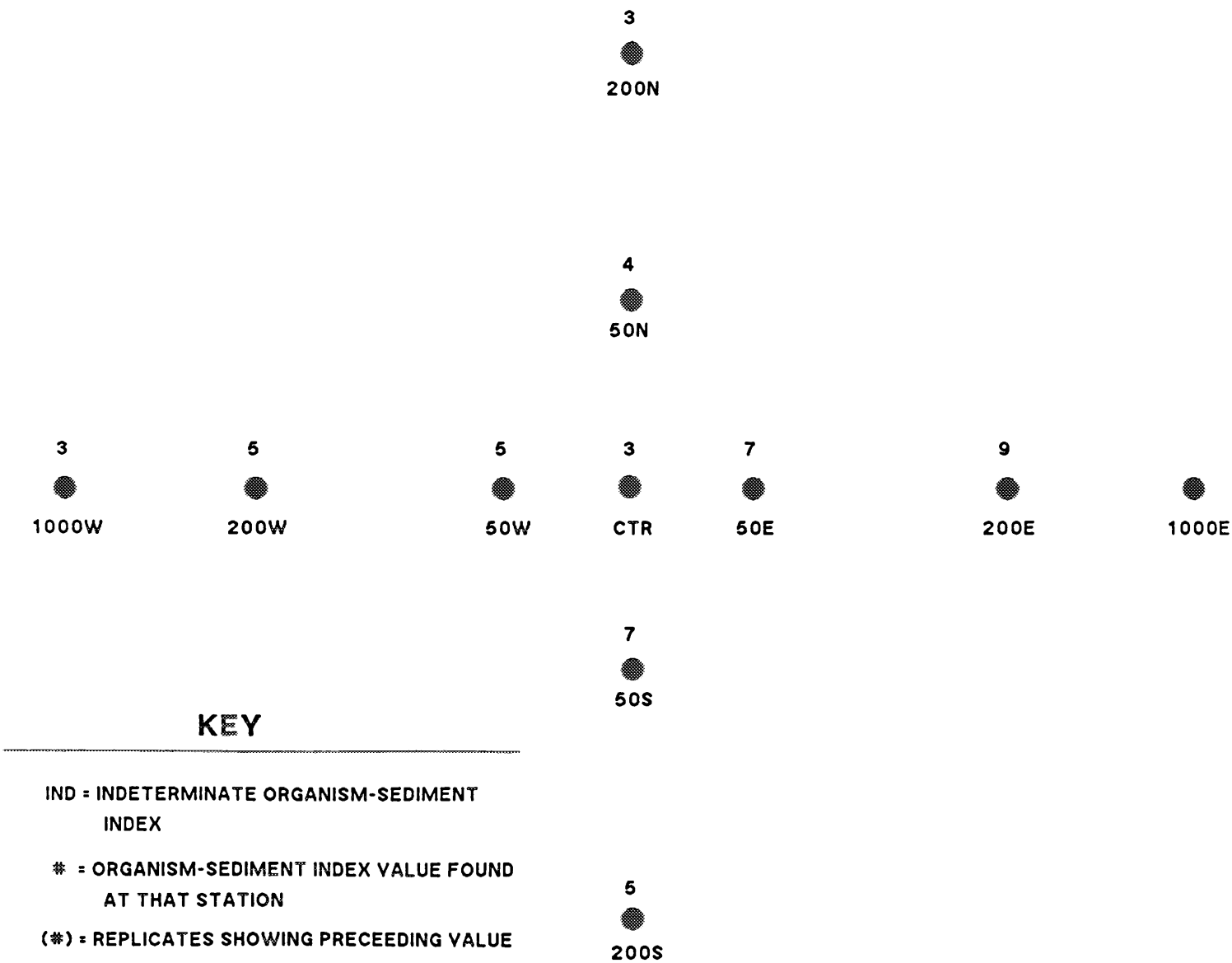

Figure 3-67 The mapped distribution of post-storm Organism-Sediment Indices (OSI) at MQR. A REMOTS® photo was not successfully obtained at 1000E.

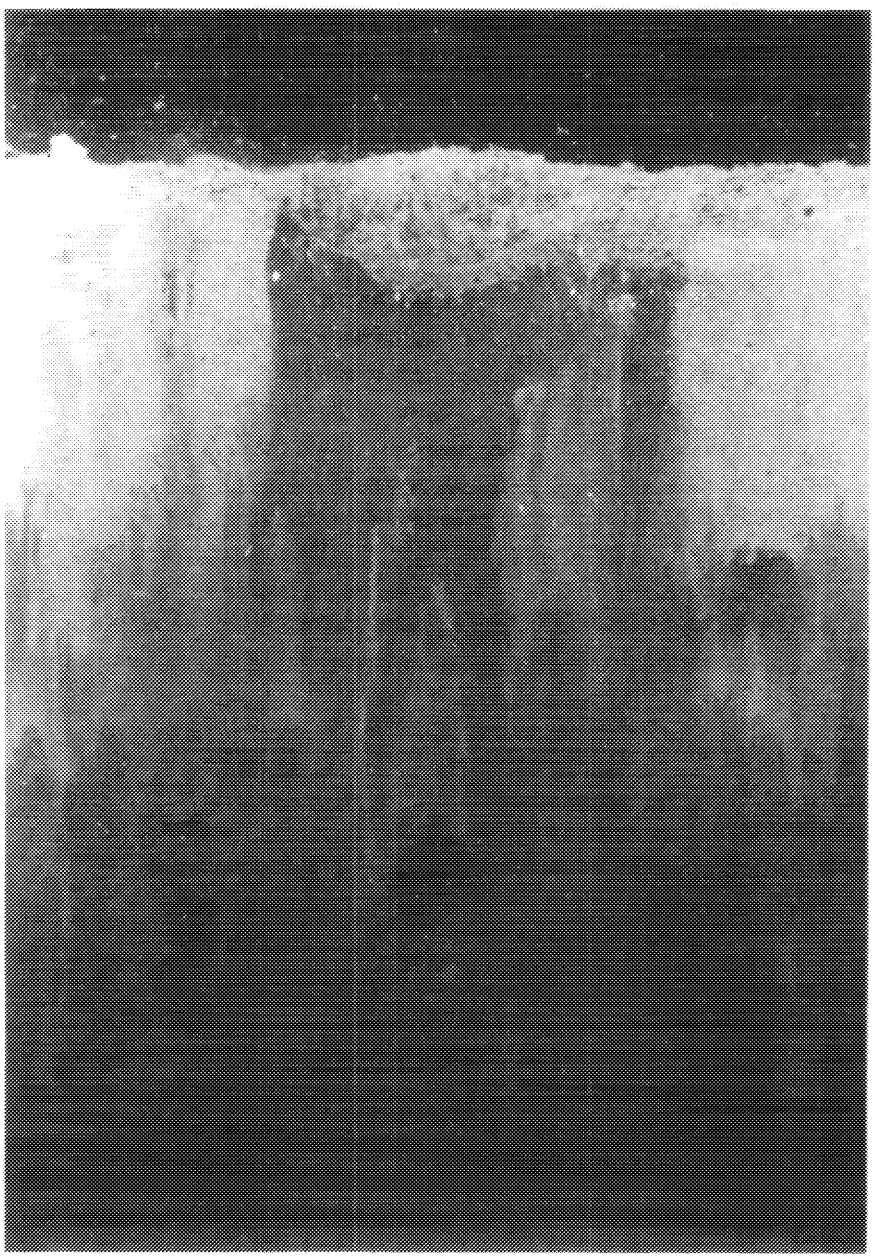

Figure 3-68 A REMOTS® image from August, station 200W, showing reduced sediment patches near the interface.

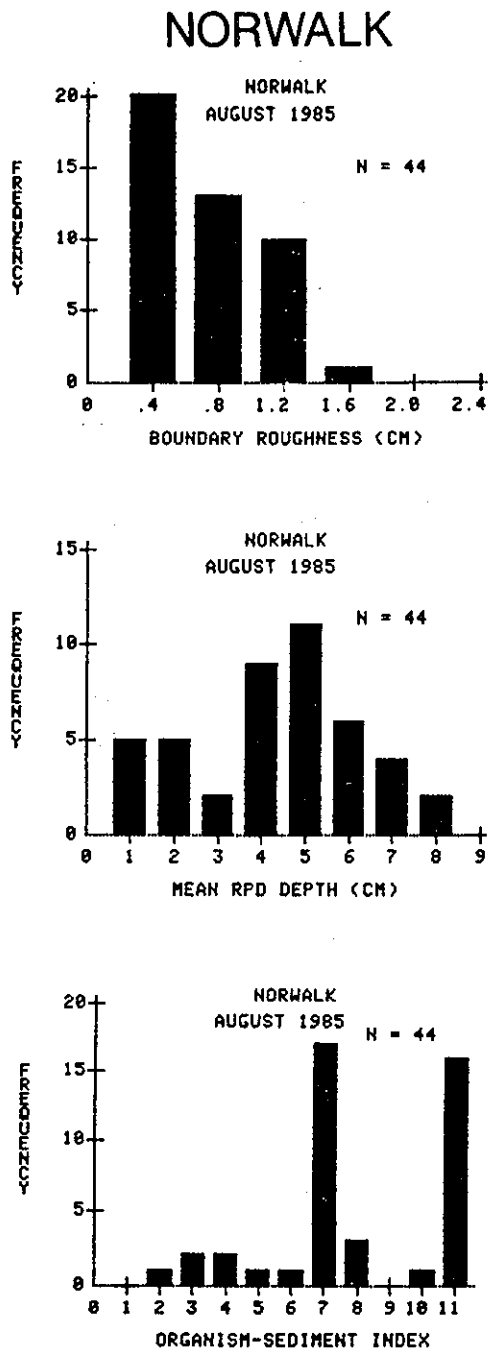

Figure 3-69 The frequency distribution of boundary roughness, redox potential discontinuity (RPD) depths, and Organism-Sediment Index (OSI) values for August 1985 at Norwalk.

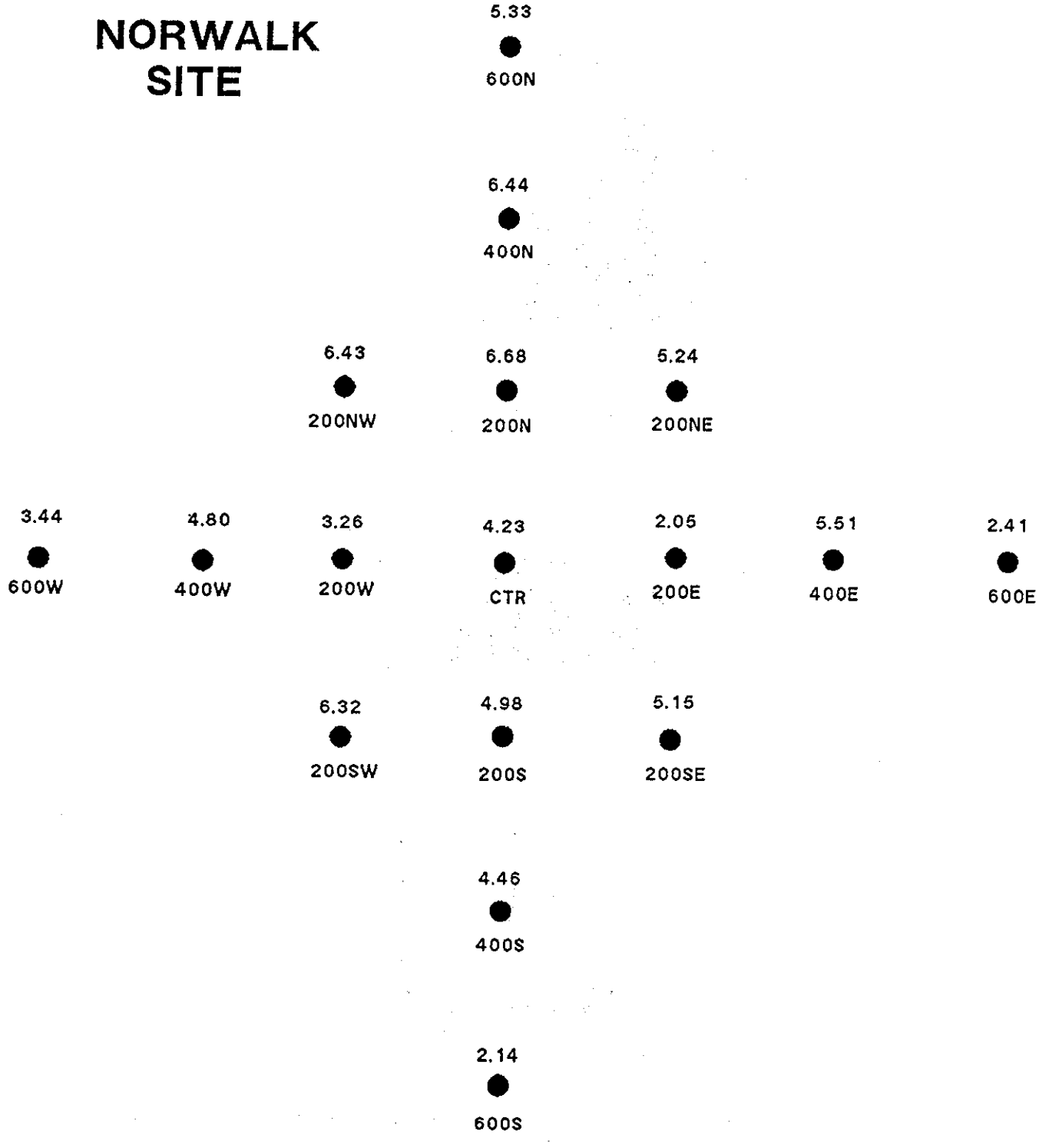

Figure 3-70 The mapped average apparent redox potential discontinuity (RPD) depth values at each station in the August survey at Norwalk.

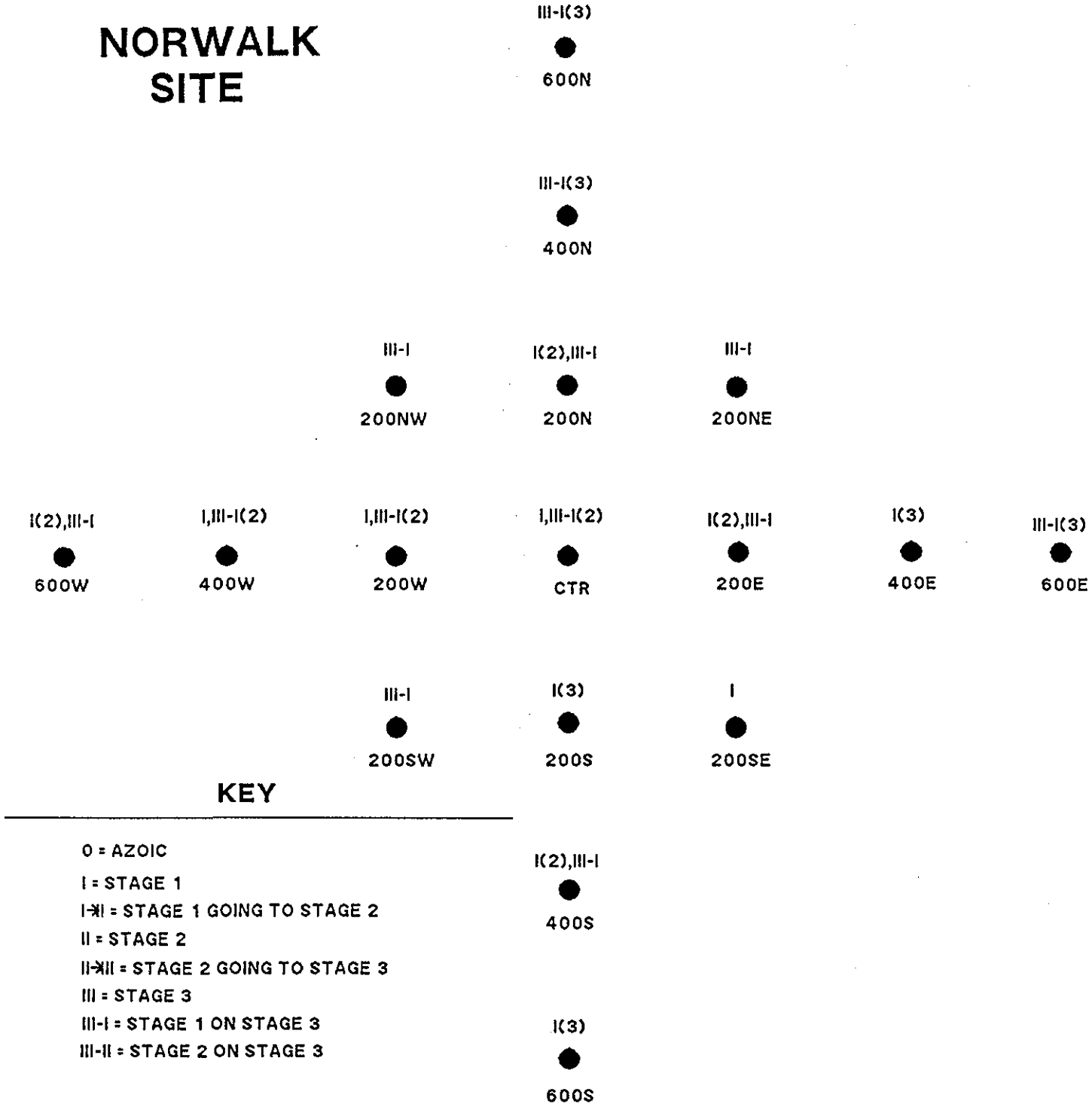

Figure 3-71 The mapped distribution of successional stages for all replicates in the August survey at Norwalk.

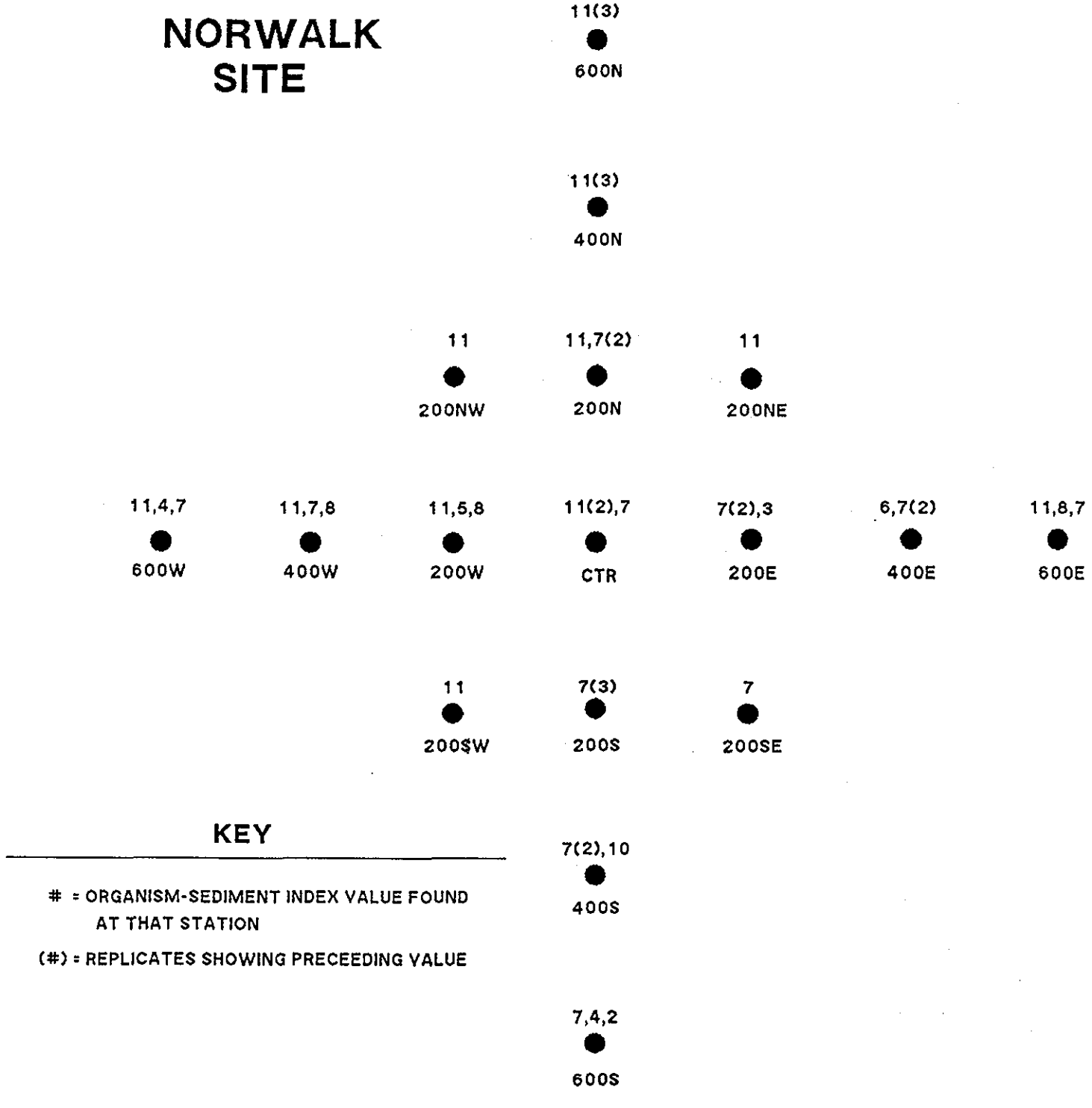

Figure 3-72 The mapped distribution of Organism- Sediment Indices (OSI) for all replicates in the August survey at Norwalk.

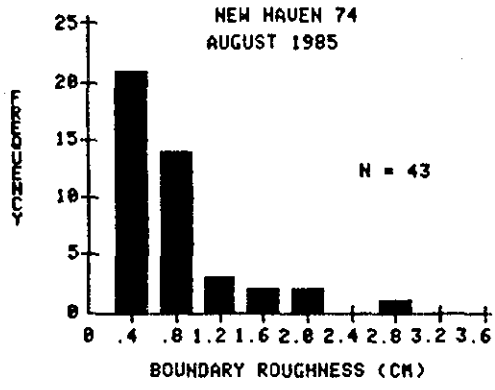

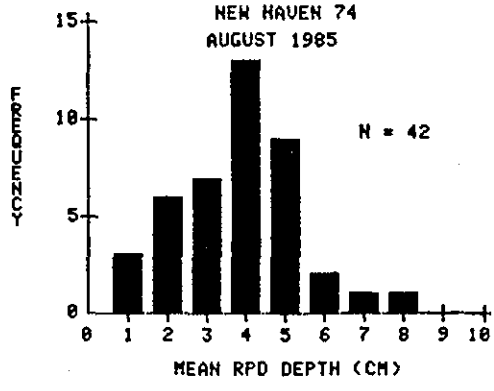

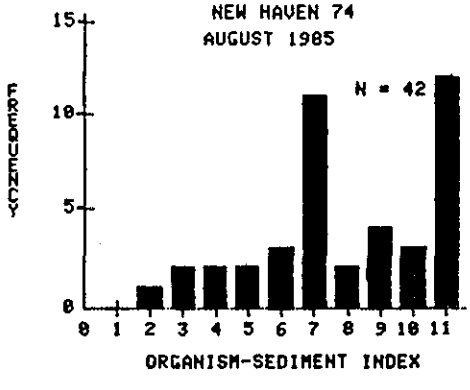

Figure 3-73 The frequency distribution of boundary roughness, redox potential discontinuity (RPD) depths, and Organism-Sediment Index (OSI) values for August, 1985 at NH-74.

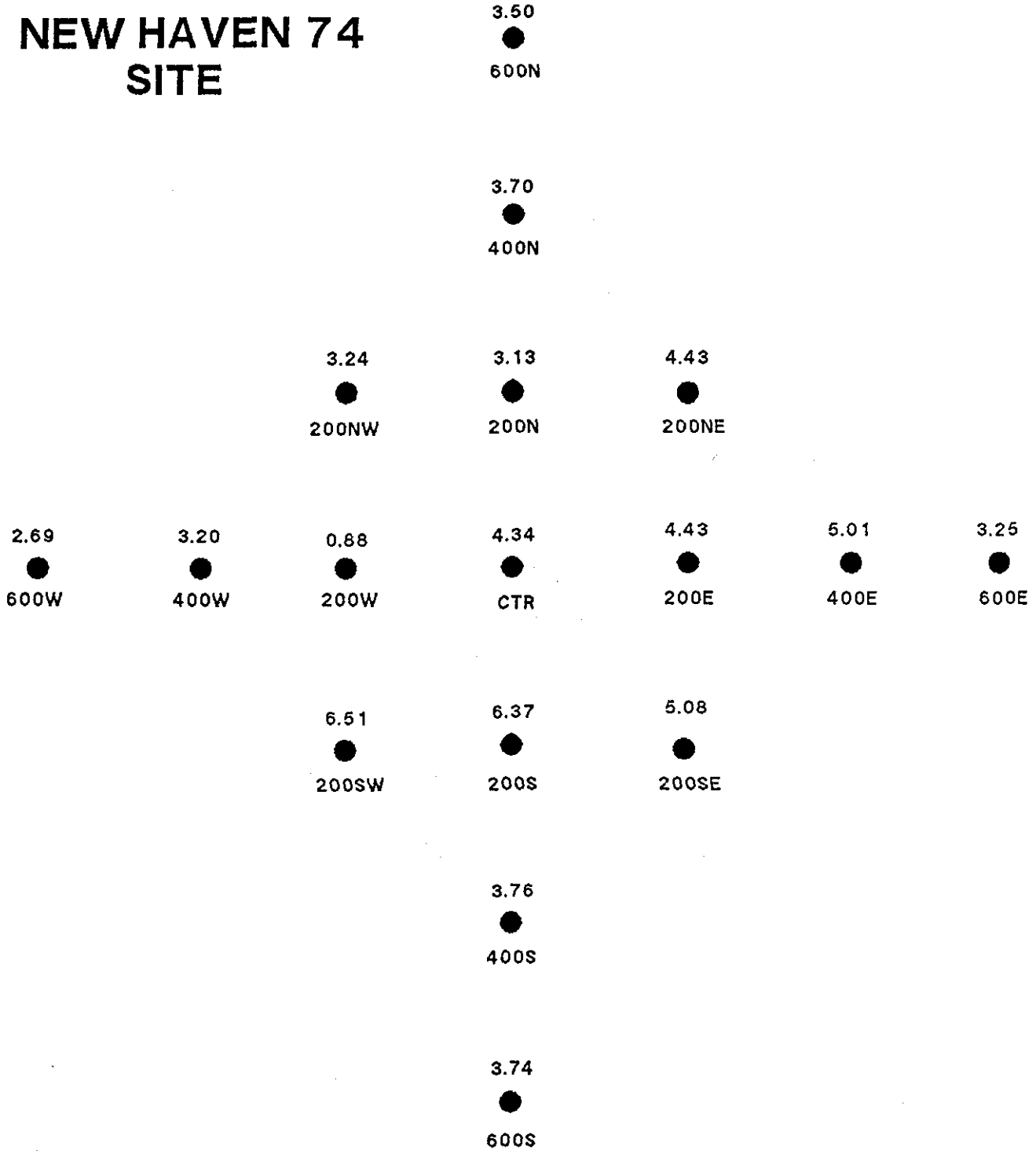

Figure 3-74 The mapped average apparent redox potential discontinuity (RPD) depth values (cm) at each station in the August survey at NH-74.

NEW HAVEN 74 SITE

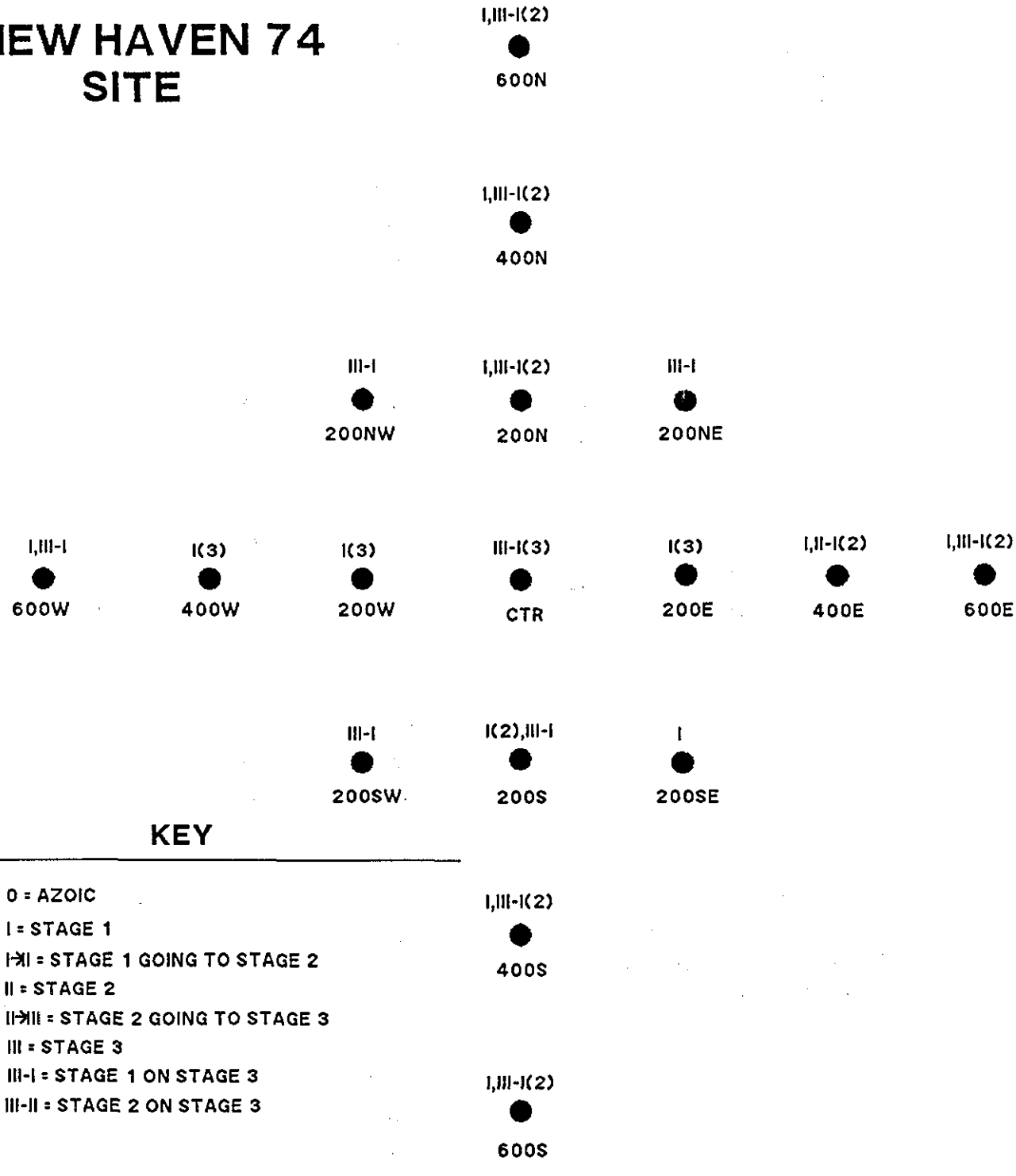

KEY

0 = AZOIC
I = STAGE 1
I→II = STAGE 1 GOING TO STAGE 2
II = STAGE 2
II→III = STAGE 2 GOING TO STAGE 3
III = STAGE 3
III-I = STAGE 1 ON STAGE 3
III-II = STAGE 2 ON STAGE 3

Figure 3-75 The mapped distribution of successional stages for all replicates in the August survey at NH-74.

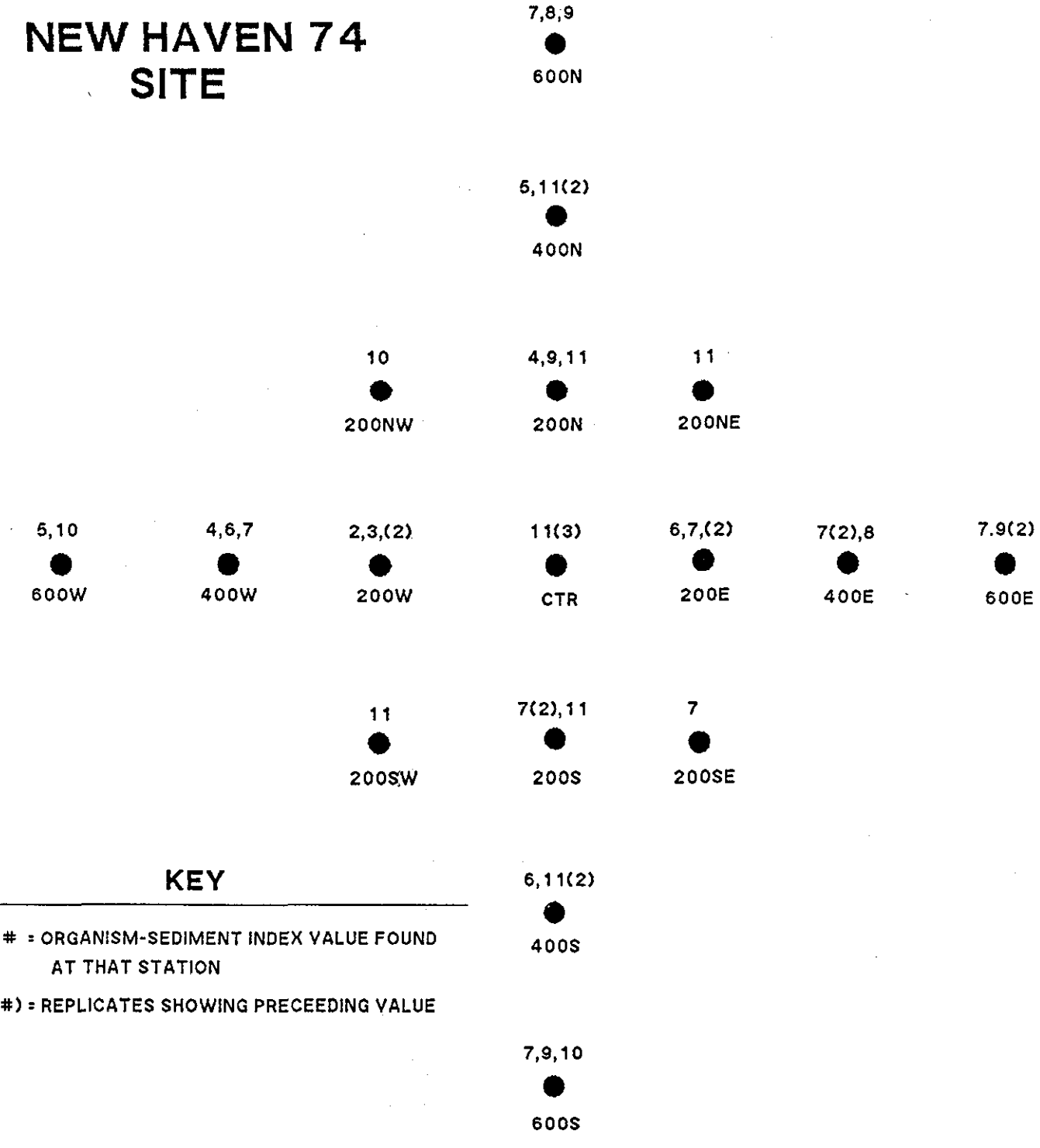

Figure 3-76 The mapped distribution of Organism- Sediment Indices (OSI) for all replicates in the August survey at NH-74.

NEW HAVEN 83

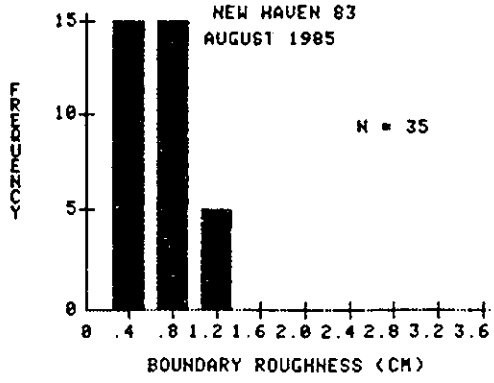

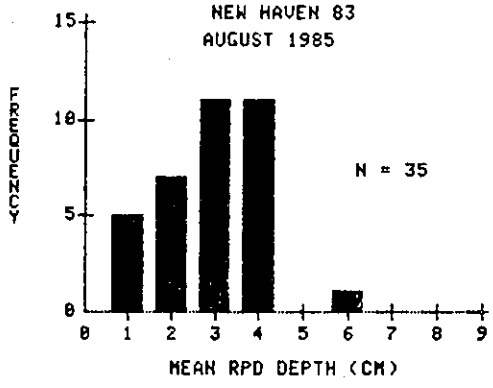

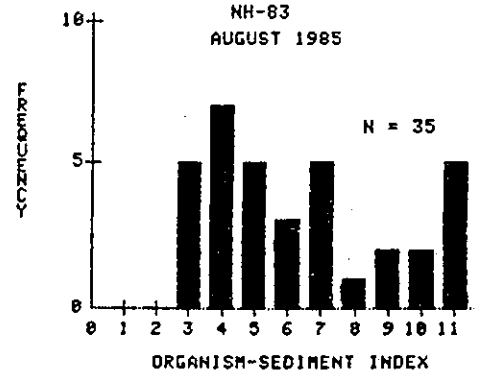

Figure 3-77 The frequency distribution of boundary roughness, redox potential discontinuity (RPD) depths, and Organism-Sediment Index (OSI) values for the August survey at NH-83.

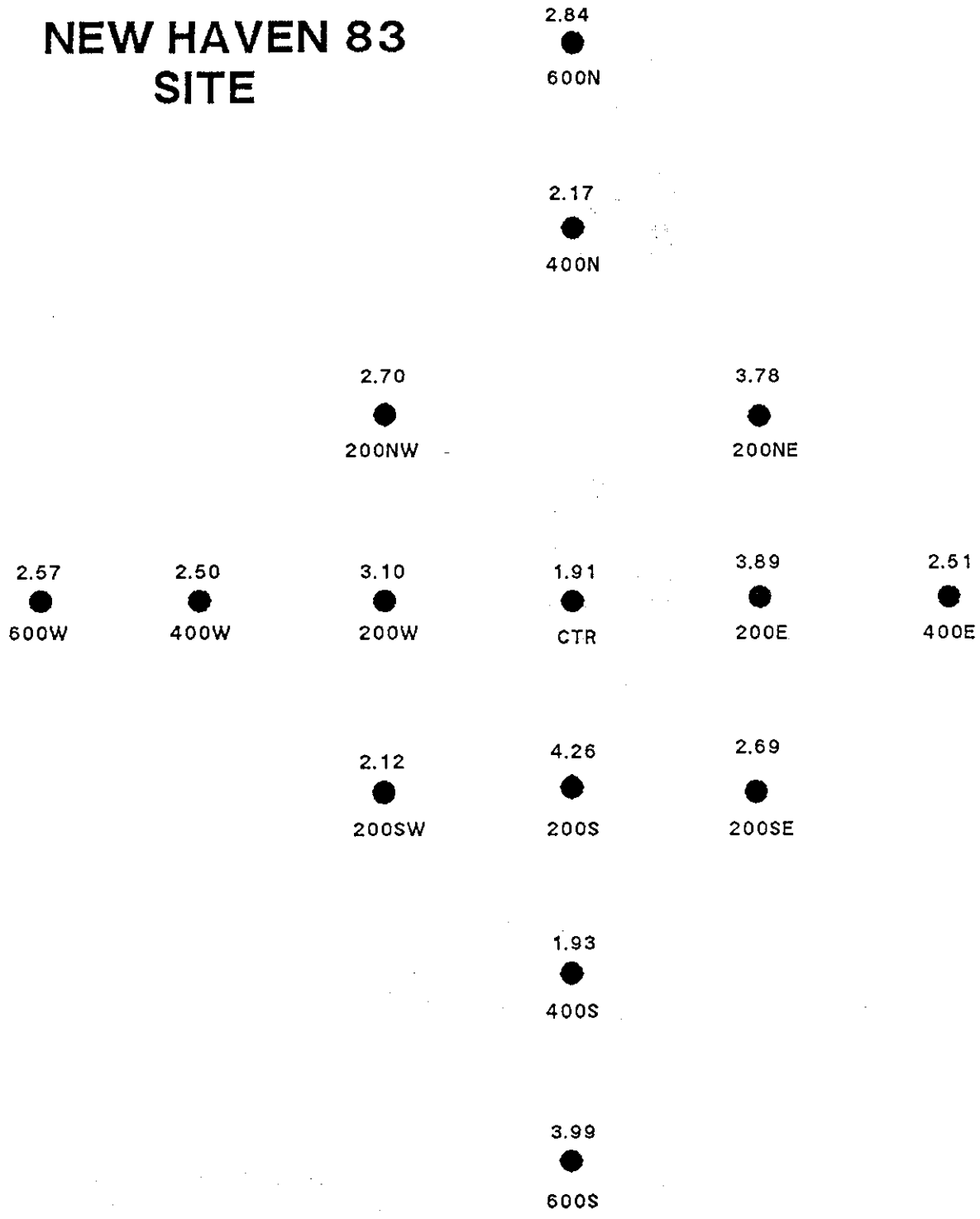

Figure 3-78 The mapped average apparent redox potential discontinuity (RPD) depth values (cm) for all replicates in the August survey at NH-83.

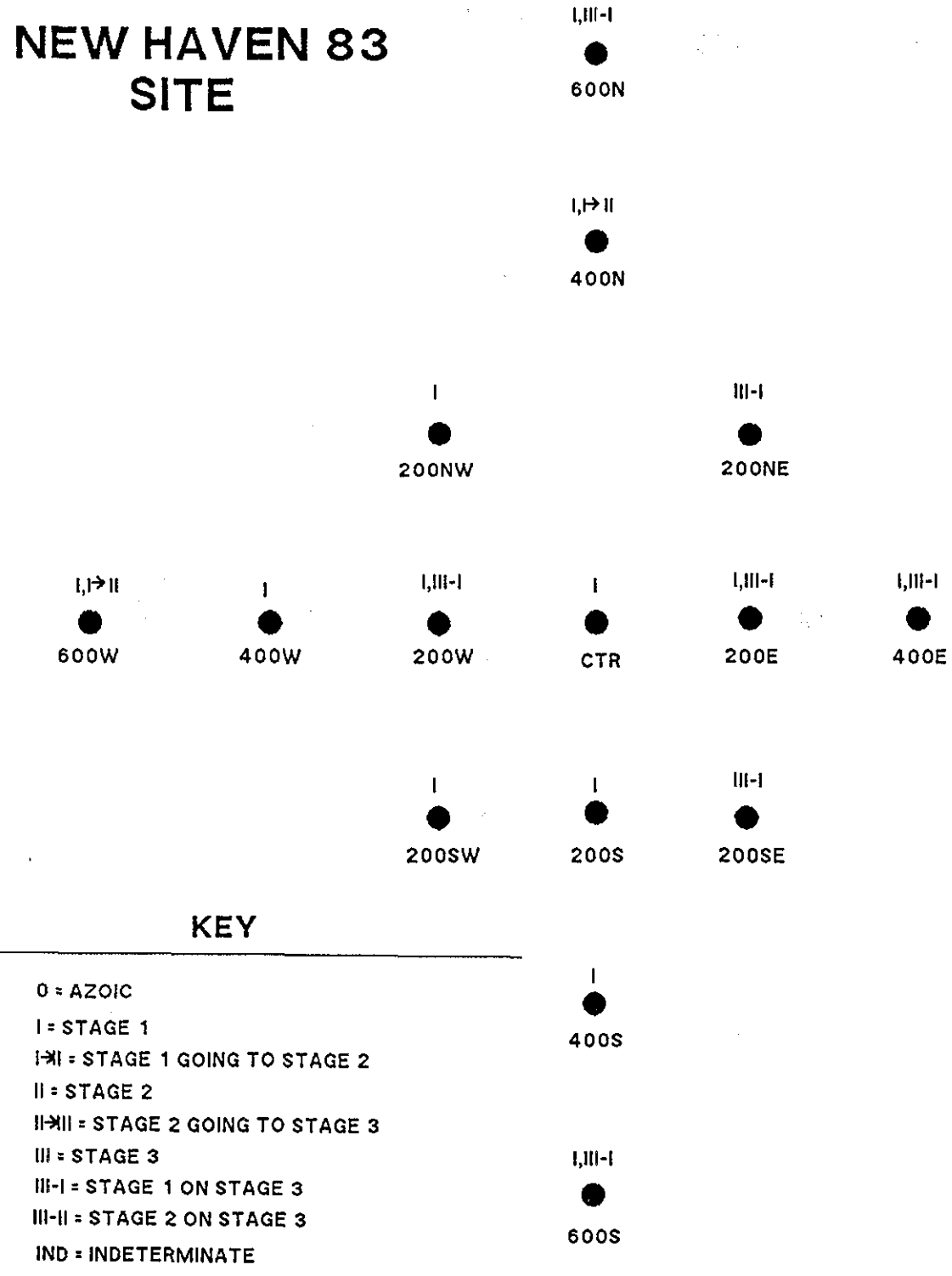

Figure 3-79 The mapped distribution of infaunal successional stages for all replicates in the August survey at NH-83.

NEW HAVEN 83 SITE

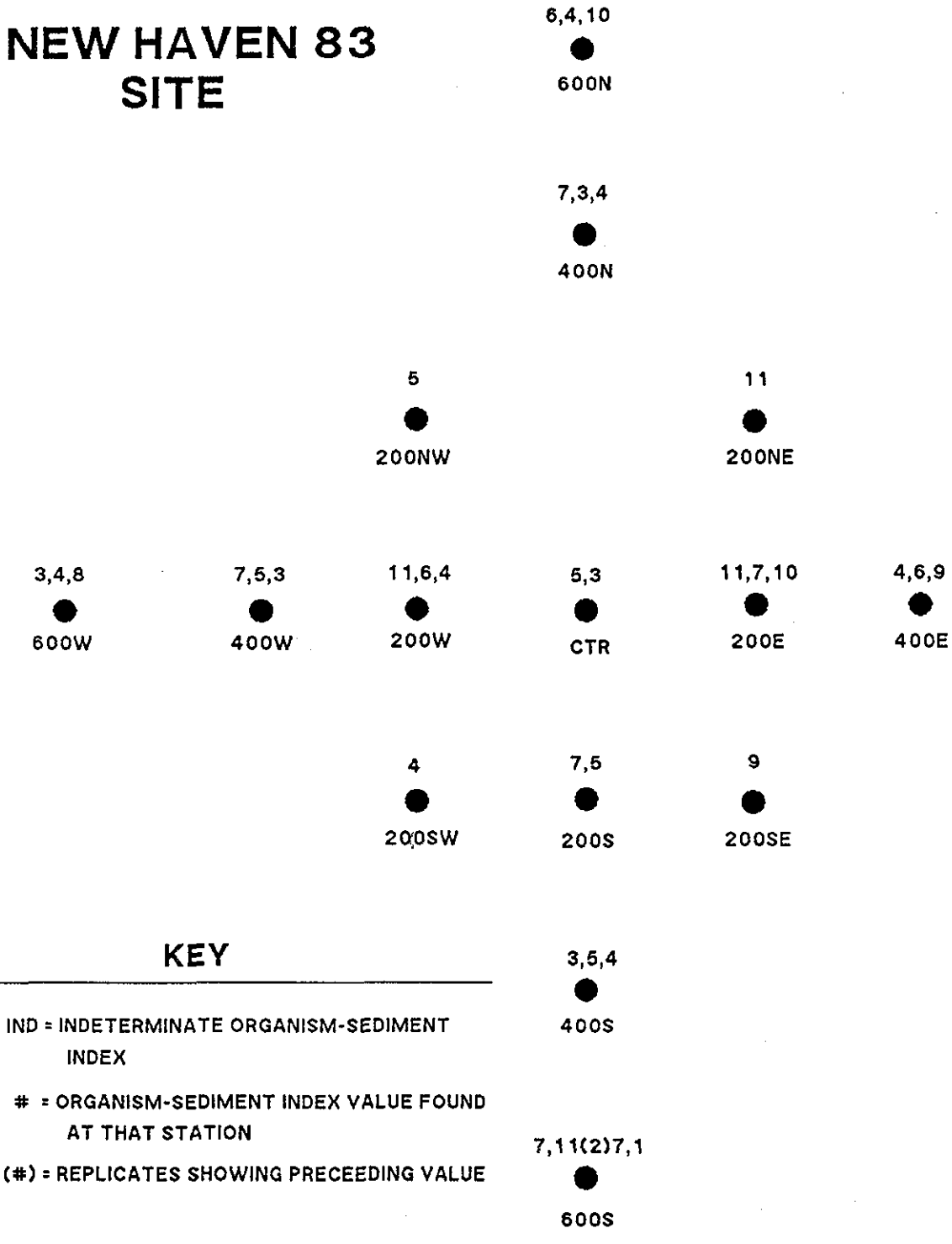

KEY

IND = INDETERMINATE ORGANISM-SEDIMENT INDEX

= ORGANISM-SEDIMENT INDEX VALUE FOUND AT THAT STATION

(#) = REPLICATES SHOWING PRECEEDING VALUE

Figure 3-80 The mapped distribution of Organism-Sediment Index (OSI) values for all replicates in the August survey at NH-83.

SE-CLIS

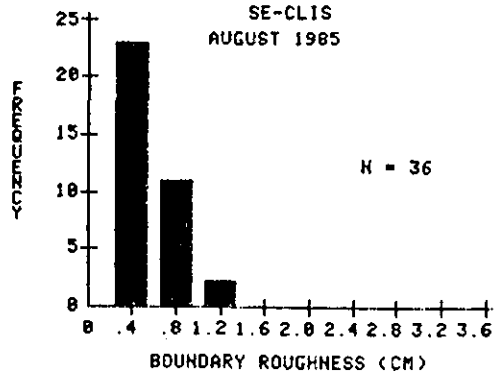

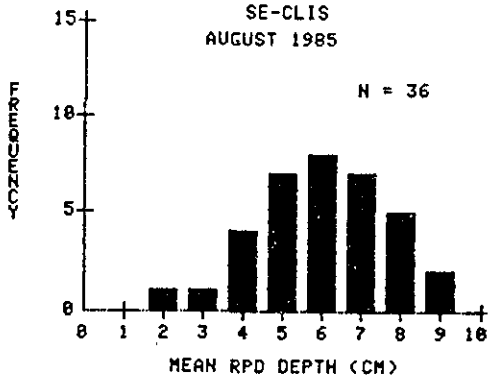

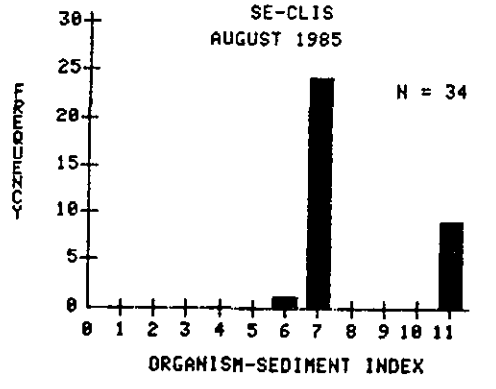

Figure 3-81 The frequency distribution of boundary roughness, redox potential discontinuity (RPD) depths, and Organism-Sediment Index (OSI) values for the August survey at CLIS-SE.

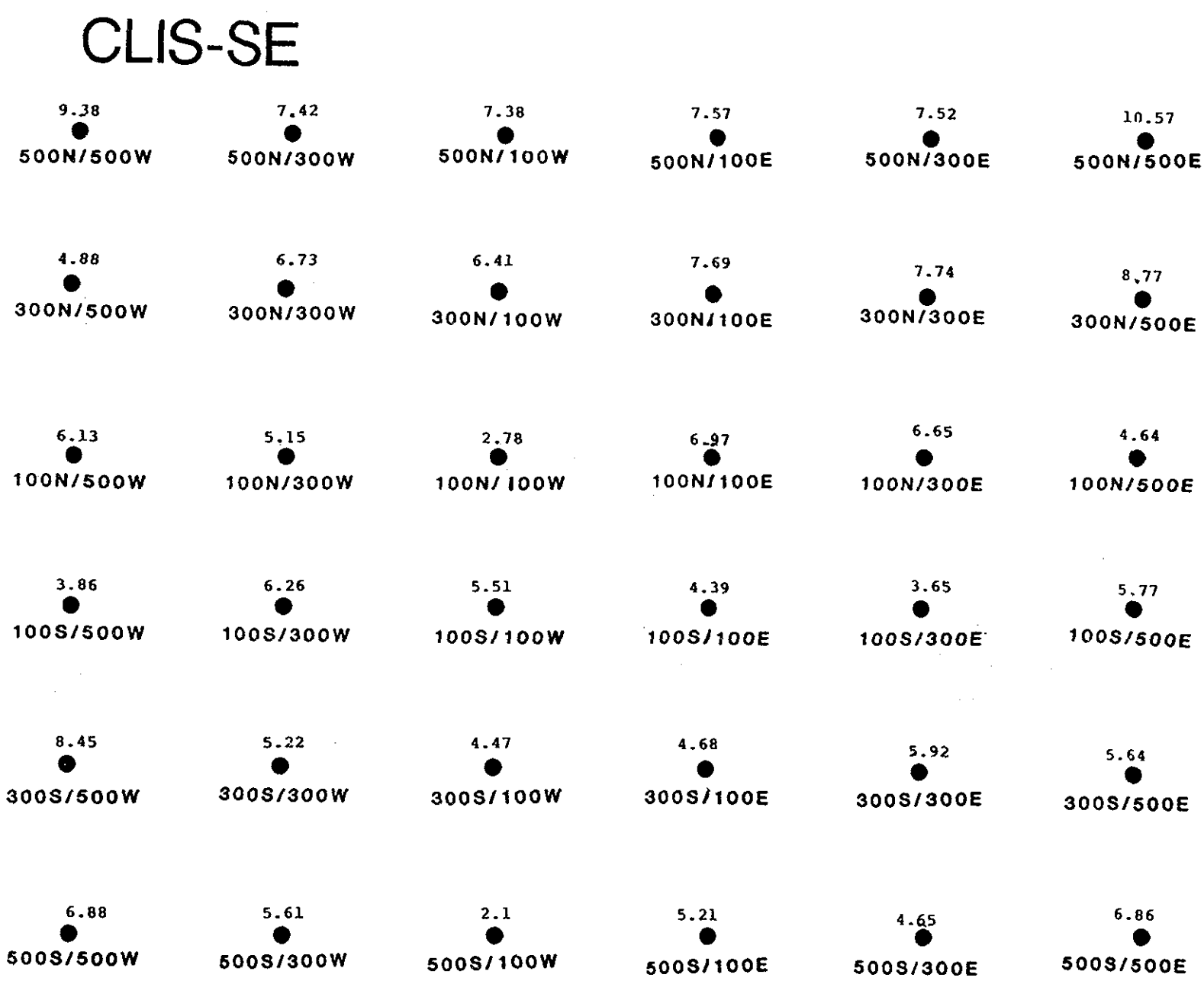

Figure 3-82 The mapped distribution of average apparent redox potential discontinuity (RPD) depth values (cm) for all replicates in the August survey at CLIS-SE.

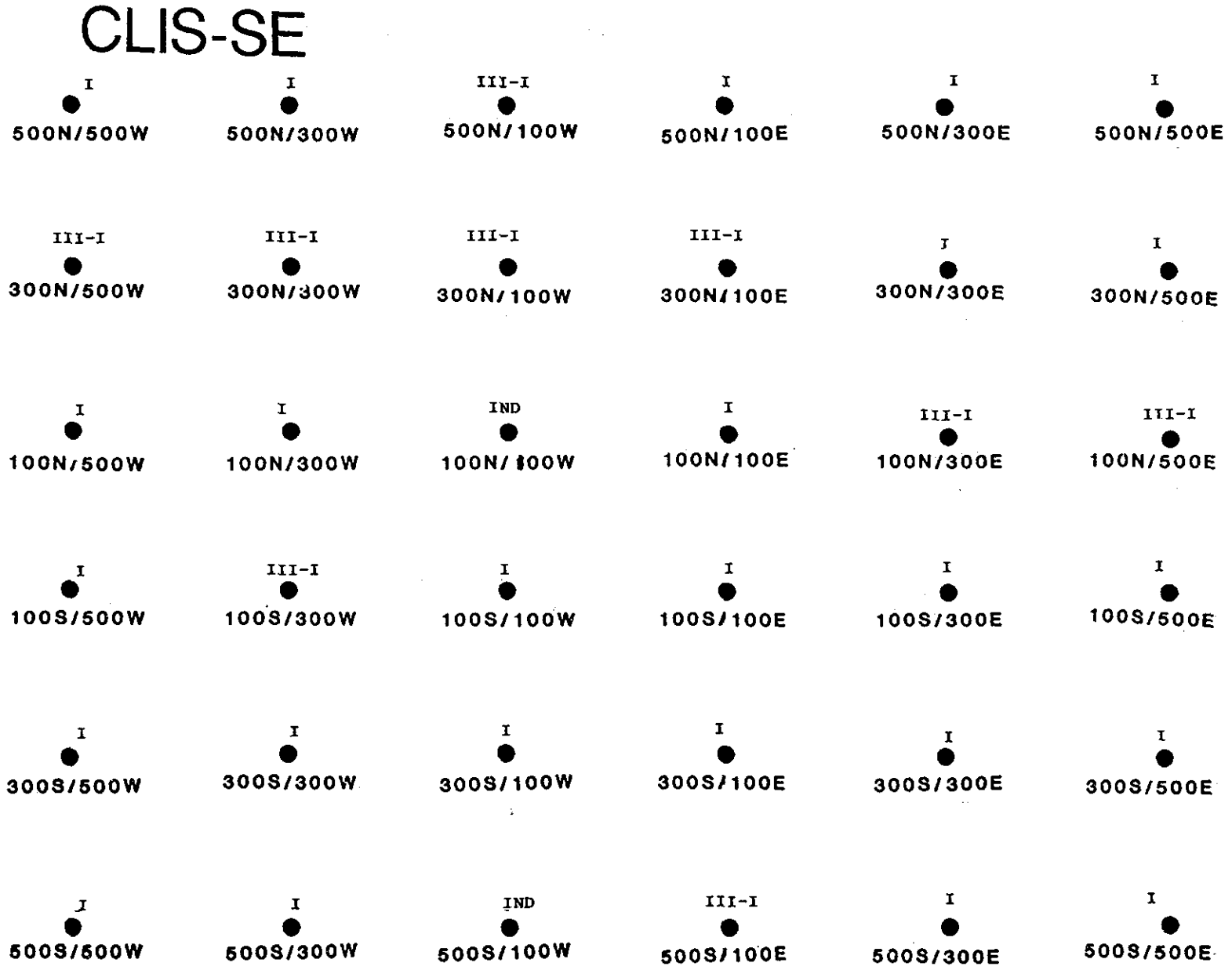

Figure 3-83 The mapped distribution of infaunal successional stages for all replicates in the August survey at CLIS-SE.

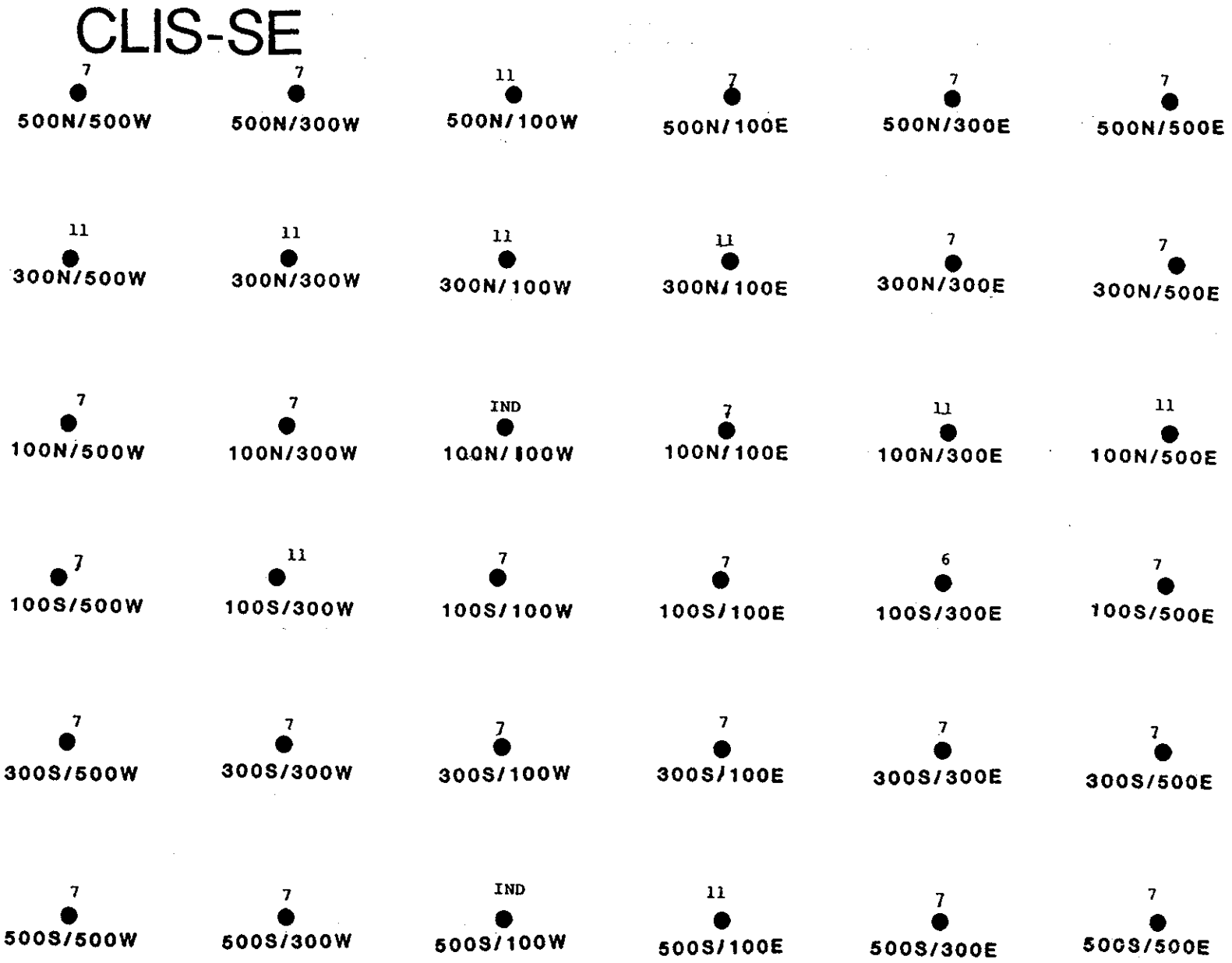

Figure 3-84 The mapped distribution of Organism-Sediment Indices (OSI) for all replicates in the August survey at CLIS-SE.

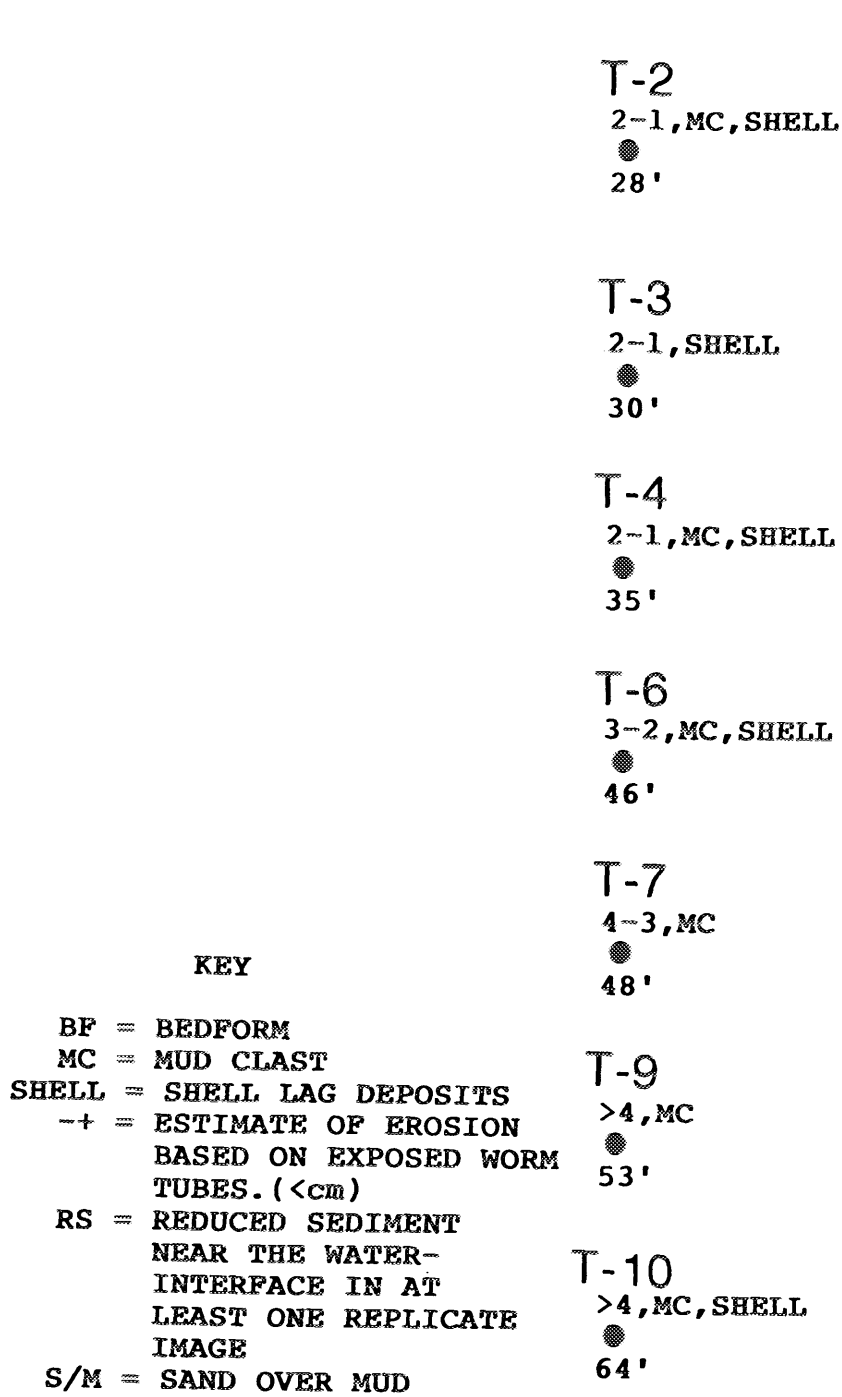

Figure 3-85 A grain-size and benthic "process" map of the post-storm CLIS Transect. Major modal grain-size in phi units are indicated for each station.

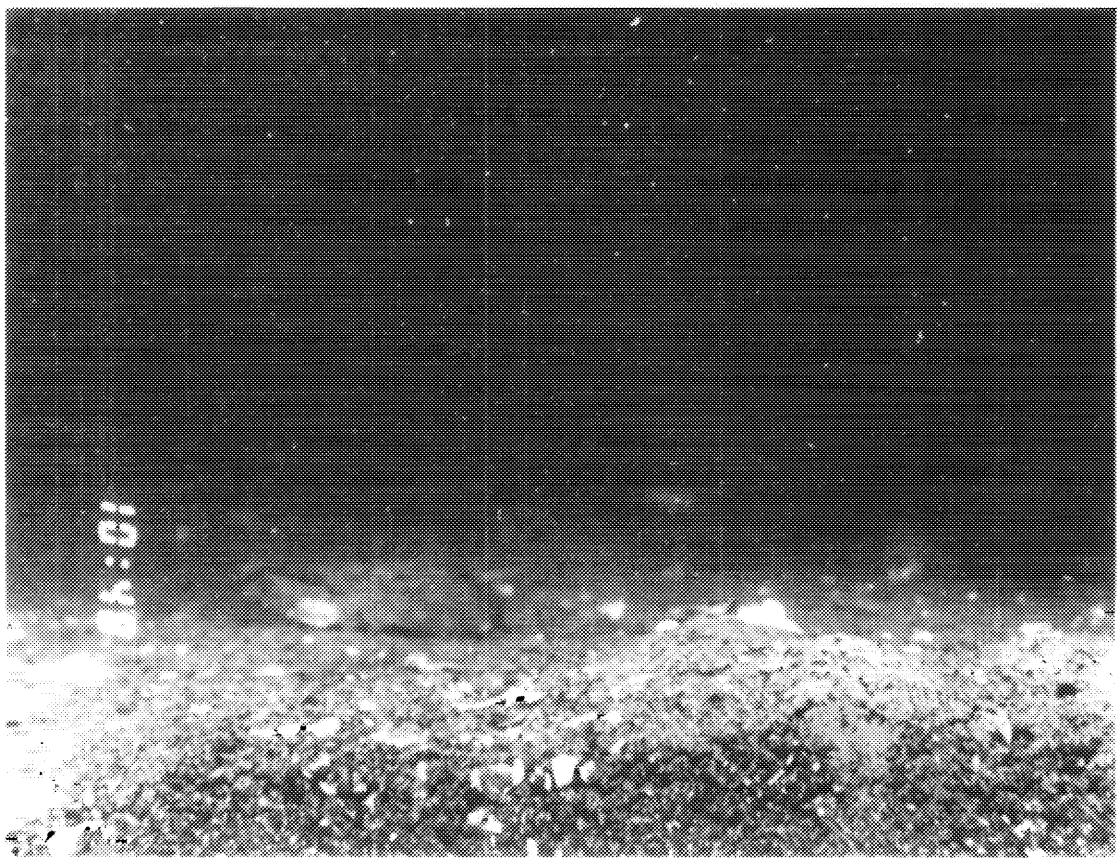

Figure 3-86 A-B Two post-storm REMOTS® images from stations T-3 and T-6 respectively, showing shell lag deposits and mud clasts indicative of bottom disturbance. Scale = 1X.

Figure 3-86B Scale = 1X.

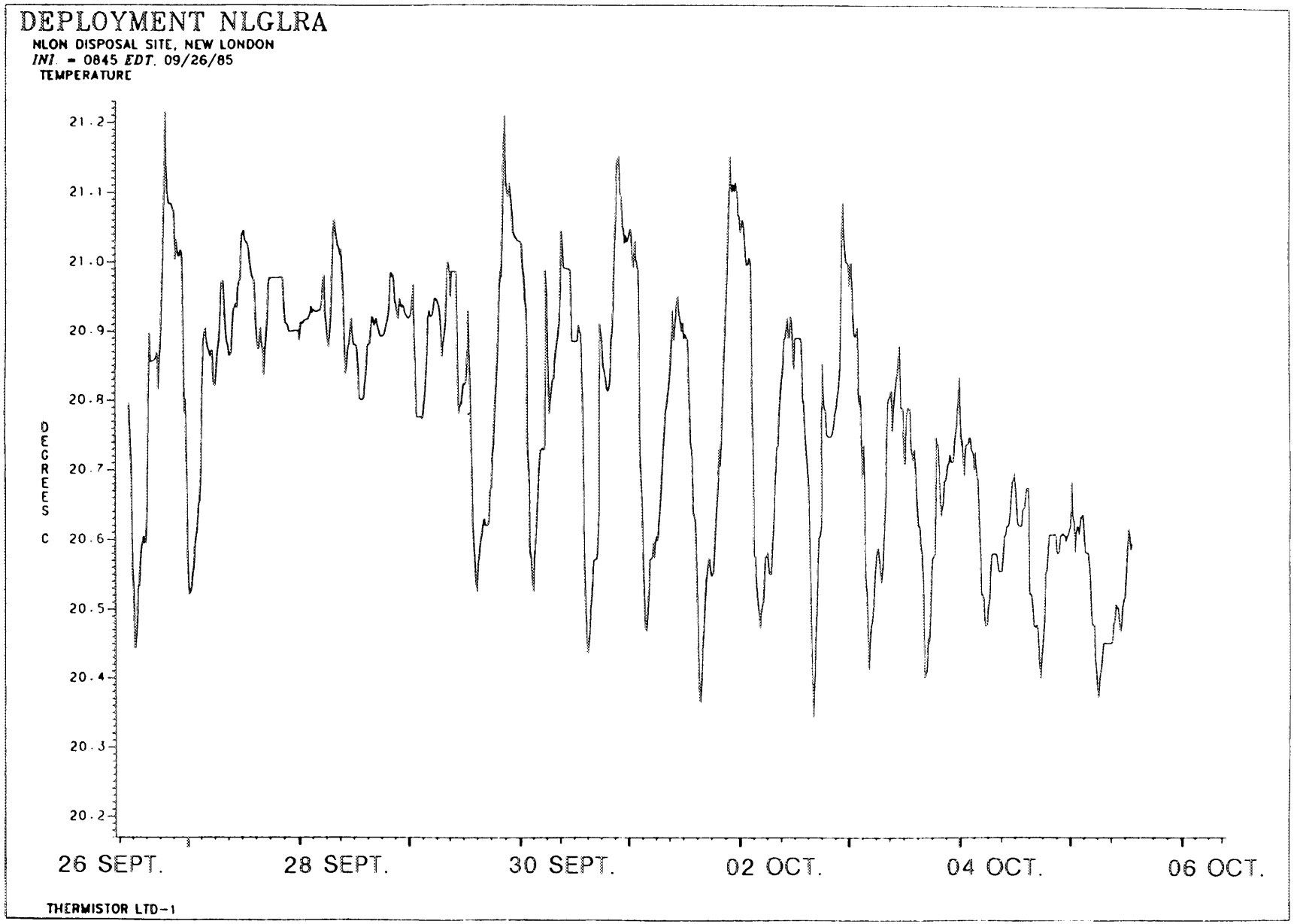

Figure 3-87 Near-bottom water temperature, Eastern Long Island Sound, September 1985.

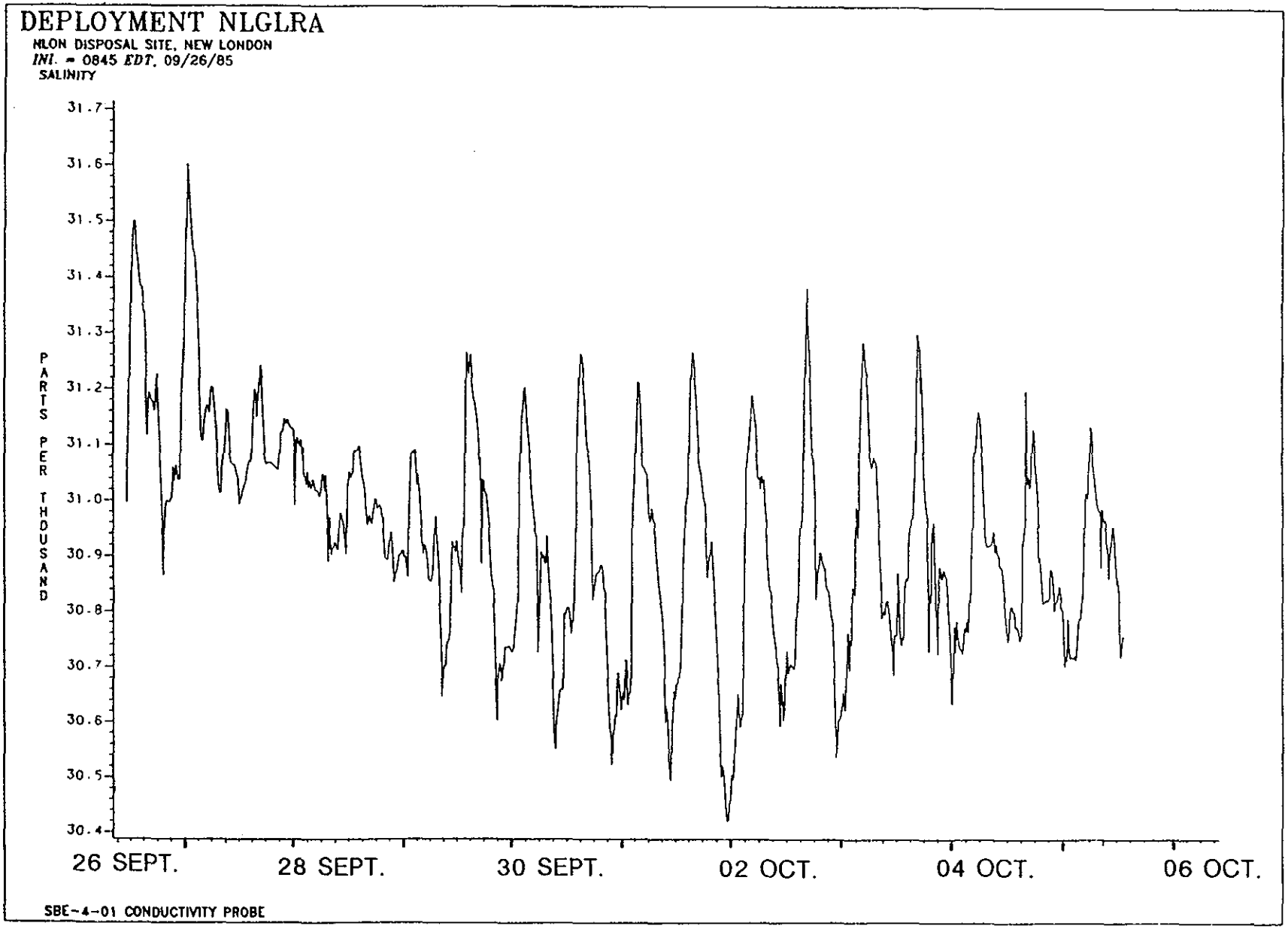

Figure 3-88 Near-bottom salinity, Eastern Long Island Sound, September 1985.

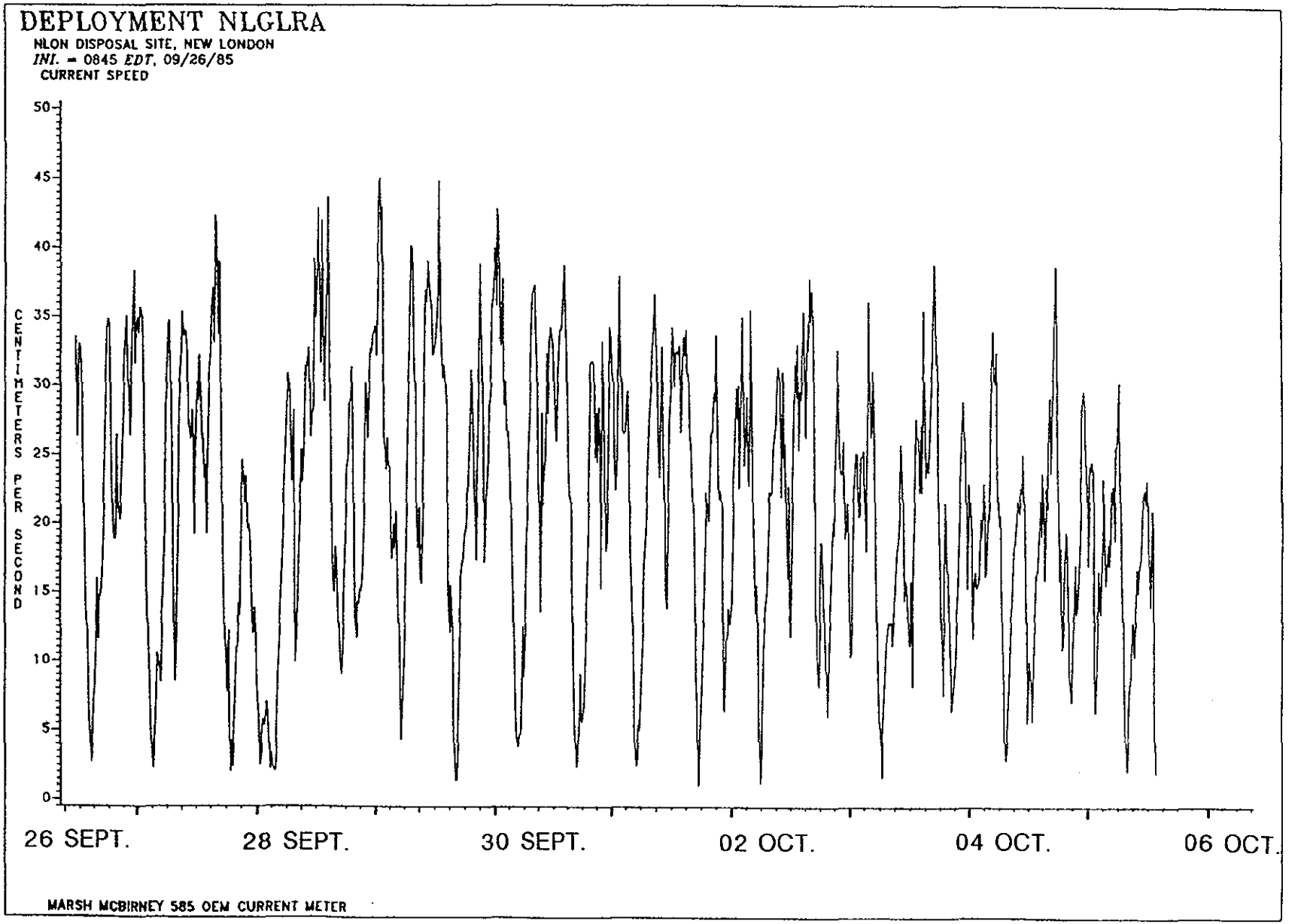

Figure 3-89 Near-bottom current speed, Eastern Long Island Sound, September 1985.

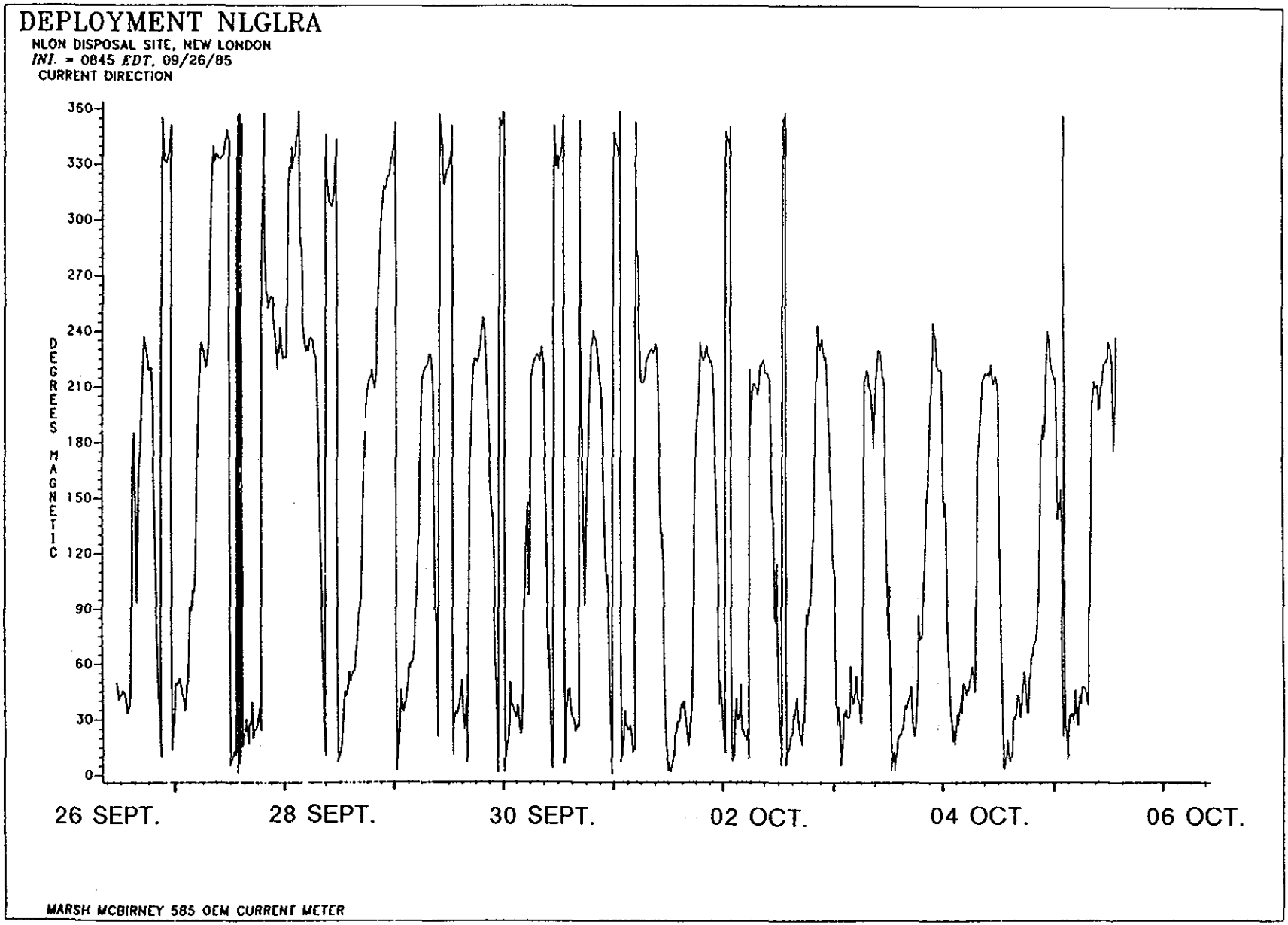

Figure 3-90 Near-bottom current direction, Eastern Long Island Sound, September 1985.

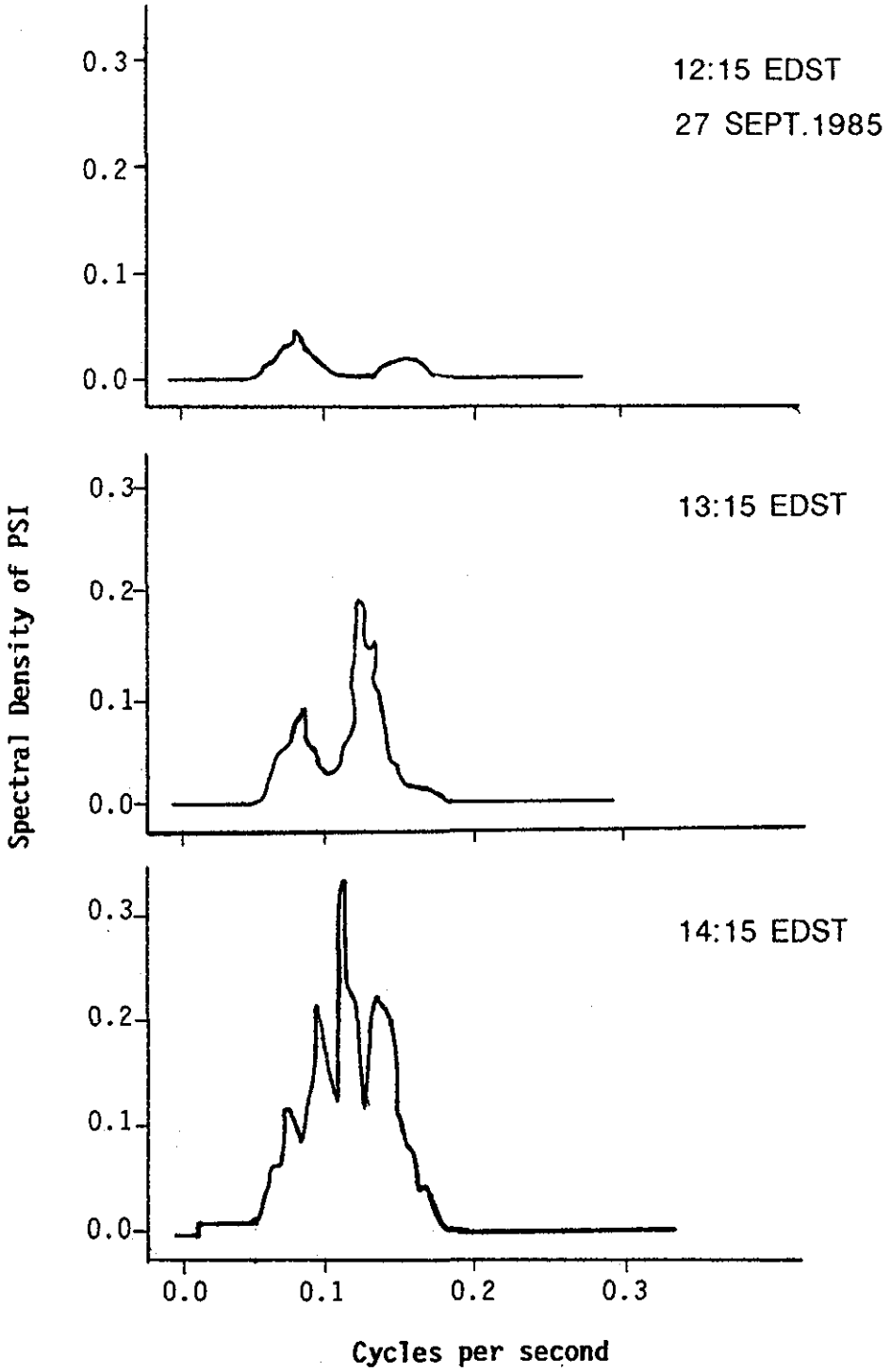

Figure 3-91 Spectral plot of near-bottom pressure at New London Disposal Area, 27 September 1985.

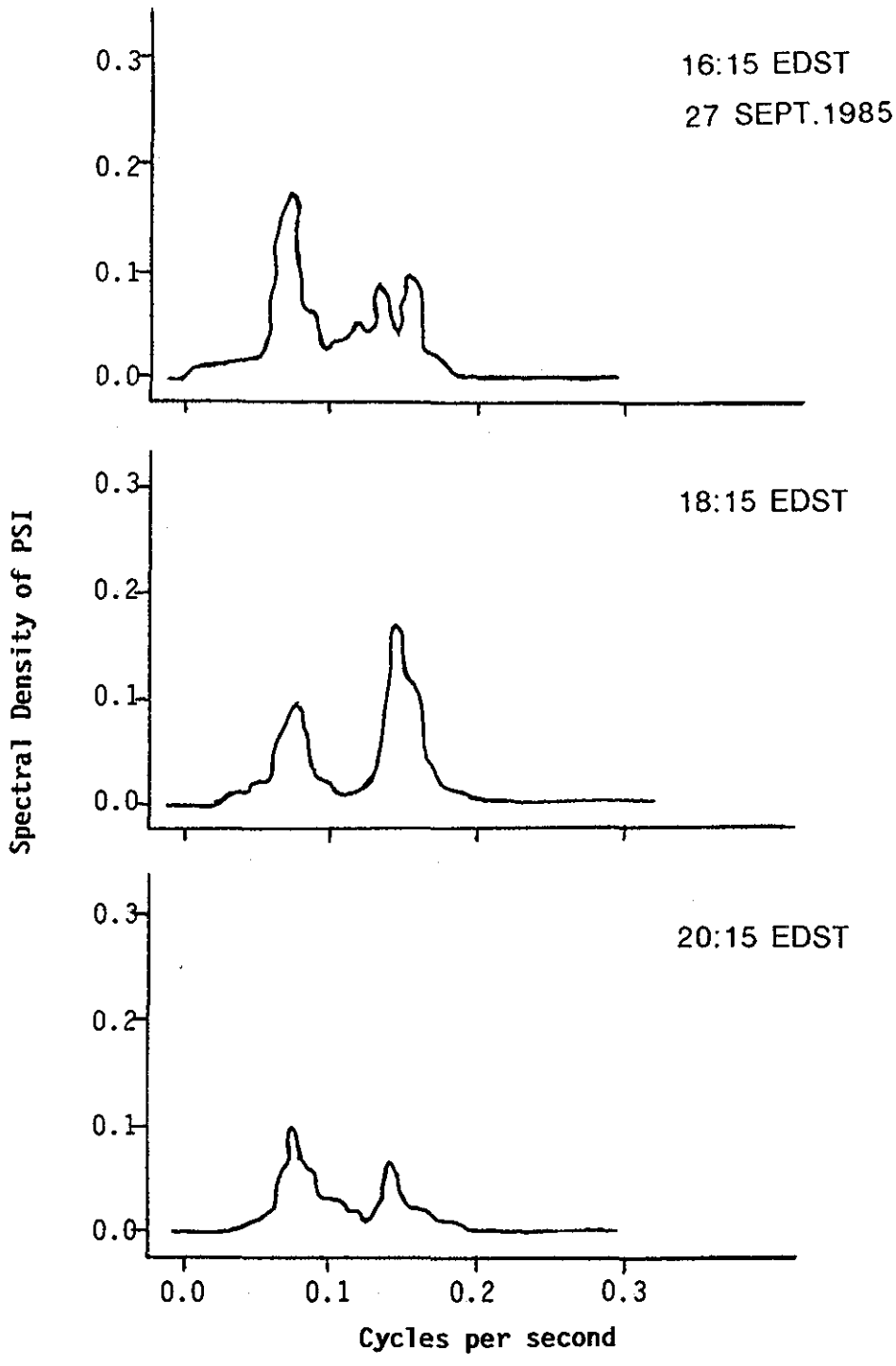

Figure 3-91 Continued.

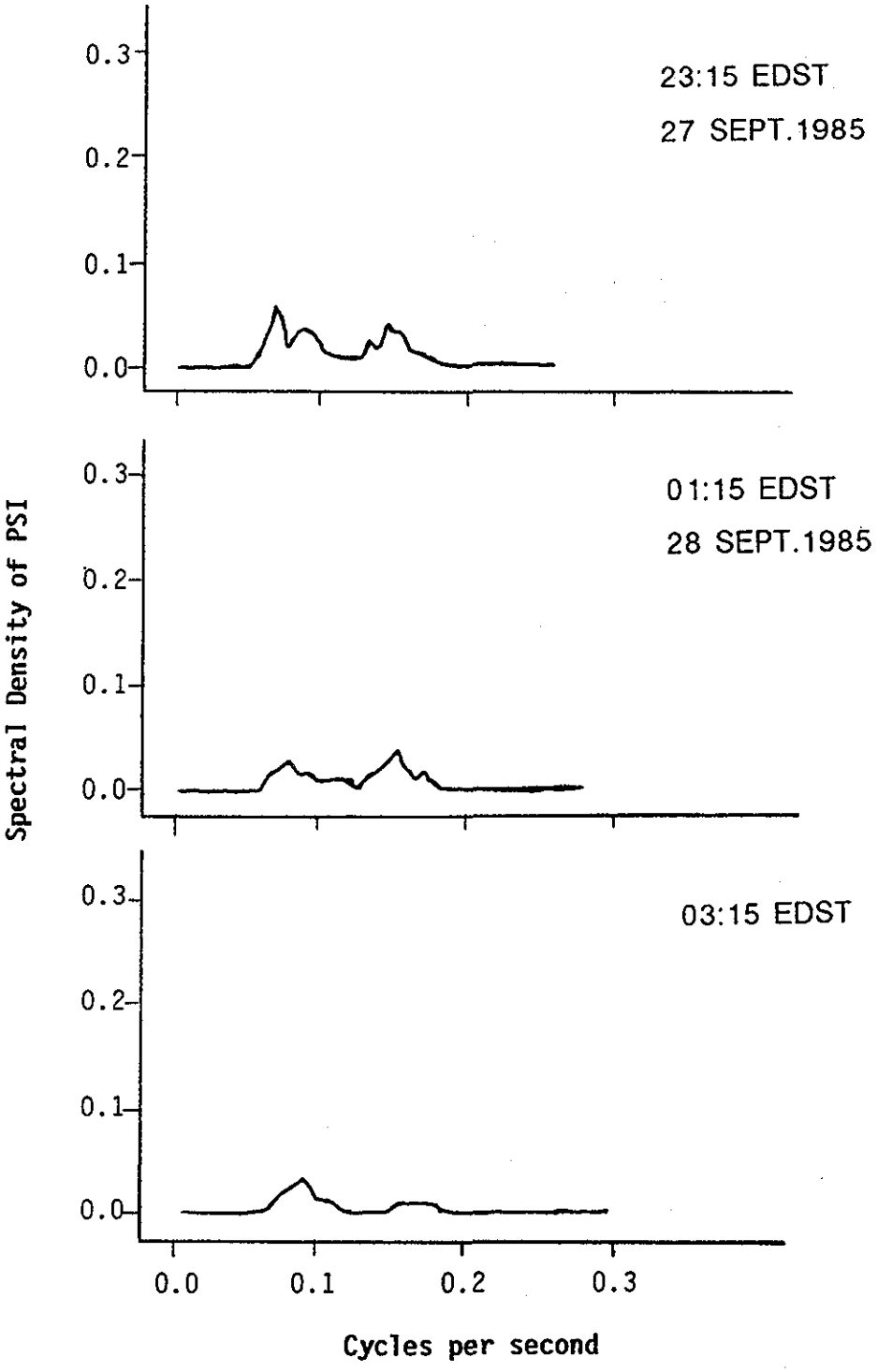

Figure 3-91 Continued.

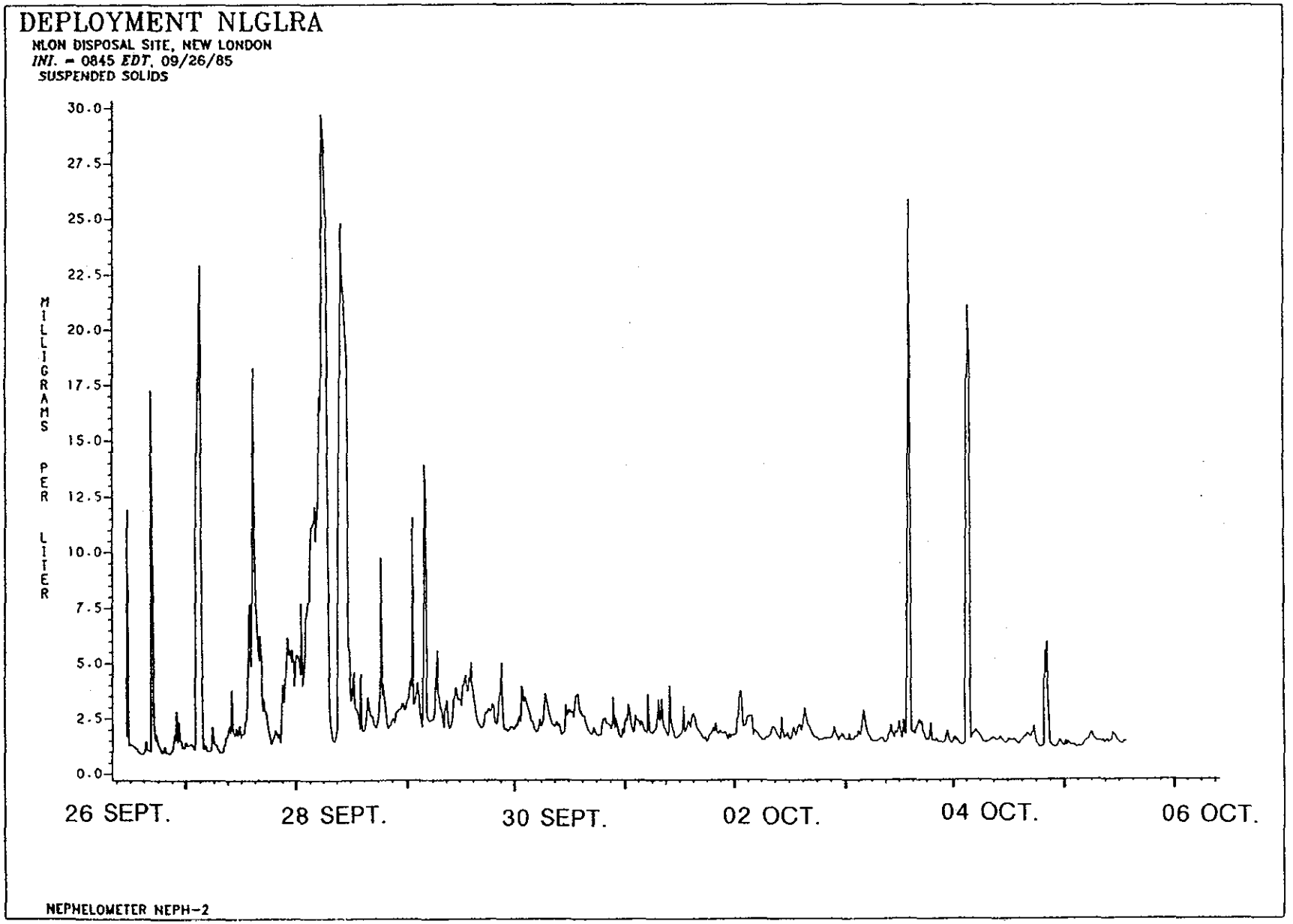

Figure 3-92 Near-bottom suspended material concentrations, Eastern Long Island Sound, September 1985.

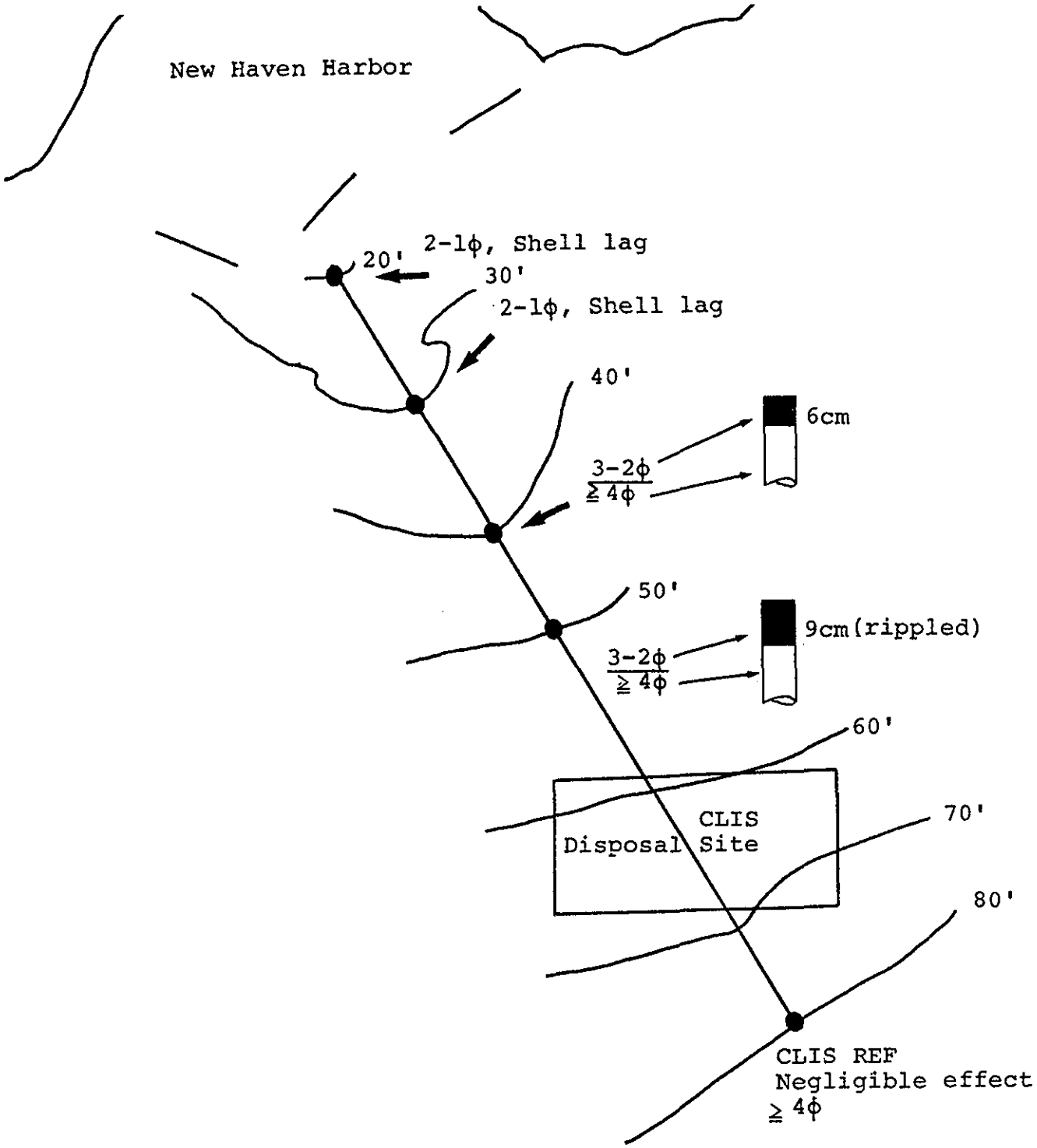

Figure 4-1 Observed grain-size (in phi units) along REMOTS® transect extending from New Haven Harbor entrance to the CLIS-REFERENCE site.

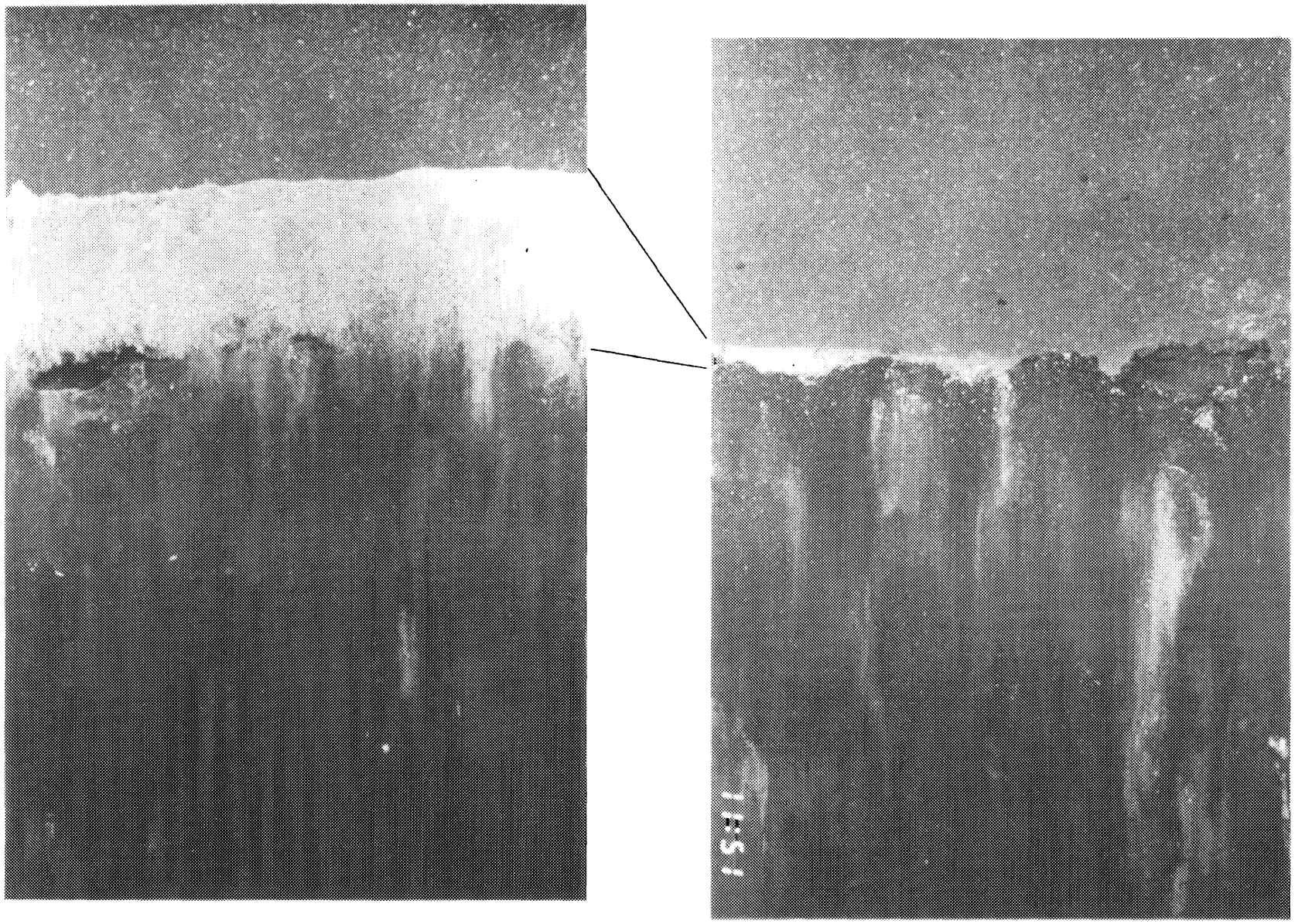

Figure 5-1 Pre and post-storm REMOTS® images from station CTR at the FVP site. In June(left), a high reflectance, sandy surface layer is evident at the interface. After the hurricane (right), this layer is no longer apparent, indicating that approximately 5 cm of material has been removed. Scale = 0.65X.

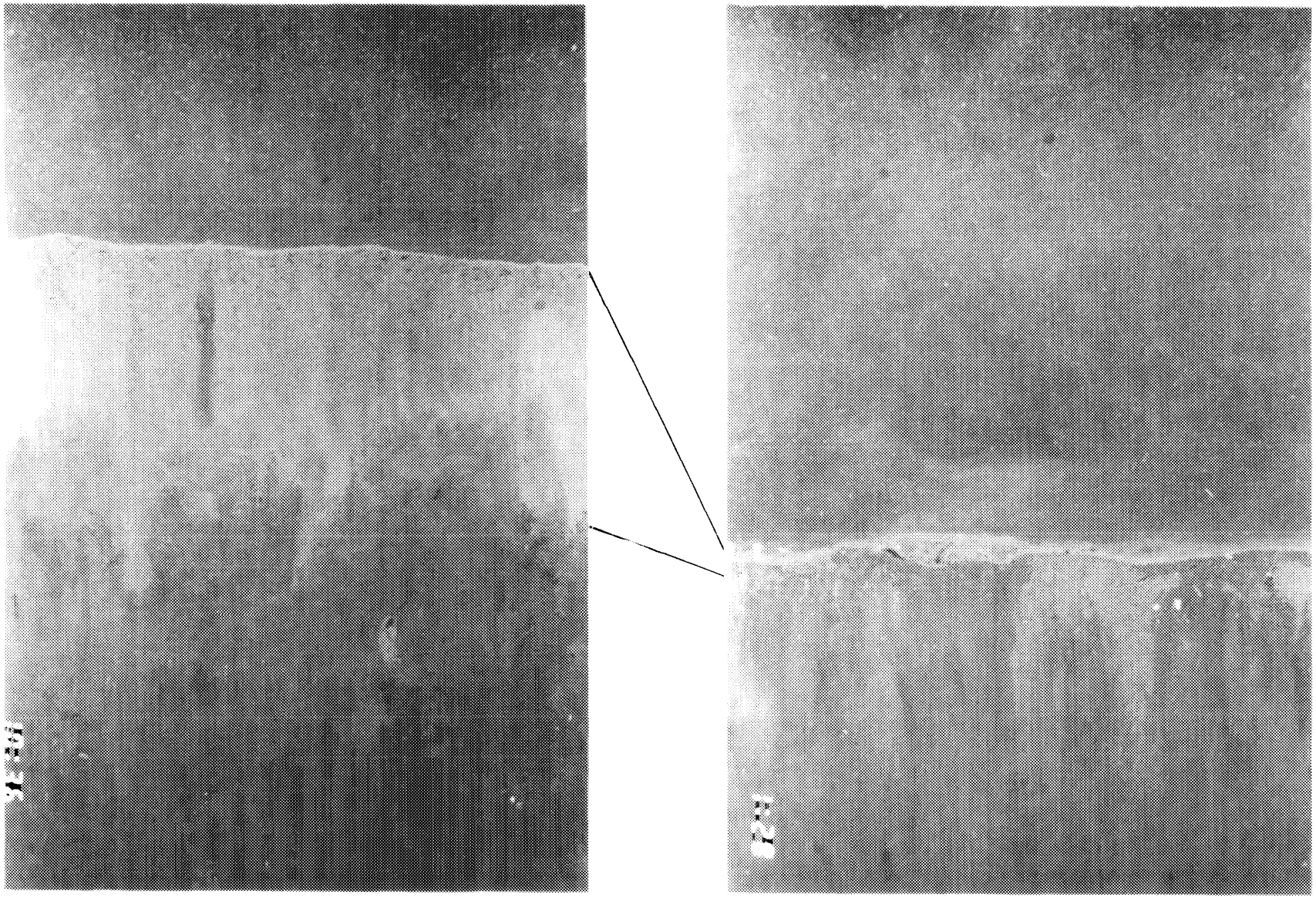

Figure 5-2 Pre and post-storm REMOTS® images from station 400S at the FVP site. In June (left), a well-developed Redox Potential Discontinuity layer (high reflectance) is evident. After the hurricane (right), much of this oxygenated material is no longer apparent and an exposed worm tube is evident at the interface, indicating the net loss of surface sediments. Scale = 0.65X.

APPENDIX

Captions to Plates

FVP

1. An aggregation of foraging hermit crabs. This activity caused erosion of fine surface sediments leaving only the coarser sediment components.

2. A partially buried whelk moving through the sediment-water interface. Note valve of the razor clam, a common prey species of the whelk.

3. A juvenile rock crab with shelter excavated under a shell fragment. All individuals were observed in softshell condition. Note molt (exuviae) at shelter entrance.

4. A vertical burrow of the rock crab with exuviae at entrance.

5. The individual rock crab removed from the burrow in the previous photograph.

6. Recent burrowing activity by a rock crab distributed anoxic sediments on the surface outside the shelter entrance.

7. Juvenile 4-spot flounder were observed foraging normally on the dredged material site.

8. A hermit crab leaving tracks on the sediment surface at the periphery of the site.

9. An association of starfish and sand shrimp (bottom of photograph, partially buried). The shrimp would winnow through sediments disturbed by the tube feet of the starfish.

CS-1

10. Hydroids fouling a clump of saltmarsh peat material.

11. Hydroid colony attached to a partially buried peat clump.

12. A winter flounder on the current sheltered side of a peat clump.

13. Mud snails attracted to the mucous trail left by a whelk on the surface of the dredged material.

CS-2

14. Remains of the molted exoskelton of a spider crab.

15. A juvenile windowpane flounder (approx. 6 cm length) on the dredged material surface.

STNH-North

16. Mud snail tracks and polychaete fecal casts are typical surface features.

17. The result of venting of sediments by mud snails burrowing below the sediment-water interface.

18. A razor clam with both valves still attached indicating recent mortality.

19. Surficial sediments reworked by the foraging activities of starfish and dense aggregations of hermit crabs.

20. Hydroids attached to shell hash material on and just under the surface.

STNH-South

21. A burrowing anemone with tentacles extended. This species was only observed at the STNH-South site during survey dives.

22. Close-up photograph of a snail burrow and degrading polychaetes fecal casts.

23. A larger burrow, possibly excavated by a juvenile rock crab.

24. A juvenile cunner taking shelter near a hydroid colony.

25. Close-up of a hydroid colony.

1.

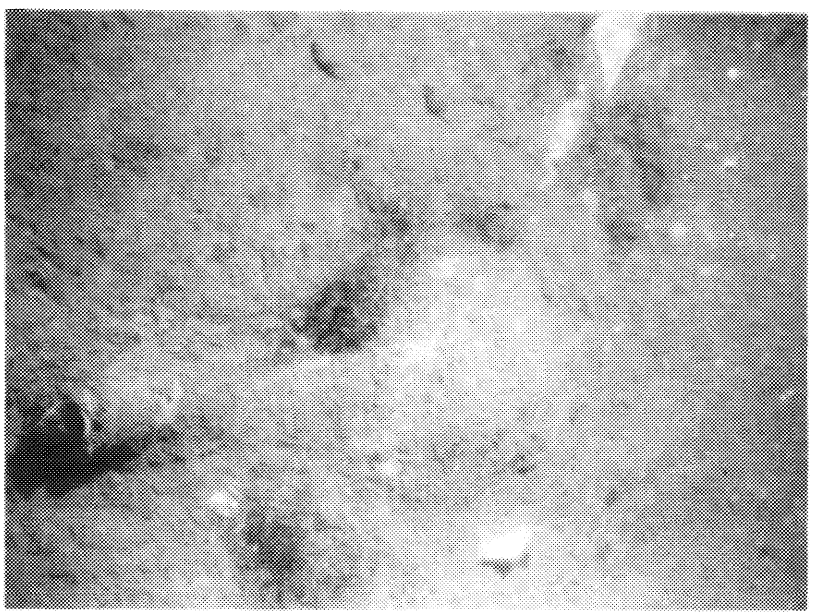

2.

3.

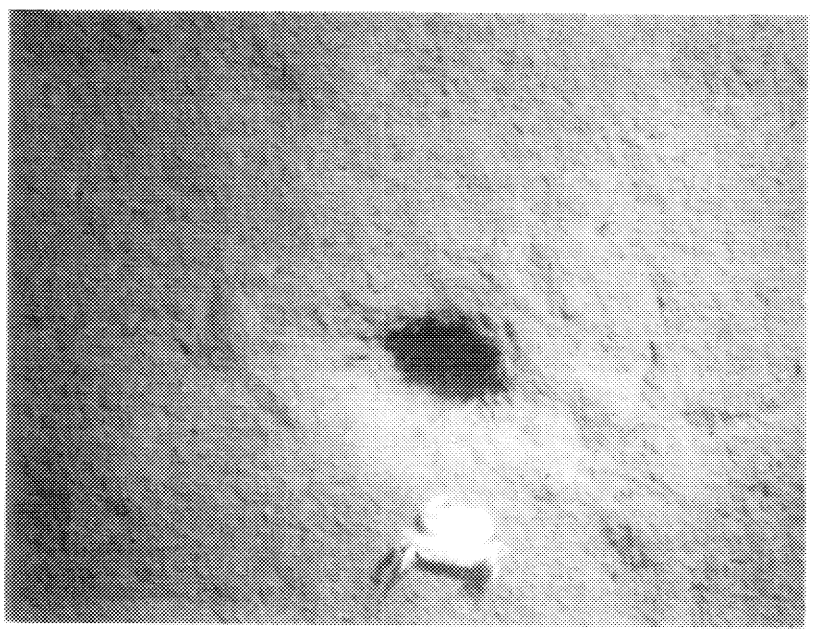

4.

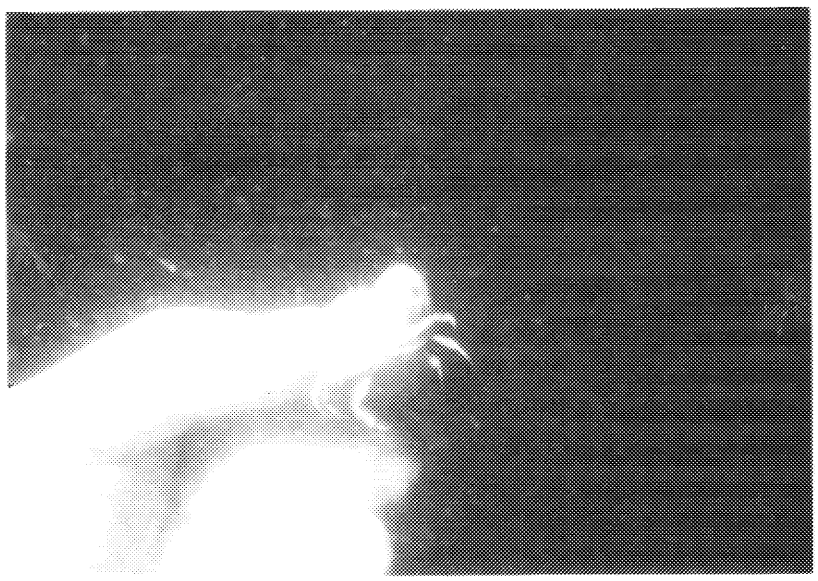

5.

6.

7.

8.

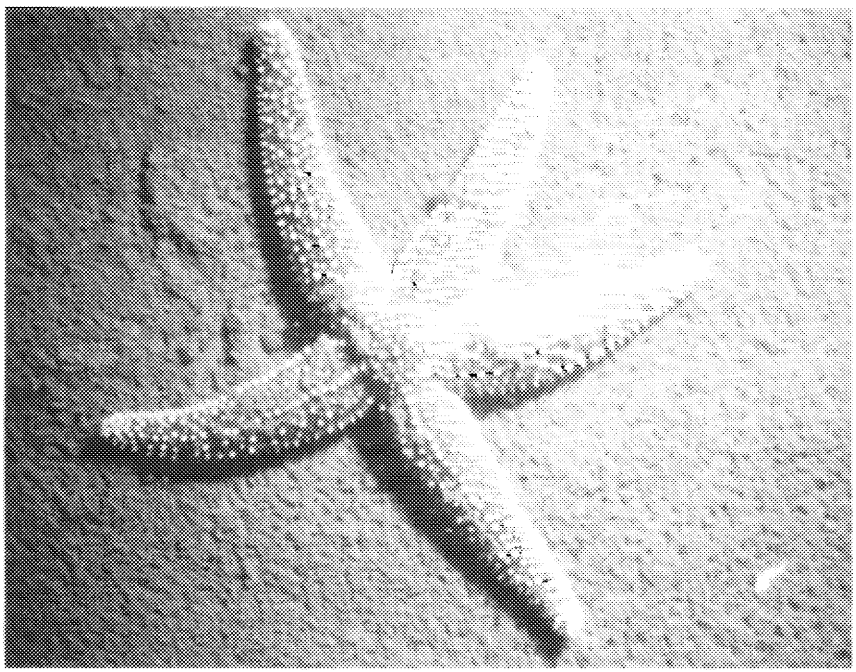

9.

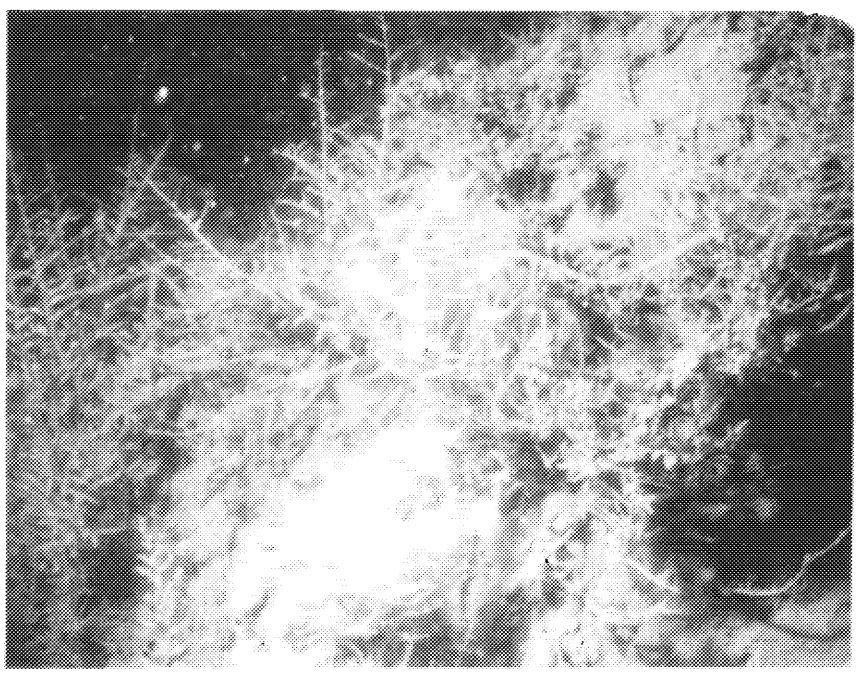

10.

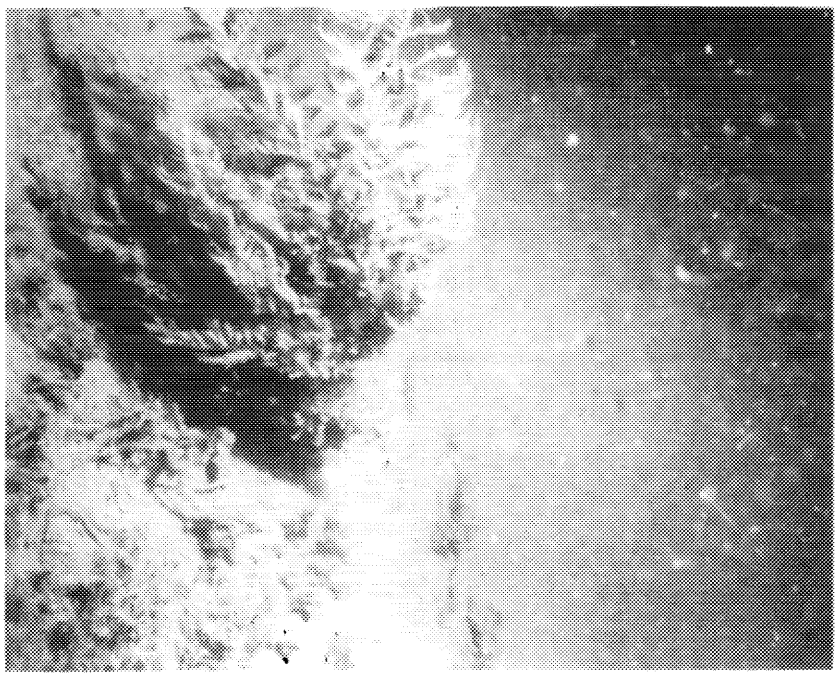

11.

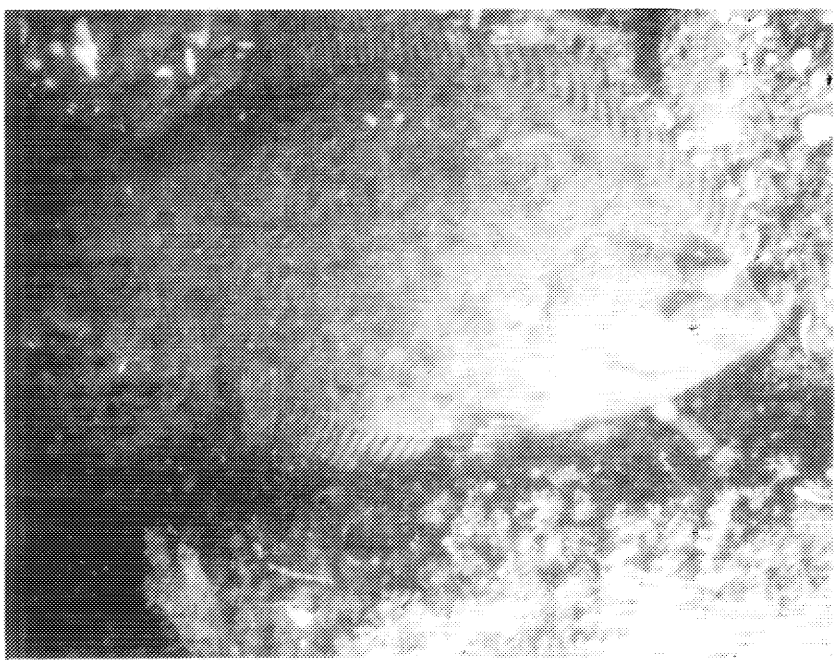

12.

13.

14.

15.

16.

17.

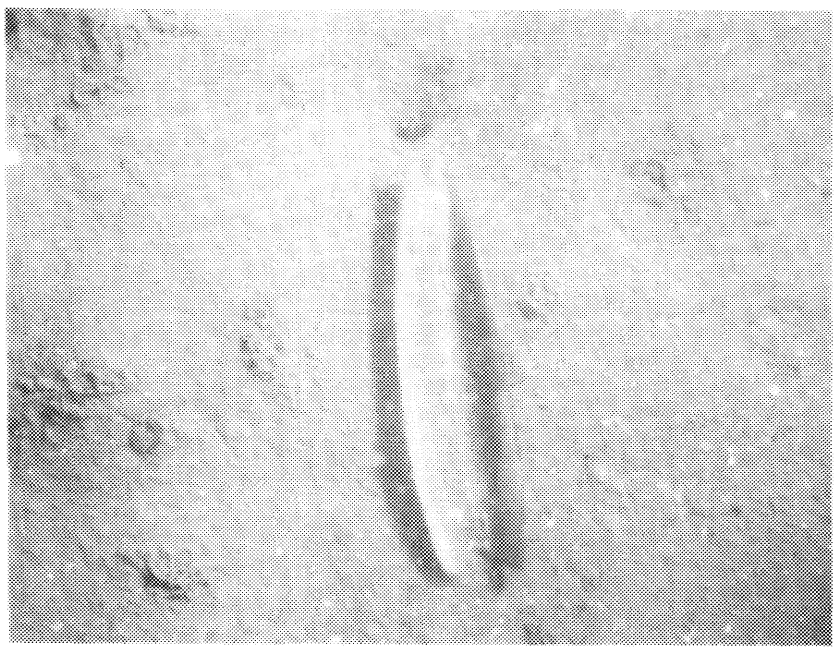

18.

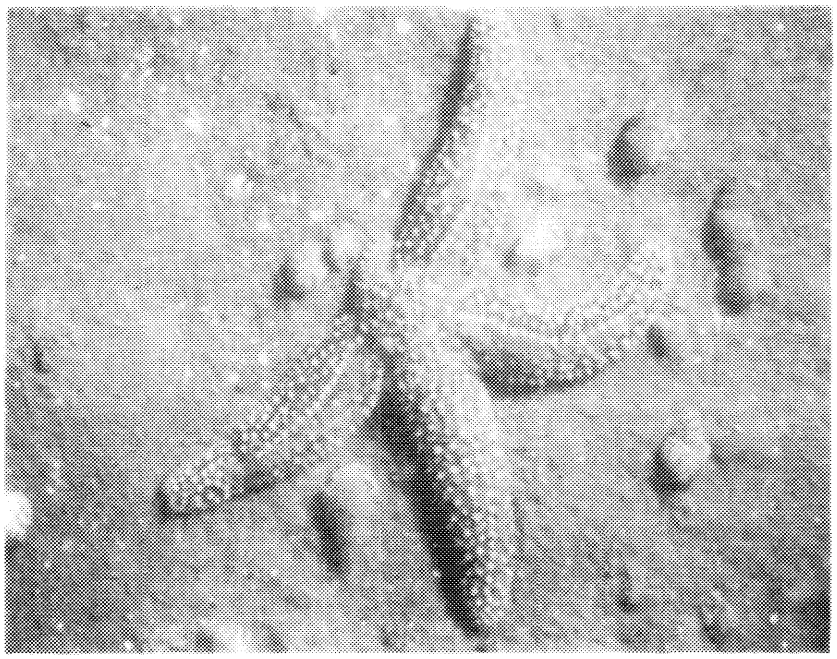

19.

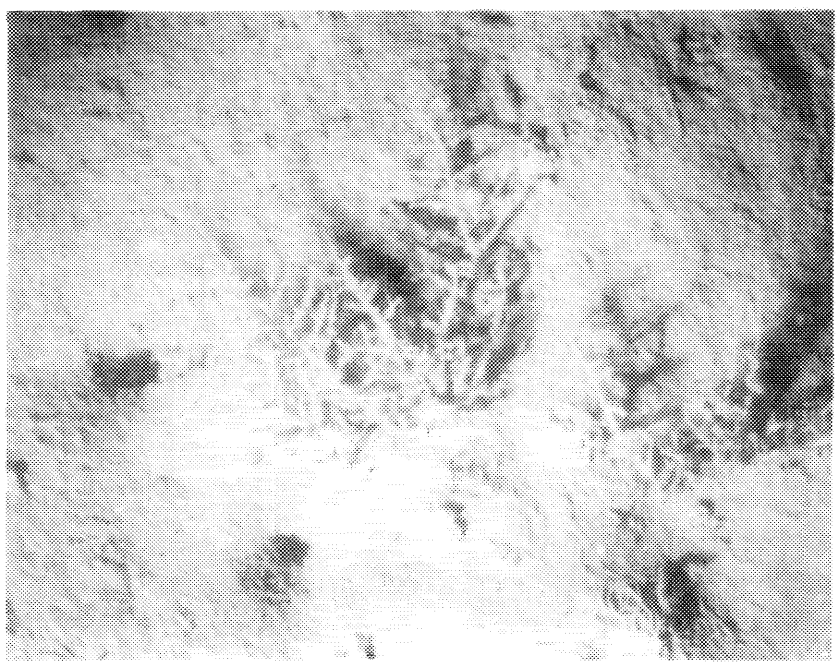

20.

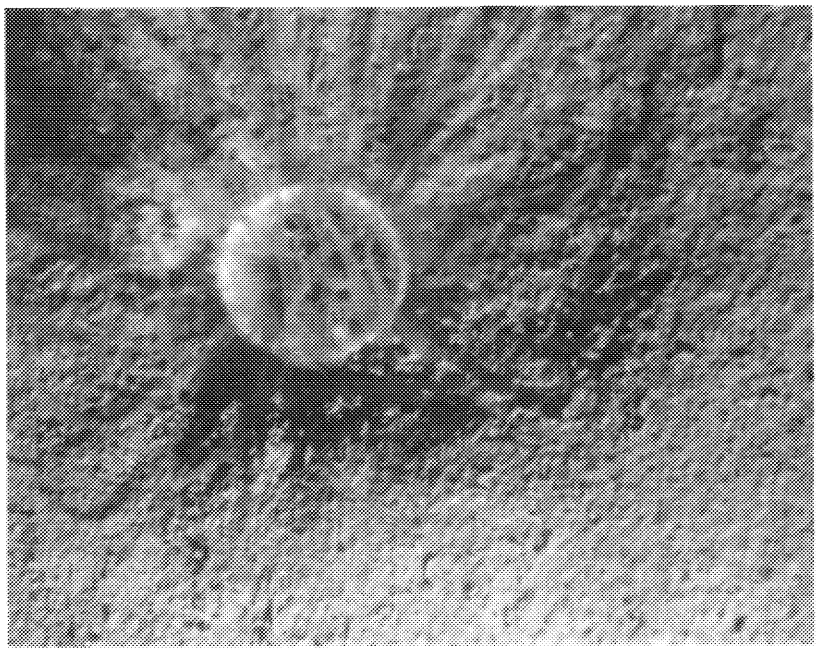

21.

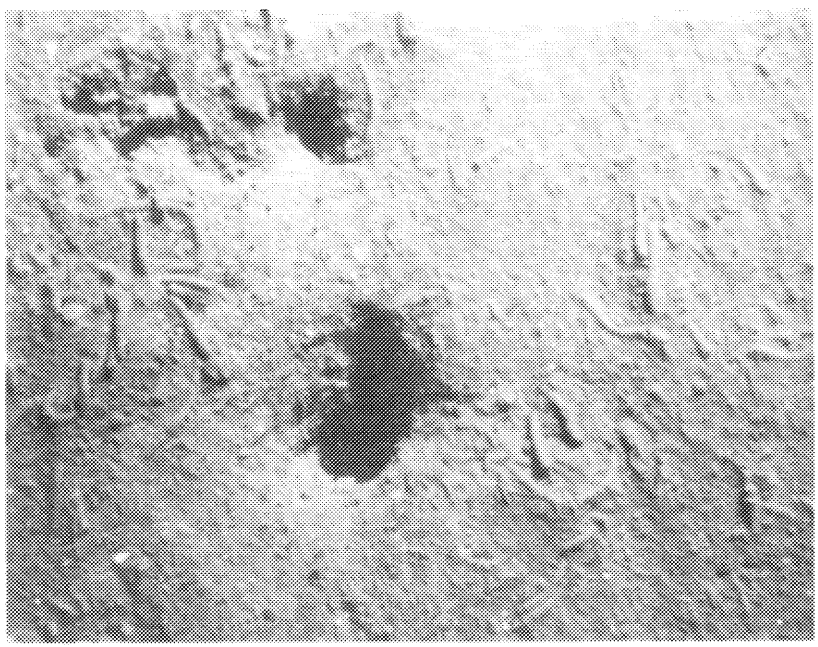

22.

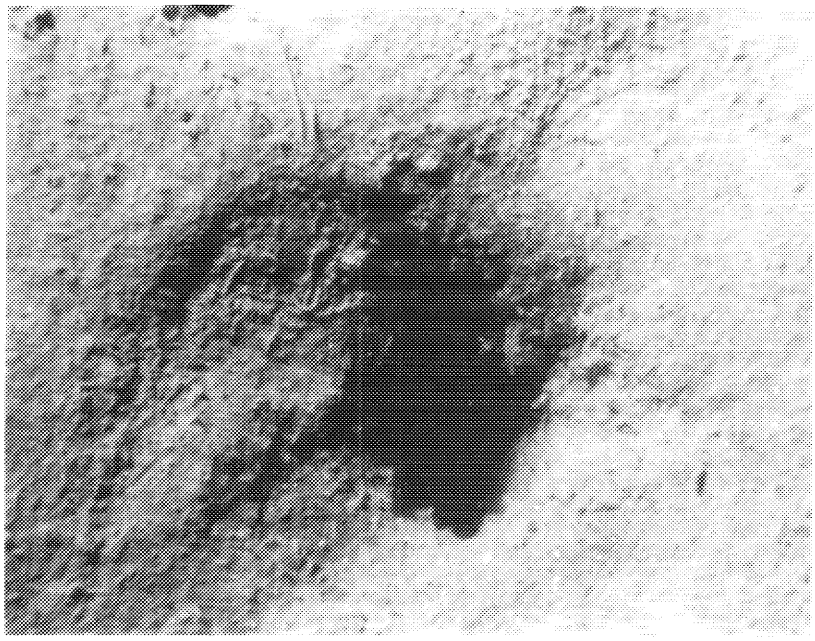

23.

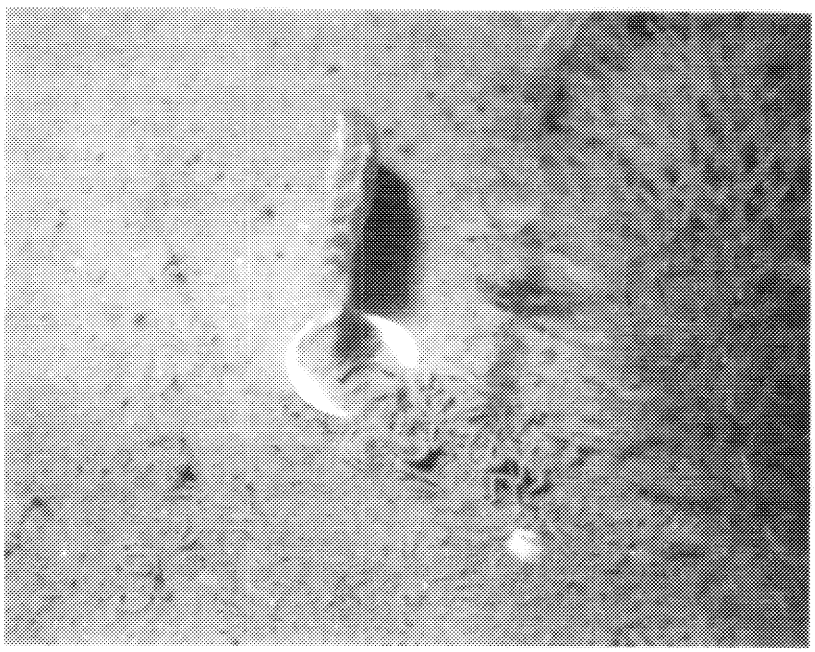

24.

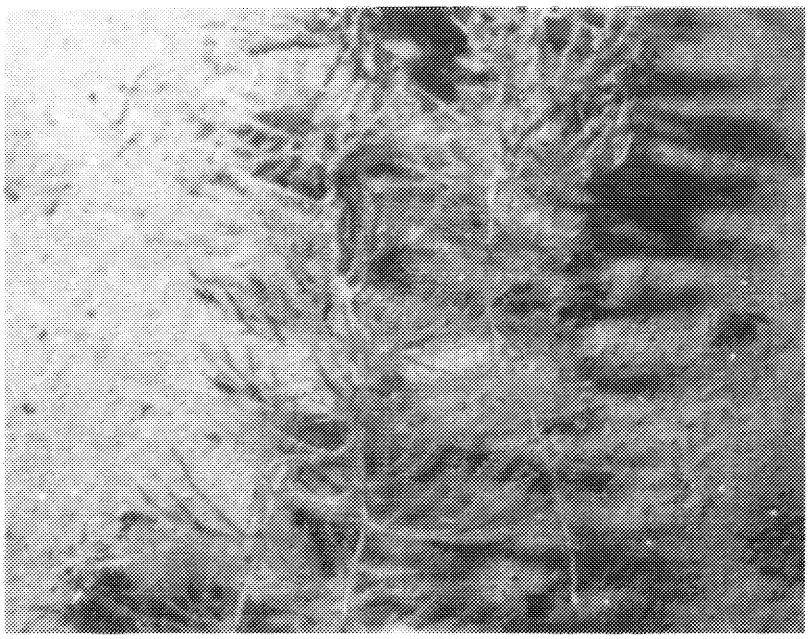

25.

☆ U. S. GOVERNMENT PRINTING OFFICE: 1990--700-017--00023